



**Calhoun: The NPS Institutional Archive**

---

Theses and Dissertations

Thesis Collection

---

1997-06

# Evaluation of the CMARC panel code software suite for the development of a UAV aerodynamic model

Pollard, Stephen J.

Monterey, California. Naval Postgraduate School

---

<http://hdl.handle.net/10945/31947>



Calhoun is a project of the Dudley Knox Library at NPS, furthering the precepts and goals of open government and government transparency. All information contained herein has been approved for release by the NPS Public Affairs Officer.

**Dudley Knox Library / Naval Postgraduate School  
411 Dyer Road / 1 University Circle  
Monterey, California USA 93943**

<http://www.nps.edu/library>

# NAVAL POSTGRADUATE SCHOOL

## Monterey, California



## THESIS

**EVALUATION OF THE CMARC PANEL CODE  
SOFTWARE SUITE FOR THE DEVELOPMENT OF A UAV  
AERODYNAMIC MODEL**

by

Stephen J. Pollard

June, 1997

Thesis Advisor:

Co-Advisor:

Max F. Platzer

Ismail H. Tuncer

Approved for public release; distribution is unlimited.

DTIC QUALITY INSPECTED 4

19980102 097

REPORT DOCUMENTATION PAGE			Form Approved OMB No. 0704-0188	
Public reporting burden for this collection of information is estimated to average 1 hour per response, including the time for reviewing instruction, searching existing data sources, gathering and maintaining the data needed, and completing and reviewing the collection of information. Send comments regarding this burden estimate or any other aspect of this collection of information, including suggestions for reducing this burden, to Washington headquarters Services, Directorate for Information Operations and Reports, 1215 Jefferson Davis Highway, Suite 1204, Arlington, VA 22202-4302, and to the Office of Management and Budget, Paperwork Reduction Project (0704-0188) Washington DC 20503.				
1. AGENCY USE ONLY (Leave blank)		2. REPORT DATE June 1997		3. REPORT TYPE AND DATES COVERED Master's Thesis
4. TITLE AND SUBTITLE EVALUATION OF THE CMARC PANEL CODE SOFTWARE SUITE FOR THE DEVELOPMENT OF A UAV AERODYNAMIC MODEL			5. FUNDING NUMBERS	
6. AUTHOR(S) Pollard, Stephen J.				
7. PERFORMING ORGANIZATION NAME(S) AND ADDRESS(ES) Naval Postgraduate School Monterey, CA 93943-5000			8. PERFORMING ORGANIZATION REPORT NUMBER	
9. SPONSORING / MONITORING AGENCY NAME(S) AND ADDRESS(ES)			10. SPONSORING / MONITORING AGENCY REPORT NUMBER	
11. SUPPLEMENTARY NOTES The views expressed in this thesis are those of the author and do not reflect the official policy or position of the Department of Defense or the U.S. Government.				
12a. DISTRIBUTION / AVAILABILITY STATEMENT Approved for public release; distribution unlimited.			12b. DISTRIBUTION CODE	
13. ABSTRACT (maximum 200 words) The CMARC panel code is evaluated to verify its accuracy and suitability for the development of an aerodynamic model of the Naval Postgraduate School (NPS) FROG Unmanned Air Vehicle (UAV). CMARC is a DOS personal computer based version of the NASA Panel Method Ames Research Center (PMARC) panel code. The core processing algorithms in CMARC are equivalent to PMARC. CMARC enhancements include improved memory management and command line functionality. Both panel codes solve for inviscid, incompressible flow over complex three-dimensional bodies using potential flow theory. Emphasis is first placed on verifying CMARC against the PMARC and NPS Unsteady Potential Flow (UPOT) panel codes. CMARC boundary layer calculations are then compared to experimental data for an inclined prolate spheroid. Finally, a complex three-dimensional panel model is developed for aerodynamic modeling of the FROG UAV. CMARC off-body flow field calculations are used to generate static-source and angle-of-attack vane position corrections. Position corrections are provided in look-up table and curve fit formats. Basic longitudinal and lateral-directional stability derivatives are also developed with CMARC data. CMARC derived stability derivatives are sufficiently accurate for incorporation into an initial aerodynamic model. Adjustments through analysis of flight test data may be required. Future CMARC studies should concentrate on the development of the damping and control power derivatives.				
14. SUBJECT TERMS Unmanned Aerial Vehicles, UAV, CMARC, PMARC, UPOT, Panel Code, Stability Derivatives, Boundary Layer Code, Computational Fluid Dynamics, CFD			15. NUMBER OF PAGES 151	
			16. PRICE CODE	
17. SECURITY CLASSIFICATION OF REPORT Unclassified	18. SECURITY CLASSIFICATION OF THIS PAGE Unclassified	19. SECURITY CLASSIFICATION OF ABSTRACT Unclassified		20. LIMITATION OF ABSTRACT UL



Approved for public release; distribution is unlimited

**EVALUATION OF THE CMARC PANEL CODE SOFTWARE SUITE FOR THE  
DEVELOPMENT OF A UAV AERODYNAMIC MODEL**

Stephen J. Pollard  
Lieutenant Commander, United States Navy  
B.S., United States Naval Academy, 1982

Submitted in partial fulfillment of the  
requirements for the degree of

**MASTER OF SCIENCE IN AERONAUTICAL ENGINEERING**

from the

**NAVAL POSTGRADUATE SCHOOL**

**June 1997**

Author:

[Redacted Signature]

Stephen J. Pollard

Approved by:

[Redacted Signature]

Max F. Platzer, Thesis Advisor

[Redacted Signature]

Ismail H. Tuncer, Co-Advisor

[Redacted Signature]

Daniel J. Collins, Chairman  
Department of Aeronautics and Astronautics



## ABSTRACT

The CMARC panel code is evaluated to verify its accuracy and suitability for the development of an aerodynamic model of the Naval Postgraduate School (NPS) FROG Unmanned Air Vehicle (UAV). CMARC is a DOS personal computer based version of the NASA Panel Method Ames Research Center (PMARC) panel code. The core processing algorithms in CMARC are equivalent to PMARC. CMARC enhancements include improved memory management and command line functionality. Both panel codes solve for inviscid, incompressible flow over complex three-dimensional bodies using potential flow theory. Emphasis is first placed on verifying CMARC against the PMARC and NPS Unsteady Potential Flow (UPOT) panel codes. CMARC boundary layer calculations are then compared to experimental data for an inclined prolate spheroid. Finally, a complex three-dimensional panel model is developed for aerodynamic modeling of the FROG UAV. CMARC off-body flow field calculations are used to generate static-source and angle-of-attack vane position corrections. Position corrections are provided in look-up table and curve fit formats. Basic longitudinal and lateral-directional stability derivatives are also developed with CMARC data. CMARC derived stability derivatives are sufficiently accurate for incorporation into an initial aerodynamic model. Adjustments through analysis of flight test data may be required. Future CMARC studies should concentrate on the development of the damping and control power derivatives.





## TABLE OF CONTENTS

I. INTRODUCTION.....	1
A. BACKGROUND.....	1
B. REQUIREMENTS.....	2
C. STATEMENT OF OBJECTIVES.....	2
II. OVERVIEW OF PERSONAL SIMULATION WORKS.....	5
A. GENERAL.....	5
B. LOFTSMAN.....	5
1. Streamlined Bodies.....	5
2. Wings and Control Surfaces.....	6
3. Patches.....	6
C. CMARC.....	6
D. POSTMARC.....	7
III. CMARC PANEL CODE THEORY.....	9
A. POTENTIAL FLOW PANEL CODE THEORY (CMARC/PMARC).....	9
B. CMARC BOUNDARY LAYER ANALYSIS THEORY.....	12
IV. CMARC VERIFICATION.....	17
A. VERIFICATION OF CMARC AGAINST PMARC.....	17
B. COMPARISON OF CMARC AND PMARC PROCESSING TIMES.....	20
C. COMPARISON OF CMARC TO THE UPOT BOUNDARY LAYER.....	23
CODE	
1. UPOT Boundary Layer Calculations.....	23
2. High AR Wing Model.....	23
3. Boundary Layer Results and Analysis (CMARC vs. UPOT).....	24
a. Boundary Layer Transition.....	24
b. Separation.....	25
c. Skin Friction Coefficient near the Stagnation Point.....	35
D. COMPARISON OF CMARC TO INCLINED PROLATE SPHEROID.....	36
EXPERIMENTAL DATA	

1. Inclined 6:1 Prolate Spheroid - AGARD AR-303 Case C-2.....	37
a. Wind Tunnel Experiment Setup.....	37
b. Experimental Data.....	38
c. Integration of Local Forces to Provide Lift Drag and.....	40
Pitching Moment	
2. CMARC Model of 6:1 Prolate Spheroid.....	42
3. Data Extraction.....	43
4. Prolate Spheroid Pressure Distribution.....	43
5. Boundary Layer Separation Locations.....	47
6. Boundary Layer Skin Friction Coefficient.....	49
7. Integrated Skin Friction Forces.....	51
8. Total Integrated Forces.....	52
V. AERODYNAMIC MODEL OF THE FROG UAV.....	55
A. BACKGROUND.....	55
B. FROG UAV DESCRIPTION.....	55
C. FROG UAV MODELING.....	58
1. General.....	58
2. Modeling Coordinate System.....	60
3. LOFTSMAN Patches.....	60
a. Fuselage Model.....	61
b. Main Wing Patch.....	61
c. Horizontal Stabilizer Patch.....	62
d. Vertical Stabilizer Patch.....	62
e. Tail Boom Patch.....	62
f. Engine Pod Patch.....	63
g. Engine Pylon Patch.....	63
4. Common CMARC Input File Errors.....	63
D. STATIC-PRESSURE SOURCE AND YAW VANE CORRECTIONS.....	64
THROUGH OFF-BODY FLOW ANALYSIS	
1. Description of the FROG UAV Pitot-Static and AOA Systems.....	64
2. Modeling Off-Body Streamlines.....	64

3. Analysis of Static Source Position Errors.....	66
4. Analysis of Alpha Vane Position Error.....	72
5. Summary of Off-Body Flow Field Analysis.....	72
E. DEVELOPMENT OF BASIC STABILITY DERIVATIVES.....	75
1. Longitudinal Stability Derivatives.....	75
a. Longitudinal Stability Derivative Methods.....	75
b. Analysis of Longitudinal Stability Data.....	78
2. Lateral Directional Stability Derivatives.....	79
a. Lateral-Directional Stability Derivative Methods.....	79
b. Analysis of Lateral-Directional Stability Data.....	81
3. Summary of CMARC Stability Derivative Analysis.....	81
VI. CONCLUSIONS AND RECOMMENDATIONS.....	83
APPENDIX A. DEVELOPMENT OF THE MOMENTUM INTEGRAL.....	85
EQUATION	
APPENDIX B. INTEGRATION OF AERODYNAMIC FORCES OVER THE ..... 89	
SURFACE OF A PROLATE SPHEROID	
APPENDIX C. MATLAB PROGRAMS TO INTEGRATE AERODYNAMIC ..... 93	
FORCES OVER THE SURFACE OF A PROLATE	
SPHEROID	
APPENDIX D. REPRESENTATIVE CMARC/PMARC SPEED TEST FILE ..... 95	
APPENDIX E. MATLAB PROGRAM FOR REORDERING AGARD DATA..... 97	
FILE	
APPENDIX F. CMARC PROLATE SPHEROID INPUT FILE ..... 99	
APPENDIX G. CMARC/PMARC DATA EXTRACTION PROGRAM ..... 107	
APPENDIX H. LOFTSMAN INPUT FILES ..... 109	
APPENDIX I. FROG UAV CMARC INPUT FILE ..... 117	
LIST OF REFERENCES ..... 137	
INITIAL DISTRIBUTION LIST ..... 139	



## I. INTRODUCTION

### A. BACKGROUND

Computational fluid dynamics (CFD) is increasingly used as a design and analysis tool. As the price of computer hardware drops and computational power increases, CFD becomes more attractive to a larger audience. CFD tools range from the high end three-dimensional (3D) Navier-Stokes solvers for compressible, viscous fluids to potential flow solvers for incompressible, inviscid flows. This paper discusses the development of a DOS personal computer hosted panel code model for the Naval Postgraduate School (NPS) Fiber Optic Guided (FROG) Unmanned Air Vehicle (UAV) program.

The Personal Simulation Works software suite, consisting of LOFTSMAN, CMARC and POSTMARC, is used for all aspects of the study. The software provides for panel model development, input file processing and the visualization of results. Emphasis is placed on verifying both the accuracy and suitability of the CFD programs for aerodynamic modeling.

Until recently, personal computers (PC) did not have the computational power or memory to be practical for panel code CFD programs. Things have changed with the introduction of the Pentium class PC and low cost RAM. AeroLogic capitalized on the power of the Pentium class PC and developed Personal Simulation Works (PSW). PSW is centered around the 3D low order, inviscid potential flow solver named CMARC. CMARC is a re-hosted version of NASA's Panel Method Ames Research Code (PMARC). PMARC was re-written in the C language and compiled for IBM compatible PCs. CMARC runs under the DOS operating system. CMARC will also run in a DOS window under the WINDOWS 3.x, 95 or NT operating systems. CMARC has enhanced capabilities that include; improved memory management, an expanded set of command line switches and provisions for expanded boundary layer post-processing capabilities. However, the core processing algorithms remain the same as implemented in PMARC.

LOFTSMAN, the PSW pre-processing program, is used to mesh complex 3D bodies and create input file patches. The program runs under the DOS operating system and allows the user to loft conics based 3D surfaces. The program automatically creates CMARC, PMARC or VSAERO input patches based on desired panel densities and distribution.

POSTMARC is used for flow visualization and integration of resultant forces. It runs under the Windows 3.x, 95 and NT operating systems. POSTMARC reads CMARC or PMARC output files and provides for the visualization of model geometry, wake stepping, on and off-body streamlines and surface phenomena.

## **B. REQUIREMENTS**

The Naval Postgraduate School Aeronautics Department is integrating UAV hardware and software to demonstrate autonomous flight, trajectory tracking and automatic landing. A core requirement for flight control development is a valid aerodynamic truth model for the UAV airframe. The introduction of each new airframe requires the development of a new aerodynamic truth model. Most recently, Papageorgiou [Ref. 1] developed and tested an aerodynamic model for the NPS FROG UAV based on classical methods. His model produced a close match to flight test results in the longitudinal axis. However, the lateral-directional axis required modifications based on measured flight test data to produce acceptable results. With the availability of low cost panel code CFD capabilities, it is suggested that a panel code model of the FROG UAV is an alternative for estimating many of the stability derivatives required for an aerodynamic truth model.

Accurate pitot-static and angle-of-attack sensors are required for highly augmented flight control systems. CMARC is well suited for solving on-body static pressure distributions and off-body flow velocities over the predominately attached flow fields of fuselage fore bodies. This proves particularly useful for generating pitot static and angle of attack correction curves and look-up tables.

## **C. STATEMENT OF OBJECTIVES**

The Naval Postgraduate School Aeronautics Department has both active CFD research and avionics development programs. The primary purpose of this investigation is to verify the accuracy and suitability of the PSW software suite while developing a panel code model for the NPS FROG UAV program. Specific objectives are as follows:

- Demonstrate panel code modeling, processing and visualization on a Pentium PC using the PSW software package.

- Verify CMARC results against PMARC.
- Investigate the CMARC integral boundary layer calculations through comparison to validated 2D CFD codes and 3D experimental data.
- Develop and analyze a panel code model for the NPS FROG UAV using PSW to estimate basic stability derivatives and produce angle-of-attack vane and pitot-static correction curves.
- Compare relative speed of CMARC hosted on 150 MHz Pentium personal computer to PMARC hosted on a Silicon Graphics Indigo<sup>2</sup> workstation.





## **II. OVERVIEW OF PERSONAL SIMULATION WORKS**

### **A. GENERAL**

Personal Simulation Works is a PC based software suite that provides for the three primary CFD requirements; 3D modeling of an aircraft (LOFTSMAN), panel code flow solver (CMARC), and post-processing of the computed flow field (POSTMARC). The software package contains three applications hosted on the IBM compatible personal computer. Each software program is discussed separately.

### **B. LOFTSMAN**

LOFTSMAN is a 3D modeling tool that generates surface panel distributions for CMARC or PMARC input files. The program is based on conics, which allows rapid lofting of streamlined bodies such as aircraft fuselages and engine nacelles. In addition, wing and control surfaces can be designed with the extensive library of airfoil templates or with user specified coordinates. The software is well documented, including a tutorial, in the Personal Simulation Works User Guide [Ref. 2]. LOFTSMAN is primarily designed for creating new objects, but an existing airframe can be matched quite closely with just a detailed three-view drawing that includes frame cross sections.

#### **1. Streamlined Bodies**

LOFTSMAN functionality is divided into Body Objects and Wing Objects. In general, they remain separate unless the intersection between a wing and body is required.

Body Objects are created using a family of curves called second-degree conics. Circles, ellipses, parabolas and hyperbolas are among this group. An entire fuselage is described by specifying just four lines. These are the top waterline (TW), bottom waterline (BW), the maximum breadth line (MB) and the waterline of the maximum breadth line (WW). For each line, the beginning, ending and a few points along the line are specified. Control points are also specified with a curvature factor that allows LOFTSMAN to generate a smooth conic between the points. The power of conic lofting will become evident when discussing the modeling of the complex FROG UAV fuselage in Chapter V.

## **2. Wings and Control Surfaces**

Wings and control surfaces are easily specified in LOFTSMAN using a short input file created with any text editor. The file specifies root, intermediate and tip rib section, location, axis, chord and incidence. LOFTSMAN then fairs a smooth surface through the rib sections. Washout is specified by varying the incidence of the root and tip ribs. Sweep-back is controlled by staggering the tip rib location with respect to the root rib. Once the general wing surface is specified, control surfaces such as ailerons, flaps and elevators can be deflected and meshed.

## **3. Patches**

LOFTSMAN automatically meshes 3D surfaces and creates patches for CMARC/PMARC input files. The distinction between a mesh and a patch is important. A mesh is a set of quadrilateral and triangular panels that represent the surface of a wing or body. When the set of panels is organized and formatted to create a sub-component portion of a CMARC or PMARC input file, it is called a patch.

A body or wing surface is first meshed at a density specified by the user. Cosine and half-cosine spacing are among the compression options. After meshing the object, one saves it to a text file as a formatted patch. One then opens the patch file with any text editor and copies/pastes the patch text into the appropriate location in the CMARC input file.

Each control surface deflection requires a separate mesh and formatted patch. For instance, to evaluate roll performance one needs to separately mesh an upward aileron deflection on the right wing and a downward deflection on the left wing. If multiple deflections of a single control surface are required, each deflection must be meshed separately.

## **C. CMARC**

CMARC is the C version of the Panel Method NASA Ames Research Center (PMARC) low order, 3D panel code. Inviscid, irrotational, incompressible, potential flow is assumed. Low order means that source and doublet strength distribution is constant across a panel. There is no attempt to match the source or doublet strength of an adjacent

panel at a common edge. Advanced features include internal flow modeling and time stepping wake models.

PMARC version 12.19 was released as FORTRAN 77 source code in 1992. CMARC was rewritten in the C language and compiled for hosting on IBM compatible personal computers by AeroLogic, Inc. The program runs under the DOS operating system. It will also run in a DOS window from Windows 3.1, 95 or NT. Enhanced features include command line options and flexible memory management. Command line options simplify batch processing by adding an extensive set of switches that can be set external to the CMARC input file. Flexible memory management provides for the automatic sizing of arrays without having to recompile the source code.

#### **D. POSTMARC**

POSTMARC is a Windows post-processing program for the visualization of CMARC and PMARC output files. Capabilities include body geometry, wake stepping, surface pressure and streamline visualization. POSTMARC also provides the capability to integrate pressure and skin friction forces over the model geometry. This proves particularly useful when one desires to recalculate loads around a different center of gravity.

An interesting feature for design work integrates panel surface area to obtain total wetted area. After lofting a new geometry in LOFTSMAN, a quick check of geometry is made by running CMARC with the -g command line toggle. The total wetted area is then checked in POSTMARC. This function is particularly useful when working to reduce skin friction drag.

Versions 1.17.3 and later of POSTMARC include the capability to integrate skin friction drag coefficient over the model geometry. It is important to note that a key piece of the drag equation is missing from a POSTMARC solution. CMARC provides induced drag from the surface pressure distribution and skin friction drag from the 2D boundary layer code. Skin friction is only calculated up to the point of boundary layer separation. Pressure drag due to separation, a major portion of the drag equation, is missing from a CMARC/POSTMARC solution.

In fact, if one isn't careful, POSTMARC drag calculations can be misleading. Take for instance two similar model configurations with only minor geometry differences that do not affect wetted area. It is possible for the model with more flow separation to

have less skin friction drag because there is no CMARC output for skin friction coefficient after the boundary layer code predicts separation. During iterative design work, this could lead to the incorrect conclusion that the design team is reducing overall drag. Perhaps a better function for LOFTSMAN than integrated skin friction drag would be a function that predicts the percentage of attached flow and laminar flow. Iterative design changes could be made that maximize laminar flow and minimize separated flow.

### III. CMARC PANEL CODE THEORY

#### A. POTENTIAL FLOW PANEL CODE THEORY (CMARC/PMARC)

Potential flow theory involves the superposition of sources and doublets to generate the desired flow field around a 3D body. It assumes inviscid, irrotational and incompressible flow. As such, valid solutions are only obtained at low Mach numbers and for flow fields without large areas of separation.

The basic concept of panel methods, as outlined by Bertin and Smith [Ref. 3], requires the modeling of the desired 3D configuration with a large number of quadrilateral and triangular panels representing the surface of the aircraft. A series of sources, doublets and vortices is then distributed on each panel. Superposition allows the simultaneous computation of the singularity strengths required to satisfy flow tangency on the surface. The inviscid, irrotational and incompressible flow field represented by the superposition of sources and doublets satisfies the Laplace equation:

$$\nabla^2 \Phi = 0 \quad 3.1$$

Using Green's Theorem, the potential at any point P in the flow is represented by:

$$\Phi_P = \frac{1}{4\pi} \iint_{S+W} (\Phi - \Phi_i) \bar{n} \nabla \left( \frac{1}{r} \right) dS - \frac{1}{4\pi} \iint_{S+W} \left( \frac{1}{r} \right) \bar{n} \cdot (\nabla \Phi - \nabla \Phi_i) dS \quad 3.2$$

Where  $(\Phi - \Phi_i)$  represents the potential from the doublet distribution and  $\bar{n} \cdot (\nabla \Phi - \nabla \Phi_i)$  represents the potential from the source distributions.

CMARC is a low order panel code that assumes constant source and doublet strength distributions across each panel. Figure 3.1 shows a panel layout for a generic 3D wing fuselage configuration. It is important to note that for a 3D solution, there is an equivalence to surface doublet and surface vortex distributions. CMARC implements source and doublet distributions.

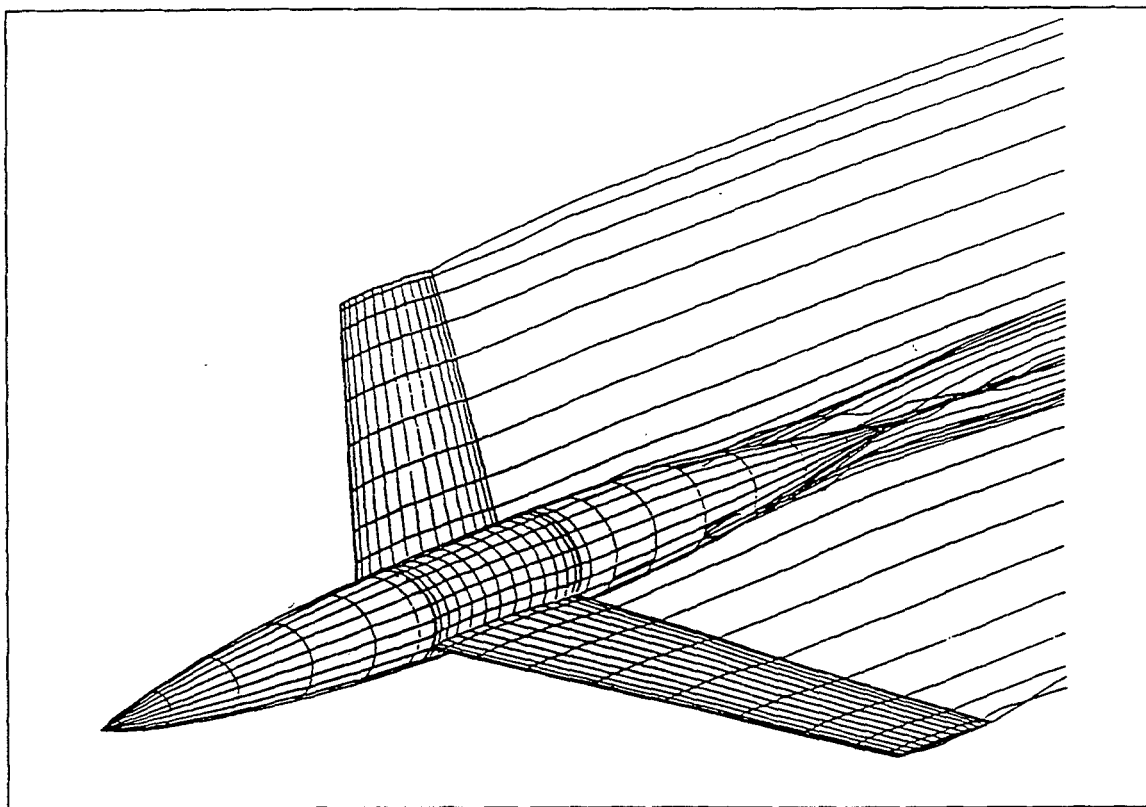


**Figure 3.1 Typical Wing-Body Panel Code Configuration, from Ref. [4].**

As mentioned previously, the general boundary condition imposed is tangential flow at the surface. CMARC, as outlined in Ref. [2], allows the modification of this boundary condition on individual panels or groups of panels. A normal surface velocity distribution may be specified to simulate flow into or out of ducts.

In order to produce lift, a potential flow panel code requires a method to implement the Kutta condition. As noted in Anderson [Ref. 5], the Kutta condition at the trailing edge implies that the circulation,  $\Gamma$ , around an airfoil is such that the flow exits the trailing edge smoothly. In addition, the velocities leaving the top and bottom surfaces are finite and equal in magnitude and direction.

Panel codes impose the Kutta condition by the shedding of wake panels along the trailing edges or separation lines. Wake panels are similar to a surface panel with only a doublet distribution. The doublet strength of the attached wake panel equals the difference in doublet strengths of the two adjacent surface panels.

The CMARC core panel code processing engine is functionally equivalent to the PMARC panel code module. The implemented equations are well documented by Ashby et al. [Ref. 4]. The PMARC documentation includes a wing-body combination, shown in Figure 3.1, evaluated by PMARC with good correlation to experimental data. The results are shown in Figures 3.2 and 3.3. In addition, Lambert [Ref. 6] compared PMARC panel code results to several theoretical and experimental test cases with good correlation at low angle-of-attack. Sensitivity to wake placement is highlighted by his studies.

Wake positioning can have a large influence on potential flow solutions. A wake is obviously attached to the trailing edge of wings and control surfaces with sharp, thin trailing edges to produce the Kutta condition. However, wake positioning on streamlined fuselages, missile airframes and nacelles is more of an art than science. Recently, Tuncer and Platzler [Ref. 7] investigated generalized wake placement techniques for cylindrical bodies of revolution with good correlation to experimental data at up to 20 degrees angle-of-attack. The techniques are used in this study with success for the verification of CMARC calculations for flow over an inclined 6:1 prolate spheroid.

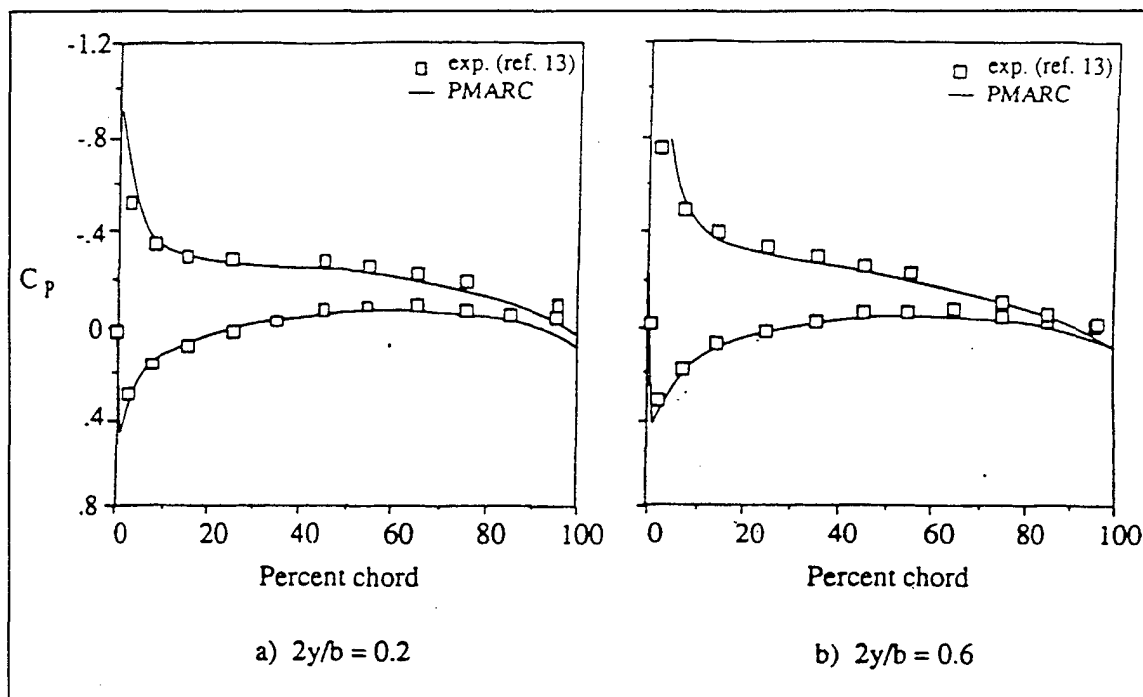


**Figure 3.2 Comparison of Experimental Data and PMARC Results for Two Spanwise Stations of the Wing/Body ( $\alpha = 4^\circ$ ), from Ref. [4].**

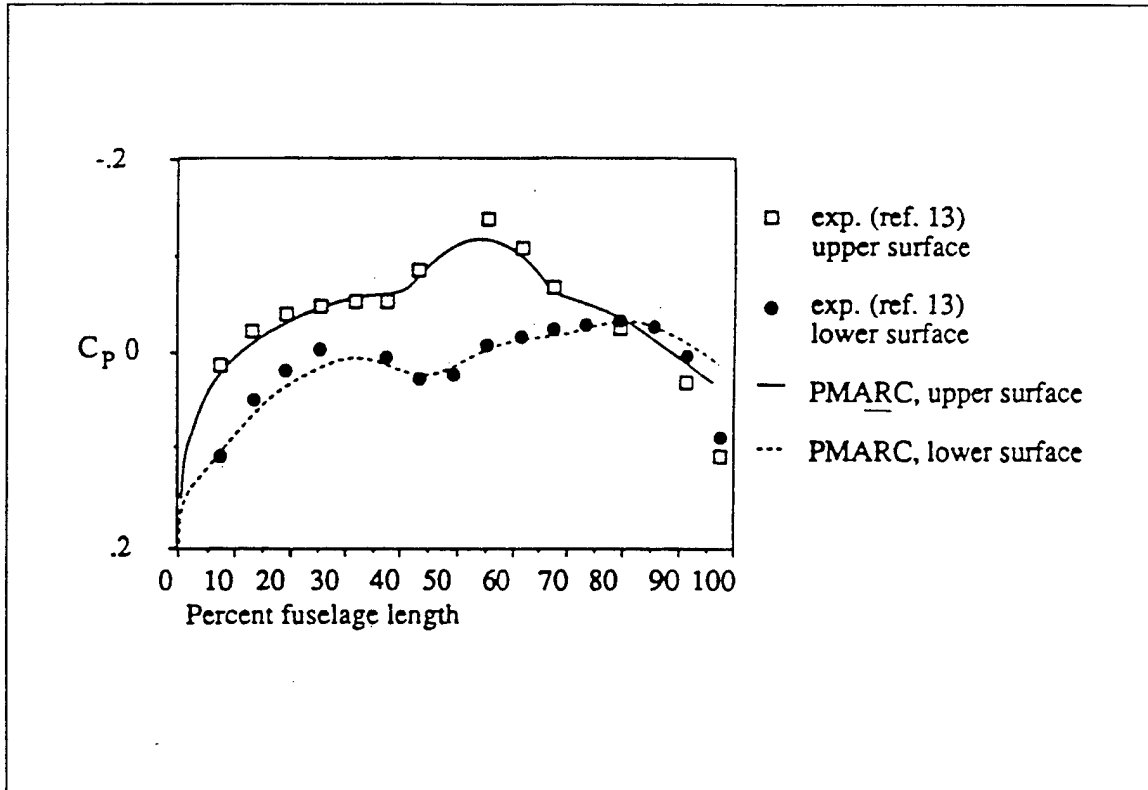


**Figure 3.3 Comparison of Experimental Data and PMARC Along the Fuselage Centerline of the Wing/Body Configuration ( $\alpha = 4^\circ$ ), from Ref. [4].**

## **B. CMARC BOUNDARY LAYER ANALYSIS THEORY**

CMARC and PMARC use the same two-dimensional integral method to calculate boundary layer characteristics along a surface streamline. A transition model automatically switches from laminar to turbulent calculations. The developers of the PMARC code chose a 2D integral routine over a 3D finite difference grid method due to speed and robustness of the calculations [Ref. 4]. Building a finite difference grid is a difficult and time consuming process requiring the user to develop grids over complex 3D surfaces. In addition, boundary layer calculation times can easily exceed that required for the basic potential flow solution. Reference [8] gives a good outline of three-dimensional finite difference methods.



The CMARC and PMARC User's Guides [Refs. 2 and 4] contain detailed discussions on the development of the CMARC/PMARC boundary layer code starting from the two-dimensional momentum equation:

$$\frac{d\theta}{d\eta} + (2 + H) \frac{\theta}{U} \frac{dU}{d\eta} = \frac{1}{2} C_f \quad 3.3$$

The momentum integral equation is numerically integrated along a surface streamline. The derivation leading to Equation 3.3 is developed in Appendix A for completeness.

The laminar region of the boundary layer is modeled by numerically integrating the following exact differential equation. The equation is solved iteratively through numerical integration along a streamline starting at a stagnation point [Ref. 4]:

$$\theta(\eta)^2 = \frac{0.45\nu}{U(\eta)^6} \int_0^\eta (1 + 2.222g(K, \mu)) U(\eta)^5 d\eta + \theta(0)^2 \left( \frac{U(0)}{U(\mu)} \right)^6 \quad 3.4$$

Where: U - velocity at outer edge of boundary layer  
 $\theta$  - momentum thickness  
 $K = \frac{\theta^2}{\nu} \frac{dU}{d\eta}$   
 $\eta$  - generalized coordinate along a streamline

The value  $g(K, u)$  is based on exact solutions for a number of pressure distributions. Initial work was conducted by Thwaites with improvements by Curle [Ref. 9]:

$$g(K, \mu) = F_0(K) - \mu G_0(K) - 0.45 + 6K \quad 3.5$$

CMARC uses an empirical transition model based on the average pressure gradient,  $\bar{K}$ , for predicting laminar to turbulent transition. The following relations are used to calculate the transition point [Ref. 4]:

$$\bar{K} = \frac{\int_{\eta_{ins}}^{\eta} K d\eta}{\eta - \eta_{ins}} \quad 3.6$$

Where  $\eta_{ins}$  is the streamline coordinate at instability. And, K is the local pressure gradient at boundary layer instability [Ref. 4]:

$$\begin{aligned} K &= -0.4709 + 0.11066 * \ln(\text{Re}_\theta) + 0.0058591 * \ln^2(\text{Re}_\theta) & (0 \leq \text{Re}_\theta \leq 650) \\ K &= 0.69412 - 0.23992 * \ln(\text{Re}_\theta) + 0.0205 * \ln^2(\text{Re}_\theta) & (650 < \text{Re}_\theta \leq 10000) \end{aligned} \quad 3.7$$

The local Reynolds number at transition is correlated to  $\bar{K}$  with the following expressions [Ref. 4]:

$$\begin{aligned} \bar{K} &= -0.0925 + 0.00007 * \text{Re}_\theta & (0 \leq \text{Re}_\theta \leq 750) \\ \bar{K} &= -0.12571 + 0.000114286 * \text{Re}_\theta & (750 < \text{Re}_\theta \leq 1100) \\ \bar{K} &= 1.59381 - 0.45543 * \ln(\text{Re}_\theta) + 0.032534 * \ln^2(\text{Re}_\theta) & (1100 < \text{Re}_\theta \leq 3000) \end{aligned} \quad 3.8$$

At transition, the initial turbulent shape factor, H, is given by the following empirical formula that is a fit to data developed by Coles [Ref. 9]:

$$H = \frac{1.4754}{\log_{10}(\text{Re}_\theta)} + 0.9698 \quad 3.9$$

Provisions are made to check for turbulent reattachment if laminar separation is encountered. At laminar separation, a point calculation is made to determine if the boundary layer will reattach. If reattachment is predicted, the boundary layer code immediately switches to turbulent calculations. No attempt is made to model the laminar separation bubble or provide a transition length. After laminar separation is predicted, the following empirical relations are used to determine if reattachment occurs [Ref. 4]:

$$\begin{aligned}
 K &= 0.0227 - 0.007575 * Re_{\theta} - 0.000001157 * Re_{\theta}^2 & (Re_{\theta} \geq 125) \\
 K &= -0.09 & (Re_{\theta} < 125)
 \end{aligned}
 \tag{3.10}$$

The boundary layer code in CMARC uses a point transition model. No attempt is made to model a more representative transition length. Turbulent calculations begin at transition using the Nash-Hicks model [Ref. 4]. Calculations continue along the streamline until turbulent separation is predicted or the end of the streamline is reached. No boundary layer data is available after separation.

The authors of PMARC caveat that their boundary layer calculations are quite accurate for predominately 2D flow but break down in regions of large cross flow near separation. This premise will be first tested by comparing predominately 2D flow over the inboard region of a high aspect ratio wing to the finite difference calculations performed by the Naval Postgraduate School Unsteady Potential Flow Code (UPOT). Then a comparison is made to experimental data for flow over an inclined prolate spheroid. The 6:1 prolate spheroid is chosen because of the availability of extensive experimental data. In addition, three-dimensional flow around the prolate spheroid is similar to flow around a streamlined slender fuselage.



## IV. CMARC VERIFICATION

### A. VERIFICATION OF CMARC AGAINST PMARC

The first step in CMARC verification is comparison with NASA's PMARC panel code. CMARC is PMARC-12 rewritten in C from FORTRAN. Additionally, CMARC is compiled for hosting on an IBM compatible PC. Other than some added command line functionality and significant memory management improvements, the CMARC basic panel code and boundary layer routines are equivalent to PMARC and should produce the same results. However, due to the recent fielding of CMARC, the author felt it prudent to spot check the solutions to verify equivalency.

CMARC and PMARC were both fed an identical input file for a straight NACA 2415 wing with a 6.4 aspect ratio at 5 degrees angle of attack. The input file is listed in full in Appendix C. Figures 4.1 and 4.2 show CMARC and PMARC pressure coefficients cross-plotted for chordwise and spanwise wing stations respectively. The results overlay as an identical match. Figure 4.3 and 4.4 display the boundary layer calculations for skin friction coefficient and displacement thickness. Again the results overlay. Integrated forces and moment listings were also identical. From this, it is inferred that CMARC and PMARC produce equivalent results.

Although both programs produce equivalent results, it is worthy to note that there are occasionally small, insignificant differences in floating point calculations and rounding. Some results differ by a digit in the sixth decimal place. In addition, with identical input files, there can be a difference in convergence likelihood. Occasionally, PMARC failed to converge when CMARC did. Again, floating point differences are the most likely source of the disparity. Regardless, difference in the rates of convergence were slight and relatively transparent to the user. However, in all cases CMARC was better behaved with a higher likelihood of convergence. It is concluded that CMARC and PMARC results are interchangeable.

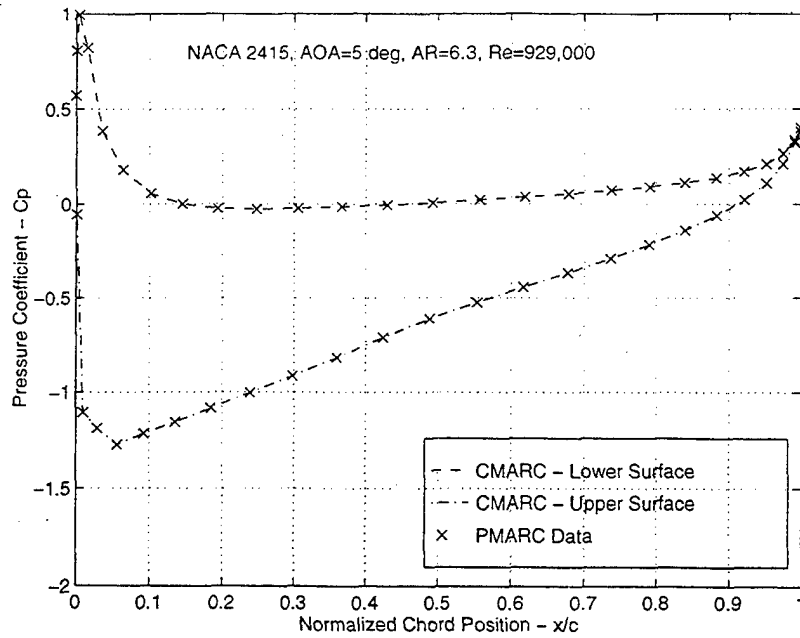


**Figure 4.1 Comparison of CMARC and PMARC Pressure Coefficients For a Chordwise Wing Station.**

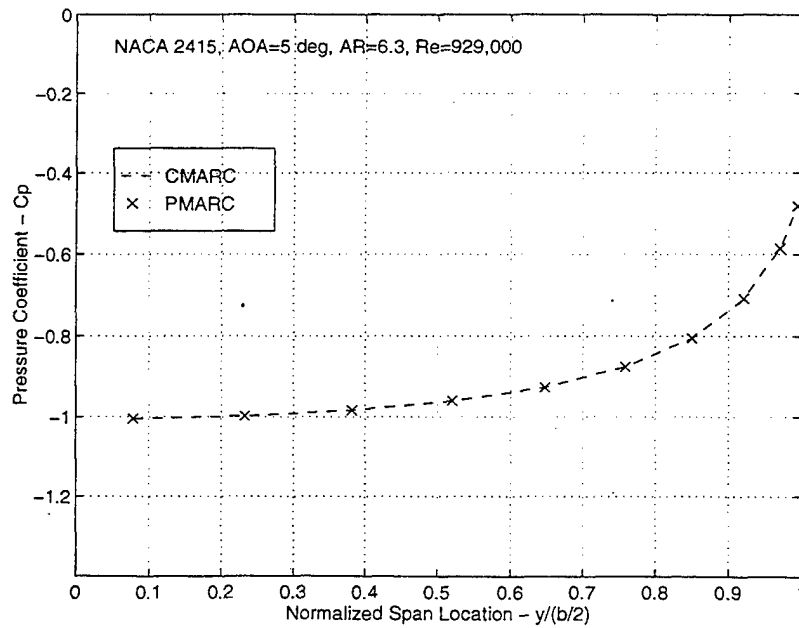


**Figure 4.2 Comparison of CMARC and PMARC Pressure Coefficients For a Spanwise Wing Station.**

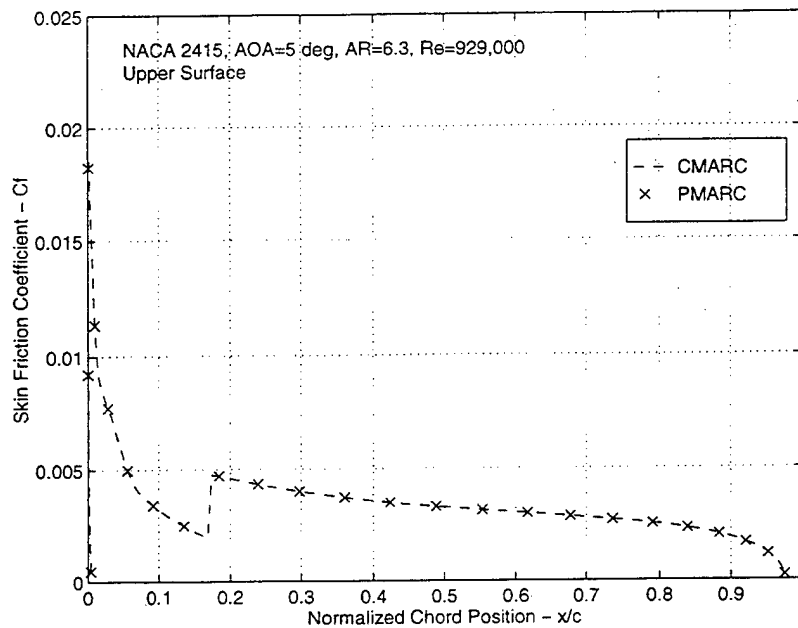


**Figure 4.3 Comparison of CMARC and PMARC Skin Friction Coefficient for an Upper Wing Surface Streamline.**

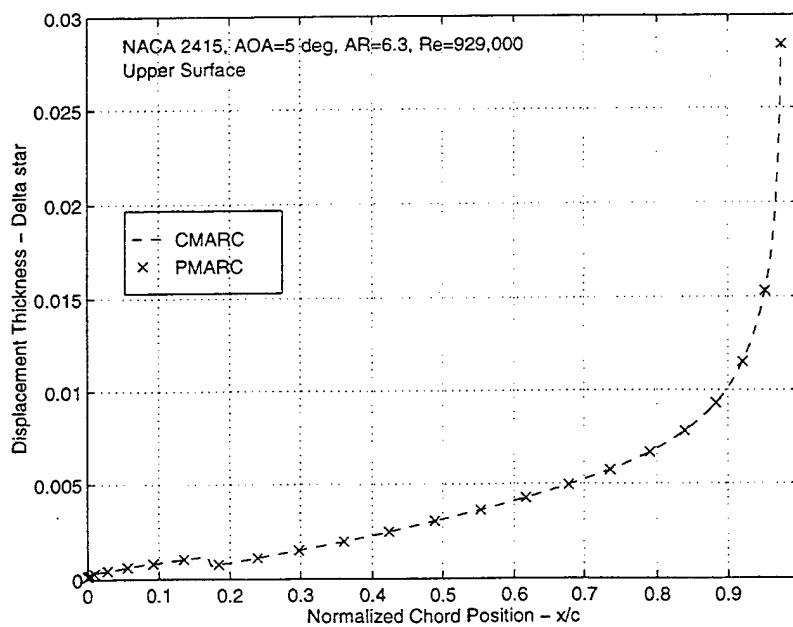


**Figure 4.4 Comparison of CMARC and PMARC Boundary Layer Displacement Thickness for an Upper Wing Surface Streamline.**

## B. COMPARISON OF CMARC AND PMARC PROCESSING TIMES

One of the primary metrics in determining suitability of a panel code hosted on an inexpensive PC is processing time. CMARC's processing speed should be within an order of magnitude of PMARC hosted on the NPS Aeronautics Department Silicon Graphics (SGI) workstations to be of much utility. To this end, processing times were compared for identical input models ranging from 200 to 1600 panels. Comparisons were performed between a 150 MHz/48 MB Pentium PC and two configurations of networked SGI Indigo<sup>2</sup> workstations. One workstation was the 150 MHz/64 MB Indigo<sup>2</sup> (Viper) running the IRIX 5.3 operating system and the other a 250 MHz/128 MB SGI Indigo<sup>2</sup> (Aurora) workstation running IRIX 6.2. With both workstations, file input/output is addressed through the network to the server.

Three versions of PMARC were tested. The first version, "pmarc12" located in the local/usr/bin, was compiled in FORTRAN to run on the older IRIX 5.3 operating system. The second version, "pmarc-inram," was compiled with Dynamic Linked Libraries (DLLs) to run on the new IRIX 6.2 operating system. These first two PMARC executable codes were compiled with the "in RAM" flag selected for matrix storage. This considerably reduced hard disk accessing time. PMARC either keeps all the matrices in RAM or all on the file server depending on whether the RAM flag is when compiled. Flexible memory management allows CMARC to fill available RAM and then automatically spill over to the hard drive. This reduces user memory management requirements.

A third version, "pmarc\_dll," was compiled with DLLs, but the matrix storage flag was inadvertently set to hard drive instead of RAM. Processing times were considerably longer with this option selected. It is not recommended unless the computer is RAM limited.

The input model used was a NACA 2415 finite wing with four time steps. The panel density was varied to obtain the desired panel count. Appendix D contains a representative input file.

The processing benchmarks showed that CMARC, hosted on a PC, is significantly faster than all three versions of PMARC hosted on the networked SGI workstations. Table 4.1 summarizes results for identical models ranging from 200 - 1600 panels.

Figure 4.5 is a plot of processing time vs. panel count for models ranging from 200 to 1600 panels. For small sized models, all configurations are relatively close to the



same speed. As the model size increases, processing time increases roughly as the square of model size. However, as model size increases, all versions of PMARC on the networked SGI workstations become significantly slower than CMARC on the PC. This is most likely due to the slower file read/write access times to the file server. The version of PMARC with the matrix storage flag set to hard drive required considerably more processing time than the two versions with RAM selected.

Platform CPU / RAM Program	Pentium PC 150 MHz / 48 MB	SGI Indigo <sup>2</sup> 150 MHz / 64 MB		SGI Indigo <sup>2</sup> 250 MHz / 128 MB	
	CMARC	PMARC	PMARC-DLL	PMARC	PMARC-DLL
Panel Count	min:sec	min:sec	min:sec	min:sec	min:sec
200	0:11	0:12	0:15	N/A	0:13
400	0:27	0:43	0:53	N/A	0:29
800	1:29	2:46	3:10	N/A	1:51
1600	5:54	9:31	17:30	N/A	10:04

**Table 4.1 CMARC and PMARC Processing Times for Models Ranging from 200 to 1600 Panels.**

It is important to note that the models compared in this study only differed in panel count. Panel count is not the only factor in determining processing time. The number of time steps selected, solution resolution, convergence rate and boundary layer calculations will all impact processing speed. As a result, the times presented should only be viewed as representative of the relative impact of panel density and not as the time required to process any other model geometry.

In conclusion, CMARC hosted on a dedicated 150 MHz Pentium PC is significantly faster than PMARC hosted on a similar or faster networked SGI workstation. In some cases, over twice as fast. Clearly, executing the CMARC panel code on the PC is a suitable alternative to running PMARC on the SGI workstations. Low cost 200-300 MHz Pentium II PCs are now available which will allow further reductions in CMARC processing times.

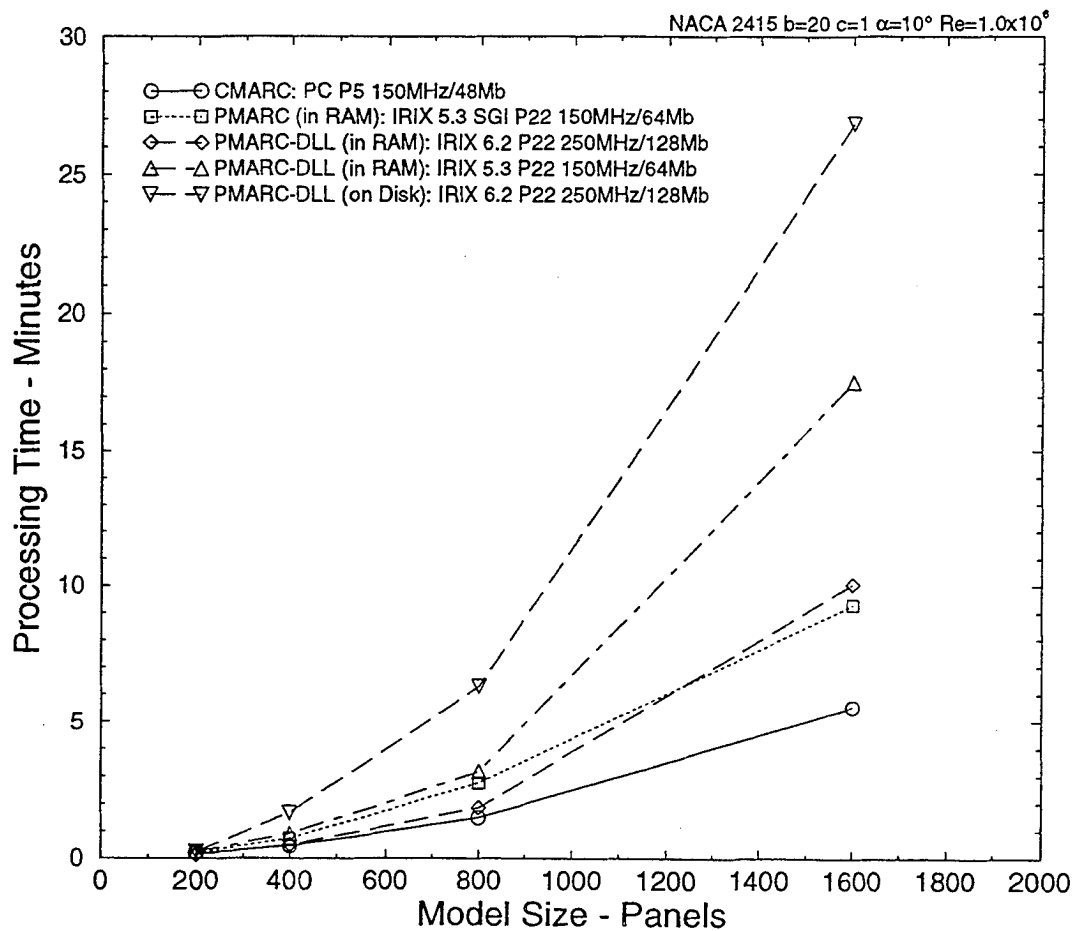


**Figure 4.5 Comparison of CMARC and PMARC Processing Times for Similar Finite Wing Models Ranging from 200 to 1600 Panels.**

## **C. COMPARISON OF CMARC TO THE UPOT BOUNDARY LAYER CODE**

As a first step in investigating CMARC boundary layer calculations and utility, CMARC results are compared to 2D calculations from the NPS Unsteady Potential Flow Code (UPOT). Although the potential flow solution used by CMARC for the boundary layer calculations is strictly a 3D solution, 2D flow can be approximated with the proper choice of geometry. In this case, flow over the inboard portion of a high aspect ratio (AR) wing is selected. A straight NACA 2415 wing with  $AR=20$  is chosen for the comparison. The NACA 2415 is the same section used in the FROG UAV. Boundary layer transition and separation points are compared at angles-of-attack ranging from 0 to 20 degrees. In addition, boundary layer solution sensitivity is investigated over four Reynolds numbers ranging from  $5.0 \times 10^5$  to  $6.0 \times 10^6$ .

### **1. UPOT Boundary Layer Calculations**

The NPS UPOT panel code was developed as a tool to assist in unsteady flow visualization over two-dimensional airfoils. It features an excellent interactive graphical user interface and rapid modeling capabilities [Ref. 10]. Unlike the integral momentum equations used by CMARC and PMARC, UPOT implements the Cebeci-Keller finite difference boundary layer code. The algorithm is documented by Nowak [Ref. 11]. The UPOT code has been compared to experimental data for a range of airfoils with favorable results. As such, it is considered to be acceptable to benchmark CMARC results.

### **2. High AR Wing Model**

A high aspect ratio NACA 2415 wing is modeled to evaluate the boundary layer over the inboard section to approximate 2D flow. CMARC's built-in modeling capability was used to generate a finite wing with dimensions of 20 ft wingspan (b) and unit chord (c) yielding an aspect ratio of 20. Fifty chordwise panels are distributed over the top and bottom surface in a full cosine distribution and 10 panel sections in a spanwise direction with half cosine distribution. There are 600 panels total, including the enclosed wing tip, over the semi-span. Figure 4.6 displays a semi-planform view of this configuration. Streamlines are placed on the upper and lower surfaces of the inboard root panels. The root area is chosen as the area where the flow is nearly two-dimensional flow.

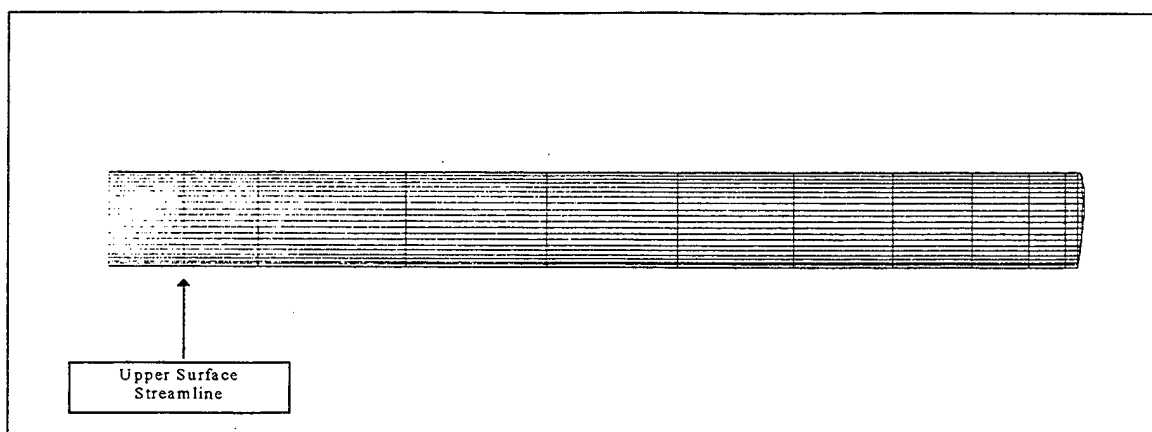


**Figure 4.6 Semi-Span of Finite Wing for the Approximation of Two-Dimensional Flow Near the Root (AR=20). 50 Chordwise x 10 Spanwise Panels.**

### **3. Boundary Layer Results and Analysis (CMARC vs. UPOT)**

CMARC and UPOT boundary layer calculations are compared for the FROG UAV NACA 2415 airfoil. Two angles-of-attack were chosen for comparison. The first,  $-2^\circ$  or zero lift, is used to compare transition models. The second angle-of-attack,  $10^\circ$  is selected for comparison to the  $10^\circ$  incidence of the inclined spheroid discussed in a later section. A comparison for Reynolds numbers ranging from  $0.5 \times 10^6$  to  $6.0 \times 10^6$  is also performed at  $10^\circ$  to investigate boundary layer calculation sensitivity to Reynolds number. In addition, boundary layer transition and separation locations are compared at angles-of-attack ranging from  $0^\circ$  to  $20^\circ$  at  $Re = 1.0 \times 10^6$ .

#### ***a. Boundary Layer Transition***

The shortcomings of the point boundary layer transition model coded in CMARC is evident when compared to the more sophisticated transition length model implemented in UPOT. UPOT uses the Michel transition onset and the Chen-Thyson transition length models [Ref. 11]. Figures 4.7 through 4.14 display skin friction coefficient as a function of chordwise location ( $x/c$ ) for the upper and lower surfaces of a NACA 2415 airfoil. Results for four Reynolds numbers ranging from  $0.5 \times 10^6$  to  $6.0 \times 10^6$  are plotted at zero lift ( $-2^\circ$ ) and  $10^\circ$  angle-of-attack. Boundary layer transition will be

discussed first, followed by boundary layer separation. Finally, differences in modeling at the stagnation point will be discussed.

In almost all cases, CMARC predicts an early transition. The transition from laminar to turbulent boundary layer occurs in CMARC as a sudden jump or point transition. The UPOT transition length model provides for a more realistic representation of the boundary layer physics. Combined, early and point transition result in higher total skin friction drag predicted by CMARC. The difference is most pronounced at the lower Reynolds numbers associated with the FROG UAV. At  $Re=0.5 \times 10^6$  and zero lift, CMARC overpredicts skin friction drag by approximately 40% on the upper surface and 20% on the lower surface. Although skin friction drag may be a relatively small portion of the total drag, airframe manufacturers go to great lengths to refine models to accurately predict it. A few percentage points of error can cause the aircraft to meet or miss performance goals.

Despite the differences in transition modeling, CMARC accurately predicts the skin friction coefficient with respect to UPOT. When comparing laminar to laminar and turbulent to turbulent regions in Figures 4.7 through 4.10 (zero lift plots), the skin friction coefficients are a close match. This indicates that an adjustment in the CMARC model delaying transition could provide more accurate results.

As another comparison of boundary layer calculations, displacement thickness ( $\delta^*$ ) is displayed in Figures 4.15 through 4.22 as a function of chord position ( $x/c$ ) for zero lift ( $-2^\circ$ ) and  $10^\circ$  angle-of-attack. In general, CMARC and UPOT predict similar trends in  $\delta^*$ . The final displacement thickness is a good relative indication of total skin friction drag. CMARC always predicts a greater  $\delta^*$  and thus more drag. This is in keeping with the previous observations indicating higher integrated skin friction forces.

### ***b. Separation***

Boundary layer separation is indicated in Figures 4.7 through 4.14 by a zero or negative skin friction coefficient. In all cases, CMARC slightly overpredicts the extent of attached flow. Again, the differences are most significant at the lower Reynolds numbers.

Figures 4.23 and 4.24 display transition and separation points for the NACA 2415 as a function of angles-of-attack ranging from  $0^\circ$  to  $20^\circ$ . The data is for  $Re=1.0 \times 10^6$  which is close to the FROG UAV high speed cruise at  $Re=929,000$ . On both

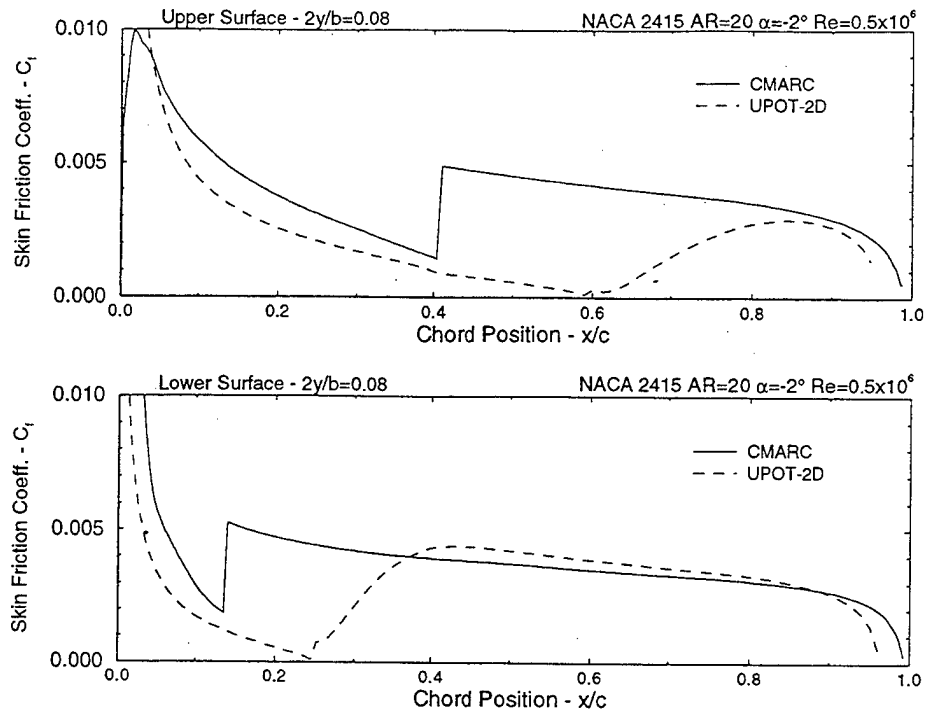


**Figure 4.7 Comparison of CMARC and UPOT Skin Friction Coefficient ( $C_f$ ) for NACA 2415 at zero lift ( $\alpha=-2^\circ$ ) and  $Re=0.5 \times 10^6$ .**

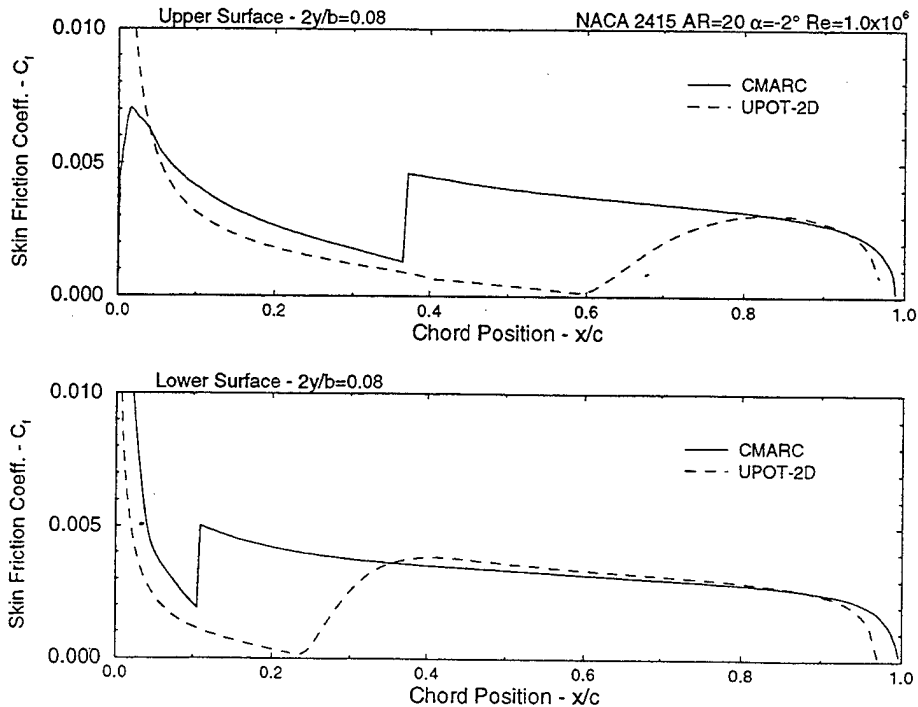


**Figure 4.8 Comparison of CMARC and UPOT Skin Friction Coefficient ( $C_f$ ) for NACA 2415 at zero lift ( $\alpha=-2^\circ$ ) and  $Re=1.0 \times 10^6$ .**

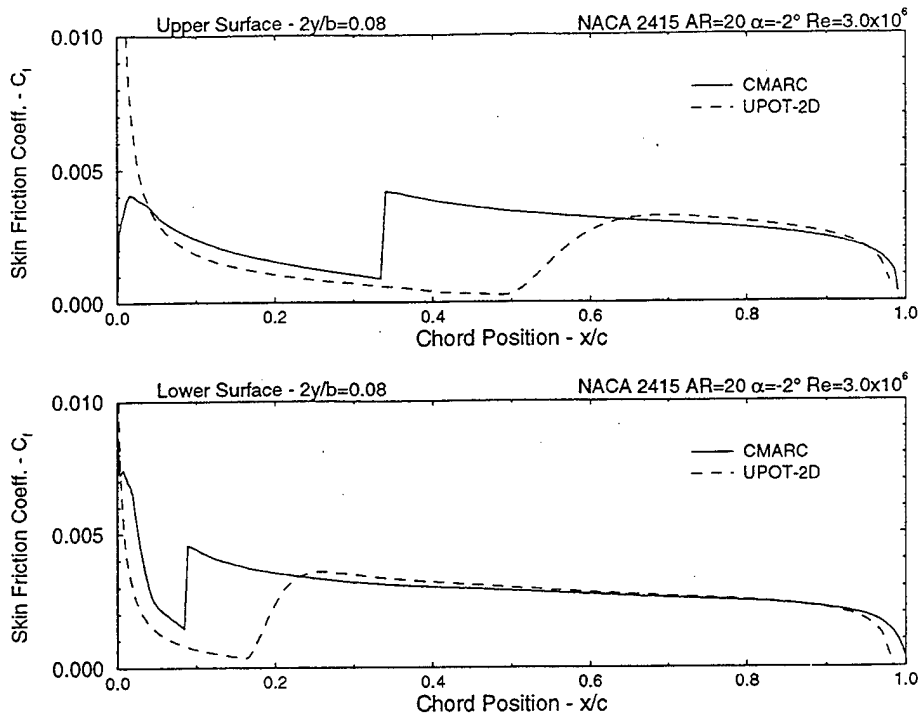


**Figure 4.9 Comparison of CMARC and UPOT Skin Friction Coefficient ( $C_f$ ) for NACA 2415 at zero lift ( $\alpha=-2^\circ$ ) and  $Re=3.0 \times 10^6$ .**

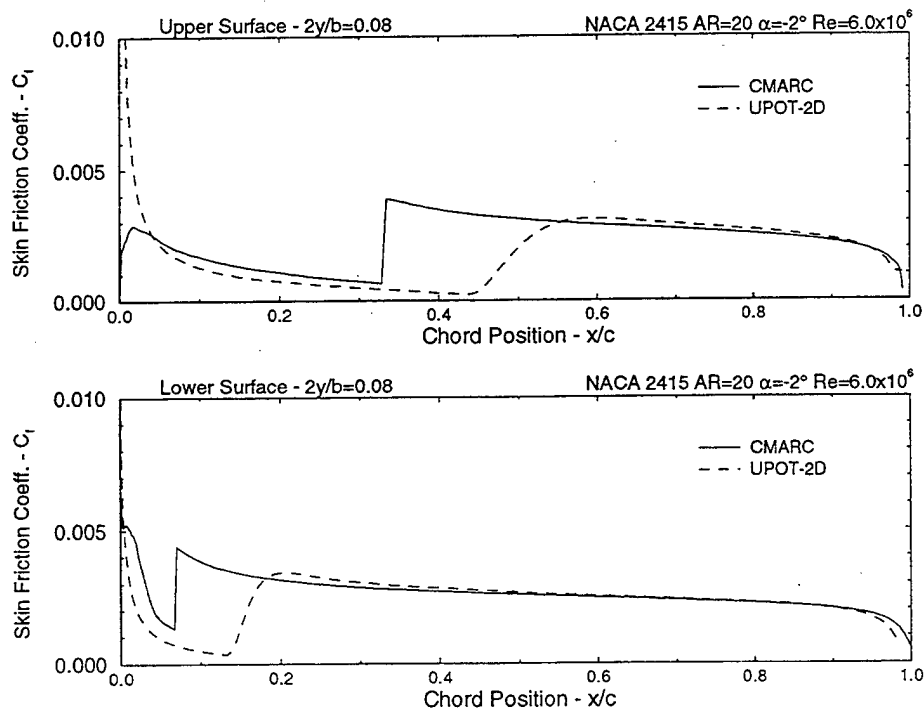


**Figure 4.10 Comparison of CMARC and UPOT Skin Friction Coefficient ( $C_f$ ) for NACA 2415 at zero lift ( $\alpha=-2^\circ$ ) and  $Re=6.0 \times 10^6$ .**

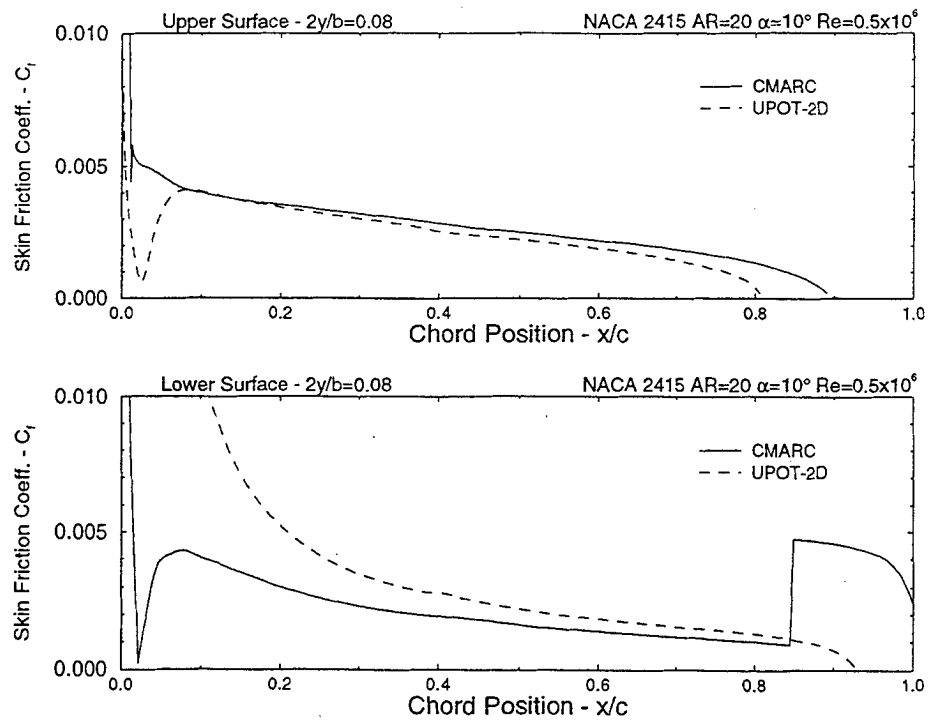


**Figure 4.11 Comparison of CMARC and UPOT Skin Friction Coefficient ( $C_f$ ) for NACA 2415 at  $\alpha=10^\circ$  and  $Re=0.5 \times 10^6$ .**

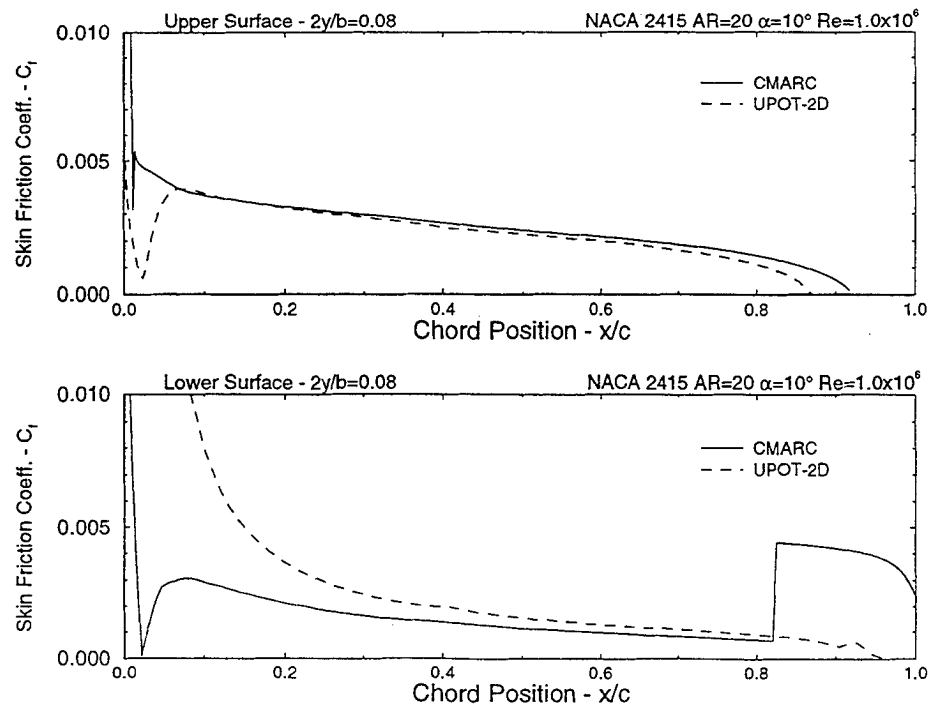


**Figure 4.12 Comparison of CMARC and UPOT Skin Friction Coefficient ( $C_f$ ) for NACA 2415 at  $\alpha=10^\circ$  and  $Re=1.0 \times 10^6$ .**



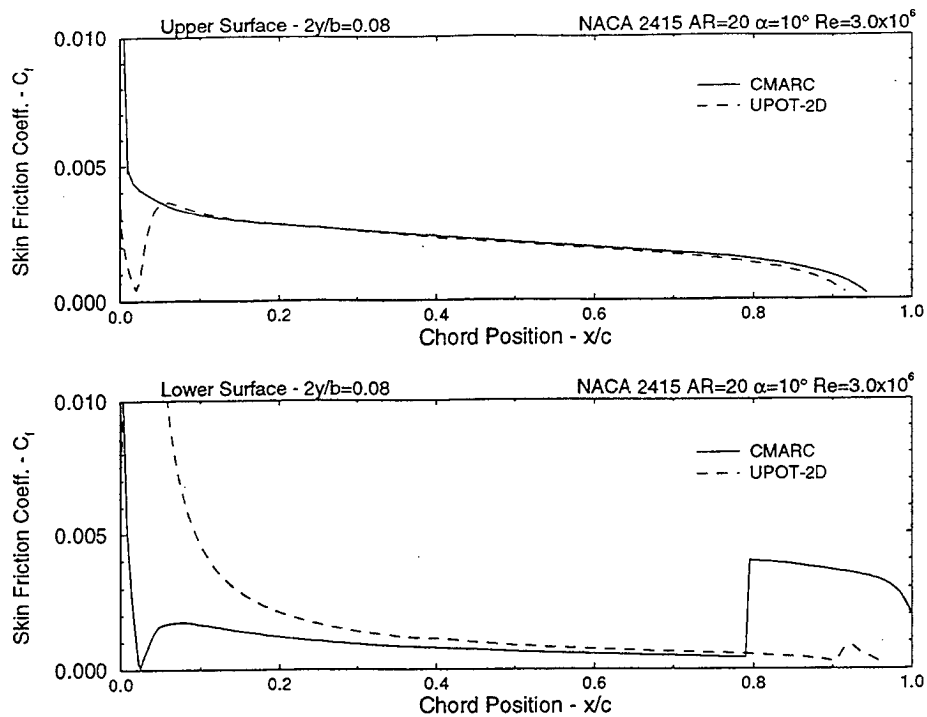


**Figure 4.13 Comparison of CMARC and UPOT Skin Friction Coefficient ( $C_f$ ) for NACA 2415 at  $\alpha=10^\circ$  and  $Re=3.0 \times 10^6$ .**

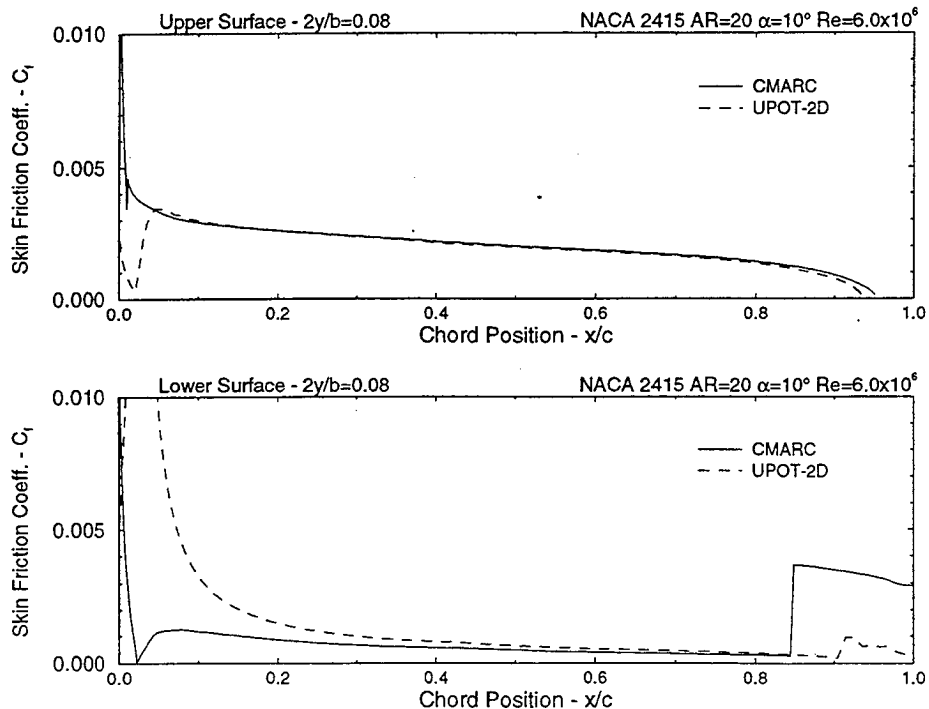


**Figure 4.14 Comparison of CMARC and UPOT Skin Friction Coefficient ( $C_f$ ) for NACA 2415 at  $\alpha=10^\circ$  and  $Re=6.0 \times 10^6$ .**

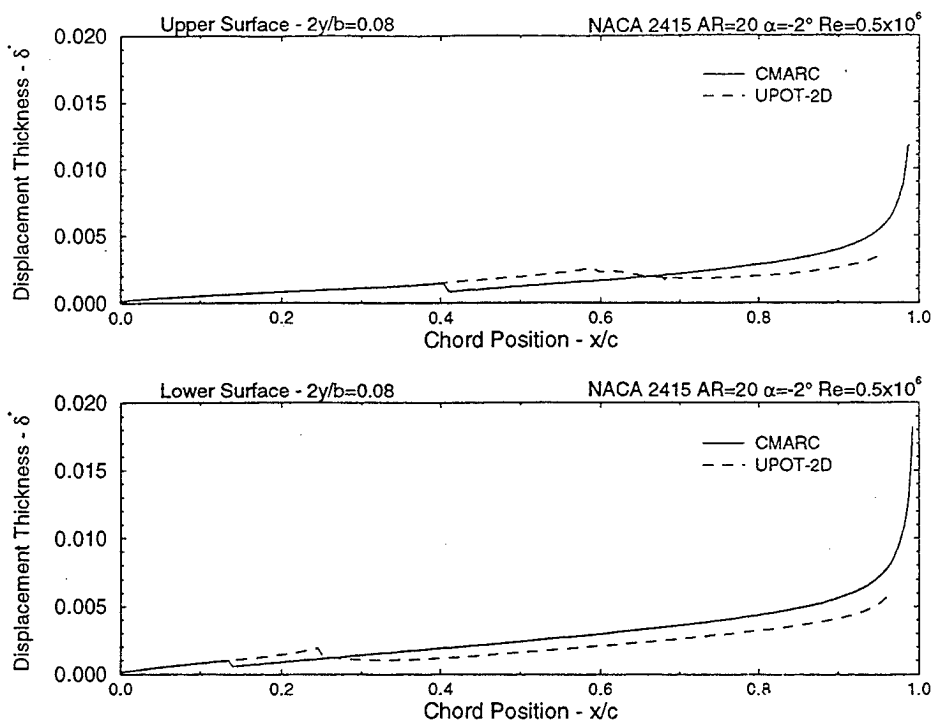


**Figure 4.15 Comparison of CMARC and UPOT Boundary Layer Displacement Thickness ( $\delta^*$ ) for NACA 2415 at zero lift ( $\alpha=-2^\circ$ ) and  $Re=0.5 \times 10^6$ .**

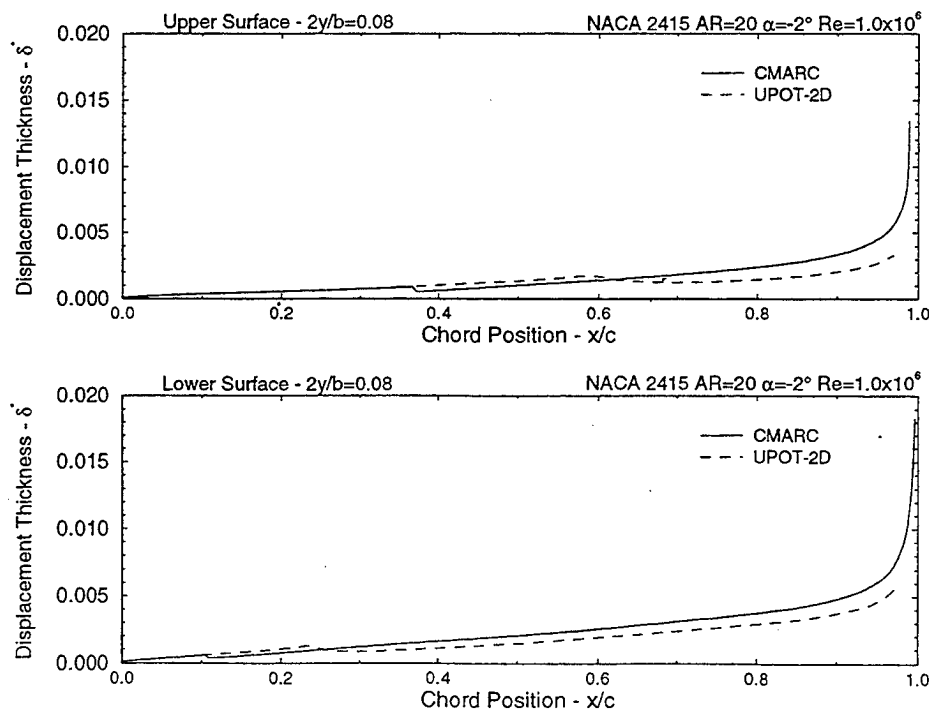


**Figure 4.16 Comparison of CMARC and UPOT Boundary Layer Displacement Thickness ( $\delta^*$ ) for NACA 2415 at zero lift ( $\alpha=-2^\circ$ ) and  $Re=1.0 \times 10^6$ .**

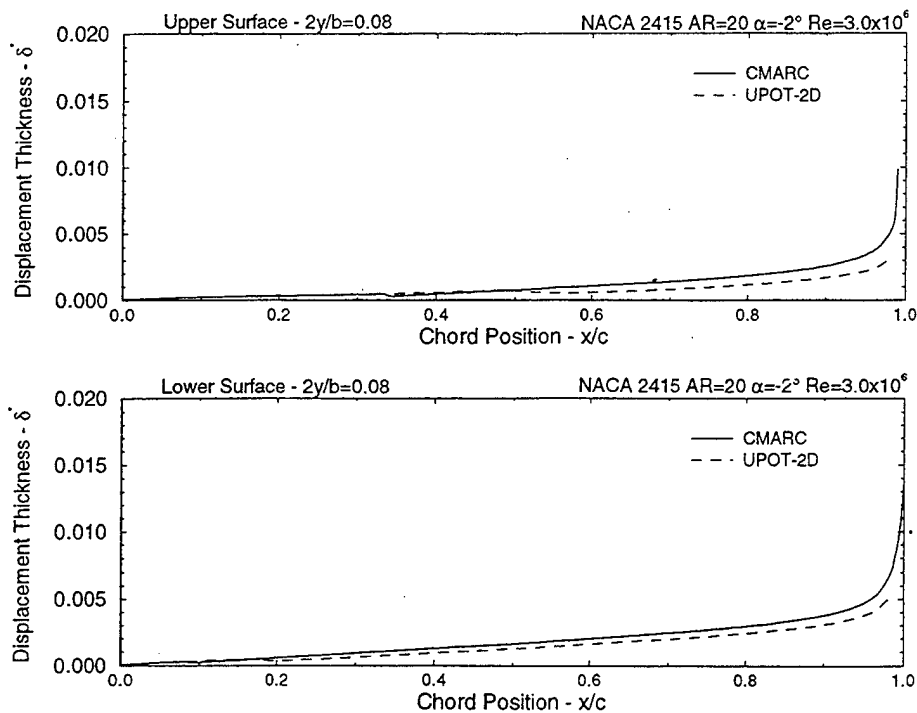


**Figure 4.17 Comparison of CMARC and UPOT Boundary Layer Displacement Thickness ( $\delta^*$ ) for NACA 2415 at zero lift ( $\alpha=-2^\circ$ ) and  $Re=3.0 \times 10^6$ .**

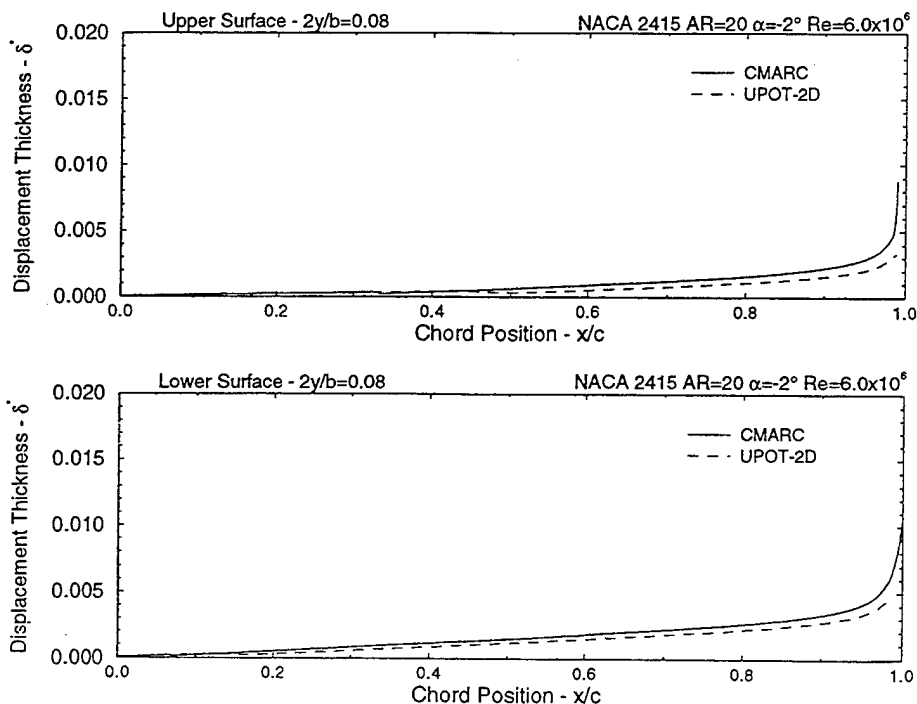


**Figure 4.18 Comparison of CMARC and UPOT Boundary Layer Displacement Thickness ( $\delta^*$ ) for NACA 2415 at zero lift ( $\alpha=-2^\circ$ ) and  $Re=6.0 \times 10^6$ .**

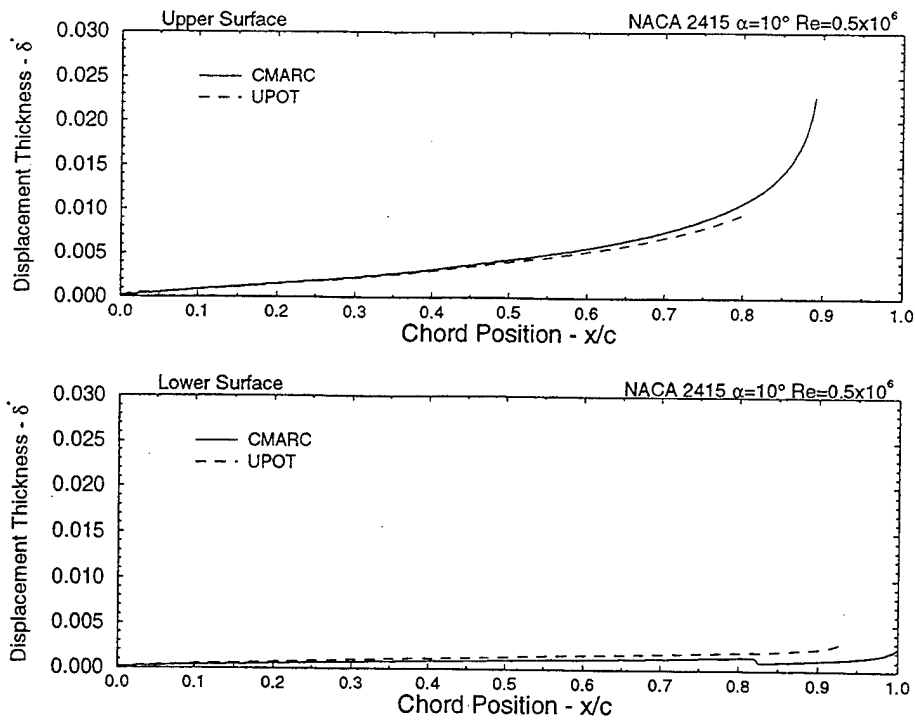


**Figure 4.19 Comparison of CMARC and UPOT Boundary Layer Displacement Thickness ( $\delta^*$ ) for NACA 2415 at  $\alpha=10^\circ$  and  $Re=0.5 \times 10^6$ .**

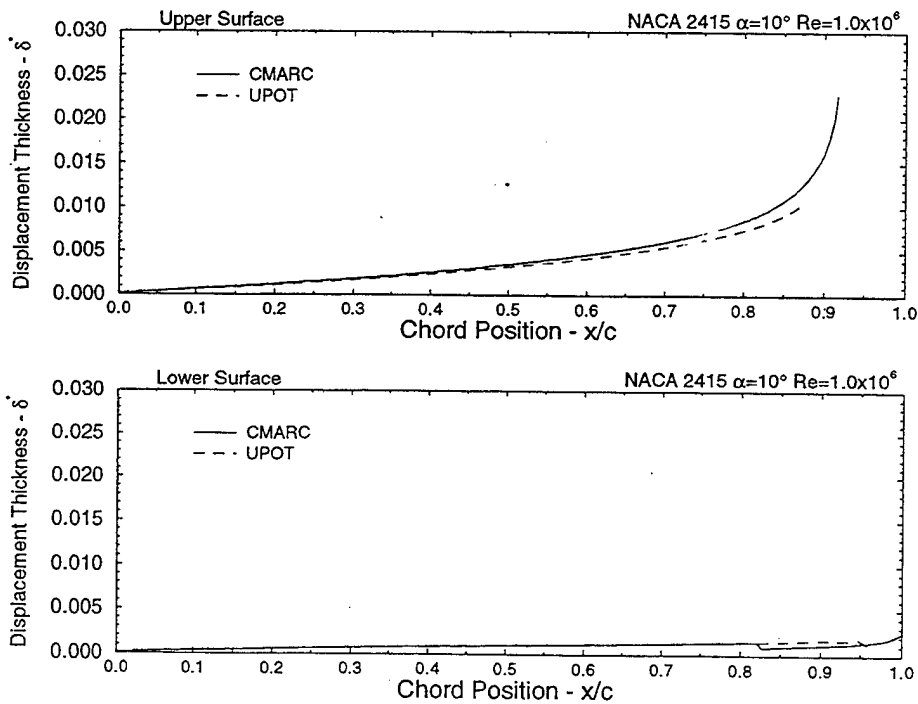


**Figure 4.20 Comparison of CMARC and UPOT Boundary Layer Displacement Thickness ( $\delta^*$ ) for NACA 2415 at  $\alpha=10^\circ$  and  $Re=1.0 \times 10^6$ .**

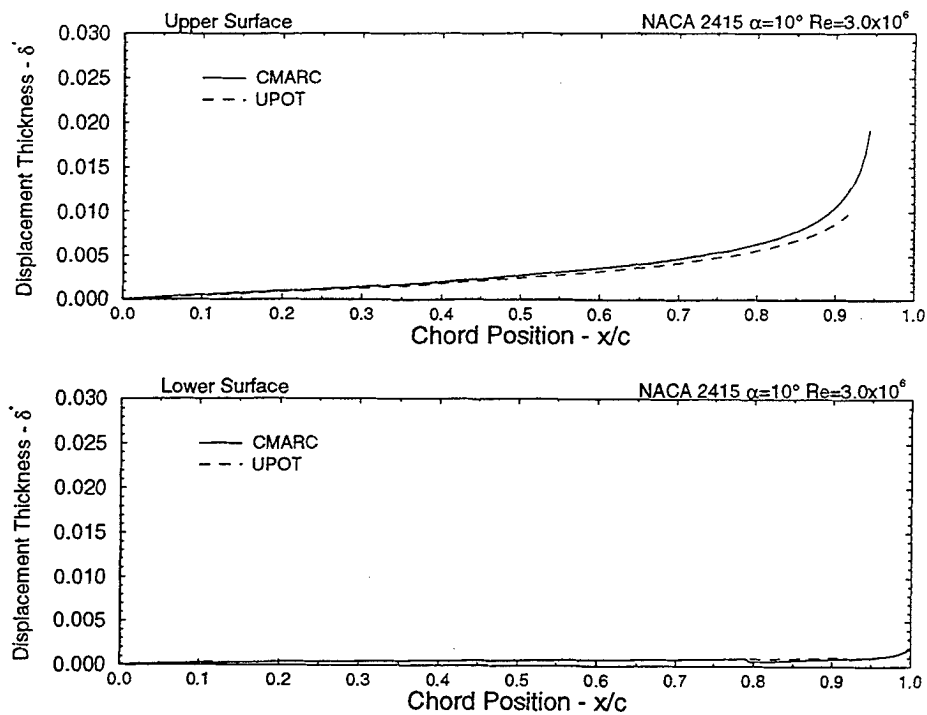


**Figure 4.21 Comparison of CMARC and UPOT Boundary Layer Displacement Thickness ( $\delta^*$ ) for NACA 2415 at  $\alpha=10^\circ$  and  $Re=3.0 \times 10^6$ .**

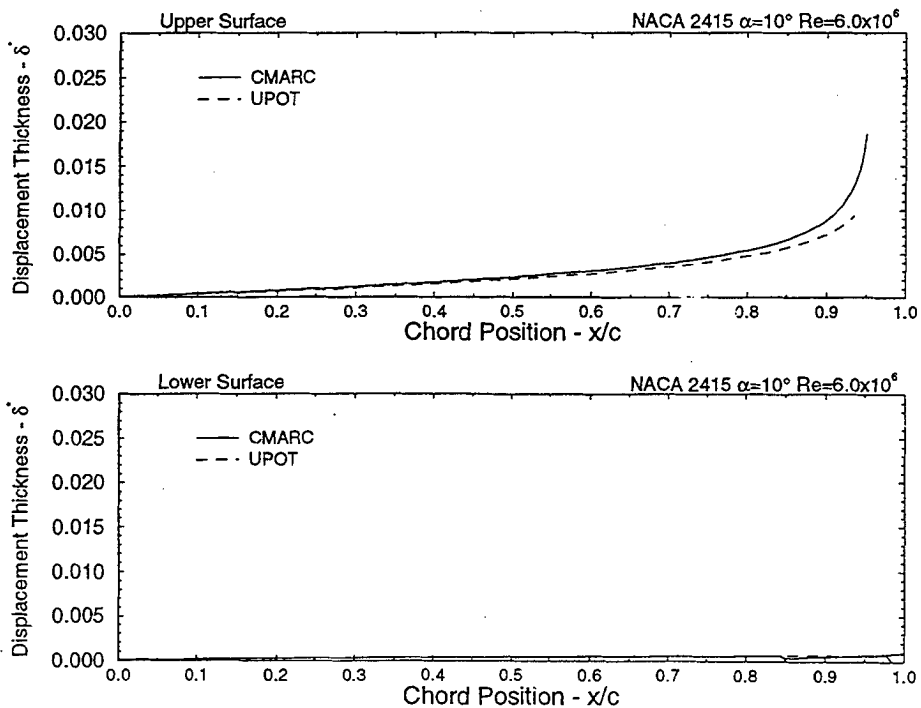


**Figure 4.22 Comparison of CMARC and UPOT Boundary Layer Displacement Thickness ( $\delta^*$ ) for NACA 2415 at  $\alpha=10^\circ$  and  $Re=6.0 \times 10^6$ .**

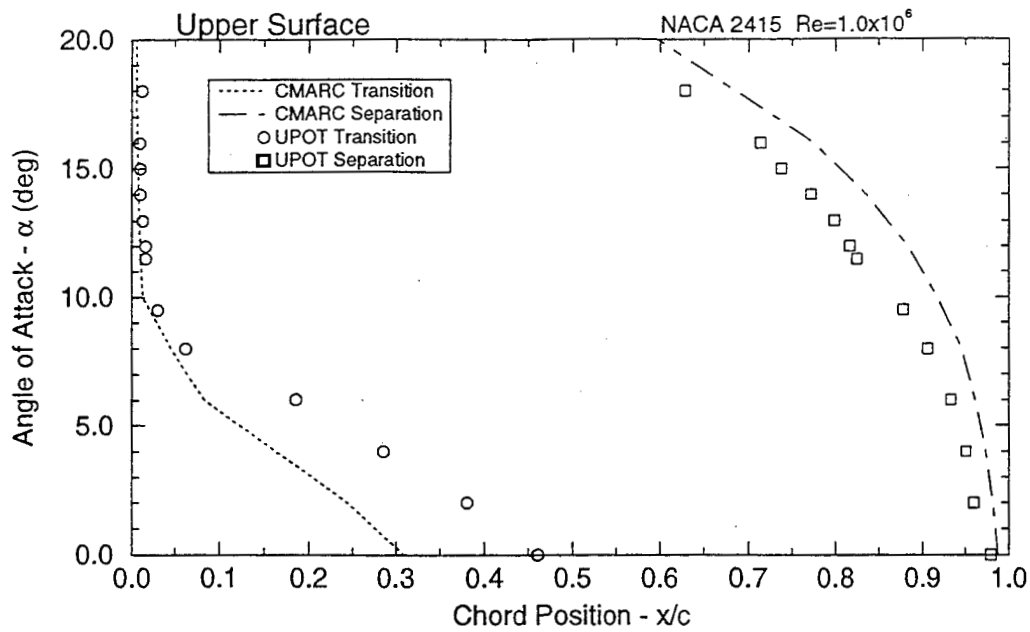


**Figure 4.23** Comparison of CMARC and UPOT Boundary Layer Transition and Separation Points for the Upper Surface of a NACA 2415 Airfoil at  $Re=1.0 \times 10^6$  from  $0^\circ$  to  $20^\circ$  AOA.

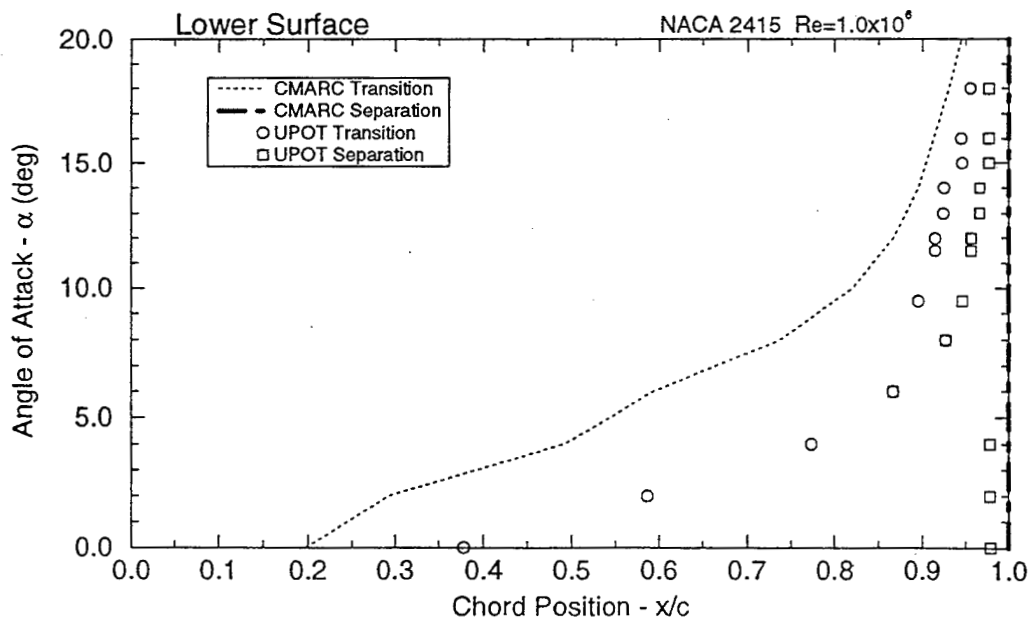


**Figure 4.24** Comparison of CMARC and UPOT Boundary Layer Transition and Separation Points for the Lower Surface of a NACA 2415 Airfoil at  $Re=1.0 \times 10^6$  from  $0^\circ$  to  $20^\circ$  AOA.

the upper and lower surface, CMARC clearly provides correct trends for both the transition and separation points. However, as seen at zero lift in Figures 4.7 through 4.10, CMARC always predicts an early transition and late separation.

Despite the inaccuracies in transition and separation points, CMARC boundary layer calculations remain useful. A low order panel code is unlikely going to be used for performance calculations. Instead, it is more useful as a design tool. It allows for rapidly visualizing the trend in transition and separation points with minor changes in configuration.

A word of caution is advised when total skin friction drag is integrated. A design change could be implemented that reduces overall skin friction drag but neglects large increases in pressure drag. In other words, one could reduce skin friction drag, but fail to realize earlier separation is taking place. The net result is a small reduction in skin friction drag that is more than offset by a large increase in separation pressure drag. Extending the extent of attached flow should always be considered preferable to reducing overall integrated skin friction drag.

#### *c. Skin Friction Coefficient near the Stagnation Point*

Another major difference between the integral boundary layer code in CMARC and the finite difference code in UPOT is highlighted at the stagnation point. In Figure 4.11, both codes locate the stagnation point on the lower surface at  $x/c=0.025$  for the NACA 2415 airfoil at 10 degrees angle-of-attack. However, it is clear that the CMARC skin friction coefficient starts at 0.0002, a small number approaching zero asymptotically, while the UPOT skin friction shoots out of the top of the chart in excess 0.7, a relatively large number approaching  $+\infty$  asymptotically.

From boundary layer theory, it is known that the skin friction coefficient is inversely proportional to the square root of the local Reynolds number or:

$$C_f = \frac{1}{\sqrt{Re_x}} \quad 4.1$$

At the stagnation point,  $C_f$  approaches  $+\infty$ . The finite difference code in UPOT correctly models this trend. On the other hand, CMARC implements a discrete

integration of the following exact differential laminar skin friction calculation:

$$\theta(\eta)^2 = \frac{0.45\nu}{U(\eta)^6} \int_0^\eta (1 + 2.222g(K, \mu))U(\eta)^5 d\eta + \theta(0)^2 \left( \frac{U(0)}{U(\mu)} \right)^6 \quad 4.2$$

Where:            U - velocity at outer edge of boundary layer  
                       θ - momentum thickness  
                       g - empirical parameter  
                        $K = \frac{\theta^2}{\nu} \frac{dU}{d\eta}$   
                       η - generalized coordinate along a streamline

At η=0, the momentum thickness starts at zero and builds rapidly from the stagnation point. Thus, the momentum integral equation reduces to:

$$\frac{d\theta}{d\eta} = \frac{1}{2} C_f = 0, \text{ at the stagnation point.} \quad 4.3$$

The integral solution for  $C_f$  starts at zero and rises quickly until the integral portion of Equation 4.2 dominates.

The incorrect modeling of  $C_f$  near the stagnation point is considered minor due to its local nature at the stagnation point. When skin friction is integrated over the entire surface the differences are bound to be relatively small. In addition, when integrated into a force, the errors in  $C_f$  at the stagnation point tend to cancel out. Close to the stagnation point on either side, skin friction forces are opposite in direction.

#### **D. COMPARISON OF CMARC TO INCLINED PROLATE SPHEROID EXPERIMENTAL DATA**

In the previous section, model geometry was selected to produce predominantly two-dimensional flow. In this section, CMARC pressure distributions and integral



boundary layer data are investigated for a model geometry that produces largely three-dimensional flow. For comparison, a suitable experimental test case was found in AGARD AR-303: A Selection of Experimental Test Cases for the Validation of CFD Codes [Ref. 12]. Case number C-2, entitled "Three-Dimensional Boundary Layer and Flow Field Data of an Inclined Prolate Spheroid" was selected. A 6:1 prolate spheroid approximates a typical streamlined fuselage. The data set was ordered from AGARD through the NASA Center for Aerospace Information (CASI).

A complete data set for all test cases in AGARD AR-303 was available for a nominal charge of \$59.00 through NASA's CASI publications office. Ordering information inside the rear cover of the publication proved to be accurate and useful. The data arrived on nine PC formatted high density disks. After copying the desired data sets to the hard drive, each file is self extracting through a built-in DOS decompression program. Detailed instructions are printed in the back section of AR-303.

#### **1. Inclined 6:1 Prolate Spheroid - AGARD AR-303 Case C-2**

AGARD AR-303 test case number C-2 contains pressure coefficient and skin friction distributions for a 6:1 prolate spheroid inclined to the flow field. Table 4.2 lists the test conditions for which data are available.

Test case I was chosen for comparison to CMARC output. At  $10^\circ$  angle-of-attack, some separated flow was expected which would provide a good comparison to CMARC integral boundary layer separation points. The only drawback to this test case is the forced transition at  $X/2a = 0.20$ . Natural transition would have been more desirable for comparison to the CMARC transition model. The test cases at  $30^\circ$  angle-of-attack are deemed to have too much separated flow to provide a meaningful comparison to a CMARC potential flow solution.

##### ***a. Wind Tunnel Experimental Set-up***

Figure 4.25 contains a diagram of the experimental set-up for the 6:1 prolate spheroid performed by Kreplin in the DLR Göttingen three meter Low Speed Wind Tunnel (NWG). Of note, the wind tunnel test section is of the Göttingen type with closed return and open test section. No corrections are applied to the data.

PARAMETER	CASE I	CASE II	CASE III
Mach Number	0.16	0.13	0.23
Reynolds Number	$7.7 \times 10^6$	$6.5 \times 10^6$	$43.0 \times 10^6$
Incidence	$10.0^\circ$	$29.7^\circ$	$30.0^\circ$
Transition	tripped at $X/2a = 0.20$	free	free

**Table 4.2 AGARD AR-303 Test Conditions, from Ref. [12].**

Figure 4.26 shows the configuration for the 6:1 prolate spheroid wind tunnel model. The 2.4 meter long model contains 42 pressure taps located along an axial meridian. The model can be rotated axially in 50 steps through just over 180 degrees providing in excess of 2000 pressure readings over half the surface. With yaw angle set to zero, symmetry is assumed for the other half. In addition to pressure ports, surface hot film sensors are located at 12 axial positions for the measurement of wall shear stress. Wall shear stress is normalized by dynamic pressure to provide skin friction coefficient ( $C_f$ ). Once again, the measurements are provided for approximately 50 rotation angles, providing coverage of half the surface.

In addition to pressure and skin friction coefficients, boundary layer velocity profiles and flow field mean velocity vectors are available at several axial locations. Although not used in this investigation, the data would prove useful for more detailed studies.

Unfortunately, the wind tunnel set-up was not instrumented for loads. As will be discussed in the next section, the number of pressure and skin friction measurements was deemed to be sufficient to allow the integration of local forces to provide a reasonable calculation of lift, drag and pitching moments.

#### ***b. Experimental Data***

Two data files from test case C-2 at  $\alpha = 10.0^\circ$  are used for comparison to CMARC data. The first file, "cp10nwg.dat," contains pressure coefficient listed as a function of axial location ( $X/2a$ ) and circumferential angle ( $\phi$ ). For each circumferential

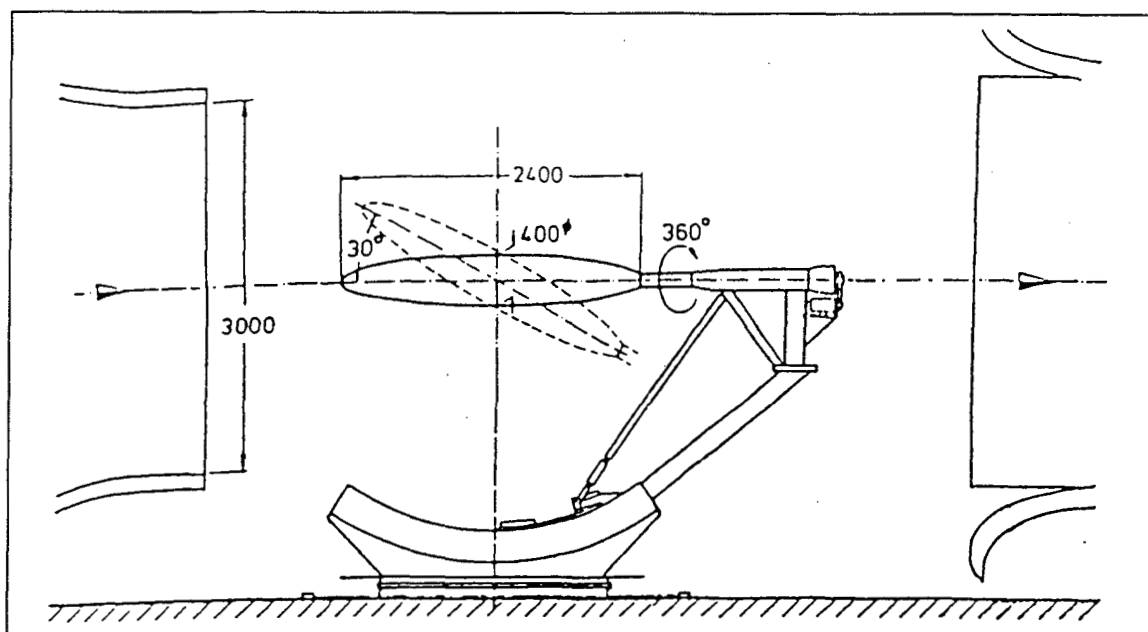


**Figure 4.25** Inclined 6:1 Prolate Spheroid Model in the DLR Göttingen Three Meter Low Speed Wind Tunnel (NWG) , from Ref. [12].

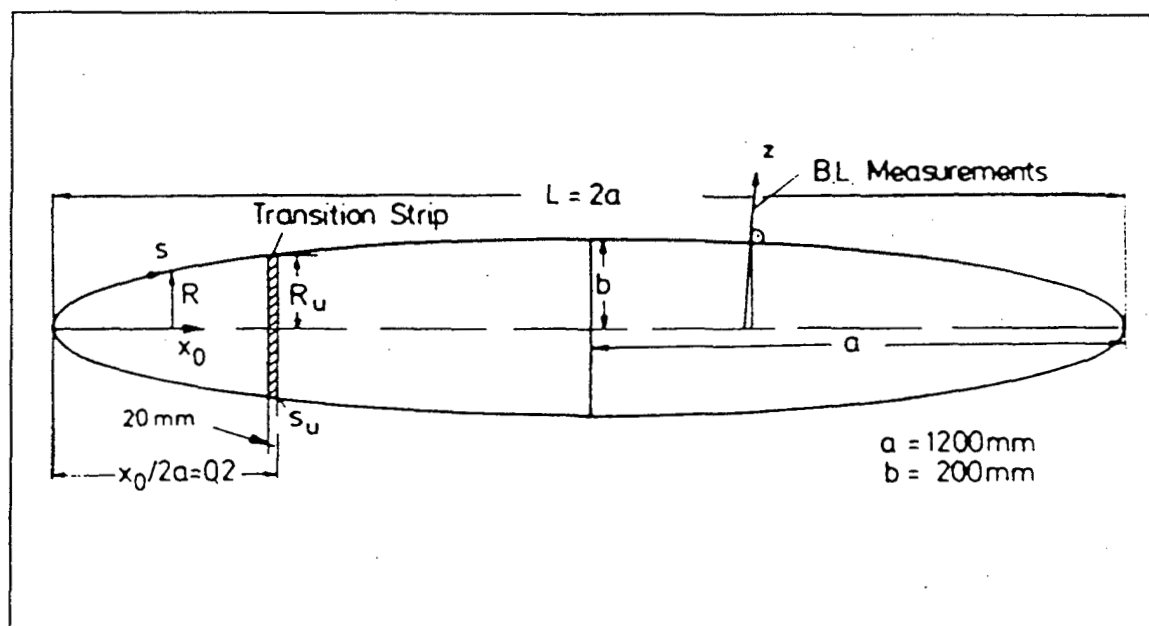


**Figure 4.26** Prolate Spheroid Wind Tunnel Model Configuration, from Ref. [12].

angle all the successive axial location pressure coefficients were listed. It is more common to plot pressure distribution as a function of circumferential angle at a given axial station. The data file was rearranged using the MATLAB M-file listed in Appendix E.

The second data file, "cf10nwg.dat," contains skin friction listed as a function of axial location ( $X/2a$ ) and circumferential angle ( $\phi$ ). The data, listed in two columns, were reordered to one column for ease of plotting.

### c. *Integration of Local Forces to Provide Lift Drag and Pitching Moment*

The experimental set-up did not include balance measurement of forces. However, it was deemed that the 2000+ pressure and 500+ skin friction measurements would be sufficient to allow the integration of measurements over the surface of the prolate spheroid for an approximation of total force and moment coefficients. The following equations were developed to provide integrated pressure and friction force coefficients. Symmetry is assumed. Appendix B outlines the development of these relations. Appendix C lists the MATLAB program which implements the discrete integration.

The pressure force coefficients normalized by  $S = \pi b^2$  and  $\bar{c} = 2b$  are yielded by discretely integrating the following equations in a cylindrical coordinate system:

$$C_{N_P} = \frac{N_P}{q_\infty S}, \quad N_P = 2 \sum_{i=1}^m \sum_{j=1}^n - (q_\infty C_P r \bar{n}) \cdot \bar{k} \Delta \phi_j \Delta x_i / 2a \quad 4.3$$

$$C_{A_P} = \frac{A_P}{q_\infty S}, \quad A_P = 2 \sum_{i=1}^m \sum_{j=1}^n - (q_\infty C_P r \bar{n}) \cdot \bar{i} \Delta \phi_j \Delta x_i / 2a \quad 4.4$$

$$C_{M_P} = \frac{M_P}{q_\infty S \bar{c}}, \quad M_P = 2 \sum_{i=1}^m \sum_{j=1}^n \left[ (q_\infty C_P r \bar{n}) \cdot (x_i / 2a \cdot \bar{k} - z_i / 2a \cdot \bar{i}) \right] \Delta \phi_j \Delta x_i / 2a \quad 4.5$$

Where the surface unit normal is given by:

$$\text{Unit Normal: } \bar{n} = -\frac{m}{\sqrt{m^2 + 1}} \bar{i} + \frac{\sin(\phi)}{\sqrt{m^2 + 1}} \bar{j} - \frac{\cos(\phi)}{\sqrt{m^2 + 1}} \bar{k} \quad 4.6$$

The skin friction coefficients normalized by  $S = \pi b^2$  and  $\bar{c} = 2b$  are yielded by discretely integrating the following equations in a cylindrical coordinate system:

$$C_{N_{SF}} = \frac{N_{SF}}{q_{\infty} S}, \quad N_{SF} = 2 \sum_{i=1}^m \sum_{j=1}^n (q_{\infty} C_f r \bar{v}) \cdot \bar{k} \Delta \phi_j \Delta x_i / 2a \quad 4.7$$

$$C_{A_{SF}} = \frac{A_{SF}}{q_{\infty} S}, \quad A_{SF} = 2 \sum_{i=1}^m \sum_{j=1}^n (q_{\infty} C_f r \bar{v}) \cdot \bar{i} \Delta \phi_j \Delta x_i / 2a \quad 4.8$$

$$C_{M_{SF}} = \frac{M_{SF}}{q_{\infty} S \bar{c}}, \quad M_{SF} = 2 \sum_{i=1}^m \sum_{j=1}^n \left[ (q_{\infty} C_f r \bar{v}) \cdot \left( -x_i / 2a \cdot \bar{k} + z_i / 2a \cdot \bar{i} \right) \right] \Delta \phi_j \Delta x_i / 2a \quad 4.9$$

Where the unit surface velocity vector is given by:

$$\bar{v} = \frac{\cos(\gamma)}{\sqrt{m^2 + 1}} \bar{i} + \left[ \frac{m \sin(\phi) \cos(\gamma)}{\sqrt{m^2 + 1}} + \cos(\phi) \sin(\gamma) \right] \bar{j} + \left[ -\frac{m \cos(\phi) \cos(\gamma)}{\sqrt{m^2 + 1}} + \sin(\phi) \sin(\gamma) \right] \bar{k} \quad 4.10$$

The surface and local slope of a prolate spheroid comes from the following relations:

$$\text{Prolate Spheroid: } \frac{x^2}{a^2} + \frac{r^2}{b^2} = 1 \quad \Rightarrow \quad \text{slope } m = \frac{dr}{dx} = -\frac{bx}{a^2 \sqrt{1 - \frac{x^2}{a^2}}} \quad 4.11$$

Note: The forces are summed over half the spheroid,  $\phi = 0 \rightarrow 180^\circ$ , and doubled.

The y-direction forces and the roll and yaw moments are neglected zero due to symmetry.

## 2. CMARC Model of 6:1 Prolate Spheroid

A 40x20 panel model of the 2.4 meter 6:1 prolate spheroid wind tunnel model was created with LOFTSMAN. The right half surface was modeled with symmetry around the  $y=0$  plane. Appendix F contains a printout of the LOFTSMAN input file which includes a fore/aft wake. The patch was created with 40 axial and 20 semi-circumferential panels. Full cosine compression was used to bunch panels at the leading and trailing edge.

After creating the patch in LOFTSMAN, it was decided that a doubling of circumferential panel count would increase wake placement flexibility. The CMARC input file was modified to create 40 circumferential panels by setting TNPC=40 in the break point input field for each cross section.

Figure 4.27 is a POSTMARC rendering of the final 1600 (40x40) panel configuration. The input file takes advantage of the plane of symmetry capability built into CMARC. It calculates just half a model symmetric around the  $y=0$  plane of symmetry provided there is zero side slip.

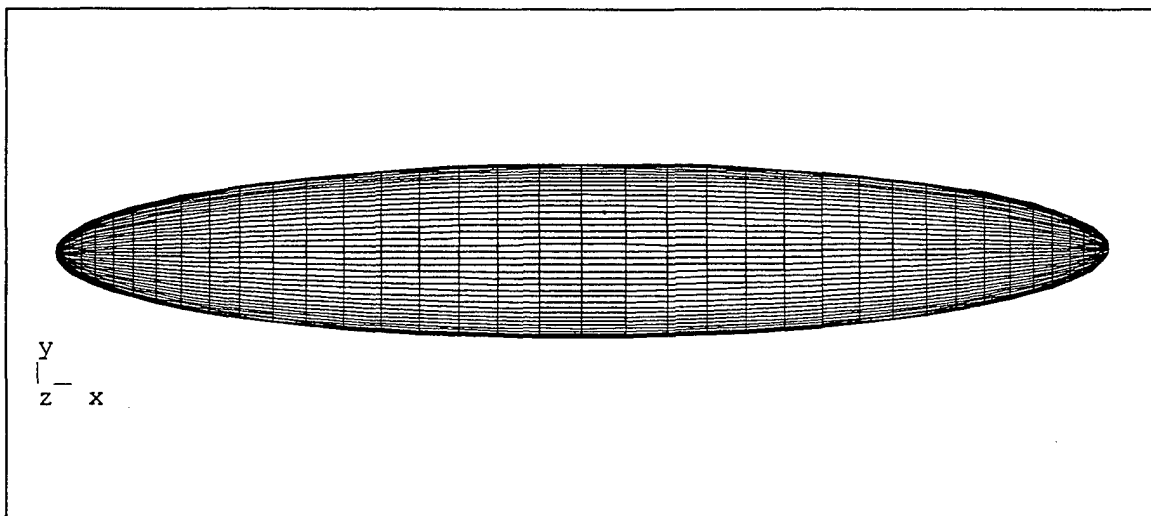


**Figure 4.27 CMARC 40x40 Prolate Spheroid Model Rendered with POSTMARC.**

### **3. Data Extraction**

Pressure coefficient data are extracted using the "postprolate.exe" FORTRAN file listed in Appendix G. This program extracts data from a CMARC or PMARC output file (DATA6) for a range of panel numbers and places them in a separate plot input file. CMARC output files are transferred to the SGI workstations for data extraction using the Windows 3.1 FTP program. Results are then plotted against experimental data with any x-y plotting program (xmgr).

#### 4. Prolate Spheroid Pressure Distribution

CMARC and experimental pressure coefficients are compared at 10 degrees angle-of-attack and  $Re=7.7 \times 10^6$ . Results are displayed as a function of axial station,  $x/2a$ , and circumferential angle,  $\phi$ , in Figure 4.28. Circumferential angle is measured starting from the lower centerline of the model. CMARC generated potential flow pressure coefficients over the forward 60% of the prolate spheroid closely match experimental results. Of note, there is a constant bias between the two sets of data.

The divergence between CMARC and experimental results aft of  $x/2a=0.60$  indicates flow separation over the top portion of the prolate spheroid. It is clear that a potential flow solution without wakes does a poor job of predicting pressure distribution over regions with separated flow.

To model the flow separation, wakes were added to the CMARC model. Tuncer and Platzer's research [Ref. 7] indicates that proper wake placement can produce a close match between panel code and experimental results for slender bodies of revolution for angles-of-attack up to 20 degrees. They concluded that a circumferential wake placement angle of 144 degrees on an ogive cylinder body provides the closest match for force and moment coefficients.

A series of wakes were placed at several circumferential angles ranging from 117 to 162 degrees. The wakes run fore-aft from  $x/2a=0.50$  to a wake separation ring at  $x/2a=0.99$ . Results are plotted in Figure 4.29. A wake angle of 117 degrees produced the closest average match to the experimental results. Figure 4.30 shows the final wake configuration.

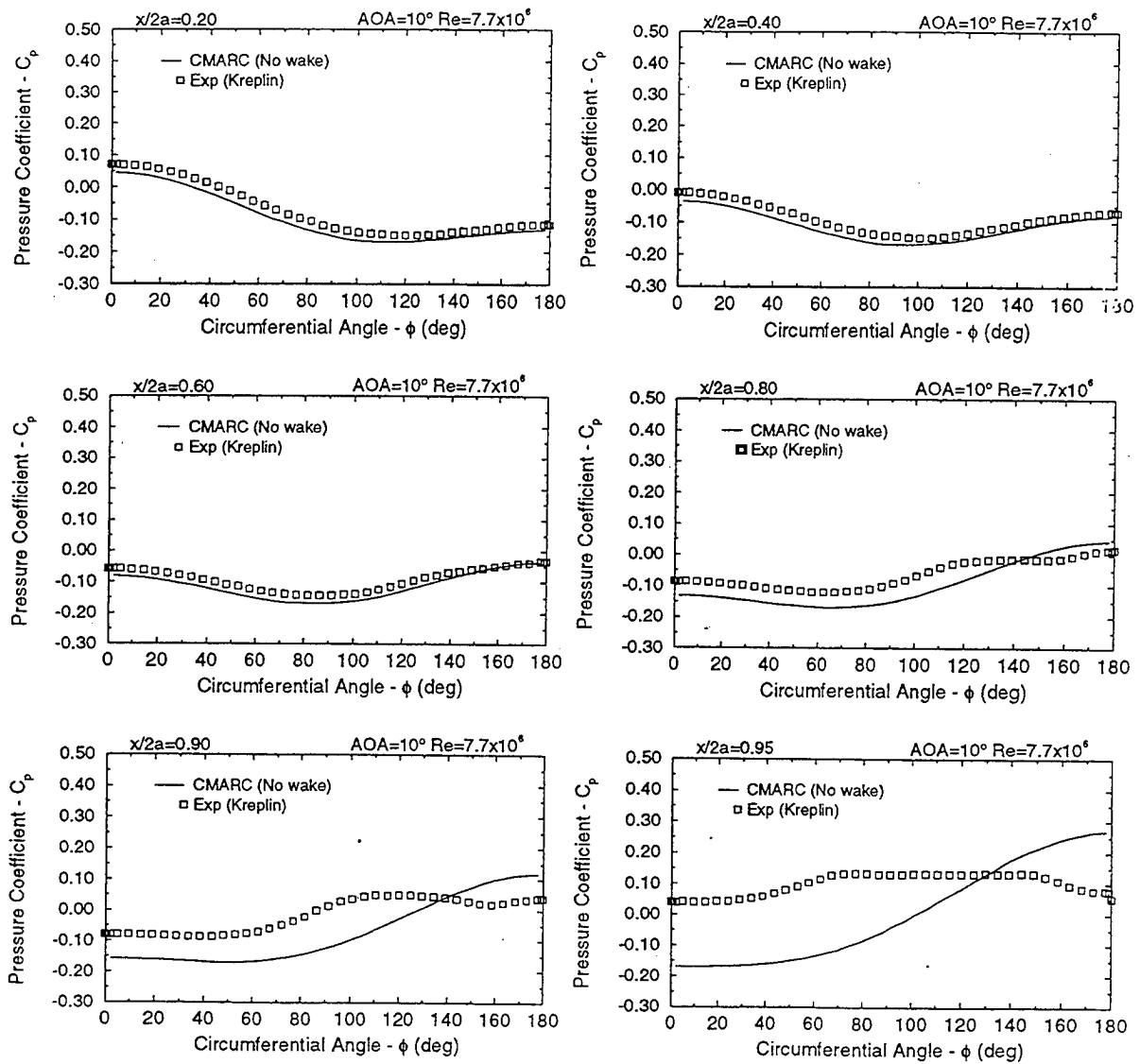


**Figure 4.28 CMARC Potential Flow (No Wakes) Pressure Distribution Compared to Experimental Data, after Ref. [12].**



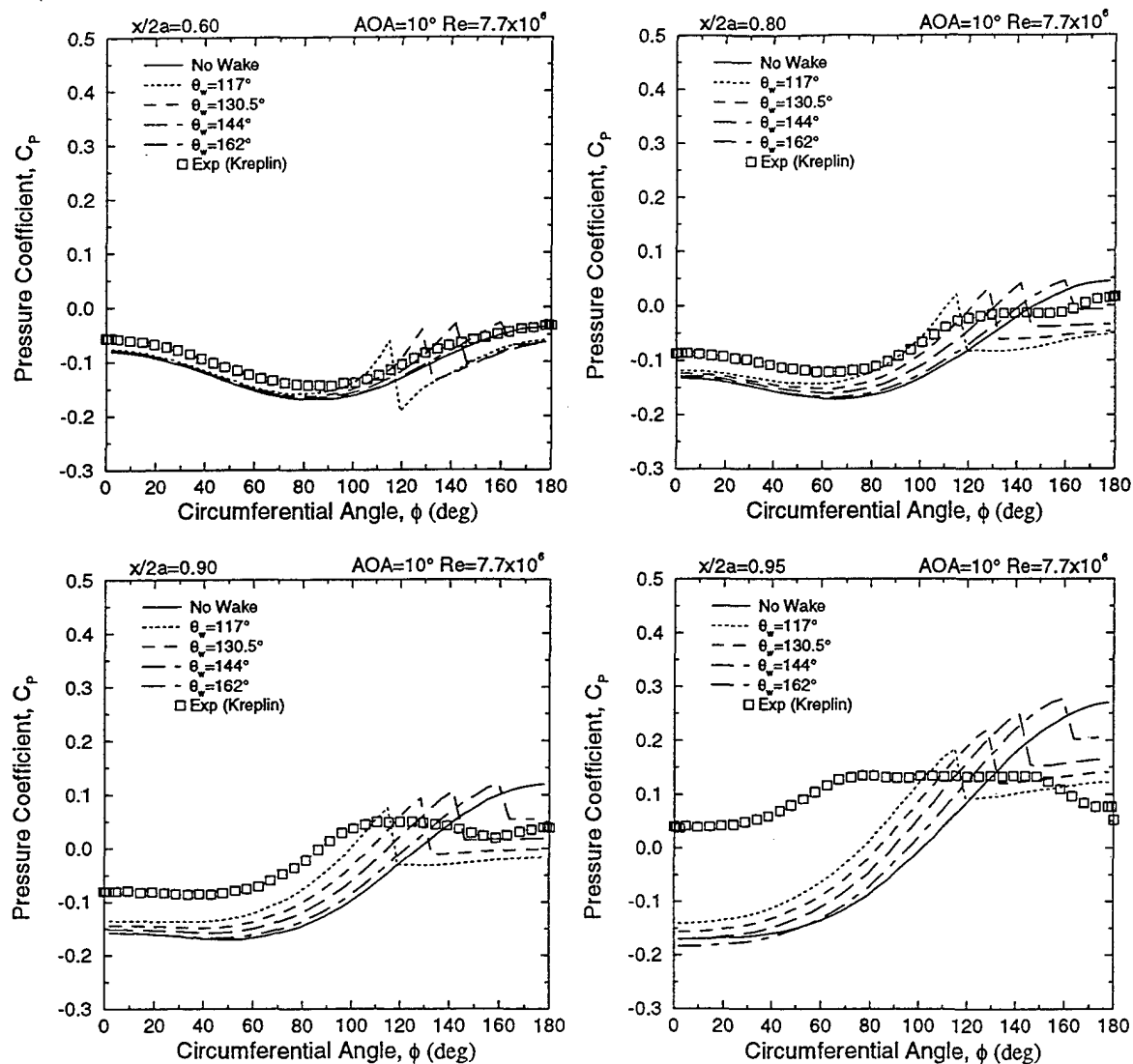


**Figure 4.29 CMARC Pressure Distribution with Wake Angles Ranging from  $117^\circ$  to  $162^\circ$  Compared to Experimental Data, after Ref. [12].**

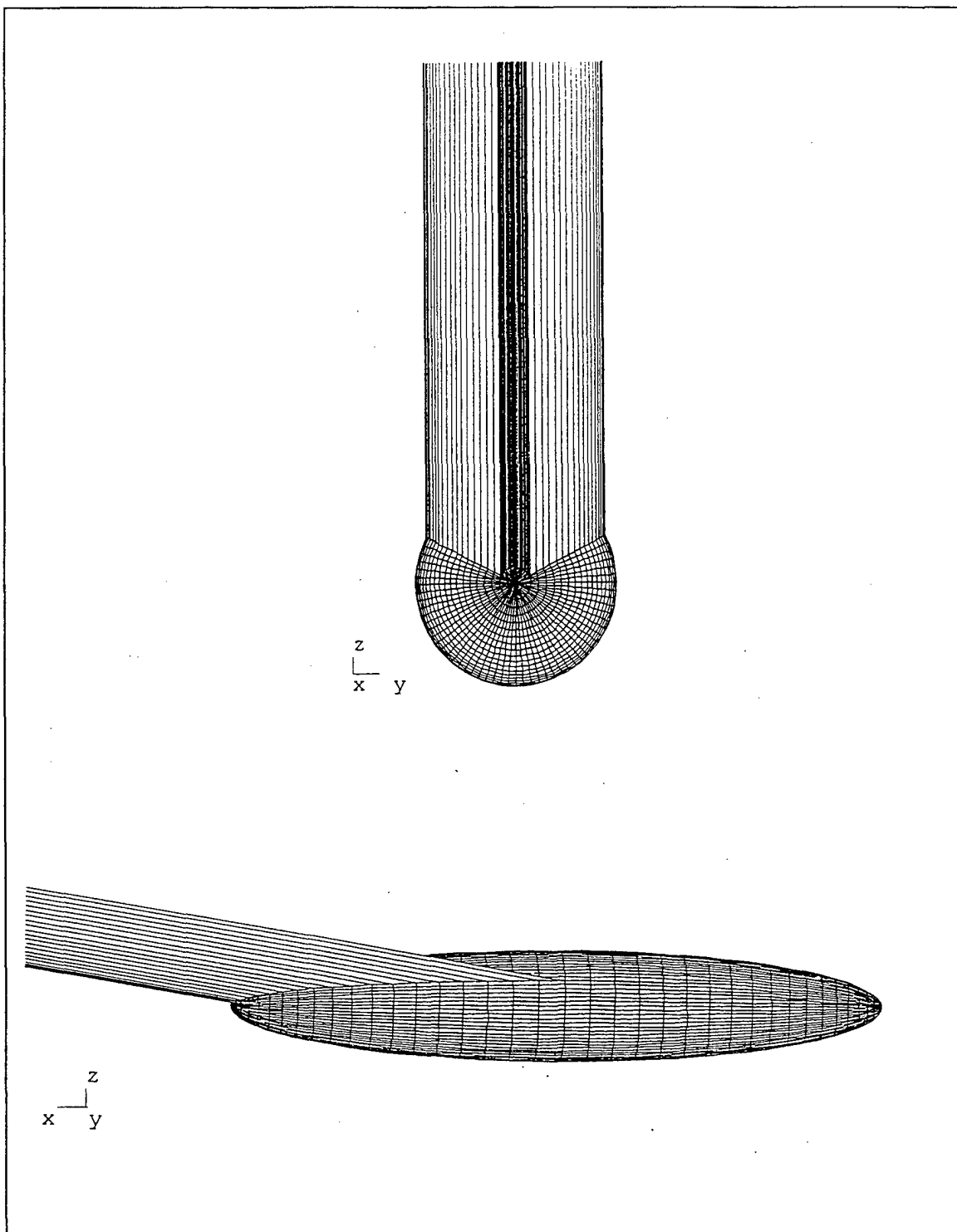


**Figure 4.30 POSTMARC Views of CMARC Model with 117° Wake Separation  
Line Running Aft from  $x/2a=0.5$  to  $x/2a=0.99$ .**

Coefficients for normal ( $C_N$ ), axial ( $C_A$ ), lift ( $C_L$ ), drag ( $C_D$ ), and pitching moment ( $C_m$ ) are compared to experimental forces in Table 4.3 for a circumferential wake angle of 117 degrees. CMARC automatically outputs the pressure load coefficients in both wind and body axes. Skin friction forces are calculated using POSTMARC and will be discussed in a later section. The experimental results are from integrated pressure forces using the method outlined in Appendix B. The coefficients are normalized by maximum diameter and cross sectional area. A wake angle of 117 degrees produces a close match to experimental results for  $C_N$ ,  $C_L$  and  $C_m$ . As expected, the axial and drag coefficients are off considerably from experimental data.

Force Origin	Force/Moment Coefficient	Experimental AGARD 303-Kreplin	CMARC $\theta_w=117^\circ$	% Difference (CMARC-exp)/exp
Pressure Forces	$C_N$	0.1924	0.1816	-5.6%
	$C_A$	0.0026	0.0411	1480.8%
	$C_L$	0.1890	0.1717	-9.2%
	$C_D$	0.0359	0.0720	100.6%
	$C_m$	0.9009	0.9003	-0.1%

**Table 4.3 Comparison of Integrated Experimental Pressure Forces to the CMARC Model with 117° Wake Placement Angle, after Ref. [12].**

It is concluded that a pure potential flow solution over a streamlined body at 10° angle-off-attack will fail to predict substantial regions of flow separation. However, pressure distributions over bodies with substantial flow separation can be approximated by proper wake distribution. As outlined by Tuncer and Platzer [Ref. 7], a wake separation angle of 144° is a good starting point.

## 5. Boundary Layer Separation Locations

Next, CMARC boundary layer calculations were visualized to see how well CMARC predicted separation points for the inclined prolate spheroid. As reported in the section on the NACA 2415 finite wing, predicted boundary layer separation points from CMARC matched those predicted by the NPS UPOT code fairly well, especially at higher

Reynolds numbers. In this case, the boundary layer points are compared to experimental data at the same  $10^\circ$  angle-of-attack over the three-dimensional prolate spheroid.

Sixty-six streamlines for boundary layer calculations were placed on the CMARC model at locations corresponding to experimental data points. Appendix F contains the input file. CMARC only predicted separation over the very aft end of the body. A separation point is best visualized with POSTMARC by selecting the on-body streamline boundary layer thickness or shape factor functions. The separation point is indicated at the last downstream point on the streamline. It is important to note that if one visualizes streamline pressure coefficient, velocity or Mach number, the streamline will travel all the way to the aft stagnation point. In other words, to visualize a separation point, phenomena derived from the boundary layer calculations and not the streamline calculations must be selected for visualization.

Figure 4.31 displays the streamline separation points on the aft end of the prolate spheroid. CMARC boundary layer separation points are compared to experimental data as a function of axial location and circumferential angle in Figure 4.32. It is to be expected that the 2D code implemented in CMARC fails to accurately predict separation regions over streamlined bodies of revolution with large cross flow velocities. Nevertheless, these results help to quantify the differences.

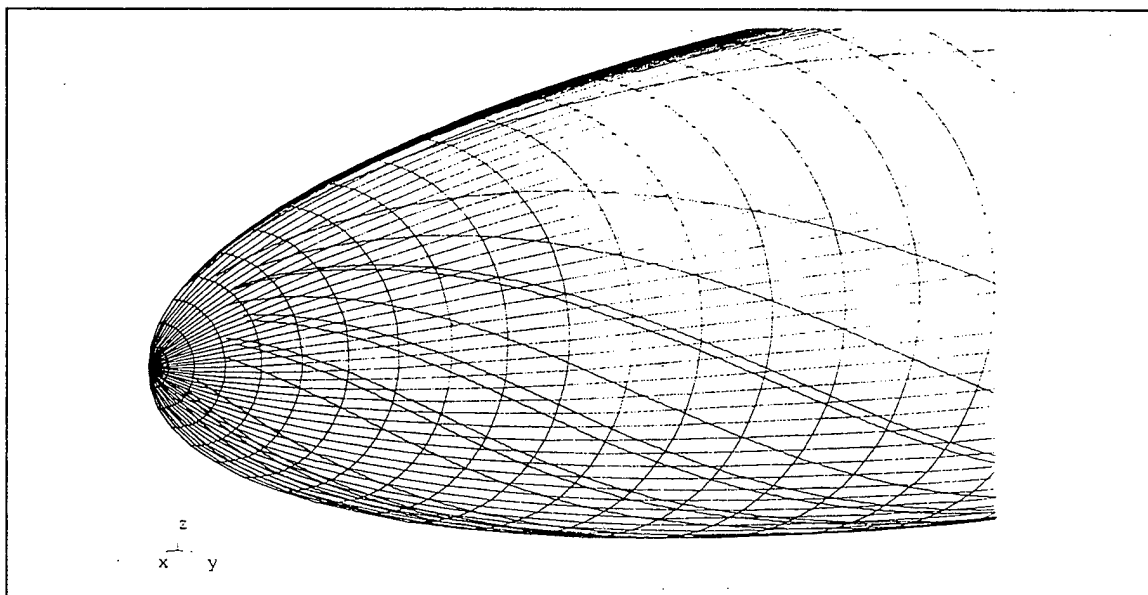


**Figure 4.31 POSTMARC Visualization of CMARC Predicted Separation Points on the Aft End of the Prolate Spheroid Model (No Wakes).**

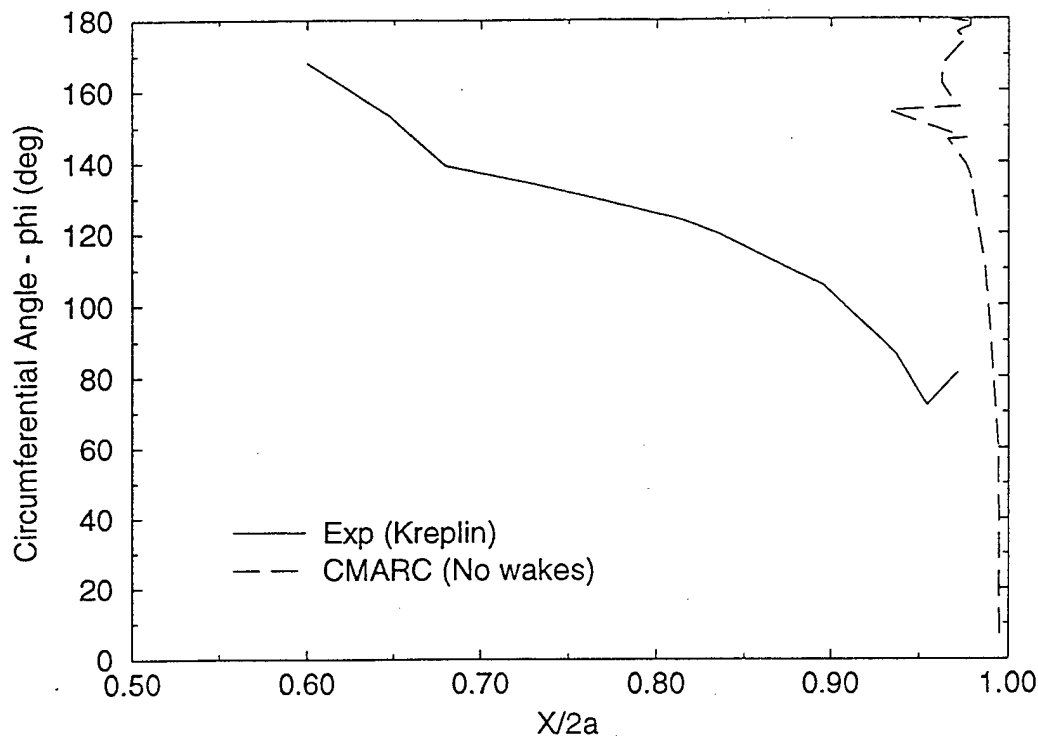


**Figure 4.32 Comparison of CMARC Predicted Separation Line to Experimental Data, after Ref. [12].**

## 6. Boundary Layer Skin Friction Coefficient

CMARC-computed skin friction coefficients were compared to experimental data obtained from hot film sensors [Ref. 12]. Sixty-six streamlines were placed through panels on the CMARC model corresponding to skin friction data points. Data were extracted manually from the CMARC output file. Data are plotted at six axial locations as a function of circumferential angle in Figure 4.33. The wind tunnel model has a transition strip located at  $x/2a=0.20$ . All CMARC boundary layer calculations are based on a built-in transition model. There are no provisions for specifying the transition location in CMARC.

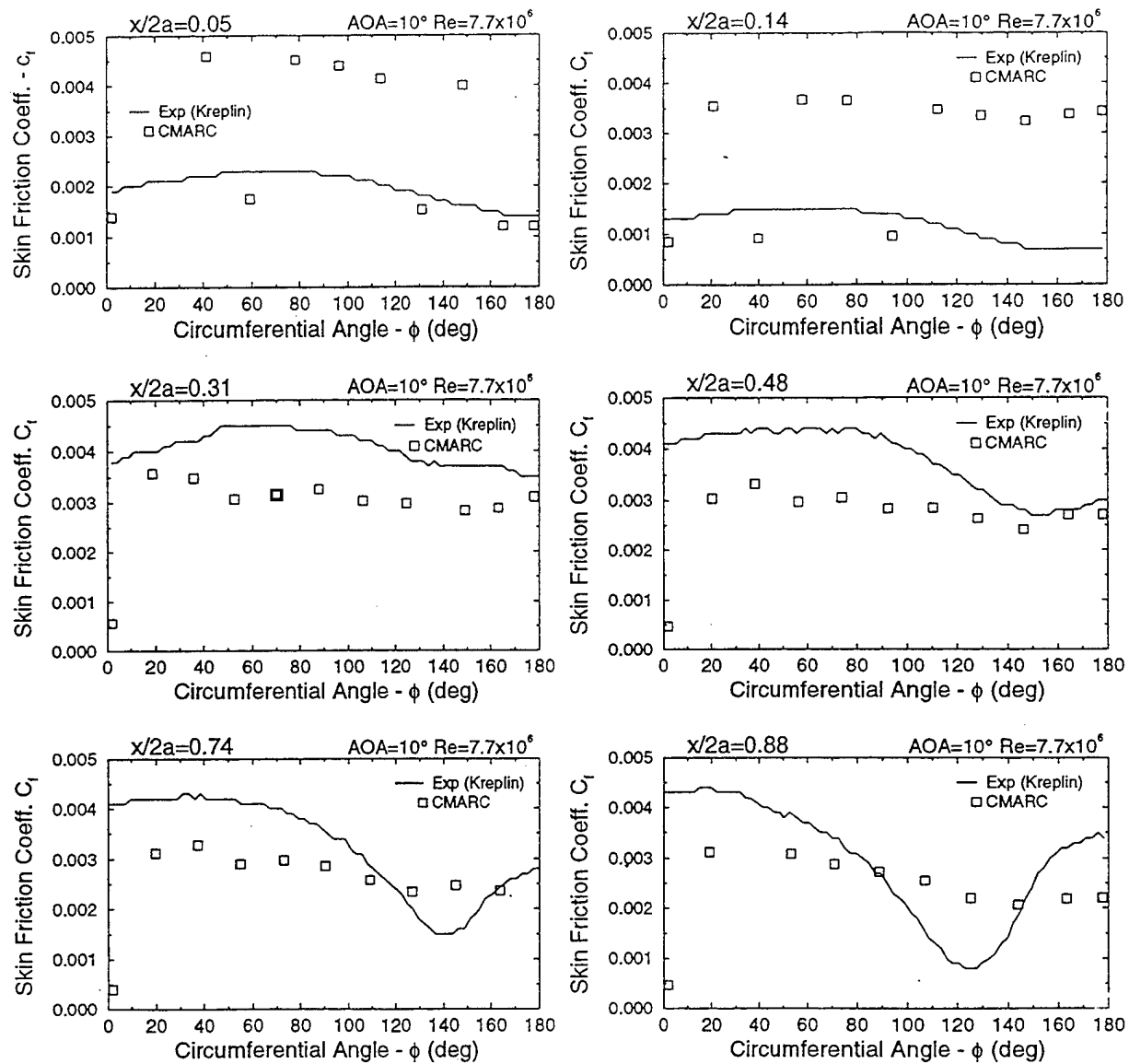


**Figure 4.33 Comparison of CMARC Predicted Skin Friction Coefficient to Experimental Data, after Ref. [12].**

For the two axial locations in front of the transition strip,  $x/2a=0.05$  and  $0.14$ , CMARC predicts a mix of laminar and turbulent flow. A laminar boundary layer is indicated by the data points where  $C_f < 0.002$ . Experimental data indicate strictly laminar flow for these axial locations. CMARC streamlines passing through each circumferential location travel a unique path across different panel geometry from the forward stagnation point to the point of interest. Being an integral two-dimensional boundary layer method, CMARC's empirical transition formula predicts separation for some of the streamlines and laminar flow for the others. In general, CMARC over-predicts skin friction drag in this region due to the mixed flow. If CMARC correctly predicted all laminar flow, the results would be close to experimental results.

Aft of the transition strip at  $x/2a=0.20$ , experimental data indicate fully turbulent flow as expected. CMARC predicts turbulent flow for all but the lower streamline which has a low adverse pressure gradient. At  $x/2a=0.31$  and  $0.48$ , computed skin friction is accurate to within 25%. Aft of  $x/2a=0.48$ , CMARC results are less meaningful due to the large region of separated flow.

## **7. Integrated Skin Friction Forces**

POSTMARC version 1.17.3 contains functionality for performing integrated skin friction calculations. When a CMARC model is processed with the "-p" command line switch, a file with a ".pm" extension is created with the information necessary for POSTMARC to perform boundary layer calculations. POSTMARC then places streamlines on every panel, performs boundary layer calculations and integrates the skin friction loads. Experimental data is integrated as outlined in Appendix B.

Integrated skin friction forces for the prolate spheroid model without wakes are compared to experimental data in Table 4.4. Normal, axial, drag and pitching moment coefficients were all within 40% of the rough estimate provided by integrating the experimental data. This is in keeping with the observations from Figure 4.33. The lift coefficient produced due to skin friction is so small that comparisons between experimental and CMARC data are meaningless.

Force Origin	Force/Moment Coefficient	Experimental AGARD 303-Kreplin	CMARC $\theta_w=117^\circ$	% Difference (CMARC-exp)/exp
Skin Friction Forces	$C_N$	0.0102	0.0071	-30.6%
	$C_A$	0.0610	0.0376	-38.4%
	$C_L$	-0.0006	0.0004	-166.7%
	$C_D$	0.0618	0.0376	-39.2%
	$C_m$	0.0022	0.0019	-12.4%

**Table 4.4 Comparison of Integrated Experimental Skin Friction Forces to the CMARC Model without Wakes, after Ref. [13].**

### **8. Total Integrated Forces**

As a final comparison of CMARC results to experimental data, the summed pressure and skin friction force coefficients are presented in Table 4.5. A simple fore/aft wake running from  $x/2a=0.5$  to a partial ring wake at  $x/2a=0.99$  provides good results for all but the axial and drag coefficients. It is concluded that CMARC, with proper wake selection, will provide meaningful force and moment coefficients for the development of stability derivative data. Results for drag coefficient are less meaningful and should be avoided for performance calculations.



Force Origin	Force/Moment Coefficient	Experimental AGARD 303-Kreplin	CMARC $\theta_w=117^\circ$	% Difference (CMARC-exp)/exp
Pressure Forces	$C_N$	0.1924	0.1816	-5.6%
	$C_A$	0.0026	0.0411	1480.8%
	$C_L$	0.1890	0.1717	-9.2%
	$C_D$	0.0359	0.0720	100.6%
	$C_m$	0.9009	0.9003	-0.1%
Skin Friction Forces	$C_N$	0.0102	0.0060	-41.2%
	$C_A$	0.0610	0.0379	-37.9%
	$C_L$	-0.0006	-0.0017	180.0%
	$C_D$	0.0618	0.0388	-37.2%
	$C_m$	0.0022	0.0017	-23.5%
Total Forces	$C_N$	0.2026	0.1876	-7.4%
	$C_A$	0.0635	0.0790	24.4%
	$C_L$	0.1884	0.1700	-9.8%
	$C_D$	0.0977	0.1108	13.4%
	$C_m$	0.9031	0.9020	-0.1%

**Table 4.5 Comparison of Integrated Experimental Forces to the CMARC Model with  $117^\circ$  Wake Placement Angle, after Ref. [12].**



## V. AERODYNAMIC MODEL OF THE FROG UAV

### A. BACKGROUND

The Naval Postgraduate School Aeronautics Department is integrating UAV hardware and software to demonstrate autonomous flight, trajectory tracking and automatic landing. A core requirement for flight control law development is a valid aerodynamic truth model for the UAV airframe. A panel code model of the FROG UAV is one method for estimating many of the stability derivatives required for an aerodynamic truth model. This development effort concentrates on finding the  $C_{L\alpha}$  and  $C_{m\alpha}$  longitudinal stability derivatives followed by the  $C_{Y\beta}$ ,  $C_{l\beta}$  and  $C_{n\beta}$  lateral-directional stability derivatives. A future study will continue the development for rate damping and control effectiveness derivatives.

Panel code modeling utility goes beyond the development of aerodynamic coefficients. Flight control systems require accurate pitot-static and angle-of-attack sensor inputs. CMARC accurately solves on-body static pressure distributions and off-body flow velocities over the predominately attached flow fields of fuselage fore bodies. In this study, correction curves are generated for static-pressure source and angle-of-attack probe position errors.

### B. FROG UAV DESCRIPTION

The FROG UAV is a small single engine flight test vehicle used for autonomous flight research by the Naval Postgraduate School Aeronautics Department. The aircraft was originally designated the FOG-R by the U. S. Army. It was designed as a small lightweight, battlefield observation platform that could be guided by a fiber optic data link. Table 5.1 presents the basic aircraft specifications.

The aircraft is somewhat unconventional in that the engine is mounted in a nacelle tractor style above the fuselage and wing. The aft fuselage consists of a 1.75 in. diameter aluminum tube which connects the tail surfaces to the main fuselage. Figure 5.1 displays a three view drawing of the FROG UAV.

PARAMETER	MEASUREMENT/UNITS	
Length	8.125 ft	97.5 in
Height	1.75 ft	21 in
Weight	67.7 lbs	
Power Plant	12 Hp / 2 Cycle	
Wing Airfoil	NACA 2415	
Horiz. Stab. Airfoil	NACA 0006 (Approx.)	
$S_w(S_{ref})$	17.57 ft <sup>2</sup>	2530 in <sup>2</sup>
$S_t$	3.174 ft <sup>2</sup>	457.1 in <sup>2</sup>
$S_v$	0.9818 ft <sup>2</sup>	141.4 in <sup>2</sup>
c	1.66 ft	20 in
$c_t$	0.958 ft	11.5 in
$b_w$	10.54 ft	126.5 in
$b_t$	3.313 ft	39.75 in
$b_v$	1.25 ft	15.0 in
$l_t$	4.44 ft	53.25 in
$l_v$	4.44 ft	53.25 in
$AR_w$	6.32	
$AR_t$	3.46	
$AR_v$	1.59	
$V_H$	0.49	
$V_v$	0.02	

**Table 5.1 FROG UAV Characteristics, after Ref. [1].**

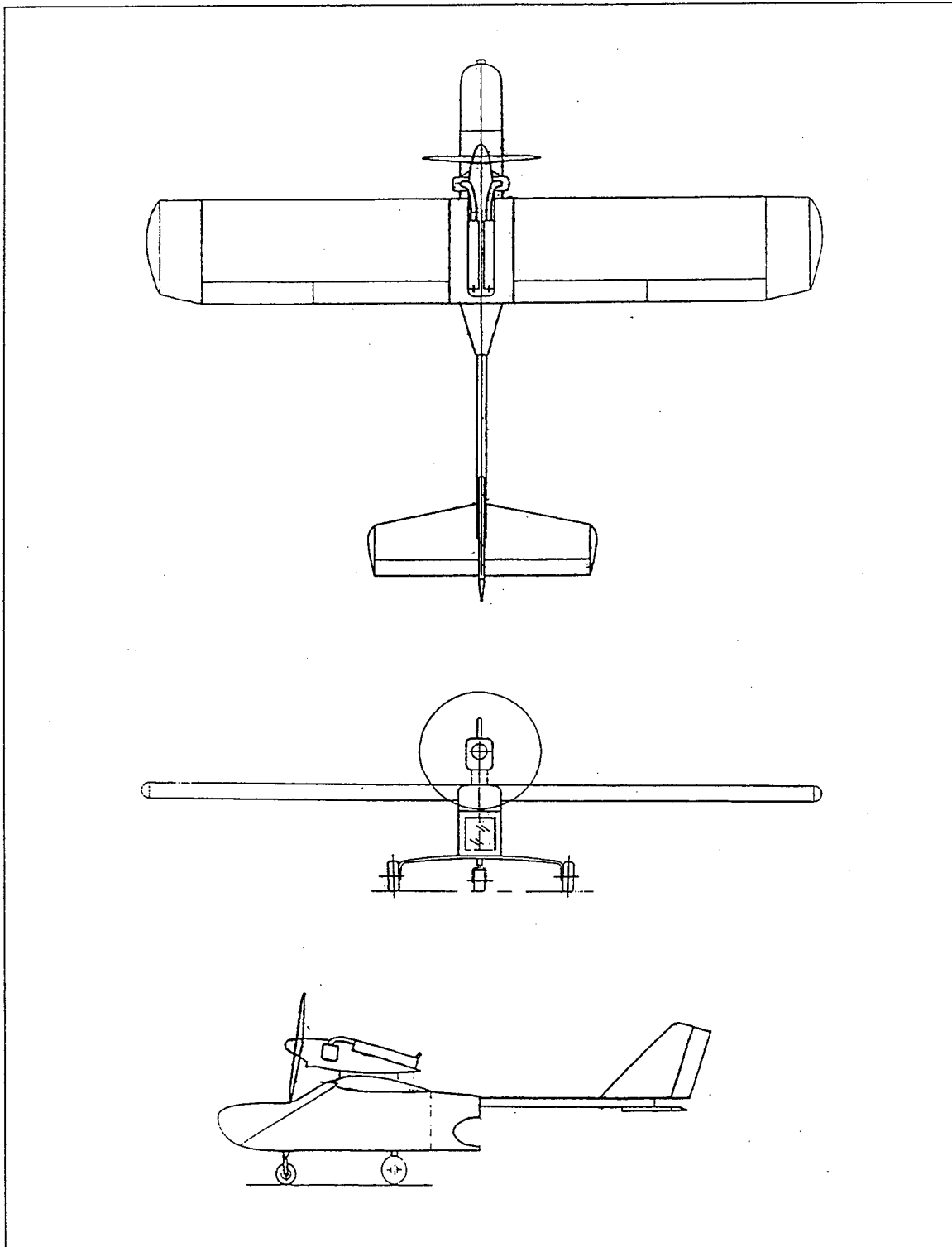


**Figure 5.1 FROG UAV Three-View Drawing.**

The FROG UAV, as operated by NPS, is equipped with airspeed, angle-of-attack, altitude and control surface sensors. In addition, a miniature Inertial Measurement Unit (IMU) captures aircraft attitude, acceleration and body rates. Data is down linked to a mobile SGI workstation through a spread spectrum modem. Onboard GPS provides differential GPS navigation capability with the ground station used as a reference. The aircraft can be flown by conventional radio control or by up-linking flight control commands from the computer workstation.

Current flight control development revolves around the cruise trim point of 60 m.p.h. or 88 ft/s. This flight condition is selected for the development of stability derivative data. Table 5.2 lists the aircraft parameters for the trim flight condition.

PARAMETER	MEASUREMENT	UNITS
Weight	67.73	lbs
IXX	12.52	slug-ft <sup>2</sup>
IYY	8.43	slug-ft <sup>2</sup>
IZZ	18.55	slug-ft <sup>2</sup>
Airspeed	60/88	mph and ft/s
Altitude	800	ft MSL
Air Density	0.002327	slug/ft <sup>3</sup>
Center of Gravity	34.5%	M.A.C
$C_{L \text{ trim}}$	0.4295	n/a
$\alpha_{\text{trim (est)}}$	-1.3	degrees
$\delta_{\text{Etrim}}$	5.1	degrees

Table 5.2 FROG UAV Trim Flight Condition, after Ref.[1].

## C. FROG UAV MODELING

### 1. General

LOFTSMAN is utilized for the creation of all CMARC input file patches except for wing tips. In some cases, CMARC's more efficient built-in capability to model standard NACA 4-digit wing surfaces could have been used. However, future studies will

require flight control surface patches meshed with LOFTSMAN. Therefore, with growth provisions in mind, all patches were created with LOFTSMAN from the start. Figure 5.2 displays the complete FROG UAV model with all patches and wakes activated.

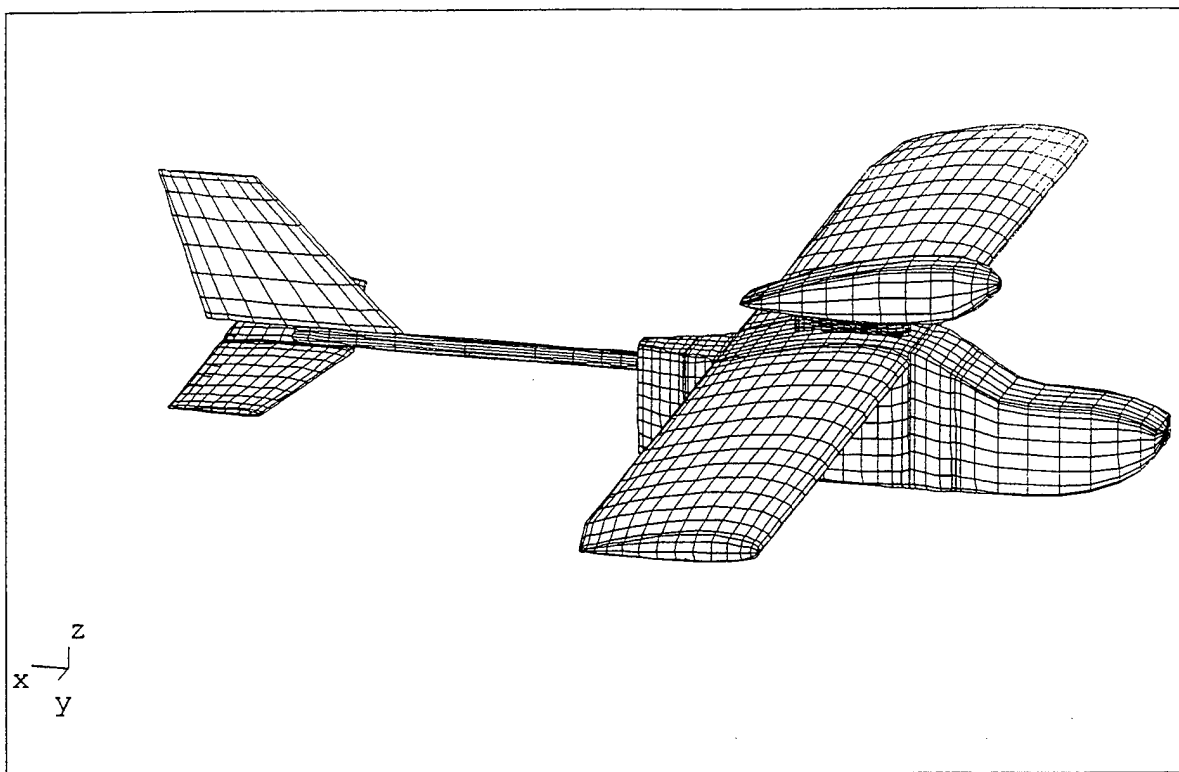


**Figure 5.2 FROG UAV Panel Code Model.**

Some assumptions are made to simplify the modeling process. First, the horizontal and vertical stabilizers are modeled with a NACA 0006 section. The actual surfaces are constructed with a flat section, rounded at the nose and tapered starting at the control surface hinge line to a sharp trailing edge. The NACA 0006 provides a close approximation and allows the use of LOFTMAN's built-in wing lofting capability. For a potential flow solution, this simplification is considered minor.

A second simplification is made regarding the vertical stabilizer's tip rib orientation. The actual rib is canted down  $5^\circ$  with respect to the longitudinal waterline.

LOFTSMAN will only model a chord line that is parallel to the waterline (constant BL). The vertical tail tip rib is modeled with a constant BL, but the span is adjusted to maintain the same overall surface area.

Finally, there is no attempt to model the tricycle landing gear struts or wheel assemblies. The landing gear components do not contribute significantly to the aerodynamic stability derivatives. However, they certainly need to be taken into account when measuring moments of inertia for a dynamic model.

## **2. Modeling Coordinate System**

The model is developed using a coordinate system selected to simplify fuselage measurements. The +x-axis starts even with the nose and runs aft along the bottom of the fuselage, parallel with the tail boom. The bottom of the fuselage is used as the waterline with +z-axis in the up direction. This allows for easy vertical measurements when the aircraft is placed flat on a horizontal surface. The +y-axis runs from centerline outboard parallel to the right wing. Figure 5.3, which displays static-pressure source and alpha vane locations, also shows the location and origin of the modeling coordinate system.

## **3. LOFTSMAN Patches**

LOFTSMAN is used to generate all the model patches except for wing tips. CMARC's built-in capability is used to create wing tip patches. Appendix H contains listings of all the LOFTSMAN input files. Once a surface is meshed, the mesh is saved to a file as a CMARC/PMARC patch. The resulting text file is then opened, and the text is copied and pasted with any text editor into the patch definition section of the CMARC input file. LOFTSMAN patch files are not listed because they are redundant with the patches in the final CMARC input file listed in Appendix I.

When saving a patch, LOFTSMAN automatically takes care of all CMARC input file formatting except for the TNODS patch continuation or final patch toggle. A patch, as formatted by LOFTSMAN, assumes additional patches will follow in the CMARC input file. Therefore, the last segment's TNODS variable is set TNODS=3. When the patch is the last patch in the input file, the TNODS variable must be manually set to TNODS=5. If CMARC hangs up while reading in geometry information, most likely TNODS=5 is missing on the last patch.



### *a. Fuselage Model*

The fuselage is lofted as a B-type body. A B-type body is used when major portions of the fuselage have a circular or oval cross section. The input file is listed in Appendix H. Only the right side is meshed, with a symmetric left side created by toggling the IPATSYM variable to IPATSYM=1. LOFTSMAN assumes that B-type bodies converge to a specific point at the fore and aft ends. The flat aft fuselage face does not provide this single point. A slight modification was made to the aft face to allow automatic meshing as a B-type body. The center of the aft face is extended very slightly, approximately 1/8 inch, to provide a convergence point for the final rear triangular panels. This small deviation is assumed not affect the aerodynamic fidelity of the model for a potential flow solution.

The right side was originally meshed separately from the wing as a 20 x 20 panel patch. This created a low order fit when the wing patch was butted to the side of the fuselage, resulting in overlapping panels. A final mesh was created that flowed around the wing root and fuselage intersection for a high order fit. All the fuselage panels at the wing root join with the adjacent wing panels. This mesh requires that the fuselage be broken up into six separate panels per side. They are the nose patch, the forward transition patch, the top and bottom wing root patches, the aft transition patch and finally the rear fuselage patch. Some manual editing is required to straighten out panels on the upper fuselage patch. When the six patches are added together, the final configuration is modeled with a 44x15 panel patch.

### *b. Main Wing Patch*

The NACA 2415 wing is created with four separate patches to allow the addition of an aileron mesh at a later date. CMARC comes with a broad selection of "\*.SD" airfoil template files that are automatically loaded during installation. The "NACA2415.SD" file is used for this model. The inboard patch runs from the wing root, past the flaps, to the start of the aileron. The mid patch covers the portion of the wing spanned by the aileron. The outboard patch creates the tapered wing extension. Finally, a semi-circular wing tip patch is added in the input file using CMARC's built-in wing tip functionality. The wing is set to a 4.5° incidence in the LOFTSMAN input file. Alternatively, the patch could be created with zero incidence and then the patch

coordinate system could be rotated in the CMARC input file. Together, the four wing patches add to make a 20 x 30 panel wing model.

#### *c. Horizontal Stabilizer Patch*

The horizontal stabilizer patch is created with a single 10 x 22 mesh using the "NACA0006.SD" airfoil template. No special modifications are required. A tip patch is not added because some of the resulting panels would be too small. In particular, the triangular panels closing out the aft end of the tip are too small in proportion to the other panels. An attempt was made to model horizontal and vertical stabilizer wing tips, but the model will not converge with them. Leaving off tip patches will not significantly influence results according to the CMARC User's Guide [Ref. 2].

#### *d. Vertical Stabilizer Patch*

The vertical stabilizer patch is created with a single 8 x 18 mesh using the "NACA0006.SD" airfoil template. The LOFTSMAN input file is different in that a vertical wing surface requires a modification to the rib axis. The rib axis must be specified with an x-axis rotation of 90°, a y-axis rotation of 0° and an unspecified (999.0) z-axis rotation. No symmetry is selected for the vertical stabilizer because the patch is already symmetric about the y=0 plane. As with the horizontal stabilizer, a tip patch is not added because some of the resulting panels would be too small.

#### *e. Tail Boom Patch*

The tail boom patch is created as a single 12 x 10 mesh using a B-type body. Again, only the right side is meshed due to symmetry. The LOFTSMAN input file requires modifications at both ends in a similar fashion to the aft fuselage. A single point is added to allow convergence of the triangular panels at either end. With this point, the tail boom has the appearance of being tapered at both ends. The point is then manually edited out in the CMARC input file by replacing the "x" coordinate of the beginning and ending section panels with the correct value. In most cases, the tail boom is left out of solution to aid in convergence. This is due to the small overlapping panels at the fuselage tail boom junction. Being a slender, round tube directly in the fuselage slip stream, the tail boom should have little influence on the stability derivatives.

#### *f. Engine Pod Patch*

The engine pod patch, or nacelle, is created as a single 15 x 10 mesh using a B-type body. Only the right side is meshed due to symmetry. The prop spinner is an integral part of the patch. No attempt is made to model the prop, engine heads or exhaust system.

#### *g. Engine Pylon Patch*

The engine pylon patch is modeled with a single 15 x 10 mesh using an A-type body. A-type bodies are used to model surfaces similar to boat hulls with cornered surfaces or sharp chines. In addition, A-type bodies do not require the body to be completely enclosed. As a result, an A-body was selected to model just the sides of the pylon. Only the right side is meshed due to symmetry. A low order fit is achieved with the adjacent fuselage and engine pod panels. This results in questionable pressure distributions. As a result, the pylon patch was turned off for most configurations. A future attempt will be made to create a high order fit between the other patches. This will probably require manual editing of the intersecting patches.

### **4. Common CMARC Input File Errors**

The patches created in LOFTSMAN are assembled into a single CMARC input file with any text editor. A default minimum input file comes with CMARC or any old file may be modified. There are many errors that will cause CMARC to hang up without an error message. The two most common errors are forgetting to designate the last patch and incorrectly numbering the wake patches.

The last patch must be designated by including a TNODS=5 setting in the last section of the last patch. If it is not included, CMARC hangs up when reading in the geometry. In a similar manner, the last wake must be designated with a NODEW=5 setting. If the last wake is not designated, CMARC hangs up while reading in the wake information.

Another common error involves incorrect wake to patch number association. Patch numbering changes whenever patches are disabled or reordered. The KWPACH field for each wake definition must be checked to make sure it reflects the current patch numbering.

#### **D. STATIC-PRESSURE SOURCE AND YAW VANE CORRECTIONS THROUGH OFF-BODY FLOW ANALYSIS**

CMARC is ideally suited for off-body flow analysis. Off-body streamlines may be placed through a point anywhere in the flow field. CMARC will then follow the streamline up and downstream the distance designated in the input file. This is particularly useful for flow visualization. In addition, CMARC calculates pressure coefficient and velocity at each point along the streamline. For this study, two streamlines are placed through the locations of the static-pressure source and alpha probe locations. Pressure coefficient is used to quantify static source position error and velocity is used to calculate alpha probe position error as a function of FROG UAV angle-of-attack. Both static pressure and AOA are digitized for down link to the ground station allowing the values to be easily corrected. Either a look-up table or curve fit correction can be applied subsequent to being passed to the flight control routines.

##### **1. Description of the FROG UAV Pitot-Static and AOA Systems**

The pitot-static system and angle-of-attack probe share a common flight test boom extending from the nose of the UAV. The boom contains both the total and static pressure ports. Figure 5.3 depicts the general dimensions of the flight test boom installation and the modeling coordinate system.

##### **2. Modeling Off-Body Streamlines**

Streamlines are placed at the two locations indicated in Figure 5.3 which correspond to the static source and alpha probe locations. Two off body streamlines were activated in CMARC by setting NSTLIN=2 in the &SLIN1 line. Only a short distance of 2 inches is selected up and downstream in the SU and SD fields to reduce the size of the output file. Figure 5.4 is a POSTMARC rendering of the two off-body streamlines used for sensor corrections. With the model at  $\alpha_t=0^\circ$ , notice that the streamline is curving up at the angle-of-attack vane location 6.5 inches in front of the aircraft nose.

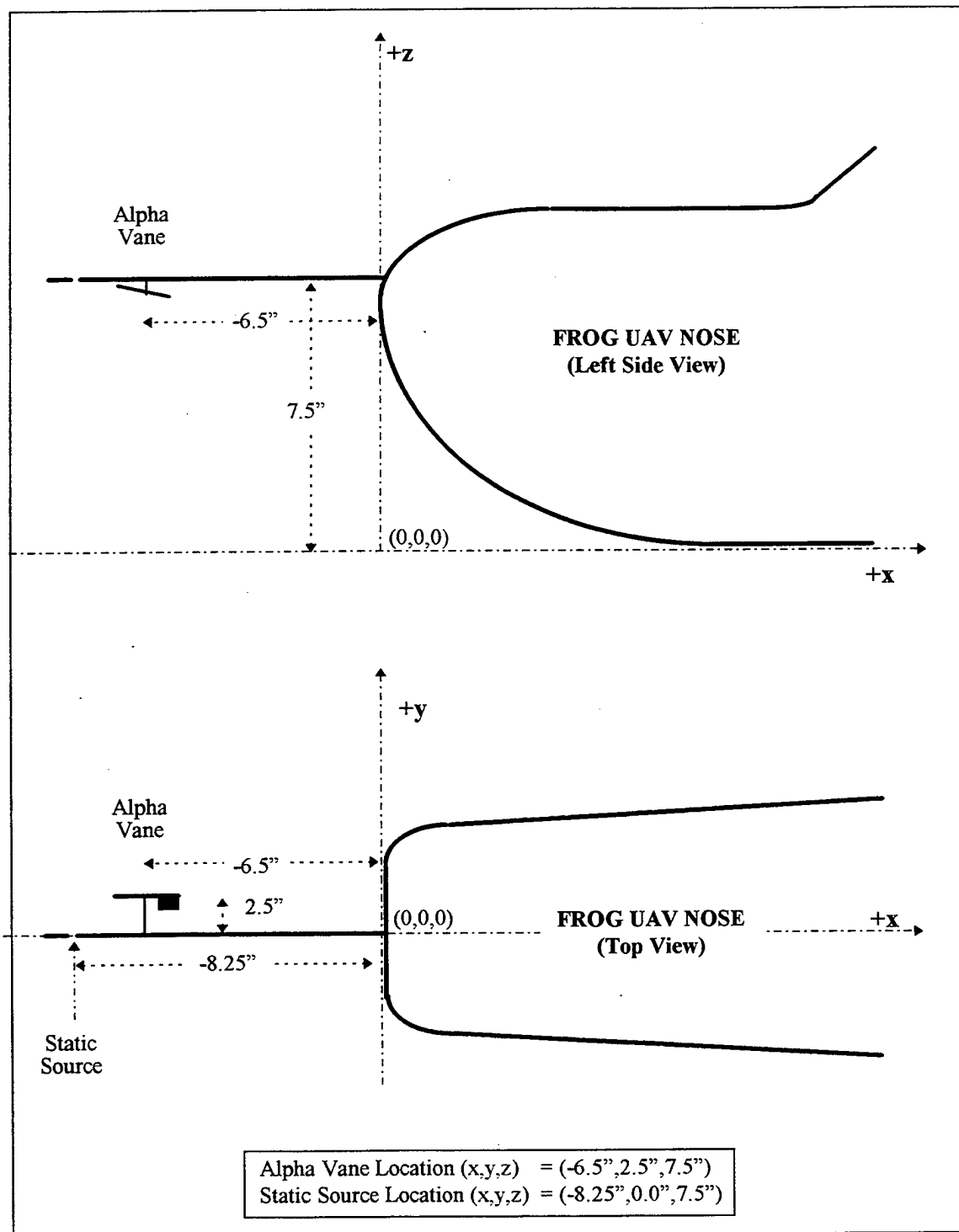


**Figure 5.3** Diagram of the FROG UAV Pitot-Static and AOA Systems.

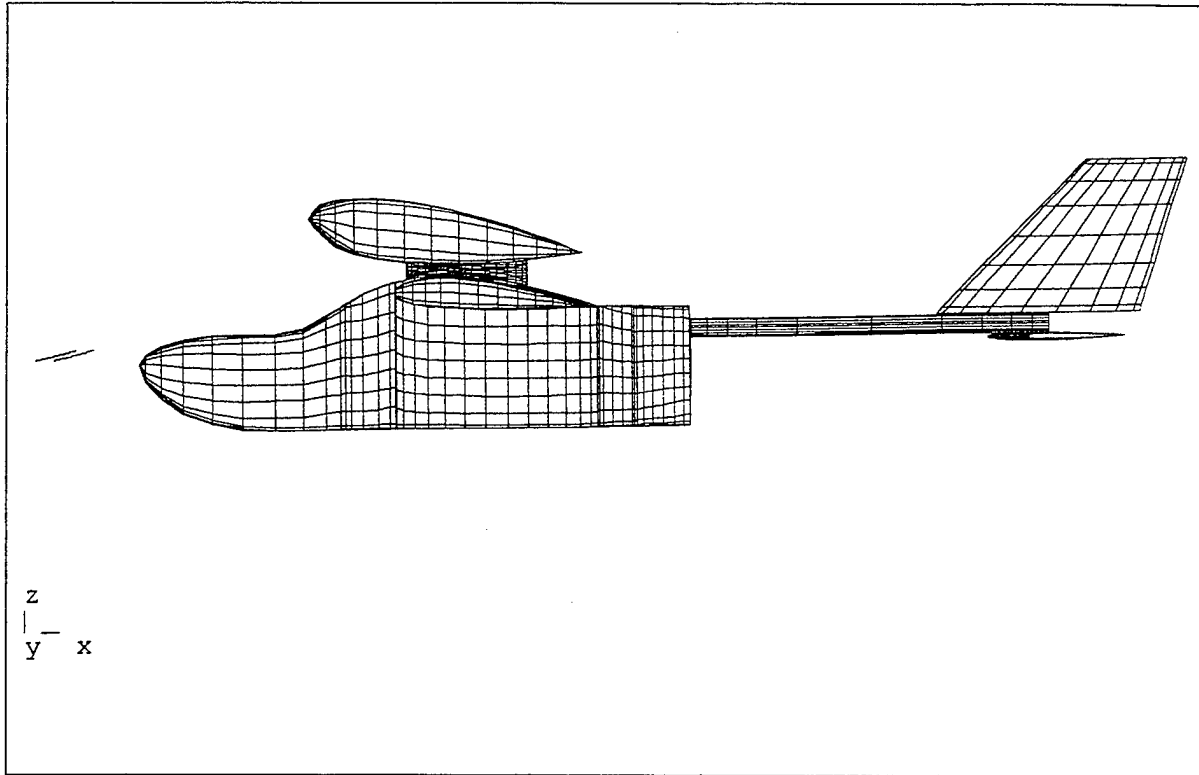


**Figure 5.4 FROG UAV Off-Body Streamline visualization with POSTMARC ( $\alpha_i=10^\circ$ ).**

### **3. Analysis of Static Source Position Errors**

In general, the position error pressure coefficient,  $\Delta C_{p_{pe}}$  or  $\Delta P_p/q_c$ , is a function of freestream Mach number and angle-of-attack provided that the static source is located outside of a thick boundary layer and sideslip is minimized [Ref. 13]. In the case of the FROG UAV with incompressible flow,  $\Delta P_p/q_c$  becomes a function of angle-of-attack only. As a result, the corrections can be simply defined as a function of measured angle-of-attack.

A DOS batch file was executed to step the CMARC model through angles-of-attack ranging from  $-8^\circ$  to  $20^\circ$ . The batch file incremented the angle-of-attack using CMARC's command line override feature. In addition, a new output file name was designated for each angle-of-attack. Position error pressure coefficient is then read from the off-body streamline listing of the output file at the location corresponding to the static

source. Table 5.3 lists the values of  $\Delta P_p/q_c$  calculated from CMARC data. Figure 5.5 displays  $\Delta C_{p_{pc}}$  as a function of indicated angle-of-attack. The second order influence of angle-of-attack is clear with the second order curve fitting tightly through the data points. Of note, the error is relatively constant for a  $\pm 8^\circ$  band around trim angle-of-attack. For incompressible flow, position error pressure coefficient is independent of airspeed and altitude.

Position error pressure coefficient can be turned into position corrections for airspeed and altitude. The following relations were developed which assume small errors and incompressible flow:

$$\Delta V_{pc} = \frac{V_i \Delta C_p}{2} \quad \text{and} \quad \Delta V_{pc} = V_c - V_i \quad 5.1$$

$$\Delta H_{pc} = \frac{\Delta V_{pc} V_i}{\sigma_{std} g_0} \quad \text{and} \quad \Delta H_{pc} = H_c - H_i \quad 5.2$$

Where:

$\Delta H_{pc}$  is the altitude position correction.

$\Delta V_{pc}$  is the velocity position correction.

$\Delta C_p = \frac{\Delta P_p}{q_c}$  or position error pressure coefficient.

$\sigma_{std}$  is standard day density ratio.

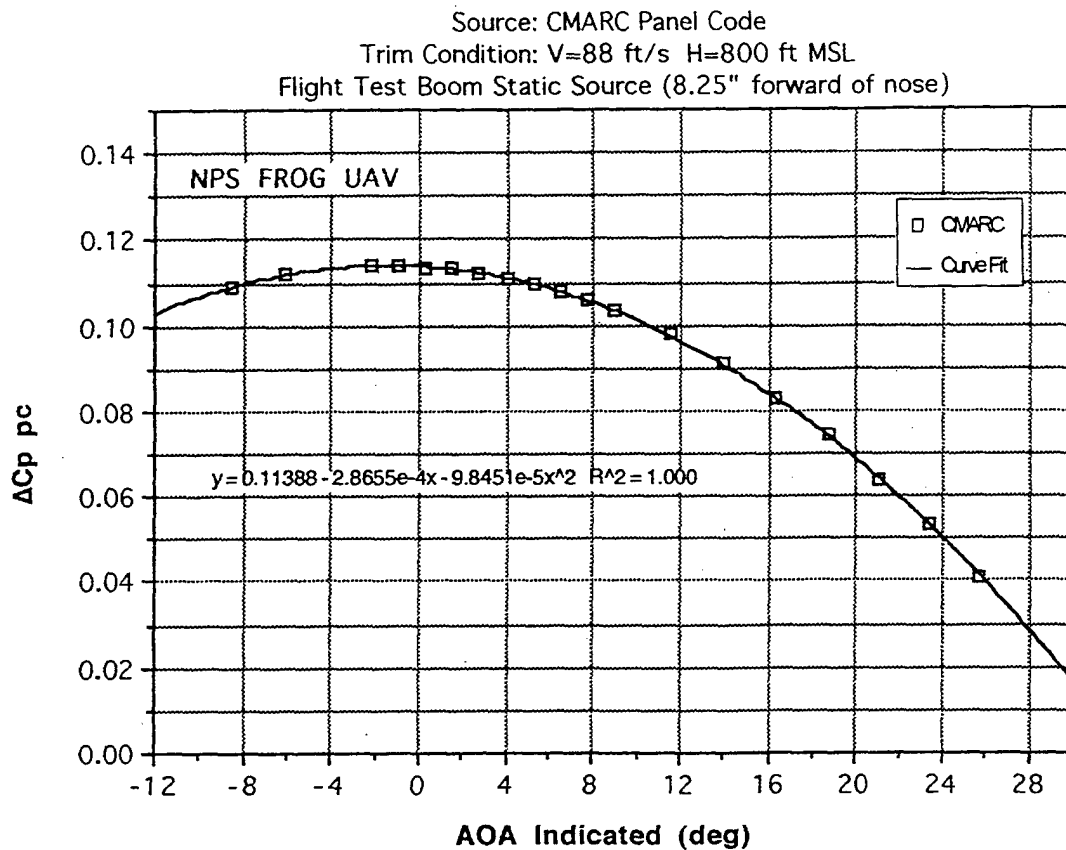
$g_0$  is the gravitational constant.

Table 5.3 displays corrections calculated for both airspeed and altitude at the FROG UAV trim condition of 88 ft/s and 800 ft MSL. The corrections are added to the indicated value to obtain the corrected value. Figures 5.6 and 5.7 display the corrections as a function of indicated angle-of-attack. Again, a second order curve fits nicely through the data points. Equations 5.1 and 5.2 can be used to implement a correction algorithm based on airspeed and altitude.

UAV AOA $\alpha_T$ (deg)	$\Delta C_{p_{pc}}$ $\Delta P/q_c$	V Correction $\Delta V_{pc}=V_c-V_i$ (ft/s)	H Correction $\Delta H_{pc}=H_c-H_i$ (ft)
-8	0.1092	4.8	13.5
-6	0.1120	4.9	13.8
-3	0.1141	5.0	14.1
-2	0.1140	5.0	14.1
-1	0.1137	5.0	14.1
0	0.1132	5.0	14.0
1	0.1123	5.0	13.9
2	0.1111	4.9	13.7
3	0.1096	4.8	13.5
4	0.1078	4.8	13.3
5	0.1057	4.7	13.1
6	0.1034	4.6	12.8
8	0.0977	4.3	12.1
10	0.0909	4.0	11.2
12	0.0831	3.7	10.3
14	0.0741	3.3	9.2
16	0.0641	2.8	7.9
18	0.0530	2.3	6.6
20	0.0410	1.8	5.1

**Table 5.3** Position Error Corrections for the NPS FROG UAV at V=88 ft/s and H=800 ft MSL. Derived from CMARC Panel Code Off-Body Flow Field Analysis.





**Figure 5.5** Position Error Pressure Coefficient,  $\Delta C_{p_{pc}}$ , for the NPS FROG UAV.  
 Derived from CMARC Panel Code Off-Body Flow Field Analysis.

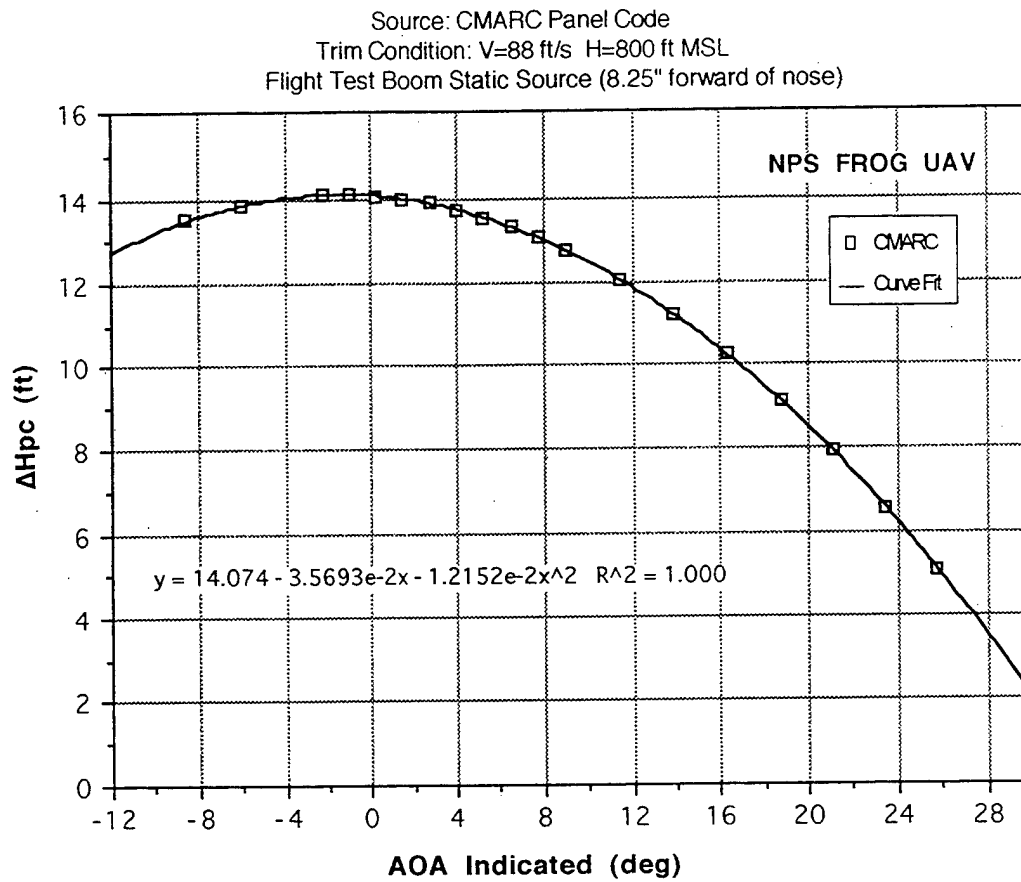


**Figure 5.6** Altitude Position Error,  $\Delta H_{pc}$ , for the NPS FROG UAV at V=88 ft/s and H=800 ft MSL. Derived from CMARC Panel Code Off-Body Flow Field Analysis.

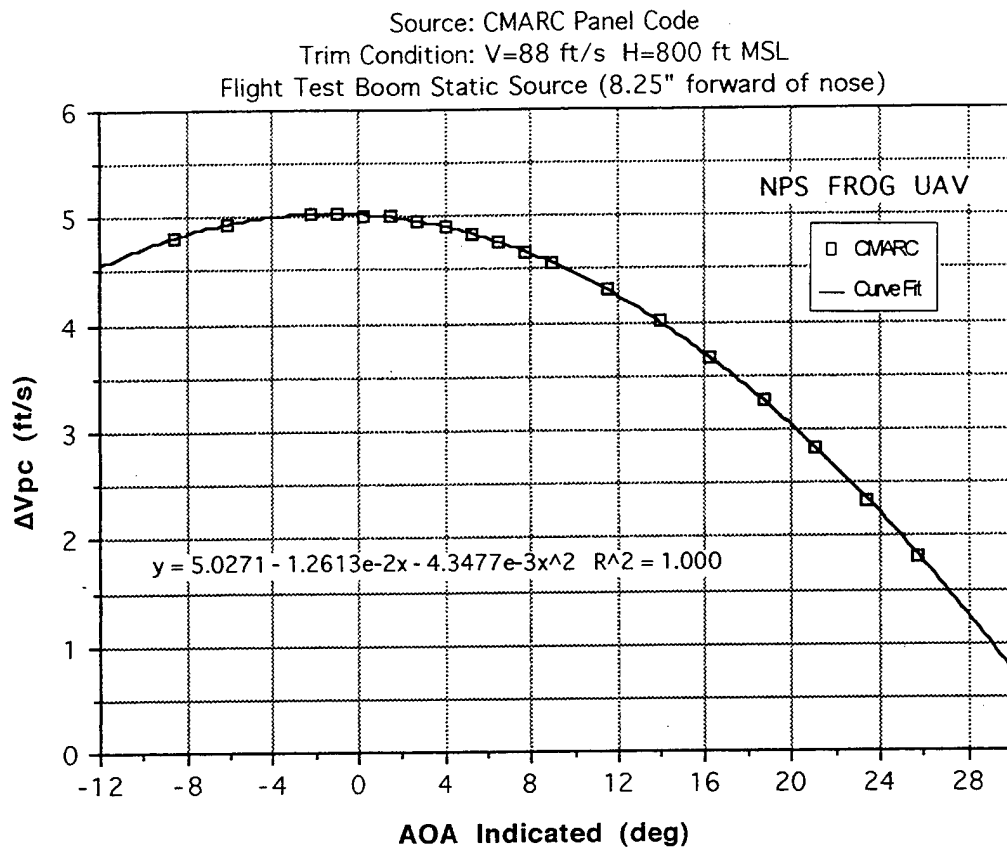


**Figure 5.7** Airspeed Position Error,  $\Delta V_{pc}$ , for the NPS FROG UAV at V=88 ft/s and H=800 ft MSL. Derived from CMARC Panel Code Off-Body Flow Field Analysis.

#### 4. Analysis of Alpha Vane Position Error

Local flow field velocity is extracted from the off-body streamline listing to obtain local angle-of-attack. The alpha vane is assumed to capture the x-z component of the local velocity field and ignore cross flow in the y direction. Flow field velocity is turned into indicated angle-of-attack and angle-of-attack position correction with the following equations:

$$\alpha_i^\circ = \tan\left(\frac{V_z}{V_x}\right) * \frac{180}{\pi} \text{ degrees} \quad 5.3$$

$$\Delta\alpha_{pc}^\circ = \alpha_t - \alpha_i \text{ degrees} \quad 5.4$$

A DOS batch file is executed to step the CMARC model, with an off-body streamline located at the vane position, through angles-of-attack ranging from -8° to 20°. Local velocity components are then read from the location corresponding to the alpha vane. Table 5.4 lists the values of  $\Delta\alpha_{pc}$  calculated from CMARC data. Figure 5.8 displays  $\Delta\alpha_{pc}$  as a function of indicated angle-of-attack. Linear and second order curve fit equations are also indicated on Figure 5.8. Angle-of-attack correction is fairly linear through the FROG operating envelope, with approximately -1.25 degrees of position error at the FROG cruise trim condition. The corrections apply at all incompressible airspeeds and all altitudes.

#### 5. Summary of Off-Body Flow Field Analysis

CMARC proved useful for both static-pressure source and alpha vane position corrections. Measured data may be corrected using look-up tables with the values in Table 5.3 and 5.4 or by using the curve fits in Figures 5.5 through 5.8. Flight testing is recommended for validation of sensor corrections obtained from this CMARC off-body flow field analysis.

UAV AOA $\alpha_T$ (deg)	Velocity at Alpha Vane			AOA <sub>Correction</sub> $\Delta\alpha = \alpha_T - \alpha_i$ (deg)	AOA <sub>Indicated</sub> $\alpha_i$ (deg)
	$V_x$ (ft/s)	$V_y$ (ft/s)	$V_z$ (ft/s)		
-8	80.92	1.66	-12.23	0.60	-8.60
-6	81.27	1.65	-8.65	0.08	-6.08
-3	81.60	1.64	-3.21	-0.75	-2.25
-2	81.67	1.63	-1.47	-0.97	-1.03
-1	81.71	1.63	0.28	-1.20	0.20
0	81.73	1.62	2.13	-1.49	1.49
1	81.73	1.61	3.93	-1.75	2.75
2	81.70	1.60	5.72	-2.00	4.00
3	81.66	1.59	7.51	-2.25	5.25
4	81.58	1.58	9.30	-2.50	6.50
5	81.48	1.57	11.08	-2.75	7.75
6	81.37	1.56	12.88	-2.99	8.99
8	81.07	1.53	16.43	-3.46	11.46
10	80.67	1.51	19.98	-3.91	13.91
12	80.17	1.48	23.50	-4.34	16.34
14	79.61	1.46	26.99	-4.73	18.73
16	78.93	1.43	30.47	-5.11	21.11
18	78.18	1.39	33.90	-5.44	23.44
20	77.34	1.36	37.31	-5.75	25.75

**Table 5.4    Angle-of Attack Vane Position Error Corrections for the NPS FROG UAV.    Derived from CMARC Panel Code Off-Body Flow Field Analysis.**

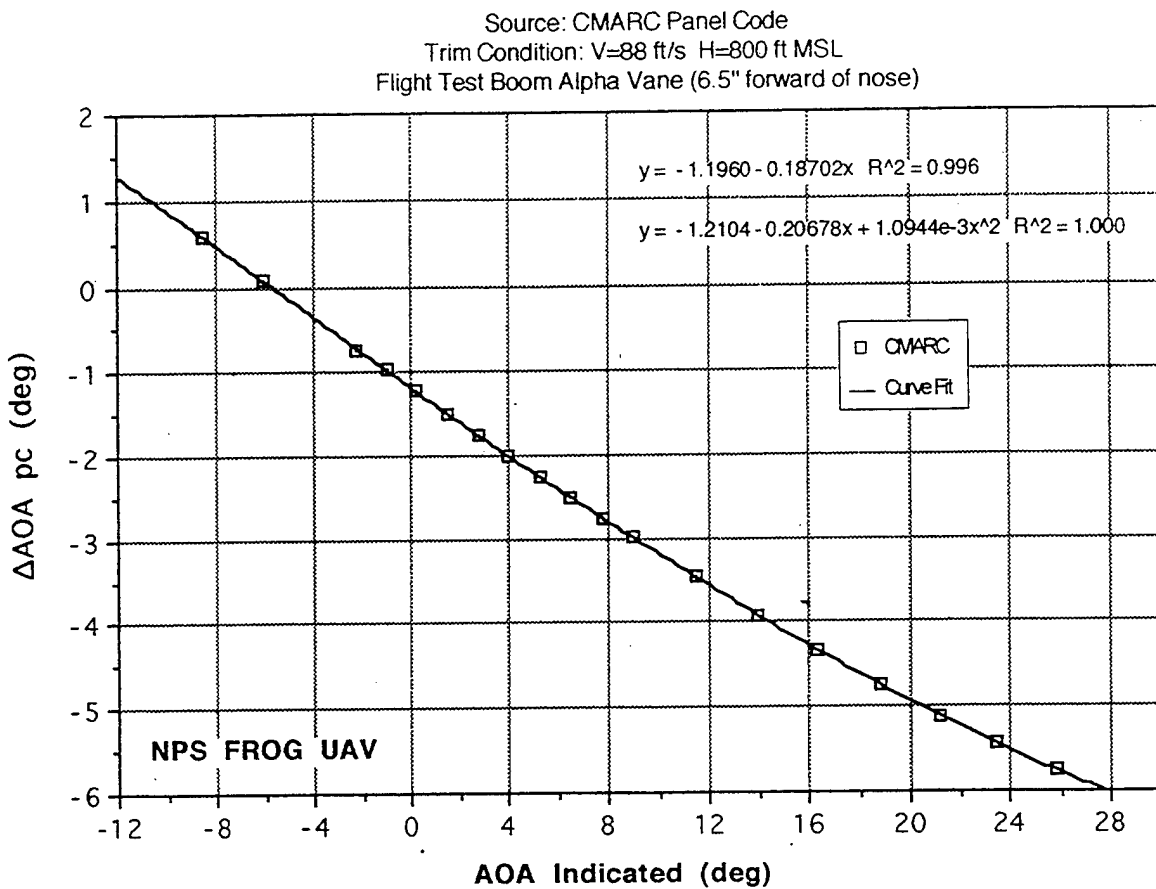


**Figure 5.8** Angle-of-Attack Vane Position Error,  $\Delta\alpha_{pc}$ , for the NPS FROG UAV.  
Derived from CMARC Panel Code Off-Body Flow Field Analysis.

## E. DEVELOPMENT OF BASIC STABILITY DERIVATIVES

In this section, CMARC is used to develop some of the basic longitudinal and lateral-directional stability derivatives for the FROG UAV. The development effort focuses on finding the  $C_{L\alpha}$  and  $C_{m\alpha}$  longitudinal stability derivatives followed by the  $C_{Y\beta}$ ,  $C_{l\beta}$  and  $C_{n\beta}$  lateral-directional stability derivatives. Control power and rate damping derivatives will be the focus of ongoing research.

CMARC contains built-in functionality to integrate forces and moments in all axes over the surface of a body. Forces and moments are automatically normalized into non-dimensional coefficients based on the mean aerodynamic chord, reference wing area, semi-span and center of gravity location in the CMARC BINP9 input line. Coefficients are presented in both wind and body axes. The CMARC model is run at two different angles-of-attack and one sideslip angle. The slope of the force and moment coefficients is then taken to produce the  $C_{L\alpha}$  and  $C_{m\alpha}$  longitudinal derivatives and the  $C_{Y\beta}$ ,  $C_{l\beta}$  and  $C_{n\beta}$  lateral-directional derivatives.

The CMARC model must be analyzed in the linear slope regions of  $\alpha$  and  $\beta$  for valid results. A potential flow solution will not produce satisfactory results for bodies with significant areas of flow separation.

### 1. Longitudinal Stability Derivatives

#### a. Longitudinal Stability Derivative Methods

Three basic longitudinal stability derivatives can be measured with just two runs of the CMARC model. The model is first analyzed at an angle-of-attack corresponding to the estimated trim condition. In this case,  $\alpha_t=0^\circ$  is selected for the first run. A second CMARC run is conducted with angle-of attack incremented one or two degrees.  $C_L$  and  $C_m$  are then extracted manually from the data files. The slope of  $C_L$  and  $C_m$  versus angle-of-attack provide the  $C_{L\alpha}$  and  $C_{m\alpha}$  longitudinal derivatives. For this study, several angles-of-attack were analyzed to check consistency of the slope. In addition,  $\alpha_{trim}$  is calculated from the lift curve slope and trim lift coefficient. Equations 5.5 through 5.7 are used for these calculations. For the longitudinal analysis, only half the model is analyzed. The symmetric calculation mode is selected by setting both  $RSYM=0.0$  and  $IPATSYM=0$  in the CMARC input file.

$$C_{L\alpha} = \frac{(C_{L2} - C_{L1})}{(\alpha_2 - \alpha_1)} * \frac{180}{\pi} \text{ per radian} \quad 5.5$$

$$C_{m\alpha} = \frac{(C_{m2} - C_{m1})}{(\alpha_2 - \alpha_1)} * \frac{180}{\pi} \text{ per radian} \quad 5.6$$

$$\alpha^\circ_{\text{trim}} = \alpha^\circ_1 + \frac{(C_{L_{\text{trim}}} - C_{L1})}{C_{L\alpha}} * \frac{180}{\pi} \text{ degrees} \quad 5.7$$

Several FROG UAV model configurations were analyzed in a build-up approach to check results against classical calculations and flight test data. Figure 5.9 shows the simplified CMARC models. First, just the wing and horizontal tail were considered. The patches for all other surfaces and wakes were turned off and the wing root was extended to centerline. The FROG fuselage was then analyzed separately and the results were added to the simplified wing and horizontal tail combination. Next, the original butted (low order fit) wing/fuselage and horizontal tail were considered. Finally, the blended wing/fuselage and horizontal tail were analyzed. Values of  $C_{L\alpha}$  and  $C_{m\alpha}$  for these four configurations are presented in Table 5.5.

Classical design calculations are also performed to estimate  $C_{m\alpha}$  for comparison to CMARC results. Equation 5.8 is used for the calculation of  $C_{m\alpha}$ . In classical design, the horizontal tail downwash derivative,  $d\epsilon/d\alpha$ , is generally selected from empirical data. Using a taper ratio of  $TR=1:1$  and aspect ratio of  $AR=6$ ,  $d\epsilon/d\alpha=0.4$  is selected from empirical charts in Ref. [14] for the FROG UAV configuration. A few other values of the horizontal tail downwash derivative,  $d\epsilon/d\alpha$ , are selected to see how well CMARC models downwash effects. Classical design estimates of  $C_{m\alpha}$  for values of  $d\epsilon/d\alpha$  ranging from 0 to 0.4 are presented in Table 5.5 for comparison with CMARC results.

$$C_{m\alpha} = a_w \left[ (h - h_{ac}) - V_H \frac{a_t}{a_w} \left( 1 - \frac{d\epsilon}{d\alpha} \right) \right] \quad 5.8$$



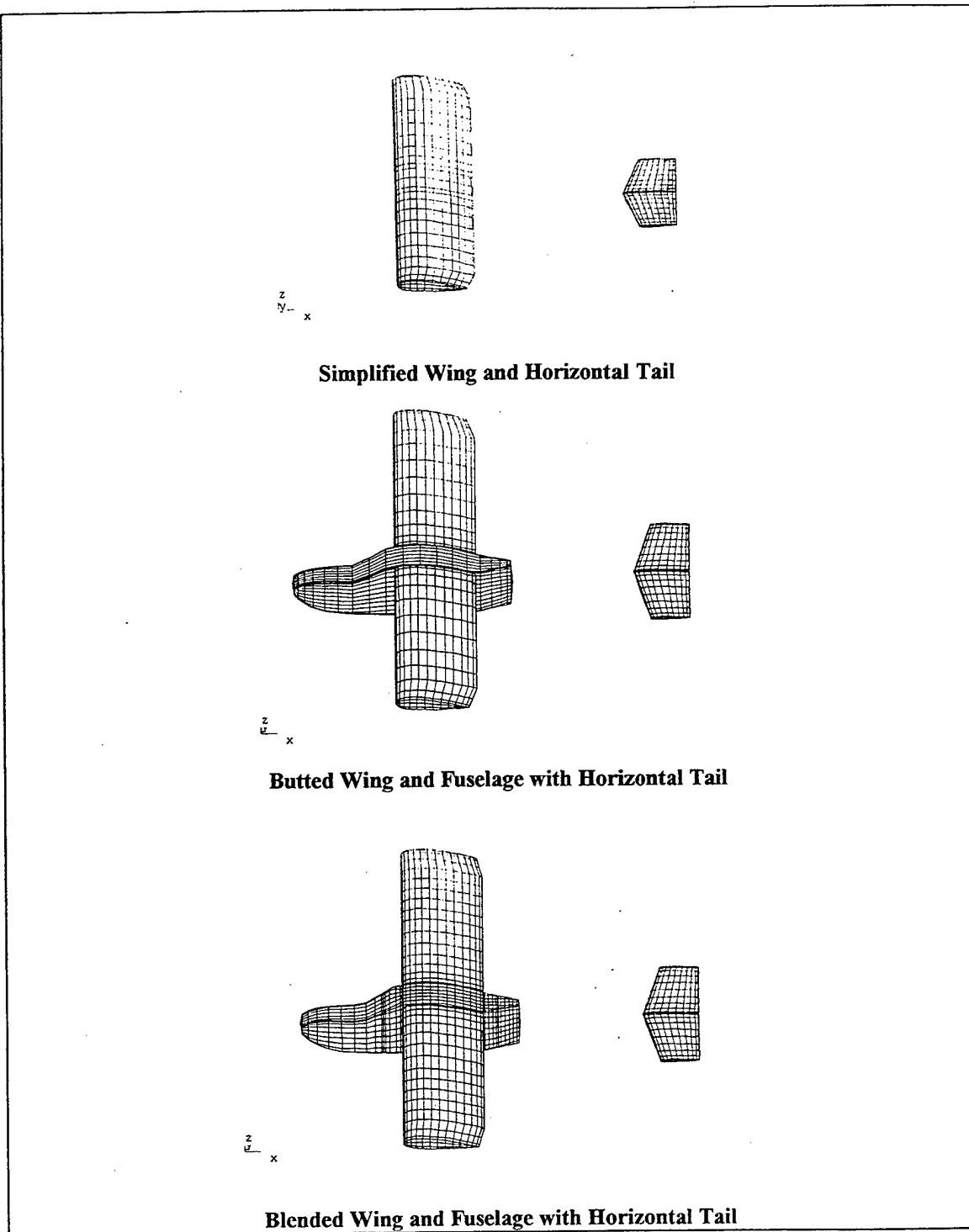


**Figure 5.9 Simplified CMARC Models of the FROG UAV for the Determination of Longitudinal Stability Derivatives.**

Flight test data for the short period and phugoid modes were used for longitudinal parameter estimation. Values for  $C_{L\alpha}$  and  $C_{m\alpha}$  based on preliminary parameter estimation work by Engdahl [pending publication] are presented in Table 5.5. Caution is advised against making definitive comparisons until the work is published.

METHOD	CONFIGURATION <sup>1</sup>	LONGITUDINAL PARAMETERS		
		$\alpha_{trim}^2$ (deg)	$C_{L\alpha}$ (per rad)	$C_{m\alpha}$ (per rad)
CMARC Panel Code	Wing/Horiz Tail	-0.87	4.86	-0.835
	Wing/Horiz Tail + Fuselage	-0.86	4.78	-0.608
	Blended Wing-Fuselage/Horiz Tail	-0.01	4.72	-1.105
	Butted Wing-Fuselage/Horiz Tail	-0.8	5.37	-1.348
Classical Design <sup>3</sup>	Wing/Horiz Tail - $\delta\epsilon/\delta\alpha=0$	-0.78	4.89	-1.50
	Wing/Horiz Tail - $\delta\epsilon/\delta\alpha=0.25$	-0.81	4.85	-1.00
	Wing/Horiz Tail - $\delta\epsilon/\delta\alpha=0.35$	-0.82	4.83	-0.80
	Wing/Horiz Tail - $\delta\epsilon/\delta\alpha=0.40$	-0.82	4.82	-0.70
Parameter Estimation <sup>4</sup>	Flying Aircraft	n/a	4.09	-0.42

NOTES: 1)  $CG_x=34.5\%$  M.A.C. /  $CG_z=8.6"$  from bottom of fuselage.

2) Zero lift wing incidence is  $+6.5^\circ$  from the longitudinal reference line.

3) Classical Design after Ref. [14].

4) Unpublished parameter estimation from flight test data by Engdahl.

**Table 5.5 Comparison of FROG UAV Longitudinal Stability Derivatives.**

***b. Analysis of Longitudinal Stability Data***

The first three configurations in Table 5.5 produce good results for  $C_{L\alpha}$  and reasonable values for  $C_{m\alpha}$ . However, the fourth configuration, the butted wing root and fuselage, produces excessively large values of both  $C_{L\alpha}$  and  $C_{m\alpha}$ . This configuration should be avoided in future models. It is recommended that CMARC model developers spend the time up front to produce the higher fidelity model from the start.

The values produced for  $C_{m\alpha}$  from CMARC are somewhat high when compared with to the classical design calculations. Clearly, some downwash is sensed by the horizontal tail in the CMARC analysis because all values for  $C_{m\alpha}$  are considerably less

than the classical calculation with  $d\varepsilon/d\alpha=0$ . Still, high values compared to flight test data indicates that CMARC has a difficult time capturing the complete  $d\varepsilon/d\alpha$  downwash effect. This could be due to the requirement to select rigid wakes to prevent the wing wake from impacting the horizontal tail. A more careful wake definition may help capture the tail downwash derivative with more fidelity. A study by Walden et al. [Ref. 15] studied wake turbulence by modeling an aircraft flying in trail of a wake generating wing. A horizontal tail trailing the main wing is a similar configuration. The study found that a streamline-based wake is the best method for modeling downwash effects. This wake definition should be investigated for modeling the  $C_{m\alpha}$  derivative. Of note, the wake diffusion process is neglected in a potential flow analysis.

In summary, CMARC produced accurate values for  $C_{L\alpha}$  and slightly high values of  $C_{m\alpha}$ . Difficulties were encountered trying to model the horizontal tail downwash derivative. A more careful study of the effects of wing wake placement on the downwash derivative is recommended.

## **2. Lateral Directional Stability Derivatives**

### ***a. Lateral-Directional Stability Derivative Methods***

Development of the lateral-directional stability derivatives is more straight forward than for the longitudinal derivatives because the vertical tail sidewash angle plays a lesser role. However, both sides must be modeled by setting both  $RSYM=1.0$  and  $IPATSYM=1$ . This creates symmetric patches around the  $y=0$  plane allowing CMARC to perform asymmetric calculations around the entire body and significantly increases processing times.

For the lateral-directional axis, the aircraft is modeled with the blended wing and fuselage in combination with the vertical and horizontal stabilizers as shown in Figure 5.10. The engine nacelle and pylon are left off because their wakes impact the vertical tail. In addition, the pylon/fuselage and pylon/nacelle junctions were meshed with a low order, butted fit. This type of junction was found to produce poor results during the longitudinal stability study.

The model is first checked for lateral directional balance at zero yaw angle. The side force, rolling and yawing coefficients should be zero when a trial run is

performed at zero yaw angle. If lateral-directional forces or moments are present, the model and wake geometry should be checked for symmetry.

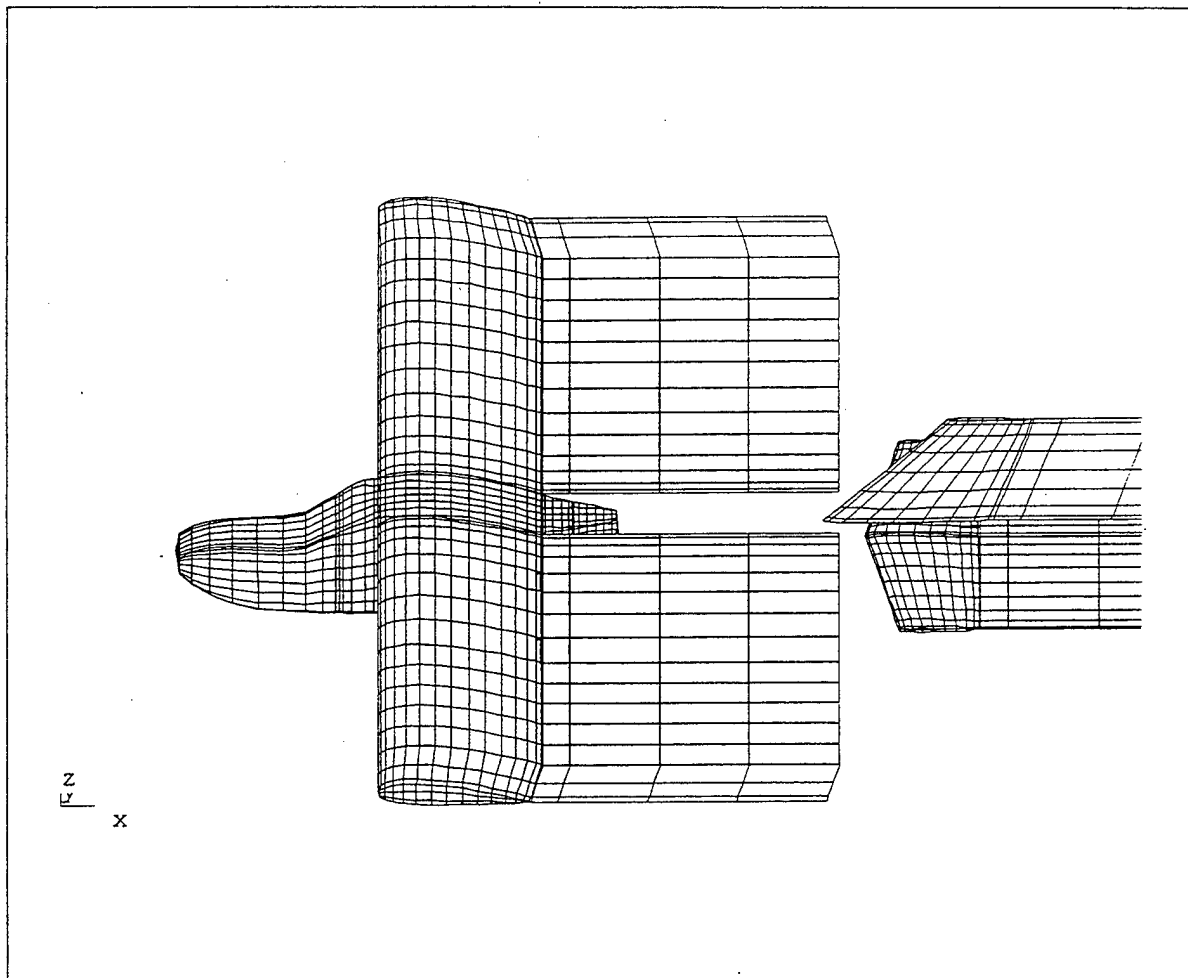


**Figure 5.10 Simplified CMARC Model of the FROG UAV for the Determination of Lateral-Directional Stability Derivatives.**

Next, a single CMARC run is performed with  $\alpha = \alpha_{\text{trim}}$  and yaw angle set to one degree. The lateral-directional derivatives,  $C_{Y\beta}$ ,  $C_{l\beta}$  and  $C_{n\beta}$ , are then obtained directly with equations 5.9 through 5.11:

$$C_{Y\beta} = \frac{C_Y}{\Delta\beta^\circ} * \frac{180}{\pi} \text{ per radian} \quad 5.9$$

$$C_{l\beta} = \frac{C_l}{\Delta\beta^\circ} * \frac{180}{\pi} \text{ per radian} \quad 5.10$$

$$C_{n\beta} = \frac{C_n}{\Delta\beta^\circ} * \frac{180}{\pi} \text{ per radian} \quad 5.11$$

It should be noted that the stability axis as modeled (x-aft and z-up) differs from the standard flight dynamics stability axis. Care must be taken to reverse the signs of the appropriate coefficients to convert from a CMARC model's stability axis into the flight dynamics stability axes

#### ***b. Analysis of Lateral-Directional Stability Data***

Lateral-directional stability derivatives obtained from CMARC are presented in Table 5.6. For comparison three other sets of data are also presented. The first comes from the classical analysis presented by Papageorgiou in Ref. [1]. The second set comes from estimates based on data recorded from flight test static sideslip maneuvers, also published in Ref. [1]. The third set comes from parameter estimation by Engdahl based on dynamic flight test data. It is unpublished and should be considered preliminary. In all cases, the CMARC lateral-directional stability derivatives produce a closer match to flight test data than those derived from classical methods. It is concluded that CMARC is a good tool for lateral-directional stability analysis.

### **3. Summary of CMARC Stability Derivative Analysis**

In summary, for the longitudinal axis, CMARC produces accurate values for  $\alpha_{trim}$  and  $C_{L\alpha}$  and slightly high values of  $C_{ma}$ . Difficulties may be encountered while trying to model the horizontal tail downwash derivative. A more careful study of the effects wing wake placement on the downwash derivative is recommended. Specifically, modeling should include streamline-based wake placement techniques [Ref. 15]. Analysis of the lateral-directional axis proves more straightforward. Lateral-directional derivatives from CMARC for  $C_{Y\beta}$ ,  $C_{l\beta}$  and  $C_{n\beta}$  provide a closer match to flight test data than the classical estimates. The engine nacelle and pylon should be re-meshed and included in future studies.

Overall, CMARC derived stability derivatives are sufficiently accurate for entry into an initial aerodynamic model. Adjustments through analysis of flight test data will still be required. Future CMARC studies should concentrate on developing the rate damping and control power derivatives.

METHOD	CONFIGURATION <sup>1</sup>	LAT-DIR PARAMETERS		
		$C_{Y\beta}$ (per rad)	$C_{l\beta}$ (per rad)	$C_{n\beta}$ (per rad)
CMARC Panel Code	Blended Wing-Fuselage/Horz/Vert Tails	-0.573	-0.063	0.120
Classical Design <sup>2</sup>	Wing/Fuselage/Vert Tail	-0.310	-0.051	0.058
Flight Test <sup>3</sup>	Flying Aircraft	-0.700	-0.053	0.057
Parameter Estimation <sup>4</sup>	Flying Aircraft	-0.987	-0.094	0.176

NOTES: 1)  $CG_x=34.5\%$  M.A.C. /  $CG_z=8.6"$  from bottom of fuselage.

2) Classical Design calculations by Papageorgio, from Ref. [1].

3) Flight test results from Steady Heading Sideslip, from Ref. [1]

4) Unpublished parameter estimation from flight test data by Engdahl.

**Table 5.6 Comparison of FROG UAV Lateral-Directional Stability Derivatives.**

## VI. CONCLUSIONS AND RECOMMENDATIONS

CMARC is a DOS personal computer hosted panel code adopted from the NASA Ames PMARC code. AeroLogic, Inc., created CMARC by converting PMARC FORTRAN 77 source code into the C language. Significant memory management and command line enhancements were also added. CMARC solves for inviscid, incompressible flow over complex three-dimensional bodies. Emphasis in this study is first placed on verifying CMARC against the PMARC and Naval Postgraduate School Unsteady Potential Flow (UPOT) panel codes. CMARC pressure distributions and boundary layer calculations are then compared to experimental data for an inclined prolate spheroid. Finally, a complex three-dimensional panel model of the Naval Postgraduate School FROG UAV is developed which successfully generates static-pressure source position corrections, alpha vane correction curves and basic stability derivatives.

CMARC results are found to be equivalent to the NASA-Ames PMARC panel code. As expected, pressure distribution and boundary layer calculations from CMARC match exactly those obtained with PMARC. The following enhancements are noteworthy. CMARC, hosted on a Pentium class PC, processes input files significantly faster than PMARC hosted on a networked SGI Indigo<sup>2</sup> UNIX workstation. CMARC's extensive command line functionality greatly enhances batch file processing capabilities. On the other side, CMARC's poor error flagging capability leaves the user frequently spending much time searching for input file mistakes. Improved input file error checking should be incorporated into CMARC functionality.

CMARC integral boundary layer calculations are compared to the two-dimensional finite difference methods implemented in the UPOT code. In general, CMARC provides correct trends for both the transition and separation points. However, in all cases, CMARC predicts early transition and late flow separation. As expected, the differences are greatest at lower Reynolds numbers where boundary layer thickness is larger. An adjustment of the empirical transition and separation models contained in CMARC may prove useful.

CMARC calculations are also compared to wind tunnel data for a 6:1 inclined prolate spheroid model at 10 degrees angle-of-attack. With proper wake placement, CMARC can produce accurate normal force and pitching moment coefficients. Over the three dimensional body, CMARC boundary layer calculations also predict early transition

and late flow separation. Despite inaccuracies, CMARC boundary layer calculations remain useful when used as a design tool for visualizing the trend in transition and separation points with configuration changes.

CMARC integrated skin friction forces are compared to prolate spheroid wind tunnel data. Normal, axial, and pitching moment coefficients for skin friction forces are underpredicted by CMARC, but remain within 40% of integrated experimental data.

The LOFTSMAN and POSTMARC portions of the Personal Simulation Works software suite are used exclusively for the pre-process modeling and post-process visualization of CMARC files. The LOFTSMAN capability to automatically format and generate CMARC input patches is an enhancing characteristic. Functionality should be added to allow the modeling of wing tip ribs that are not parallel to the aircraft butt line.

POSTMARC is an excellent tool for visualizing CMARC output files. The capability to create streamlines and perform boundary layer calculations external to CMARC is extremely useful. However, much time could be saved if POSTMARC maintained previous settings and selections following translations, rotations and re-scaling. Additionally, a capability to overlay multiple data types is desired.

CMARC off-body flow field analysis is useful for both static-pressure source and alpha vane position corrections. Measured data may be corrected using look-up tables or through curve fits of CMARC derived data. Flight testing is recommended for validation of sensor corrections obtained from the CMARC off-body analysis.

For the longitudinal analysis, CMARC produces accurate values for  $\alpha_{trim}$  and  $C_{L\alpha}$  and slightly high values of  $C_{m\alpha}$ . Some difficulties are encountered trying to model the horizontal tail downwash derivative. A more careful study of the effects of wing wake placement on the downwash derivative is recommended.

Analysis of the lateral-directional axis proves more straightforward. Lateral-directional derivatives from CMARC for  $C_{Y\beta}$ ,  $C_{l\beta}$  and  $C_{n\beta}$  provide a closer match to flight test data than classical design calculations. Adjustments through analysis of flight test data may still be required. The engine nacelle and pylon should be re-meshed and included in future studies.

Overall, the CMARC panel code is found to be suitable for aerodynamic modeling of the Naval Postgraduate School FROG UAV. CMARC derived stability derivatives are sufficiently accurate for incorporation into an initial aerodynamic model. Future CMARC studies should concentrate on the development of the rate damping and control power derivatives.



## APPENDIX A.

### DEVELOPMENT OF THE MOMENTUM INTEGRAL EQUATION

The CMARC and PMARC User's Guides contain the development of the implemented boundary layer equations starting from the two-dimensional momentum integral equation. For completeness, the momentum integral equation is developed here to provide continuity.

The development of the momentum boundary layer equations is outlined by Young in Ref. [9]. In 1904 Prandtl first presented his *Boundary Layer Theory* based on the following observations:

- 1) However small the viscosity of a fluid, it cannot be ignored. At the surface, the fluid is at rest compared to the body (no slip condition).
- 2) Shear stresses are directly proportional to the rates of strain.
- 3) The ratio of inertial forces to viscous forces, or Reynolds number, is important in characterizing flow phenomena.
- 4) The full non-linear viscous Navier-Stokes equations are difficult to solve directly. Prandtl observed that simplifications could be made when assuming a thin boundary layer. Viscosity can be ignored outside the boundary layer allowing the use of classical inviscid methods.

Thin boundary layer theory also assumes that the pressure distribution outside the thin boundary layer is transmitted normally through the boundary layer to the surface without loss. CMARC takes advantage of this assumption by neglecting the thickness of the boundary layer and imposes a potential flow solution over the surface.

The momentum integral equation for two-dimensional incompressible flow is the starting point for the boundary layer analysis outlined in References [2] and [4]. It is obtained through the following total energy integral analysis as outlined by Young in Ref. [9].

Figure A.1 depicts an incremental portion of a two-dimensional boundary layer. The mass flow rate ( $\dot{m}$ ) across each side is given by:

$$\dot{m}_{AD} = 0$$

$$\dot{m}_{DC} - \dot{m}_{AB} = \frac{d}{dx} \left[ \int_0^h \rho u dz \right] \Delta x + O(\Delta x^2)$$

$$\dot{m}_{BC} = \rho_e w_h \Delta x \quad \text{and} \quad \dot{m}_{DC} - \dot{m}_{AB} = \dot{m}_{BC} \quad \text{from continuity.}$$

A.1

$$\therefore \rho_e w_h = \frac{d}{dx} \left[ \int_0^h \rho u dz \right] + O(\Delta x)$$

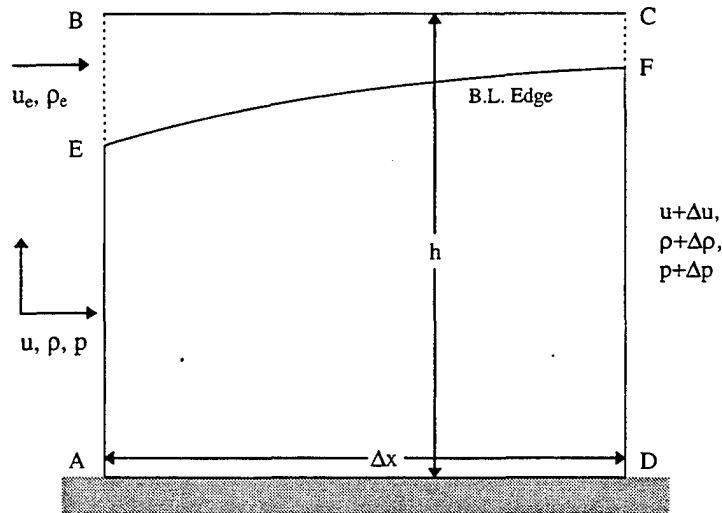


**Figure A.1** Elementary boundary layer section for deriving the momentum integral equation for two-dimensional flow, after Ref. [9].

Similarly, the rate of momentum transport across each boundary is given by:

$$\begin{aligned}
 AD: &= 0 \\
 DC - AB: &= \frac{d}{dx} \left[ \int_0^h \rho u^2 dw \right] + O(\Delta x^2) \\
 BC: &= \rho w_h \cdot u_e \Delta x = u_e \frac{d}{dx} \left[ \int_0^h \rho u dz \right] \Delta x + O(\Delta x^2)
 \end{aligned} \tag{A.2}$$

The force due to pressure on the sectional boundary layer element is given by:

$$= -h \Delta p = -h \left( \frac{dp}{dx} \right) \Delta x + O(\Delta x^2) \tag{A.3}$$

And, the friction force exerted by the wall is:

$$= -\tau_w \cdot \Delta x \tag{A.4}$$

Summing the momentum terms and equating them to the forces while taking the limit as  $\Delta x \rightarrow 0$  yields the momentum integral equation:

$$\frac{d}{dx} \left( \int_0^h \rho u dz \right) = -h \frac{dp}{dx} - \tau_w \tag{A.5}$$

It is more convenient to express the relation in terms of displacement and momentum thickness by substituting the following:

$$-\frac{dp}{dx} = \rho_e u_e \frac{du_e}{dx} \tag{A.6}$$

The momentum integral is then reduced to:

$$\frac{d}{dx} \left[ \int_0^h \rho u (u - u_e) dz \right] + \frac{du_e}{dx} \left[ \int_0^h \rho u dz \right] = h \rho_e u_e \frac{du_e}{dx} - \tau_w \rightarrow \frac{d}{dx} \left[ \int_0^h \rho u (u - u_e) dz \right] + \frac{du_e}{dx} \left[ \int_0^h (\rho u - \rho u_e) dz \right] = -\tau_w$$

$$\text{or } \frac{d}{dx} (\rho_e u_e^2 \theta) + \frac{du_e}{dx} \rho_e u_e \delta^* = \tau_w \tag{A.7}$$

$$\text{Where } d^* = \int_0^h \left(1 - \frac{ru}{r_e u_e}\right) dz \quad \text{and} \quad q = \int_0^h \frac{ru}{r_e u_e} \left(1 - \frac{u}{u_e}\right) dz \quad \text{A.8}$$

Substituting  $H = \delta^*/\theta$ , where H is the boundary layer shape factor, and rearranging after the chain rule, the momentum integral can be written in as:

$$\frac{d\theta}{dx} + \frac{1}{u_e} \frac{du_e}{dx} \theta(H+2) + \frac{\theta}{\rho_e} \frac{d\rho_e}{dx} = \frac{\tau_w}{\rho_e u_e^2} \quad \text{A.9}$$

And finally, by substituting  $C_f = \frac{\tau_w}{\frac{1}{2} \rho_e u_e^2} = \frac{2\tau_w}{\rho_e u_e^2}$ , one obtains Equation 16 in References [2]

and [4]:

$$\frac{d\theta}{dx} + \frac{1}{u_e} \frac{du_e}{dx} \theta(H+2) + \frac{\theta}{\rho_e} \frac{d\rho_e}{dx} = \frac{C_f}{2} \quad \text{A.10}$$

From here, the CMARC or PMARC guides provide a detailed development of the implemented boundary layer models.

## APPENDIX B.

### INTEGRATION OF AERODYNAMIC FORCES OVER THE SURFACE OF A PROLATE SPHEROID

The experimental set-up in Ref. [12] did not include measurement of forces. However, it was deemed that the 2000+ pressure and 500+ skin friction measurements would be sufficient to allow the integration of measurements over the surface of the prolate spheroid for a good approximation of total force and moment coefficients. The following technique is developed to provide an estimate of integrated pressure and friction forces. Symmetry is assumed. Appendix C lists the entire MATLAB program which implements the technique that follows.

In general the pressure force is given by:

$$\bar{F}_p = \iint_S P \bar{n} dS, \quad \bar{n} \text{ is a unit surface normal} \quad \text{B.1}$$

However, the test data is provided discretely in cylindrical coordinates, resulting in the following discrete double summation:

$$\bar{F}_p = \sum_{x/2a} \sum_{\phi} P \bar{n} r \Delta \phi \Delta x / 2a, \quad \text{where } dS = r \Delta \phi \Delta x / 2a \quad \text{B.2}$$

Figure B.1 shows a diagram of the pressure and skin friction acting over the incremental surface areas,  $\Delta S$ . The pressure and skin friction coefficients, scalars, are assumed to be constant over the incremental surface.

$$\Delta \bar{F}_p = P \bar{n} r \Delta \phi \Delta x / 2a = (q C_p + p_\infty) \bar{n} \Delta S, \quad \text{B.3}$$

$$\text{where } C_p = \frac{P - P_\infty}{q} \Rightarrow P = C_p \cdot q + P_\infty \quad \text{B.4}$$

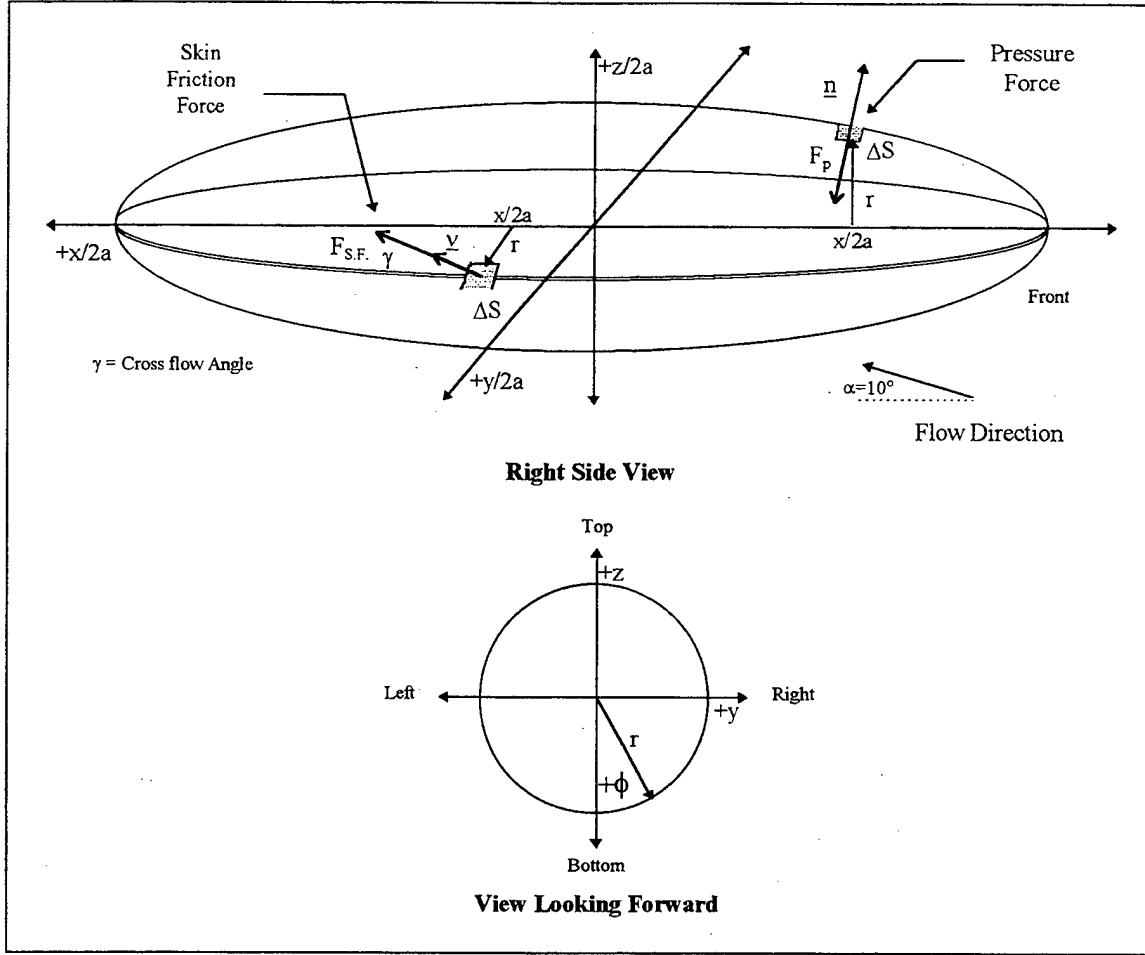


**Figure B.1 Prolate Spheroid Geometry and Forces**

Free stream pressure ( $P_\infty$ ), assumed to be constant, can be dropped from the integration due to symmetry. This leaves the following relation:

$$F_p = \sum_{x/2a=0}^1 \sum_{\phi=0}^{360} q C_p \bar{n} r \Delta \phi \Delta x / 2a \quad \text{B.5}$$

Likewise, skin friction can also be integrated using the following relations:

$$\Delta F_{sf} = q C_f \bar{v} \Delta S = q C_f \bar{v} r \Delta \phi \Delta x / 2a, \text{ where } \bar{v} \text{ is a unit velocity vector} \quad \text{B.6}$$

$$F_{SF} = \sum_{x/2a=0}^1 \sum_{\phi=0}^{360} q C_f r \bar{v} \Delta \phi \Delta x / 2a$$

B.7

The pressure force coefficients, normalized by  $S = \pi b^2$  and  $\bar{c} = 2b$ , are yielded by discretely integrating the following equations in a cylindrical coordinate system:

$$C_{N_p} = \frac{N_p}{q_\infty S}, \quad N_p = 2 \sum_{i=1}^m \sum_{j=1}^n - (q_\infty C_p r \bar{n}) \cdot \bar{k} \Delta \phi_j \Delta x_i / 2a \quad \text{B.8}$$

$$C_{A_p} = \frac{A_p}{q_\infty S}, \quad A_p = 2 \sum_{i=1}^m \sum_{j=1}^n - (q_\infty C_p r \bar{n}) \cdot \bar{i} \Delta \phi_j \Delta x_i / 2a \quad \text{B.9}$$

$$C_{M_p} = \frac{M_p}{q_\infty S \bar{c}}, \quad M_p = 2 \sum_{i=1}^m \sum_{j=1}^n [(q_\infty C_p r \bar{n}) \cdot (x_i / 2a \cdot \bar{k} - z_i / 2a \cdot \bar{i})] \Delta \phi_j \Delta x_i / 2a \quad \text{B.10}$$

Where the surface unit normal is given by:

$$\text{Unit Normal: } \bar{n} = -\frac{m}{\sqrt{m^2 + 1}} \bar{i} + \frac{\sin(\phi)}{\sqrt{m^2 + 1}} \bar{j} - \frac{\cos(\phi)}{\sqrt{m^2 + 1}} \bar{k} \quad \text{B.11}$$

The skin friction coefficients, normalized by  $S = \pi b^2$  and  $\bar{c} = 2b$ , are yielded by discretely integrating the following equations in a cylindrical coordinate system:

$$C_{N_{SF}} = \frac{N_{SF}}{q_\infty S}, \quad N_{SF} = 2 \sum_{i=1}^m \sum_{j=1}^n (q_\infty C_f r \bar{v}) \cdot \bar{k} \Delta \phi_j \Delta x_i / 2a \quad \text{B.12}$$

$$C_{A_{SF}} = \frac{A_{SF}}{q_\infty S}, \quad A_{SF} = 2 \sum_{i=1}^m \sum_{j=1}^n (q_\infty C_f r \bar{v}) \cdot \bar{i} \Delta \phi_j \Delta x_i / 2a \quad \text{B.13}$$

$$C_{M_{SF}} = \frac{M_{SF}}{q_\infty S \bar{c}}, \quad M_{SF} = 2 \sum_{i=1}^m \sum_{j=1}^n [(q_\infty C_f r \bar{v}) \cdot (-x_i / 2a \cdot \bar{k} + z_i / 2a \cdot \bar{i})] \Delta \phi_j \Delta x_i / 2a \quad \text{B.14}$$

Where the unit surface velocity vector is given by:

$$\bar{v} = \frac{\cos(\gamma)}{\sqrt{m^2 + 1}} \bar{i} + \left[ \frac{m \sin(\phi) \cos(\gamma)}{\sqrt{m^2 + 1}} + \cos(\phi) \sin(\gamma) \right] \bar{j} + \left[ -\frac{m \cos(\phi) \cos(\gamma)}{\sqrt{m^2 + 1}} + \sin(\phi) \sin(\gamma) \right] \bar{k}$$

B.15

The surface and local slope of a prolate spheroid comes from the following relations:

$$\text{Prolate Spheroid: } \frac{x^2}{a^2} + \frac{r^2}{b^2} = 1 \quad \Rightarrow \quad \text{slope } m = \frac{dr}{dx} = -\frac{bx}{a^2 \sqrt{1 - \frac{x^2}{a^2}}} \quad \text{B.16}$$

Note: The forces are summed over half the spheroid,  $\phi = 0 \rightarrow 180^\circ$ , and doubled.

The y-direction forces and the roll and yaw moments are neglected zero due to symmetry.



## APPENDIX C.

### MATLAB PROGRAMS TO INTEGRATE AERODYNAMIC FORCES OVER THE SURFACE OF A PROLATE SPHEROID

Jun 4 1997 02:18	icp_prolate.m	Page 1
------------------	---------------	--------

```

% This Matlab M-file script performs a first order (linear approximation)
% integration of pressure forces over a 6:1 prolate spheroid. Central Differencing
% of location is used for the first order integration routine. Data is input from
% AGARD AR-303 Test C-2 as rotation angle, x/c, and Cp. Data is for two test
% conditions, AOA = 10 and 29.7 degrees.

clear
% Load in experimental data for AOA = 10 degrees, Re = 7.7x10e6, Vinf = 55 m/s:
% M = 0.162
load cpl0data
fid1=fopen('icp10raw','r+'); %open file for printing step data for error checking
fprintf(fid1,'i      j      l      phi      dphi      x      M      r      dx      Cp
nx      ny      nz      dS      dN      dA      dm      \n');
data = [cpl0data(:,2) cpl0data(:,4) cpl0data(:,5)]; % Extract columns 2,4,5
nphi = 40; nxc = 42; %Initialize # of rotation steps and pressure ports
m = 0; N = 0; A = 0; Si = 0; % Initialize summed forces to zero
a = 0.5; b = 0.5/6; % a and b for 6:1 Prolate Spheroid
S = pi*b^2; % Reference area - max cross section
for i = 1:nphi
    for j = 1:nxc
        l = (i-1)*nxc+j;
        phi = data(l,1);
        x = data(l,2)-a;
        Cp = data(l,3);
        r = b*sqrt(1-x^2/a^2);
        M = -b*x/(a^2*sqrt(1-x^2/a^2+.000001));
        z = -r*cos(phi);
        nx = -M/sqrt(M^2+1);
        ny = sin(phi/57.296)/sqrt(M^2+1);
        nz = -cos(phi/57.296)/sqrt(M^2+1);
        nt=sqrt(nx^2+ny^2+nz^2);
        if j == 1
            dx = data(l+1,2)/2; % dx at first pressure port
        elseif j == nxc
            dx = (2*a-data(l-1,2))/2; % dx at last pressure port
        else
            dx = (data(l+1,2)-data(l-1,2))/2; % central differencing at interme
diate pressure ports
        end
        if i == 1
            dphi = data((i*nxc+1),1)/2;
        elseif i == nphi
            dphi = (180-data(((i-1)*nxc),1))/2;
        else
            dphi = (data((i*nxc+1),1)-data(((i-1)*nxc),1))/2;
        end
        dS = r*dphi/57.296*dx*sqrt(M^2+1);
        dN = 2*(-Cp)*dS*nz;
        dA = 2*(-Cp)*dS*nx;
        dm = 2*(-Cp)*dS*(-x*nz+z*nx);
        N = N+dN;
        A = A+dA;
        m = m+dm;
        raw(l,:)=[i j l phi dphi x M r dx Cp nx ny nz dS dN
dA dm];
        Si=Si+2*dS;
    end
end
end
CN_AOA10 = N/S
CA_AOA10 = A/S
CM_AOA10 = m/(S*2*b)
Si
fprintf(fid1,'%3.0f %3.0f %5.0f %5.2f %6.4f %4.3f %5.2f %6.3f %6.4f %4.3f
%4.3f %4.3f %4.3f %8.7f %8.7f %8.7f %8.7f\n','raw');
fprintf(fid1,'i      j      l      phi      dphi      x      M      r      dx      Cp
nx      ny      nz      dS      dN      dA      dm      \n');
fclose('all');
```

```

% This Matlab M-file script performs a first order (linear approximation)
% integration of skin friction over a 6:1 prolate spheroid. Central Differencing
% of location is used for the first order integration routine. Data is input from
% AGARD AR-303 Test C-2 as rotation angle, x/c, Cf and gamma (crossflow angle). Data
% is for two test
% conditions, AOA = 10
clear
% Load in experimental data for AOA = 10 degrees, Re = 7.7x10e6, Vinf = 55 m/s:
% M = 0.162
load cf10reorder
%fid1=fopen('icf10raw','r+');
%fprintf(fid1,'i      j      l      phi      dphi      x      r      m      dx      Cf
gamma      vx      vy      vz      dS      dN      dA      dm \n');

data = [cf10reorder(:,2) cf10reorder(:,1) cf10reorder(:,3) cf10reorder(:,4)]; % Extract
columns 2,4,5
nphi = 74; nxc = 12; % Initialize # of rotation steps and pressure ports
Nsf=0; Asf=0; msf=0;
m = 0; N = 0; A = 0; Si=0; % Initialize summed forces to zero
a = 0.5; b = 0.5/6; % a and b for 6:1 Prolate Spheroid
S = pi*b^2; % Reference area - max cross section
for i = 1:nxc
    for j = 1:nphi
        l = (i-1)*nphi+j;
        phi = data(l,1);
        x = data(l,2)-a;
        Cf = data(l,3);
        gamma = data(l,4);
        r = b*sqrt(1-x^2/a^2);
        M = -b*x/(a^2*sqrt(1-x^2/a^2+.000001));
        z = -r*cos(phi);
        vx = cos(gamma/57.3)/sqrt(M^2+1);
        vy = M*sin(phi/57.296)*cos(gamma/57.3)/sqrt(M^2+1)+cos(phi/57.3)*sin(gamma/
57.3);
        vz = -M*cos(phi/57.296)*sin(gamma/57.3)/sqrt(M^2+1)+sin(phi/57.3)*sin(gamma
/57.3);
        nt=sqrt(vx^2+vy^2+vz^2);
        if i == 1
            dx = data(nphi+1,2)/2; % dx at first hot film sensor
        elseif i == nxc
            dx = (2*a-data(((i-1)*nphi),2))/2; % dx at last hot film
sensor
        else
            dx = (data((i*nphi+1),2)-data(((i-1)*nphi),2))/2;
        end
        if j == 1
            dphi = data((l+1),1)/2;
        elseif j == nphi
            dphi = (180-data(l-1,1))/2;
        else
            dphi = (data(l+1,1)-data(l-1,1))/2;
        end
        dS = r*dphi/57.296*dx*sqrt(M^2+1);
        dN = 2*(Cf)*dS*vz;
        dA = 2*(Cf)*dS*vx;
        dm = 2*(Cf)*dS*(-x*vz+z*vx);
        Nsf = Nsf+dN;
        Asf = Asf+dA;
        msf = msf+dm;
        raw(l,:)=[i j l phi dphi x M r dx Cf gamma vx vy vz
% ds dN dA
end
end
end
CNsf_AOA10 = Nsf/S
CAsf_AOA10 = Asf/S
CMsf_AOA10 = msf/(S^2*b)
%fprintf(fid1,'%3.0f %3.0f %5.0f %5.2f %6.4f %4.3f %5.2f %6.3f %6.4f %6.5f
%4.1f %4.3f %4.3f %8.7f %8.7f %8.7f %8.7f\n ',raw');
%fclose('all');

```

Jun 20 1997 04:39 24p1600.in Page 1

HACA2415 RECTANGULAR WING - 1600 Panels for CHARC/PHARC Time Trials  
 b=20 FT, cbar=1.00 FT, AR = 20 Re = 1,000,000 Vinf = 157.23 FT/S  
 File purpose: For comparison of CHARC / PHARC processing times.

Created: 5/18 by Steve Pollard

```

&BINP2 LSTINP=2, LSTOUT=0, LSTFRQ=0, LENRUN=0, LPLTYP=1, &END
&BINP3 LSTGEO=0, LSTNAB=0, LSTWAK=0, LSTCPV=0, &END
&BINP4 MAXIT=500, SOLRES=0.0005, &END
&BINP5 NTSTPS= 10, DTSTEP=0.5, &END
&BINP6 RSYM=0.0, RGPR=0.0, RFF=5.0, RCORES=0.0080, RCREW=0.0080, &END
&BINP7 VINF=157.23, VSOUND=1116.0, &END
&BINP8 ALDEC= 10.00, YAWDEC=0.0, PHIDOT=0.0, THEDOT=0.0, PSIDOT=0.0, &END
&BINP8A PHIMAX= 0.0, THEMAX= 0.0, PSIMAX=0.0, &END
&BINP8B WRX=0.0, WRY=0.0, WRZ=0.0, &END
&BINP8B DXMAX=0.0, DYMAX=0.0, DZMAX=0.0, &END
&BINP8B WTX=0.0, WTY=0.0, WTZ=0.0, &END
&BINP9 CBAR=1.00, SREF=20, SSPAN= 10, &END
&BINP9 RMPX=0.25, RMPY=0.00, RMPZ=0.00, &END
&BINP10 NORSET=0, NBCHGE=0, HCZONE=0, &END
&BINP10 NCZPCH=0, CZDPCH=0.0, VREF=0.0, &END
&BINP11 NORPCH=0, NORF=0, NORL=0, &END
&BINP11 NOCL=0, VNORM=0.0, &END
&BINP12 KPAI=0, KSIDE=0, NEWNAB=0, NEWSID=0, &END
&BINP13 NBLIT=0, &END

&ASEM1 ASEMXX=0.00, ASEMYY=0.00, ASEMZZ=0.00, &END
&ASEM1 ASCAL=1.00, ATHET=0.00, NODEA=5, &END
&ASEM2 APXX=0.00, APYY=0.00, APZZ=0.00, &END
&ASEM2 AHXX=0.00, AHYY=1.00, AHZZ=0.00, &END

&COMP1 COMPMX= 0.0000, COMPMY= 0.0000, COMPMZ= 0.0000, &END
&COMP1 CSCAL= 1.000, CTHET= 0.0, NODEC= 5, &END
&COMP2 CPXX= 0.0000, CPYY= 0.0000, CPZZ= 0.0000, &END
&COMP2 CHXX= 0.0000, CHYY= 1.000, CHZZ= 0.0000, &END

&PATCH1 IREV= 0, IDPAT= 1, MAKE= 0, KCOMP= 1, KASS= 1, IPATSYN=0, &END
&PATCH1 IPATCOP=0, &END
&PATCH1 WING &END
&SECT1 STX= 0.0000, STY= 0.0000, STZ= 0.0000, SCALE= 1.00, &END
&SECT1 ALF= 0.0, THETA= 0.0, &END
&SECT1 INMODE= 5, TNODS= 0, TNPS= 0, TINTS= 3, &END
&SECT2 RTC= 0.1500, RMC= 0.0200, RPC= 0.4000, &END
&SECT2 IPLANE= 2, THPC= 40, TINTC= 3, &END
&SECT1 STX= 0.00, STY= 10, STZ= 0.0000, SCALE= 1.00, &END
&SECT1 ALF= 0.0, THETA= 0.0, &END
&SECT1 INMODE= 0, TNODS= 5, TNPS= 20, TINTS= 3, &END

&PATCH1 IREV= 0, IDPAT= 1, MAKE= 1, KCOMP= 1, KASS= 1, IPATSYN=0, &END
&PATCH1 IPATCOP=0, &END
&PATCH1 WING_TIP &END
&PATCH2 ITYP= 2, TNODS= 5, TNPS= 4, TINTS= 3, &END

&WAKE1 IDWAK=1, IFLXW=0, ITRFT2= 0, INTRW= 0, &END
&WAKE1 WING_WAKE &END
&WAKE2 KWPACH=2, KWSIDE=4, KWLINE=0, KWPAI=0, &END
&WAKE2 KWPAN2=0, NODEW=0, INITIAL=0, &END
&WAKE2 KWPACH=1, KWSIDE=2, KWLINE=0, KWPAI=0, &END
&WAKE2 KWPAN2=0, NODEW=5, INITIAL=0, &END

&ONSTRM NONSL =0, KPSL = 1.50, &END

&BLPAPAM RH =1000000, VISC = 0.00015723, NSLBL = 1.2, &END

&VS1 NVOLR= 0, NVOLC= 0, &END
&VS2 X0= -0.1000, Y0= 1.5000, Z0= -0.1000, INTVSR= 1, &END

```

Jun 20 1997 04:39 24p1600.in Page 2

```

&VS3 X1= -0.1000, Y1= 1.5000, Z1= 0.1000, NPT1= 0, &END
&VS4 X2= -0.1000, Y2= 1.5000, Z2= 0.1000, NPT2= 20, &END
&VS5 X3= 1.1000, Y3= 1.5000, Z3= -0.1000, NPT3= 25, &END

&VS6 XRO= 2.0000, YRO= 2.0000, ZRO= 0.0000, INTVSC= 1, &END
&VS7 XR1= 4.0000, YR1= 2.0000, ZR1= 0.0000, &END
&VS7 XR2= 2.0000, YR2= 2.0000, ZR2= 1.0000, &END
&VS8 R1= 0.1000, R2= 1.0000, PHI1= 0.0, PHI2=360.0, &END
&VS9 NRAD= 5, NPHI= 12, NLEN= 3, &END

&SLIN1 NSTLIN=0, &END
&SLIN2 SX0= -2.0000, SY0= 1.0000, SZ0= -0.5000, &END
&SLIN2 SU= 0.0000, SD= 10.0000, DS= 0.2500, INTSL= 1, &END

```



## APPENDIX E. MATLAB PROGRAM FOR REORDERING AGARD DATA FILE

Jun 20 1997 04:42	reorder.m	Page 1
-------------------	-----------	--------

```

% This Matlab M-file transforms AGARD Prolate Spheroid Cp data listed
% in a chordwise direction and converts it into slices for a given x/c location.

% Created by: Steve Pollard

load cwcp10;
load cwcp30;
fid1=fopen('swcp10','r+');
fid2=fopen('swcp30','r+');
fprintf(fid1,'# DPN PHI I X0/L CP \n');
fprintf(fid2,'# DPN PHI I X0/L CP \n');
for i=1:42
    for j=1:42
        swcp10((i-1)*42+j,:)=cwcp10((j-1)*42+i,:);
    end
end
for i=1:42
    for j=1:51
        swcp30((i-1)*51+j,:)=cwcp30((j-1)*42+i,:);
    end
end
fprintf(fid1,'%6.0f %7.2f %3.1f %8.5f %8.5f \n',swcp10');
fprintf(fid2,'%6.0f %7.2f %3.1f %8.5f %8.5f \n',swcp30');
fclose('all');

```



99

```

Jun 11 1997 05:33                                pr10w117.in                                Page 2
0.0037      0.0110      -0.0111
0.0037      0.0126      -0.0094
0.0037      0.0139      -0.0073
0.0037      0.0148      -0.0052
0.0037      0.0154      -0.0028
0.0037      0.0157      -0.0003
0.0037      0.0154      0.0032
0.0037      0.0147      0.0055
0.0037      0.0137      0.0077
0.0037      0.0124      0.0096
0.0037      0.0110      0.0112
0.0037      0.0090      0.0128
0.0037      0.0071      0.0140
0.0037      0.0049      0.0149
0.0037      0.0025      0.0155
0.0037      0.0000      0.0157
&BPNODE TNODE=3, TNPC=40, TINTC=3, &END
&SECT1 STX=0.0, STY=0.0, STZ=0.0, SCALE=1.0, ALF=0.0, THETA=0.0, INMODE=4,
TNODS=0, TNPS=0, TINTS=0, &END
0.0148      0.0000      -0.0313
0.0148      0.0055      -0.0308
0.0148      0.0104      -0.0295
0.0148      0.0149      -0.0275
0.0148      0.0188      -0.0250
0.0148      0.0221      -0.0221
0.0148      0.0252      -0.0188
0.0148      0.0277      -0.0145
0.0148      0.0296      -0.0100
0.0148      0.0308      -0.0051
0.0148      0.0313      0.0000
0.0148      0.0308      0.0055
0.0148      0.0295      0.0104
0.0148      0.0275      0.0149
0.0148      0.0250      0.0188
0.0148      0.0221      0.0221
0.0148      0.0185      0.0252
0.0148      0.0145      0.0277
0.0148      0.0100      0.0296
0.0148      0.0051      0.0308
0.0148      0.0000      0.0313
&BPNODE TNODE=3, TNPC=40, TINTC=3, &END
&SECT1 STX=0.0, STY=0.0, STZ=0.0, SCALE=1.0, ALF=0.0, THETA=0.0, INMODE=4,
TNODS=0, TNPS=0, TINTS=0, &END
0.0332      0.0000      -0.0467
0.0332      0.0081      -0.0460
0.0332      0.0155      -0.0440
0.0332      0.0222      -0.0410
0.0332      0.0282      -0.0372
0.0332      0.0332      -0.0328
0.0332      0.0374      -0.0278
0.0332      0.0412      -0.0219
0.0332      0.0441      -0.0151
0.0332      0.0460      -0.0077
0.0332      0.0467      0.0000
0.0332      0.0460      0.0081
0.0332      0.0440      0.0155
0.0332      0.0410      0.0222
0.0332      0.0372      0.0282
0.0332      0.0328      0.0332
0.0332      0.0278      0.0374
0.0332      0.0219      0.0412
0.0332      0.0151      0.0441
0.0332      0.0077      0.0460
0.0332      0.0000      0.0467
&BPNODE TNODE=3, TNPC=40, TINTC=3, &END
&SECT1 STX=0.0, STY=0.0, STZ=0.0, SCALE=1.0, ALF=0.0, THETA=0.0, INMODE=4,
TNODS=0, TNPS=0, TINTS=0, &END
0.0587      0.0000      -0.0618
0.0587      0.0106      -0.0609
0.0587      0.0203      -0.0583
0.0587      0.0293      -0.0544
0.0587      0.0371      -0.0494
0.0587      0.0437      -0.0436
0.0587      0.0496      -0.0368
0.0587      0.0546      -0.0289
0.0587      0.0584      -0.0200

```

Jun 11 1997 05:33 pr10w117.in Page 3

0.0587	0.0609	-0.0102
0.0587	0.0618	0.0000
0.0587	0.0609	0.0106
0.0587	0.0583	0.0203
0.0587	0.0544	0.0293
0.0587	0.0494	0.0371
0.0587	0.0436	0.0437
0.0587	0.0368	0.0496
0.0587	0.0289	0.0546
0.0587	0.0200	0.0584
0.0587	0.0102	0.0609
0.0587	0.0000	0.0618

&BPNODE TNODE=3, TNPC=40, TINTC=3, &END  
&SECT1 STX=0.0, STY=0.0, STZ=0.0, SCALE=1.0, ALF=0.0, THETA=0.0, INMODE=4,  
TNODS=0, TNPS=0, TINTS=0, &END

0.0913	0.0000	-0.0765
0.0913	0.0130	-0.0754
0.0913	0.0251	-0.0722
0.0913	0.0362	-0.0674
0.0913	0.0459	-0.0612
0.0913	0.0541	-0.0541
0.0913	0.0614	-0.0456
0.0913	0.0676	-0.0359
0.0913	0.0724	-0.0248
0.0913	0.0754	-0.0127
0.0913	0.0765	0.0000
0.0913	0.0754	0.0130
0.0913	0.0722	0.0251
0.0913	0.0674	0.0362
0.0913	0.0612	0.0459
0.0913	0.0541	0.0541
0.0913	0.0456	0.0614
0.0913	0.0359	0.0676
0.0913	0.0248	0.0724
0.0913	0.0127	0.0754
0.0913	0.0000	0.0765

&BPNODE TNODE=3, TNPC=40, TINTC=3, &END  
&SECT1 STX=0.0, STY=0.0, STZ=0.0, SCALE=1.0, ALF=0.0, THETA=0.0, INMODE=4,  
TNODS=0, TNPS=0, TINTS=0, &END

0.1308	0.0000	-0.0908
0.1308	0.0154	-0.0894
0.1308	0.0298	-0.0857
0.1308	0.0429	-0.0799
0.1308	0.0545	-0.0726
0.1308	0.0642	-0.0641
0.1308	0.0728	-0.0541
0.1308	0.0801	-0.0426
0.1308	0.0858	-0.0294
0.1308	0.0895	-0.0150
0.1308	0.0908	0.0000
0.1308	0.0894	0.0154
0.1308	0.0857	0.0298
0.1308	0.0799	0.0429
0.1308	0.0726	0.0545
0.1308	0.0641	0.0642
0.1308	0.0541	0.0728
0.1308	0.0426	0.0801
0.1308	0.0294	0.0858
0.1308	0.0150	0.0895
0.1308	0.0000	0.0908

&BPNODE TNODE=3, TNPC=40, TINTC=3, &END  
&SECT1 STX=0.0, STY=0.0, STZ=0.0, SCALE=1.0, ALF=0.0, THETA=0.0, INMODE=4,  
TNODS=0, TNPS=0, TINTS=0, &END

0.1768	0.0000	-0.1045
0.1768	0.0177	-0.1029
0.1768	0.0343	-0.0987
0.1768	0.0495	-0.0920
0.1768	0.0628	-0.0835
0.1768	0.0739	-0.0737
0.1768	0.0837	-0.0624
0.1768	0.0922	-0.0491
0.1768	0.0988	-0.0339
0.1768	0.1030	-0.0174
0.1768	0.1045	0.0000
0.1768	0.1029	0.0177
0.1768	0.0987	0.0343

Jun 11 1997 05:33 pr10w117.in Page 4

0.1768	0.0920	0.0495
0.1768	0.0835	0.0628
0.1768	0.0737	0.0739
0.1768	0.0624	0.0837
0.1768	0.0491	0.0922
0.1768	0.0339	0.0988
0.1768	0.0174	0.1030
0.1768	0.0000	0.1045

&BPNODE TNODE=3, TNPC=40, TINTC=3, &END  
&SECT1 STX=0.0, STY=0.0, STZ=0.0, SCALE=1.0, ALF=0.0, THETA=0.0, INMODE=4,  
TNODS=0, TNPS=0, TINTS=0, &END

0.2292	0.0000	-0.1175
0.2292	0.0198	-0.1158
0.2292	0.0385	-0.1110
0.2292	0.0556	-0.1035
0.2292	0.0705	-0.0940
0.2292	0.0831	-0.0831
0.2292	0.0942	-0.0702
0.2292	0.1037	-0.0552
0.2292	0.1111	-0.0382
0.2292	0.1159	-0.0195
0.2292	0.1175	0.0000
0.2292	0.1158	0.0198
0.2292	0.1110	0.0385
0.2292	0.1035	0.0556
0.2292	0.0940	0.0705
0.2292	0.0831	0.0831
0.2292	0.0702	0.0942
0.2292	0.0552	0.1037
0.2292	0.0382	0.1111
0.2292	0.0195	0.1159
0.2292	0.0000	0.1175

&BPNODE TNODE=3, TNPC=40, TINTC=3, &END  
&SECT1 STX=0.0, STY=0.0, STZ=0.0, SCALE=1.0, ALF=0.0, THETA=0.0, INMODE=4,  
TNODS=0, TNPS=0, TINTS=0, &END

0.2875	0.0000	-0.1298
0.2875	0.0219	-0.1280
0.2875	0.0426	-0.1227
0.2875	0.0614	-0.1144
0.2875	0.0780	-0.1038
0.2875	0.0919	-0.0917
0.2875	0.1041	-0.0776
0.2875	0.1146	-0.0611
0.2875	0.1228	-0.0422
0.2875	0.1280	-0.0216
0.2875	0.1298	0.0000
0.2875	0.1280	0.0219
0.2875	0.1227	0.0426
0.2875	0.1144	0.0614
0.2875	0.1038	0.0780
0.2875	0.0917	0.0919
0.2875	0.0776	0.1041
0.2875	0.0611	0.1146
0.2875	0.0422	0.1228
0.2875	0.0216	0.1280
0.2875	0.0000	0.1298

&BPNODE TNODE=3, TNPC=40, TINTC=3, &END  
&SECT1 STX=0.0, STY=0.0, STZ=0.0, SCALE=1.0, ALF=0.0, THETA=0.0, INMODE=4,  
TNODS=0, TNPS=0, TINTS=0, &END

0.3515	0.0000	-0.1414
0.3515	0.0239	-0.1393
0.3515	0.0464	-0.1336
0.3515	0.0669	-0.1245
0.3515	0.0850	-0.1130
0.3515	0.1001	-0.0998
0.3515	0.1132	-0.0846
0.3515	0.1247	-0.0666
0.3515	0.1337	-0.0460
0.3515	0.1394	-0.0235
0.3515	0.1414	0.0000
0.3515	0.1393	0.0239
0.3515	0.1336	0.0464
0.3515	0.1245	0.0669
0.3515	0.1130	0.0850
0.3515	0.0998	0.1001
0.3515	0.0846	0.1132



Jun 11 1997 05:33			pr10w117.in	Page 5
0.3515	0.0666	0.1247		
0.3515	0.0460	0.1337		
0.3515	0.0235	0.1394		
0.3515	0.0000	0.1414		
&BPNODE TNODE=3, TNPC=40, TINTC=3, &END				
&SECT1 STX=0.0, STY=0.0, STZ=0.0, SCALE=1.0, ALF=0.0, THETA=0.0, INMODE=4,				
TNODES=0, TNPS=0, TINTS=0, &END				
0.4207	0.0000	-0.1520		
0.4207	0.0257	-0.1499		
0.4207	0.0499	-0.1436		
0.4207	0.0720	-0.1339		
0.4207	0.0914	-0.1215		
0.4207	0.1077	-0.1073		
0.4207	0.1217	-0.0910		
0.4207	0.1341	-0.0717		
0.4207	0.1437	-0.0495		
0.4207	0.1499	-0.0253		
0.4207	0.1520	0.0000		
0.4207	0.1499	0.0257		
0.4207	0.1436	0.0499		
0.4207	0.1339	0.0720		
0.4207	0.1215	0.0914		
0.4207	0.1073	0.1077		
0.4207	0.0910	0.1217		
0.4207	0.0717	0.1341		
0.4207	0.0495	0.1437		
0.4207	0.0253	0.1499		
0.4207	0.0000	0.1520		
&BPNODE TNODE=3, TNPC=40, TINTC=3, &END				
&SECT1 STX=0.0, STY=0.0, STZ=0.0, SCALE=1.0, ALF=0.0, THETA=0.0, INMODE=4,				
TNODES=0, TNPS=0, TINTS=0, &END				
0.4947	0.0000	-0.1618		
0.4947	0.0273	-0.1595		
0.4947	0.0530	-0.1528		
0.4947	0.0765	-0.1425		
0.4947	0.0972	-0.1293		
0.4947	0.1145	-0.1143		
0.4947	0.1296	-0.0968		
0.4947	0.1427	-0.0762		
0.4947	0.1530	-0.0526		
0.4947	0.1595	-0.0269		
0.4947	0.1618	0.0000		
0.4947	0.1595	0.0273		
0.4947	0.1528	0.0530		
0.4947	0.1425	0.0765		
0.4947	0.1293	0.0972		
0.4947	0.1143	0.1145		
0.4947	0.0968	0.1296		
0.4947	0.0762	0.1427		
0.4947	0.0526	0.1530		
0.4947	0.0269	0.1595		
0.4947	0.0000	0.1618		
&BPNODE TNODE=3, TNPC=40, TINTC=3, &END				
&SECT1 STX=0.0, STY=0.0, STZ=0.0, SCALE=1.0, ALF=0.0, THETA=0.0, INMODE=4,				
TNODES=0, TNPS=0, TINTS=0, &END				
0.5730	0.0000	-0.1705		
0.5730	0.0287	-0.1681		
0.5730	0.0558	-0.1611		
0.5730	0.0806	-0.1502		
0.5730	0.1023	-0.1364		
0.5730	0.1206	-0.1205		
0.5730	0.1366	-0.1020		
0.5730	0.1504	-0.0802		
0.5730	0.1612	-0.0554		
0.5730	0.1681	-0.0283		
0.5730	0.1705	0.0000		
0.5730	0.1681	0.0287		
0.5730	0.1611	0.0558		
0.5730	0.1502	0.0806		
0.5730	0.1364	0.1023		
0.5730	0.1205	0.1206		
0.5730	0.1020	0.1366		
0.5730	0.0802	0.1504		
0.5730	0.0554	0.1612		
0.5730	0.0283	0.1681		
0.5730	0.0000	0.1705		

Jun 11 1997 05:33			pr10w117.in	Page 6
&BPNODE TNODE=3, TNPC=40, TINTC=3, &END				
&SECT1 STX=0.0, STY=0.0, STZ=0.0, SCALE=1.0, ALF=0.0, THETA=0.0, INMODE=4,				
TNODES=0, TNPS=0, TINTS=0, &END				
0.6552	0.0000	-0.1782		
0.6552	0.0300	-0.1756		
0.6552	0.0584	-0.1683		
0.6552	0.0843	-0.1569		
0.6552	0.1071	-0.1424		
0.6552	0.1261	-0.1258		
0.6552	0.1427	-0.1067		
0.6552	0.1571	-0.0840		
0.6552	0.1685	-0.0580		
0.6552	0.1757	-0.0297		
0.6552	0.1782	0.0000		
0.6552	0.1756	0.0300		
0.6552	0.1683	0.0584		
0.6552	0.1569	0.0843		
0.6552	0.1424	0.1071		
0.6552	0.1258	0.1261		
0.6552	0.1067	0.1427		
0.6552	0.0840	0.1571		
0.6552	0.0580	0.1685		
0.6552	0.0297	0.1757		
0.6552	0.0000	0.1782		
&BPNODE TNODE=3, TNPC=40, TINTC=3, &END				
&SECT1 STX=0.0, STY=0.0, STZ=0.0, SCALE=1.0, ALF=0.0, THETA=0.0, INMODE=4,				
TNODES=0, TNPS=0, TINTS=0, &END				
0.7408	0.0000	-0.1848		
0.7408	0.0311	-0.1821		
0.7408	0.0604	-0.1746		
0.7408	0.0873	-0.1628		
0.7408	0.1109	-0.1478		
0.7408	0.1306	-0.1306		
0.7408	0.1480	-0.1105		
0.7408	0.1630	-0.0870		
0.7408	0.1747	-0.0601		
0.7408	0.1822	-0.0307		
0.7408	0.1848	0.0000		
0.7408	0.1821	0.0311		
0.7408	0.1746	0.0604		
0.7408	0.1628	0.0873		
0.7408	0.1478	0.1109		
0.7408	0.1306	0.1306		
0.7408	0.1105	0.1480		
0.7408	0.0870	0.1630		
0.7408	0.0601	0.1747		
0.7408	0.0307	0.1822		
0.7408	0.0000	0.1848		
&BPNODE TNODE=3, TNPC=40, TINTC=3, &END				
&SECT1 STX=0.0, STY=0.0, STZ=0.0, SCALE=1.0, ALF=0.0, THETA=0.0, INMODE=4,				
TNODES=0, TNPS=0, TINTS=0, &END				
0.8292	0.0000	-0.1902		
0.8292	0.0320	-0.1875		
0.8292	0.0623	-0.1797		
0.8292	0.0900	-0.1675		
0.8292	0.1143	-0.1520		
0.8292	0.1346	-0.1343		
0.8292	0.1523	-0.1139		
0.8292	0.1677	-0.0897		
0.8292	0.1798	-0.0620		
0.8292	0.1875	-0.0317		
0.8292	0.1902	0.0000		
0.8292	0.1875	0.0320		
0.8292	0.1797	0.0623		
0.8292	0.1675	0.0900		
0.8292	0.1520	0.1143		
0.8292	0.1343	0.1346		
0.8292	0.1139	0.1523		
0.8292	0.0897	0.1677		
0.8292	0.0620	0.1798		
0.8292	0.0317	0.1875		
0.8292	0.0000	0.1902		
&BPNODE TNODE=3, TNPC=40, TINTC=3, &END				
&SECT1 STX=0.0, STY=0.0, STZ=0.0, SCALE=1.0, ALF=0.0, THETA=0.0, INMODE=4,				
TNODES=0, TNPS=0, TINTS=0, &END				
0.9199	0.0000	-0.1945		

Jun 11 1997 05:33			pr10w117.in	Page 7
0.9199	0.0327	-0.1917		
0.9199	0.0637	-0.1837		
0.9199	0.0920	-0.1713		
0.9199	0.1168	-0.1554		
0.9199	0.1377	-0.1373		
0.9199	0.1557	-0.1165		
0.9199	0.1715	-0.0917		
0.9199	0.1838	-0.0633		
0.9199	0.1917	-0.0324		
0.9199	0.1945	0.0000		
0.9199	0.1917	0.0327		
0.9199	0.1837	0.0637		
0.9199	0.1713	0.0920		
0.9199	0.1554	0.1168		
0.9199	0.1373	0.1377		
0.9199	0.1165	0.1557		
0.9199	0.0917	0.1715		
0.9199	0.0633	0.1838		
0.9199	0.0324	0.1917		
0.9199	0.0000	0.1945		
&BPNODE TNODE=3, TNPC=40, TINTC=3, &END				
&SECT1 STX=0.0, STY=0.0, STZ=0.0, SCALE=1.0, ALF=0.0, THETA=0.0, INMODE=4,				
TNODES=0, TNPS=0, TINTS=0, &END				
1.0123	0.0000	-0.1975		
1.0123	0.0332	-0.1947		
1.0123	0.0646	-0.1867		
1.0123	0.0934	-0.1741		
1.0123	0.1185	-0.1580		
1.0123	0.1397	-0.1396		
1.0123	0.1582	-0.1182		
1.0123	0.1742	-0.0930		
1.0123	0.1868	-0.0643		
1.0123	0.1948	-0.0328		
1.0123	0.1975	0.0000		
1.0123	0.1947	0.0332		
1.0123	0.1867	0.0646		
1.0123	0.1741	0.0934		
1.0123	0.1580	0.1185		
1.0123	0.1396	0.1397		
1.0123	0.1182	0.1582		
1.0123	0.0930	0.1742		
1.0123	0.0643	0.1868		
1.0123	0.0328	0.1948		
1.0123	0.0000	0.1975		
&BPNODE TNODE=3, TNPC=40, TINTC=3, &END				
&SECT1 STX=0.0, STY=0.0, STZ=0.0, SCALE=1.0, ALF=0.0, THETA=0.0, INMODE=4,				
TNODES=0, TNPS=0, TINTS=0, &END				
1.1058	0.0000	-0.1994		
1.1058	0.0335	-0.1965		
1.1058	0.0653	-0.1884		
1.1058	0.0943	-0.1756		
1.1058	0.1198	-0.1594		
1.1058	0.1411	-0.1408		
1.1058	0.1596	-0.1194		
1.1058	0.1758	-0.0940		
1.1058	0.1885	-0.0649		
1.1058	0.1966	-0.0332		
1.1058	0.1994	0.0000		
1.1058	0.1965	0.0335		
1.1058	0.1884	0.0653		
1.1058	0.1756	0.0943		
1.1058	0.1594	0.1198		
1.1058	0.1408	0.1411		
1.1058	0.1194	0.1596		
1.1058	0.0940	0.1758		
1.1058	0.0649	0.1885		
1.1058	0.0332	0.1966		
1.1058	0.0000	0.1994		
&BPNODE TNODE=3, TNPC=40, TINTC=3, &END				
&SECT1 STX=0.0, STY=0.0, STZ=0.0, SCALE=1.0, ALF=0.0, THETA=0.0, INMODE=4,				
TNODES=0, TNPS=0, TINTS=0, &END				
1.2000	0.0000	-0.2000		
1.2000	0.0336	-0.1971		
1.2000	0.0655	-0.1890		
1.2000	0.0946	-0.1762		
1.2000	0.1201	-0.1599		

Jun 11 1997 05:33			pr10w117.in	Page 8
1.2000	0.1415	-0.1413		
1.2000	0.1601	-0.1198		
1.2000	0.1764	-0.0943		
1.2000	0.1891	-0.0651		
1.2000	0.1972	-0.0333		
1.2000	0.2000	0.0000		
1.2000	0.1971	0.0336		
1.2000	0.1890	0.0655		
1.2000	0.1762	0.0946		
1.2000	0.1599	0.1201		
1.2000	0.1413	0.1415		
1.2000	0.1198	0.1601		
1.2000	0.0943	0.1764		
1.2000	0.0651	0.1891		
1.2000	0.0333	0.1972		
1.2000	0.0000	0.2000		
&BPNODE TNODE=3, TNPC=40, TINTC=3, &END				
&SECT1 STX=0.0, STY=0.0, STZ=0.0, SCALE=1.0, ALF=0.0, THETA=0.0, INMODE=4,				
TNODES=0, TNPS=0, TINTS=0, &END				
1.2942	0.0000	-0.1994		
1.2942	0.0335	-0.1965		
1.2942	0.0653	-0.1884		
1.2942	0.0943	-0.1756		
1.2942	0.1198	-0.1594		
1.2942	0.1411	-0.1408		
1.2942	0.1596	-0.1194		
1.2942	0.1758	-0.0940		
1.2942	0.1885	-0.0649		
1.2942	0.1966	-0.0332		
1.2942	0.1994	0.0000		
1.2942	0.1965	0.0335		
1.2942	0.1884	0.0653		
1.2942	0.1756	0.0943		
1.2942	0.1594	0.1198		
1.2942	0.1408	0.1411		
1.2942	0.1194	0.1596		
1.2942	0.0940	0.1758		
1.2942	0.0649	0.1885		
1.2942	0.0332	0.1966		
1.2942	0.0000	0.1994		
&BPNODE TNODE=3, TNPC=40, TINTC=3, &END				
&SECT1 STX=0.0, STY=0.0, STZ=0.0, SCALE=1.0, ALF=0.0, THETA=0.0, INMODE=4,				
TNODES=0, TNPS=0, TINTS=0, &END				
1.3877	0.0000	-0.1975		
1.3877	0.0332	-0.1947		
1.3877	0.0646	-0.1867		
1.3877	0.0934	-0.1741		
1.3877	0.1185	-0.1580		
1.3877	0.1397	-0.1396		
1.3877	0.1582	-0.1182		
1.3877	0.1742	-0.0930		
1.3877	0.1868	-0.0643		
1.3877	0.1948	-0.0328		
1.3877	0.1975	0.0000		
1.3877	0.1947	0.0332		
1.3877	0.1867	0.0646		
1.3877	0.1741	0.0934		
1.3877	0.1580	0.1185		
1.3877	0.1396	0.1397		
1.3877	0.1182	0.1582		
1.3877	0.0930	0.1742		
1.3877	0.0643	0.1868		
1.3877	0.0328	0.1948		
1.3877	0.0000	0.1975		
&BPNODE TNODE=3, TNPC=40, TINTC=3, &END				
&SECT1 STX=0.0, STY=0.0, STZ=0.0, SCALE=1.0, ALF=0.0, THETA=0.0, INMODE=4,				
TNODES=0, TNPS=0, TINTS=0, &END				
1.4801	0.0000	-0.1945		
1.4801	0.0327	-0.1917		
1.4801	0.0637	-0.1837		
1.4801	0.0920	-0.1713		
1.4801	0.1168	-0.1554		
1.4801	0.1377	-0.1373		
1.4801	0.1557	-0.1165		
1.4801	0.1715	-0.0917		
1.4801	0.1838	-0.0633		

Jun 11 1997 05:33 pr10w117.in Page 9		
1.4801	0.1917	-0.0324
1.4801	0.1945	0.0000
1.4801	0.1917	0.0327
1.4801	0.1837	0.0637
1.4801	0.1713	0.0920
1.4801	0.1554	0.1168
1.4801	0.1373	0.1377
1.4801	0.1165	0.1557
1.4801	0.0917	0.1715
1.4801	0.0633	0.1838
1.4801	0.0324	0.1917
1.4801	0.0000	0.1945
&BPNODE TNODE=3, TNPC=40, TINTC=3, &END		
&SECT1 STX=0.0, STY=0.0, STZ=0.0, SCALE=1.0, ALF=0.0, THETA=0.0, INMODE=4,		
TNODS=0, TNPS=0, TINTS=0, &END		
1.5708	0.0000	-0.1902
1.5708	0.0320	-0.1875
1.5708	0.0623	-0.1797
1.5708	0.0900	-0.1675
1.5708	0.1143	-0.1520
1.5708	0.1346	-0.1343
1.5708	0.1523	-0.1139
1.5708	0.1677	-0.0897
1.5708	0.1798	-0.0620
1.5708	0.1875	-0.0317
1.5708	0.1902	0.0000
1.5708	0.1875	0.0320
1.5708	0.1797	0.0623
1.5708	0.1675	0.0900
1.5708	0.1520	0.1143
1.5708	0.1343	0.1346
1.5708	0.1139	0.1523
1.5708	0.0897	0.1677
1.5708	0.0620	0.1798
1.5708	0.0317	0.1875
1.5708	0.0000	0.1902
&BPNODE TNODE=3, TNPC=40, TINTC=3, &END		
&SECT1 STX=0.0, STY=0.0, STZ=0.0, SCALE=1.0, ALF=0.0, THETA=0.0, INMODE=4,		
TNODS=0, TNPS=0, TINTS=0, &END		
1.6592	0.0000	-0.1848
1.6592	0.0311	-0.1821
1.6592	0.0604	-0.1746
1.6592	0.0873	-0.1628
1.6592	0.1109	-0.1478
1.6592	0.1306	-0.1306
1.6592	0.1480	-0.1105
1.6592	0.1630	-0.0870
1.6592	0.1747	-0.0601
1.6592	0.1822	-0.0307
1.6592	0.1848	0.0000
1.6592	0.1821	0.0311
1.6592	0.1746	0.0604
1.6592	0.1628	0.0873
1.6592	0.1478	0.1109
1.6592	0.1306	0.1306
1.6592	0.1105	0.1480
1.6592	0.0870	0.1630
1.6592	0.0601	0.1747
1.6592	0.0307	0.1822
1.6592	0.0000	0.1848
&BPNODE TNODE=3, TNPC=40, TINTC=3, &END		
&SECT1 STX=0.0, STY=0.0, STZ=0.0, SCALE=1.0, ALF=0.0, THETA=0.0, INMODE=4,		
TNODS=0, TNPS=0, TINTS=0, &END		
1.7448	0.0000	-0.1782
1.7448	0.0300	-0.1756
1.7448	0.0584	-0.1683
1.7448	0.0843	-0.1569
1.7448	0.1071	-0.1424
1.7448	0.1261	-0.1258
1.7448	0.1427	-0.1067
1.7448	0.1571	-0.0840
1.7448	0.1685	-0.0580
1.7448	0.1757	-0.0297
1.7448	0.1782	0.0000
1.7448	0.1756	0.0300
1.7448	0.1683	0.0584

Jun 11 1997 05:33 pr10w117.in Page 10		
1.7448	0.1569	0.0843
1.7448	0.1424	0.1071
1.7448	0.1258	0.1261
1.7448	0.1067	0.1427
1.7448	0.0840	0.1571
1.7448	0.0580	0.1685
1.7448	0.0297	0.1757
1.7448	0.0000	0.1782
&BPNODE TNODE=3, TNPC=40, TINTC=3, &END		
&SECT1 STX=0.0, STY=0.0, STZ=0.0, SCALE=1.0, ALF=0.0, THETA=0.0, INMODE=4,		
TNODS=0, TNPS=0, TINTS=0, &END		
1.8270	0.0000	-0.1705
1.8270	0.0287	-0.1681
1.8270	0.0559	-0.1611
1.8270	0.0806	-0.1502
1.8270	0.1023	-0.1364
1.8270	0.1206	-0.1205
1.8270	0.1366	-0.1020
1.8270	0.1504	-0.0802
1.8270	0.1612	-0.0554
1.8270	0.1681	-0.0283
1.8270	0.1705	0.0000
1.8270	0.1681	0.0287
1.8270	0.1611	0.0559
1.8270	0.1502	0.0806
1.8270	0.1364	0.1023
1.8270	0.1205	0.1206
1.8270	0.1020	0.1366
1.8270	0.0802	0.1504
1.8270	0.0554	0.1612
1.8270	0.0283	0.1681
1.8270	0.0000	0.1705
&BPNODE TNODE=3, TNPC=40, TINTC=3, &END		
&SECT1 STX=0.0, STY=0.0, STZ=0.0, SCALE=1.0, ALF=0.0, THETA=0.0, INMODE=4,		
TNODS=0, TNPS=0, TINTS=0, &END		
1.9053	0.0000	-0.1618
1.9053	0.0273	-0.1595
1.9053	0.0530	-0.1528
1.9053	0.0765	-0.1425
1.9053	0.0972	-0.1293
1.9053	0.1145	-0.1143
1.9053	0.1296	-0.0968
1.9053	0.1427	-0.0762
1.9053	0.1530	-0.0526
1.9053	0.1595	-0.0269
1.9053	0.1618	0.0000
1.9053	0.1595	0.0273
1.9053	0.1528	0.0530
1.9053	0.1425	0.0765
1.9053	0.1293	0.0972
1.9053	0.1143	0.1145
1.9053	0.0968	0.1296
1.9053	0.0762	0.1427
1.9053	0.0526	0.1530
1.9053	0.0269	0.1595
1.9053	0.0000	0.1618
&BPNODE TNODE=3, TNPC=40, TINTC=3, &END		
&SECT1 STX=0.0, STY=0.0, STZ=0.0, SCALE=1.0, ALF=0.0, THETA=0.0, INMODE=4,		
TNODS=0, TNPS=0, TINTS=0, &END		
1.9793	0.0000	-0.1520
1.9793	0.0257	-0.1499
1.9793	0.0499	-0.1436
1.9793	0.0720	-0.1339
1.9793	0.0914	-0.1215
1.9793	0.1077	-0.1073
1.9793	0.1217	-0.0910
1.9793	0.1341	-0.0717
1.9793	0.1437	-0.0495
1.9793	0.1499	-0.0253
1.9793	0.1520	0.0000
1.9793	0.1499	0.0257
1.9793	0.1436	0.0499
1.9793	0.1339	0.0720
1.9793	0.1215	0.0914
1.9793	0.1073	0.1077
1.9793	0.0910	0.1217

Jun 11 1997 05:33			pr10w117.in	Page 11
1.9793	0.0717	0.1341		
1.9793	0.0495	0.1437		
1.9793	0.0253	0.1499		
1.9793	0.0000	0.1520		
&BPNODE TNODE=3, TNPC=40, TINTC=3, &END				
&SECT1 STX=0.0, STY=0.0, STZ=0.0, SCALE=1.0, ALF=0.0, THETA=0.0, INMODE=4,				
TNODES=0, TNPS=0, TINTS=0, &END				
2.0485	0.0000	-0.1414		
2.0485	0.0239	-0.1393		
2.0485	0.0464	-0.1336		
2.0485	0.0669	-0.1245		
2.0485	0.0850	-0.1130		
2.0485	0.1001	-0.0998		
2.0485	0.1132	-0.0846		
2.0485	0.1247	-0.0666		
2.0485	0.1337	-0.0460		
2.0485	0.1394	-0.0235		
2.0485	0.1414	0.0000		
2.0485	0.1393	0.0239		
2.0485	0.1336	0.0464		
2.0485	0.1245	0.0669		
2.0485	0.1130	0.0850		
2.0485	0.0998	0.1001		
2.0485	0.0846	0.1132		
2.0485	0.0666	0.1247		
2.0485	0.0460	0.1337		
2.0485	0.0235	0.1394		
2.0485	0.0000	0.1414		
&BPNODE TNODE=3, TNPC=40, TINTC=3, &END				
&SECT1 STX=0.0, STY=0.0, STZ=0.0, SCALE=1.0, ALF=0.0, THETA=0.0, INMODE=4,				
TNODES=0, TNPS=0, TINTS=0, &END				
2.1125	0.0000	-0.1298		
2.1125	0.0219	-0.1280		
2.1125	0.0426	-0.1227		
2.1125	0.0614	-0.1144		
2.1125	0.0780	-0.1038		
2.1125	0.0919	-0.0917		
2.1125	0.1041	-0.0776		
2.1125	0.1146	-0.0611		
2.1125	0.1228	-0.0422		
2.1125	0.1280	-0.0216		
2.1125	0.1298	0.0000		
2.1125	0.1280	0.0219		
2.1125	0.1227	0.0426		
2.1125	0.1144	0.0614		
2.1125	0.1038	0.0780		
2.1125	0.0917	0.0919		
2.1125	0.0776	0.1041		
2.1125	0.0611	0.1146		
2.1125	0.0422	0.1228		
2.1125	0.0216	0.1280		
2.1125	0.0000	0.1298		
&BPNODE TNODE=3, TNPC=40, TINTC=3, &END				
&SECT1 STX=0.0, STY=0.0, STZ=0.0, SCALE=1.0, ALF=0.0, THETA=0.0, INMODE=4,				
TNODES=0, TNPS=0, TINTS=0, &END				
2.1708	0.0000	-0.1175		
2.1708	0.0198	-0.1158		
2.1708	0.0385	-0.1110		
2.1708	0.0556	-0.1035		
2.1708	0.0705	-0.0940		
2.1708	0.0831	-0.0831		
2.1708	0.0942	-0.0702		
2.1708	0.1037	-0.0552		
2.1708	0.1111	-0.0382		
2.1708	0.1159	-0.0195		
2.1708	0.1175	0.0000		
2.1708	0.1158	0.0198		
2.1708	0.1110	0.0385		
2.1708	0.1035	0.0556		
2.1708	0.0940	0.0705		
2.1708	0.0831	0.0831		
2.1708	0.0702	0.0942		
2.1708	0.0552	0.1037		
2.1708	0.0382	0.1111		
2.1708	0.0195	0.1159		
2.1708	0.0000	0.1175		

Jun 11 1997 05:33			pr10w117.in	Page 12
&BPNODE TNODE=3, TNPC=40, TINTC=3, &END				
&SECT1 STX=0.0, STY=0.0, STZ=0.0, SCALE=1.0, ALF=0.0, THETA=0.0, INMODE=4,				
TNODES=0, TNPS=0, TINTS=0, &END				
2.2232	0.0000	-0.1045		
2.2232	0.0177	-0.1029		
2.2232	0.0343	-0.0987		
2.2232	0.0495	-0.0920		
2.2232	0.0628	-0.0835		
2.2232	0.0739	-0.0737		
2.2232	0.0837	-0.0624		
2.2232	0.0922	-0.0491		
2.2232	0.0988	-0.0339		
2.2232	0.1030	-0.0174		
2.2232	0.1045	0.0000		
2.2232	0.1029	0.0177		
2.2232	0.0987	0.0343		
2.2232	0.0920	0.0495		
2.2232	0.0835	0.0628		
2.2232	0.0737	0.0739		
2.2232	0.0624	0.0837		
2.2232	0.0491	0.0922		
2.2232	0.0339	0.0988		
2.2232	0.0174	0.1030		
2.2232	0.0000	0.1045		
&BPNODE TNODE=3, TNPC=40, TINTC=3, &END				
&SECT1 STX=0.0, STY=0.0, STZ=0.0, SCALE=1.0, ALF=0.0, THETA=0.0, INMODE=4,				
TNODES=0, TNPS=0, TINTS=0, &END				
2.2692	0.0000	-0.0908		
2.2692	0.0154	-0.0894		
2.2692	0.0298	-0.0857		
2.2692	0.0429	-0.0799		
2.2692	0.0545	-0.0726		
2.2692	0.0642	-0.0641		
2.2692	0.0728	-0.0541		
2.2692	0.0801	-0.0426		
2.2692	0.0858	-0.0294		
2.2692	0.0895	-0.0150		
2.2692	0.0908	0.0000		
2.2692	0.0894	0.0154		
2.2692	0.0857	0.0298		
2.2692	0.0799	0.0429		
2.2692	0.0726	0.0545		
2.2692	0.0641	0.0642		
2.2692	0.0541	0.0728		
2.2692	0.0426	0.0801		
2.2692	0.0294	0.0858		
2.2692	0.0150	0.0895		
2.2692	0.0000	0.0908		
&BPNODE TNODE=3, TNPC=40, TINTC=3, &END				
&SECT1 STX=0.0, STY=0.0, STZ=0.0, SCALE=1.0, ALF=0.0, THETA=0.0, INMODE=4,				
TNODES=0, TNPS=0, TINTS=0, &END				
2.3087	0.0000	-0.0755		
2.3087	0.0130	-0.0754		
2.3087	0.0251	-0.0722		
2.3087	0.0362	-0.0674		
2.3087	0.0459	-0.0612		
2.3087	0.0541	-0.0541		
2.3087	0.0614	-0.0456		
2.3087	0.0676	-0.0359		
2.3087	0.0724	-0.0248		
2.3087	0.0754	-0.0127		
2.3087	0.0765	0.0000		
2.3087	0.0754	0.0130		
2.3087	0.0722	0.0251		
2.3087	0.0674	0.0362		
2.3087	0.0612	0.0459		
2.3087	0.0541	0.0541		
2.3087	0.0456	0.0614		
2.3087	0.0359	0.0676		
2.3087	0.0248	0.0724		
2.3087	0.0127	0.0754		
2.3087	0.0000	0.0765		
&BPNODE TNODE=3, TNPC=40, TINTC=3, &END				
&SECT1 STX=0.0, STY=0.0, STZ=0.0, SCALE=1.0, ALF=0.0, THETA=0.0, INMODE=4,				
TNODES=0, TNPS=0, TINTS=0, &END				
2.3413	0.0000	-0.0618		

Jun 11 1997 05:33

pr10w117.in

Page 13

```

2.3413 0.0106 -0.0609
2.3413 0.0203 -0.0583
2.3413 0.0293 -0.0544
2.3413 0.0371 -0.0494
2.3413 0.0437 -0.0436
2.3413 0.0496 -0.0368
2.3413 0.0546 -0.0289
2.3413 0.0584 -0.0200
2.3413 0.0609 -0.0102
2.3413 0.0618 0.0000
2.3413 0.0609 0.0106
2.3413 0.0583 0.0203
2.3413 0.0544 0.0293
2.3413 0.0494 0.0371
2.3413 0.0436 0.0437
2.3413 0.0368 0.0496
2.3413 0.0289 0.0546
2.3413 0.0200 0.0584
2.3413 0.0102 0.0609
2.3413 0.0000 0.0618
&BPNODE TNODE=3, TNPC=40, TINTC=3, &END
&SECT1 STX=0.0, STY=0.0, STZ=0.0, SCALE=1.0, ALF=0.0, THETA=0.0, INMODE=4,
TNODES=0, TNPS=0, TINTS=0, &END
2.3668 0.0000 -0.0467
2.3668 0.0081 -0.0460
2.3668 0.0155 -0.0440
2.3668 0.0222 -0.0410
2.3668 0.0282 -0.0372
2.3668 0.0332 -0.0328
2.3668 0.0374 -0.0278
2.3668 0.0412 -0.0219
2.3668 0.0441 -0.0151
2.3668 0.0460 -0.0077
2.3668 0.0467 0.0000
2.3668 0.0460 0.0081
2.3668 0.0440 0.0155
2.3668 0.0410 0.0222
2.3668 0.0372 0.0282
2.3668 0.0328 0.0332
2.3668 0.0278 0.0374
2.3668 0.0219 0.0412
2.3668 0.0151 0.0441
2.3668 0.0077 0.0460
2.3668 0.0000 0.0467
&BPNODE TNODE=3, TNPC=40, TINTC=3, &END
&SECT1 STX=0.0, STY=0.0, STZ=0.0, SCALE=1.0, ALF=0.0, THETA=0.0, INMODE=4,
TNODES=0, TNPS=0, TINTS=0, &END
2.3852 0.0000 -0.0313
2.3852 0.0055 -0.0308
2.3852 0.0104 -0.0295
2.3852 0.0149 -0.0275
2.3852 0.0188 -0.0250
2.3852 0.0221 -0.0221
2.3852 0.0252 -0.0185
2.3852 0.0277 -0.0145
2.3852 0.0296 -0.0100
2.3852 0.0308 -0.0051
2.3852 0.0313 0.0000
2.3852 0.0308 0.0055
2.3852 0.0295 0.0104
2.3852 0.0275 0.0149
2.3852 0.0250 0.0188
2.3852 0.0221 0.0221
2.3852 0.0185 0.0252
2.3852 0.0145 0.0277
2.3852 0.0100 0.0296
2.3852 0.0051 0.0308
2.3852 0.0000 0.0313
&BPNODE TNODE=3, TNPC=40, TINTC=3, &END
&SECT1 STX=0.0, STY=0.0, STZ=0.0, SCALE=1.0, ALF=0.0, THETA=0.0, INMODE=4,
TNODES=0, TNPS=0, TINTS=0, &END
2.3963 0.0000 -0.0157
2.3963 0.0029 -0.0154
2.3963 0.0053 -0.0148
2.3963 0.0075 -0.0138
2.3963 0.0095 -0.0125
2.3963 0.0111 0.0111
2.3963 0.0092 0.0127
2.3963 0.0072 0.0139
2.3963 0.0049 0.0149
2.3963 0.0025 0.0155
2.3963 0.0000 0.0157
&BPNODE TNODE=3, TNPC=40, TINTC=3, &END
&SECT1 STX=0.0, STY=0.0, STZ=0.0, SCALE=1.0, ALF=0.0, THETA=0.0, INMODE=4,
TNODES=5, TNPS=0, TINTS=0, &END
2.4000 0.0000 0.0000
2.4000 0.0000 0.0000
2.4000 0.0000 0.0000
2.4000 0.0000 0.0000
2.4000 0.0000 0.0000
2.4000 0.0000 0.0000
2.4000 0.0000 0.0000
2.4000 0.0000 0.0000
2.4000 0.0000 0.0000
2.4000 0.0000 0.0000
2.4000 0.0000 0.0000
2.4000 0.0000 0.0000
2.4000 0.0000 0.0000
2.4000 0.0000 0.0000
2.4000 0.0000 0.0000
2.4000 0.0000 0.0000
2.4000 0.0000 0.0000
2.4000 0.0000 0.0000
&BPNODE TNODE=3, TNPC=40, TINTC=3, &END
&WAKE1 IDWAK=1, IFLXW=1, ITRFTZ=0, INTRW=0, &END
Wake_1_Partial_Ring_at_x/c=0.99_closes_side_wakes
&WAKE2 KWPACH=1, KWSIDE=1, KWLIN=39, KWPAN1=25, &END
KWPAN2=40, NODEW=3, INITIAL=0, &END
&WAKE1 IDWAK=1, IFLXW=1, ITRFTZ=0, INTRW=0, &END
Wake_2_117_deg_wake_from_x/c=0.50
&WAKE2 KWPACH=1, KWSIDE=2, KWLIN=26, KWPAN1=21, &END
KWPAN2=38, NODEW=5, INITIAL=0, &END
&ONSTRM NONSL=1, KPSL=201,205,209,213,217,221,225,229,233,237,240,361,365,369,
373,377,381,385,389,393,397,400,601,605,609,613,117,621,625,629,634,637,600,761,765,7
69,773,777,781,785,789,793,797,800,1041,1045,1049,1053,1057,1061,1065,1069,1073,1077,
1080,1241,1245,1249,1253,1257,1261,
1265,1269,1273,1277,1280, &END
&BLPARAM RN=7700000, VISC=0.000017143, NSLBL=1,2,3,4,5,6,7,8,9,10,11,12,13,1
4,15,16,17,18,19,20,21,22,23,24,25,26,27,28,29,30,31,32,33,34,35,36,37,38,39,40,41,42
43,44,45,46,47,48,49,50,51,52,53,54,55,56,57,58,59,60,61,62,63,64,65,
66, &END
&VS1 NVOLR=0, NVOLC=0, &END
&VS2 X0=-0.1000, Y0=1.5000, Z0=-0.1000, INTVSR=1, &END
&VS3 X1=-0.1000, Y1=1.5000, Z1=0.1000, NPT1=0, &END
&VS4 X2=-0.1000, Y2=1.5000, Z2=0.1000, NPT2=20, &END
&VS5 X3=1.1000, Y3=1.5000, Z3=-0.1000, NPT3=25, &END
&VS6 X0=2.0000, Y0=2.0000, Z0=0.0000, INTVSC=1, &END
&VS7 X1=4.0000, Y1=2.0000, Z1=0.0000, &END
X2=2.0000, Y2=2.0000, Z2=1.0000, &END
&VS8 R1=0.1000, R2=1.0000, PHI1=0.0, PHI2=360.0, &END
&VS9 NRAD=5, NPHI=12, NLEN=3, &END

```

Jun 11 1997 05:33

pr10w117.in

Page 14

```

2.3963 0.0111 -0.0111
2.3963 0.0127 -0.0092
2.3963 0.0139 -0.0072
2.3963 0.0149 -0.0049
2.3963 0.0155 -0.0025
2.3963 0.0157 0.0000
2.3963 0.0154 0.0029
2.3963 0.0148 0.0053
2.3963 0.0138 0.0075
2.3963 0.0125 0.0095
2.3963 0.0111 0.0111
2.3963 0.0092 0.0127
2.3963 0.0072 0.0139
2.3963 0.0049 0.0149
2.3963 0.0025 0.0155
2.3963 0.0000 0.0157
&BPNODE TNODE=3, TNPC=40, TINTC=3, &END
&SECT1 STX=0.0, STY=0.0, STZ=0.0, SCALE=1.0, ALF=0.0, THETA=0.0, INMODE=4,
TNODES=5, TNPS=0, TINTS=0, &END
2.4000 0.0000 0.0000
2.4000 0.0000 0.0000
2.4000 0.0000 0.0000
2.4000 0.0000 0.0000
2.4000 0.0000 0.0000
2.4000 0.0000 0.0000
2.4000 0.0000 0.0000
2.4000 0.0000 0.0000
2.4000 0.0000 0.0000
2.4000 0.0000 0.0000
2.4000 0.0000 0.0000
2.4000 0.0000 0.0000
2.4000 0.0000 0.0000
2.4000 0.0000 0.0000
2.4000 0.0000 0.0000
2.4000 0.0000 0.0000
2.4000 0.0000 0.0000
2.4000 0.0000 0.0000
&BPNODE TNODE=3, TNPC=40, TINTC=3, &END
&WAKE1 IDWAK=1, IFLXW=1, ITRFTZ=0, INTRW=0, &END
Wake_1_Partial_Ring_at_x/c=0.99_closes_side_wakes
&WAKE2 KWPACH=1, KWSIDE=1, KWLIN=39, KWPAN1=25, &END
KWPAN2=40, NODEW=3, INITIAL=0, &END
&WAKE1 IDWAK=1, IFLXW=1, ITRFTZ=0, INTRW=0, &END
Wake_2_117_deg_wake_from_x/c=0.50
&WAKE2 KWPACH=1, KWSIDE=2, KWLIN=26, KWPAN1=21, &END
KWPAN2=38, NODEW=5, INITIAL=0, &END
&ONSTRM NONSL=1, KPSL=201,205,209,213,217,221,225,229,233,237,240,361,365,369,
373,377,381,385,389,393,397,400,601,605,609,613,117,621,625,629,634,637,600,761,765,7
69,773,777,781,785,789,793,797,800,1041,1045,1049,1053,1057,1061,1065,1069,1073,1077,
1080,1241,1245,1249,1253,1257,1261,
1265,1269,1273,1277,1280, &END
&BLPARAM RN=7700000, VISC=0.000017143, NSLBL=1,2,3,4,5,6,7,8,9,10,11,12,13,1
4,15,16,17,18,19,20,21,22,23,24,25,26,27,28,29,30,31,32,33,34,35,36,37,38,39,40,41,42
43,44,45,46,47,48,49,50,51,52,53,54,55,56,57,58,59,60,61,62,63,64,65,
66, &END
&VS1 NVOLR=0, NVOLC=0, &END
&VS2 X0=-0.1000, Y0=1.5000, Z0=-0.1000, INTVSR=1, &END
&VS3 X1=-0.1000, Y1=1.5000, Z1=0.1000, NPT1=0, &END
&VS4 X2=-0.1000, Y2=1.5000, Z2=0.1000, NPT2=20, &END
&VS5 X3=1.1000, Y3=1.5000, Z3=-0.1000, NPT3=25, &END
&VS6 X0=2.0000, Y0=2.0000, Z0=0.0000, INTVSC=1, &END
&VS7 X1=4.0000, Y1=2.0000, Z1=0.0000, &END
X2=2.0000, Y2=2.0000, Z2=1.0000, &END
&VS8 R1=0.1000, R2=1.0000, PHI1=0.0, PHI2=360.0, &END
&VS9 NRAD=5, NPHI=12, NLEN=3, &END

```

Jun 11 1997 05:33		pr10w117.in				Page 15
&SLIN1	NSTLIN=0,					&END
&SLIN2	SX0=	-2.0000,	SY0=	1.0000,	SZ0=	-0.5000,
	SU=	0.0000,	SD=	10.0000,	DS=	0.2500, INTSL= 1,
&SLIN2	SX0=	-2.0000,	SY0=	1.0000,	SZ0=	-0.4000,
	SU=	0.0000,	SD=	10.0000,	DS=	0.2500, INTSL= 1,
&SLIN2	SX0=	-2.0000,	SY0=	1.0000,	SZ0=	-0.3000,
	SU=	0.0000,	SD=	10.0000,	DS=	0.2500, INTSL= 1,
&SLIN2	SX0=	-2.0000,	SY0=	1.0000,	SZ0=	-0.2000,
	SU=	0.0000,	SD=	10.0000,	DS=	0.2500, INTSL= 1,
&SLIN2	SX0=	-2.0000,	SY0=	1.0000,	SZ0=	-0.1000,
	SU=	0.0000,	SD=	10.0000,	DS=	0.2500, INTSL= 1,
&SLIN2	SX0=	-2.0000,	SY0=	1.0000,	SZ0=	0.0000,
	SU=	0.0000,	SD=	10.0000,	DS=	0.2500, INTSL= 1,
						&END

Jun 20 1997 04:45 postprolate.f Page 1

```

program postprolate.exe !..for CMARC Prolate output file
!..by Tuncer, 3/96 modified by Steve Pollard 2/97
!..Steve Pollard 5/97 to extract and normalize Prolate
!..Spheroid CMARC Data

parameter nm=400
dimension npanel(nm)
character yn*1, line*132, fname*25, fnamee*20, byte*8
real x,y,z,phi
integer q
logical ok, out, tstep
data tstep,out /.false.,.false./, fname /"post.d"/
!..

>
print*, ' This program reads in CMARC.OUT file formats and'
print*, ' pulls out panel #, xyz location, cp and velocity.'
print*, ' The program requires the following steps: '
print*, ' 1) First the program checks for the file "post.d".'
print*, ' Data will be harvested from the PMARC output file'
print*, ' based on which panels are designated in "post.d".'
print*, ' You need to create a file "post.d" and put it in'
print*, ' this directory. The file has the following format:'
print*, ' First panel # Last Panel # Step Size'
print*, ' 2) Next, you will be asked to input a filename. It'
print*, ' should be a CMARC.OUT file.'
print*, ' 3) The program then prompts you for which time step'
print*, ' data should be harvested. Your choices are the'
print*, ' first time step (0) or the last time step'
print*, ' (usually 10). You should pick the last time'
print*, ' state to approx steady state.'
print*, ' 4) Finally, the program harvests the PMARC data and'
print*, ' outputs it into a file named "p<data file name>".'
print*, ' Program is starting:'
print*, '

1 inquire(FILE='post.d',EXIST=ok)
if (.not. ok) then
print*, '
print*, ' Input the filename containing the PMARC output - ', fname, '- d
oes NOT exist.'
print*, ' Enter the file name :>'
read*,'(A20)' fname
goto 1
endif
OPEN(1,FILE=FNAME,FORM='formatted',STATUS='OLD')
np = 0
do nr = 1,100
read(1,'end=2, err=2) ns,ne,ninc
do n = ns,ne,ninc
np = np+1
npanel(np) = n
enddo
if ( np .gt. nm ) then
print*, ' CHECK prog. dimensions '
stop
endif
enddo
2 close(1)

5 print*, '
PRINT*, ' Enter the PMARC DATA file name :>'
read*,'(A20)' fname
if( fname .eq. '' ) fname='out'
inquire(FILE=fname,EXIST=ok)
if (.not. ok) then
print*, ' ', fname, ' does NOT exist.'
goto 5
endif

```

107

Jun 20 1997 04:45 postprolate.f Page 2

```

OPEN(2,FILE=FNAME,FORM='formatted',STATUS='OLD')
fnamee = 'p'//fname
print*, ' Output FileName: ', fnamee
open(3,file=fnamee,form='formatted') !..output file

10 continue
nline = nline+1
read(2,'(a132)',end=100,err=10) line
read(line,'(a8)') byte
print*, 'Line :',nline, byte
IF( byte .eq. " TIME ST" ) then
read(line,'(a12,i10)') byte, nstep
out = .false.
tstep = .true.
nc = 1
ELSEIF( tstep .and. byte .eq. " AERODYN" ) then
print*, ' TIME STEP =',nstep
print*, ' Output panel info? [y/n]:> '
read*,'(A1)' yn
if( yn .eq. "y" .and. tstep ) then
out = .true.
elseif( yn .eq. "q" ) then
goto 100
endif
tstep = .false.
ELSEIF( out .and. nc .le. np ) then
read(1,'end=100,err=10) ipanel,x,y,z,cp,vx,vy,vz,v,dub,dphi,xmach
if ( npanel(nc) .eq. ipanel ) then
phi=atan(y/(-z))*57.3
if (phi .eq. 0) then
q=q+1
endif
if (phi .lt. 0) then
phi=180+phi
endif
if (phi .eq. 0) then
if (q .gt. 1) then
phi=180
endif
endif
x=x/2.4
y=y/2.4
z=z/2.4
write(3,'(i5,6f11.4)') ipanel,phi,x,y,z,cp,v
nc = nc+1
endif
ENDIF
goto 10

100 continue
close(2)
close(3)
print*, '
print*, '
print*, '**** Note: The output file does not contain column'
print*, ' headers, allowing the data to be easily'
print*, ' loaded into MATLAB using the "load"'
print*, ' command.'
print*, ' The data has the following format:'
print*, '
print*, ' *panel phi(deg) x/c y/c z/c cp v '
print*, '
print*, '

STOP
END

```





# APPENDIX H. LOFTSMAN INPUT FILES

Jun 11 1997 05:39	fogfusa.lft	Page 1
BOX MOLDLINES DATA TEMPLATE		
File name: fogfusa		
Last revision: 4/12/97		
-----		
BOTTOM WATERLINE		
Segments: 3		
Fore end	0,6.5	
Aft end	12,0	53.0,0 53.5,5.75
Corner	0,0	S 53.5,0
Curvature	.69	0.95
-----		
WAIST WATERLINE		
Segments: 1		
Fore end	0,6.5	
Aft end	53.5,6.5	
Corner	S	
Curvature		
-----		
TOP WATERLINE		
Segments: 7		
Fore end	0,6.5	
Aft end	8,9.3	15.2,9.3 21.6,13.0 29.0,14.6 44.6,11.6 53.0,11.5 53.5,6.5
Corner	0,9.3	S S 24.3,14.6 35.4,14.6 S 53.5,11.5
Curvature	0.7	0.71 0.81 .95
-----		
MAXIMUM BUTTLINE DISTANCE FROM PLANE OF SYMMETRY		
Segments: 6		
Fore end	0,0	
Aft end	1,3	1,3 22,4.5 43.6,4.5 53.1,1.3 53.5,0
Corner	0,2.9	S S S S 53.5,1.3
Curvature	.9	0.8 0.95
-----		
BOTTOM K FACTOR		
Segments: 3		
Fore end	0,0.93	
Aft end	12.0,0.98	43.6,0.98 53.5,0.95
Corner	S	S S
Curvature		
-----		
TOP K FACTOR		
Segments: 4		
Fore end	0,0.90	
Aft end	15.20,0.95	24,1.0 44.65,1.0 53.5,0.95
Corner	S	S S S
Curvature		
-----		
BUTTLINE AT PLANE OF SYMMETRY		
Segments: 0		

## NPS FROG UAV Main Wing - Loftsmen Input File

Date: 5/29/97

Breaks: 5

## Break 1

Axis: 24.65,0,13.1

Axis/chord: 0

Chord: 20.0

Incidence: 4.5

Cant: 0

Section file: N2415

T/C ratio: 0.1500

Spars: 0

Panel rib angles: 0,999.0000,0.0000

## Break 2

Axis: 24.65,6,13.1

Axis/chord: 0

Chord: 20.0

Incidence: 4.5

Cant: 0

Section file: N2415

T/C ratio: 0.1500

Spars: 0

Panel rib angles: 0,999.0000,0.0000

## Break 3

Axis: 24.65,31.5,13.1

Axis/chord: 0

Chord: 20.0

Incidence: 4.5

Cant: 0

Section file: N2415

T/C ratio: 0.1500

Spars: 0

Panel rib angles: 0,999.0000,0.0000

## Break 4

Axis: 24.65,53.0,13.1

Axis/chord: 0

Chord: 20.0

Incidence: 4.5

Cant: 0

Section file: N2415

T/C ratio: 0.1500

Spars: 0

Panel rib angles: 0,999.0000,0.0000

## Break 5

Axis: 24.65,61.0,13.1

Axis/chord: 0

Chord: 18.5

Incidence: 4.5

Cant: 0

Section file: N2415

T/C ratio: 0.1500

Spars: 0

Jun 11 1997 05:24

fogenpod.lft

Page 1

## FROG UAV ENGINE NACELLE

File name: fogenpod  
Last revision: 4/13/97-----  
BOTTOM WATERLINE

Segments: 4

Fore end	16.5,20.4			
Aft end	18.2,18.6	21.0,16.8	31.0,15.75	43.0, 16.8
Corner	16.6,19.6	19.15,17.35	23.8,15.9	35.6,15.65
Curvature	0.79	0.83	0.72	0.73

-----  
WAIST WATERLINE

Segments: 1

Fore end	16.5,20.4
Aft end	43.0,16.8
Corner	S
Curvature	

-----  
TOP WATERLINE

Segments: 4

Fore end	16.3,20.4			
Aft end	18.45,22.1	27.0,21.75	35.0,19.8	43.0,16.8
Corner	16.75,21.3	21.4,22.5	30.4,21.3	38.3,18.75
Curvature	0.79	0.80	0.70	0.75

-----  
MAXIMUM BUTTLINE DISTANCE FROM PLANE OF SYMMETRY

Segments: 4

Fore end	16.5,0			
Aft end	18.2,1.6	23.0,2.3	40.8,2.3	43.0,0
Corner	16.5,0.70	20.1,2.25	S	43.0,2.3
Curvature	0.72	0.75		0.90

-----  
BOTTOM K FACTOR

Segments: 4

Fore end	16.5,0.707			
Aft end	18.2,0.707	24.0,0.93	42.0,0.93	43.0,0.75
Corner	S	20,0.93	S	S
Curvature		0.9		

-----  
TOP K FACTOR

Segments: 4

Fore end	16.5,0.707			
Aft end	18.45,0.707	24.5,0.93	42.0,0.93	43.0,0.75
Corner	S	20.3,0.93	S	S
Curvature		0.9		

-----  
BUTTLINE AT PLANE OF SYMMETRY

Segments: 0

Jun 11 1997 05:27

fogpylo1.lft

Page 1

FROG UAV ENGINE PYLON (Lofted as A-Body Type)

-Basic pylon model modified so as not to have a top and bottom  
-Single strip which is the side of the pylon.

File name: FOGPYLO1  
Last revision: 4/23/97

Strips: 1  
Sym: Y

M1B

Segments: 1  
Fore end 25.8,0  
Aft end 37.7,0  
Corner 25.8,3.8  
K factor 0.71

M1W

Segments: 1  
Fore end 25.8,14.31  
Aft end 37.7,13.65  
Corner 31.0,15.45  
K factor 0.72

C1B

Segments: S

C1W

Segments: S

K1

Segments: S

M2B

Segments: =M1B

M2W

Segments: 1  
Fore end 25.8,16.01  
Aft end 37.7,16.1  
Corner 33.65,15.35  
K factor 0.65

Jun 11 1997 05:22

fogboom.lft

Page 1

FROG UAV Tail Boom

File name: fogboom  
Last revision: 4/28/97

4/28: added rounded start and finish to close ends

-----  
BOTTOM WATERLINE

Segments: 3

Fore end	53.5,9.375		
Aft end	54,8.5	88,8.5	88.5,9.375
Corner	53.5,8.5	S	88.5,8.5
Curvature	0.707		0.707

-----  
WAIST WATERLINE

Segments: 1

Fore end	53.5,9.375
Aft end	88.5, 9.375
Corner	S
Curvature	

-----  
TOP WATERLINE

Segments: 3

Fore end	53.5,9.375		
Aft end	54.0,10.25	88,10.25	88.5,9.375
Corner	53.5,10.25	S	88.5,10.25
Curvature	0.707		0.707

-----  
MAXIMUM BUTTLINE DISTANCE FROM PLANE OF SYMMETRY

Segments: 3

Fore end	53.5,0		
Aft end	54,0.875	88,0.875	88.5,0
Corner	53.5,0.875	S	88.5,0.875
Curvature	0.707		0.707

-----  
BOTTOM K FACTOR

Segments: 1

Fore end	53.5,0.707
Aft end	88.5, 0.707
Corner	S
Curvature	

-----  
TOP K FACTOR

Segments: 1

Fore end	53.5,0.707
Aft end	88.5, 0.707
Corner	S
Curvature	

-----  
BUTTLINE AT PLANE OF SYMMETRY

Segments: 0

FROG Horizontal Tail

Date: 4/14/97

Breaks: 2

Break 1

Axis: 82.5,0,8.09

Axis/chord: 0

Chord: 13.5

Incidence: 0

Cant: 0

Section file: N0006

T/C ratio: 0.06

Spars: 0

Panel rib angles: 0,999.0000,0.0000

Break 2

Axis: 86.5,19.875,8.09

Axis/chord: 0

Chord: 9.55

Incidence: 0

Cant: 0

Section file: N0006

T/C ratio: 0.06

Spars: 0

Panel rib angles: 0,999.0000,0.0000

FROG UAV Vertical Tail - LOFTSMAN input file

Date: 4/14/97

Breaks: 2

Break 1

Axis: 77.5,0,10.4

Axis/chord: 0

Chord: 20

Incidence: 0

Cant: 90

Section file: N0006

T/C ratio: 0.06

Spars: 0

Panel rib angles: 90,0,999

Break 2

Axis: 92.35,0,25.15

Axis/chord: 0

Chord: 10

Incidence: 0

Cant: 90

Section file: N0006

T/C ratio: 0.06

Spars: 0

Panel rib angles: 90,0,999





Jun 11 1997 05:30      froguav.in      Page 1

NPS FROG UAV CMARC/PNARC/PANEL MODEL - Units = inches

Complete FROG UAV Model (3790 Patches)

Blended Wing/Fuselage Patches  
Off-body Streamlines at Alpha/Static Probe Locations  
Symmetric Calculations turned off - Symmetric patches selected.

Created by: Steve Pollard 5/29/97  
Revised: 6/10/97

```

&BINP2 LSTINP=2, LSTOUT=0, LSTFRQ=0, LENRUN=0, LPLTYP=1, &END
&BINP3 LSTGEO=0, LSTNAB=0, LSTWAK=0, LSTCPV=0, &END
&BINP4 MAXIT=400, SOLRES=0.001, &END
&BINP5 NTSTPS= 4, DTSTEP=0.5, &END
&BINP6 RSYM=1.0, RGPR=0.0, RFF=5.0, RCORES=0.0080, RCREW=0.0080, &END
&BINP7 VINP=1056.00, VSOUND=13392.0, &END
&BINP8 ALDEG= 0.00, YAWDEG=0.0, PHIDOT=0.0, THEDOT=0.0, PSIDOT=0.0, &END
&BINP8A PHIMAX= 0.0, THEMEX= 0.0, PSIMAX=0.0, &END
&BINP8B WRX=0.0, WRY=0.0, WRZ=0.0, &END
&BINP8C DXMAX=0.0, DYMAX=0.0, DZMAX=0.0, &END
&BINP8D WTX=0.0, WTY=0.0, WTZ=0.0, &END
&BINP9 CBAR=20, SREF=2530.0, SSPAN= 62, &END
&BINP9A RMPX=31.55, RMPY=0.00, RMPZ=8.57, &END
&BINP10 NORSET=0, NBCHGE=0, NCZONE=0, &END
&BINP10A NCZPCH=0, CZDUB=0.0, VREF=0.0, &END
&BINP11 NORPCH=0, NORF=0, NORL=0, &END
&BINP11A NOCF=0, NOCL=0, VNORM=0.0, &END
&BINP12 KPAN=0, KSIDE=0, NEWSID=0, &END
&BINP13 NBLIT=0, &END

&ASEM1 ASEMXX=0.00, ASEMYY=0.00, ASEMZZ=0.00, &END
&ASEM2 ASCAL=1.00, ATHET=0.00, NODEA=5, &END
&ASEM3 APXX=0.00, APYY=0.00, APZZ=0.00, &END
&ASEM4 AHXX=0.00, AHYY=1.00, AHZZ=0.00, &END

&COMP1 COMPM= 0.0000, COMPY= 0.0000, COMPM= 0.0000, &END
&COMP2 CSCAL= 1.000, CTNET= 0.0, NODEC= 5, &END
&COMP3 CPXX= 0.0000, CPYY= 0.0000, CPZZ= 0.0000, &END
&COMP4 CHXX= 0.0000, CHYY= 1.000, CHZZ= 0.0000, &END

&PATCH1 IREV=0, IDPAT=2, MAKE=0, KCOMP=1, KASS=1, IPATSYM=1, IPATCOP=0, &END
&END
FUSELAGE_NOSE
&SECT1 STX=0.0, STY=0.0, STZ=0.0, SCALE=1.0, ALF=0.0, THETA=0.0, INMODE=4,
TNODS=0, TNPS=0, TINTS=0, &END
0.0000 0.0000 6.5000
0.0000 0.0000 6.5000
0.0000 0.0000 6.5000
0.0000 0.0000 6.5000
0.0000 0.0000 6.5000
0.0000 0.0000 6.5000
0.0000 0.0000 6.5000
0.0000 0.0000 6.5000
0.0000 0.0000 6.5000
0.0000 0.0000 6.5000
0.0000 0.0000 6.5000
0.0000 0.0000 6.5000
0.0000 0.0000 6.5000
0.0000 0.0000 6.5000
0.0000 0.0000 6.5000
0.0000 0.0000 6.5000
0.0000 0.0000 6.5000
0.0000 0.0000 6.5000
0.0000 0.0000 6.5000
&BPNODE TNODE=3, TNPC=0, TINTC=0, &END
&SECT1 STX=0.0, STY=0.0, STZ=0.0, SCALE=1.0, ALF=0.0, THETA=0.0, INMODE=4,
TNODS=0, TNPS=0, TINTS=0, &END
0.4894 0.0000 4.8456
0.4894 0.9694 4.8472
0.4894 1.8700 4.8569
0.4894 2.4101 4.8828
0.4894 2.6949 4.9422
0.4894 2.8308 5.0656
0.4894 2.8941 5.1171
0.4894 2.9200 5.7981

```

Jun 11 1997 05:30      froguav.in      Page 2

```

0.4894 2.9252 6.5846
0.4894 2.9005 6.9893
0.4894 2.8237 7.2119
0.4894 2.6669 7.3254
0.4894 2.3672 7.3842
0.4894 1.8372 7.4126
0.4894 0.9694 7.4244
0.4894 0.0000 7.4266
&BPNODE TNODE=3, TNPC=0, TINTC=0, &END
&SECT1 STX=0.0, STY=0.0, STZ=0.0, SCALE=1.0, ALF=0.0, THETA=0.0, INMODE=4,
TNODS=0, TNPS=0, TINTS=0, &END
1.9098 0.0000 3.2261
1.9098 1.2120 3.2304
1.9098 2.1514 3.2527
1.9098 2.6464 3.3105
1.9098 2.8844 3.4400
1.9098 2.9946 3.7159
1.9098 3.0431 4.2715
1.9098 3.0617 5.2972
1.9098 3.0650 6.5092
1.9098 3.0481 7.3382
1.9098 2.9862 7.8079
1.9098 2.8504 8.0540
1.9098 2.5827 8.1796
1.9098 2.0806 8.2410
1.9098 1.1960 8.2673
1.9098 0.0000 8.2731
&BPNODE TNODE=3, TNPC=0, TINTC=0, &END
&SECT1 STX=0.0, STY=0.0, STZ=0.0, SCALE=1.0, ALF=0.0, THETA=0.0, INMODE=4,
TNODS=0, TNPS=0, TINTS=0, &END
4.1221 0.0000 1.8058
4.1221 1.3792 1.8110
4.1221 2.3922 1.8401
4.1221 2.8791 1.9216
4.1221 3.0873 2.1152
4.1221 3.1756 2.5617
4.1221 3.2104 3.4985
4.1221 3.2210 4.8740
4.1221 3.2230 6.2532
4.1221 3.2129 7.5020
4.1221 3.1635 8.2308
4.1221 3.0419 8.6115
4.1221 2.7927 8.7934
4.1221 2.2900 8.8905
4.1221 1.3537 8.9164
4.1221 0.0000 8.9243
&BPNODE TNODE=3, TNPC=0, TINTC=0, &END
&SECT1 STX=0.0, STY=0.0, STZ=0.0, SCALE=1.0, ALF=0.0, THETA=0.0, INMODE=4,
TNODS=0, TNPS=0, TINTS=0, &END
6.9098 0.0000 0.7304
6.9098 1.4829 0.7343
6.9098 2.6474 0.7608
6.9098 3.1478 0.8479
6.9098 3.3299 1.0887
6.9098 3.3948 1.7151
6.9098 3.4159 3.0358
6.9098 3.4209 4.5188
6.9098 3.4221 6.0017
6.9098 3.4168 7.4676
6.9098 3.3779 8.4328
6.9098 3.2701 8.9147
6.9098 3.0302 9.1303
6.9098 2.5077 9.2266
6.9098 1.4679 9.2637
6.9098 0.0000 9.2711
&BPNODE TNODE=3, TNPC=0, TINTC=0, &END
&SECT1 STX=0.0, STY=0.0, STZ=0.0, SCALE=1.0, ALF=0.0, THETA=0.0, INMODE=4,
TNODS=0, TNPS=0, TINTS=0, &END
10.0000 0.0000 0.1152
10.0000 1.5156 0.1169
10.0000 2.8805 0.1323
10.0000 3.4347 0.2022
10.0000 3.5900 0.4599
10.0000 3.6111 1.2905
10.0000 3.6402 2.7963
10.0000 3.6423 4.3320

```

Jun 11 1997 05:30

froguav.in

Page 3

```

10.0000 3.6428 5.8276
10.0000 3.6400 7.3433
10.0000 3.6087 8.4519
10.0000 3.5110 8.9679
10.0000 3.2695 9.1801
10.0000 2.7005 9.2654
10.0000 1.5113 9.2951
10.0000 0.0000 9.3000
&BPNODE TNODE=3, TNPC=0, TINTC=0, &END
&SECT1 STX=0.0, STY=0.0, STZ=0.0, SCALE=1.0, ALF=0.0, THETA=0.0, INMODE=4,
TNODES=0, TNPS=0, TINTS=0, &END
13.0902 0.0000 0.0000
13.0902 1.5138 0.0007
13.0902 3.0061 0.0077
13.0902 3.6868 0.0552
13.0902 3.8313 0.3019
13.0902 3.8583 1.3036
13.0902 3.8623 2.8174
13.0902 3.8633 4.3312
13.0902 3.8636 5.8451
13.0902 3.8614 7.3589
13.0902 3.8344 8.5203
13.0902 3.7416 9.0232
13.0902 3.4903 9.2092
13.0902 2.8478 9.2766
13.0902 1.5130 9.2971
13.0902 0.0000 9.3000
&BPNODE TNODE=3, TNPC=0, TINTC=0, &END
&SECT1 STX=0.0, STY=0.0, STZ=0.0, SCALE=1.0, ALF=0.0, THETA=0.0, INMODE=4,
TNODES=0, TNPS=0, TINTS=0, &END
15.8779 0.0000 0.0000
15.8779 1.5558 0.0007
15.8779 3.1041 0.0070
15.8779 3.8653 0.0517
15.8779 4.0270 0.2880
15.8779 4.0569 1.2775
15.8779 4.0614 2.8332
15.8779 4.0624 4.3890
15.8779 4.0627 5.9448
15.8779 4.0612 7.5006
15.8779 4.0415 8.8474
15.8779 3.9629 9.4248
15.8779 3.7146 9.6156
15.8779 3.0056 9.6748
15.8779 1.5544 9.6899
15.8779 0.0000 9.6919
&BPNODE TNODE=3, TNPC=0, TINTC=0, &END
&SECT1 STX=0.0, STY=0.0, STZ=0.0, SCALE=1.0, ALF=0.0, THETA=0.0, INMODE=4,
TNODES=0, TNPS=0, TINTS=0, &END
18.0902 0.0000 0.0000
18.0902 1.6509 0.0007
18.0902 3.2889 0.0077
18.0902 4.0453 0.0611
18.0902 4.1913 0.3563
18.0902 4.2164 1.5673
18.0902 4.2198 3.2182
18.0902 4.2206 4.8691
18.0902 4.2207 6.5200
18.0902 4.2195 8.1710
18.0902 4.2094 9.8015
18.0902 4.1567 10.6520
18.0902 3.9490 10.8950
18.0902 3.2238 10.9567
18.0902 1.6504 10.9694
18.0902 0.0000 10.9709
&BPNODE TNODE=3, TNPC=0, TINTC=0, &END
&SECT1 STX=0.0, STY=0.0, STZ=0.0, SCALE=1.0, ALF=0.0, THETA=0.0, INMODE=4,
TNODES=0, TNPS=0, TINTS=0, &END
19.5106 0.0000 0.0000
19.5106 1.7043 0.0007
19.5106 3.3938 0.0081
19.5106 4.1553 0.0661
19.5106 4.2955 0.3979
19.5106 4.3184 1.7232
19.5106 4.3214 3.4275
19.5106 4.3221 5.1318

```

Printed by pollard from hawkkeye

Jun 11 1997 05:30

froguav.in

Page 4

```

19.5106 4.3222 6.8361
19.5106 4.3214 8.5405
19.5106 4.3169 10.2448
19.5106 4.2840 11.4245
19.5106 4.1133 11.7224
19.5106 3.3665 11.7816
19.5106 1.7041 11.7911
19.5106 0.0000 11.7920
&BPNODE TNODE=3, TNPC=0, TINTC=0, &END
&SECT1 STX=0.0, STY=0.0, STZ=0.0, SCALE=1.0, ALF=0.0, THETA=0.0, INMODE=4,
TNODES=3, TNPS=0, TINTS=0, &END
20.0000 0.0000 0.0000
20.0000 1.7202 0.0007
20.0000 3.4256 0.0081
20.0000 4.1917 0.0673
20.0000 4.3314 0.4135
20.0000 4.3535 1.7754
20.0000 4.3564 3.4956
20.0000 4.3571 5.2158
20.0000 4.3571 6.9360
20.0000 4.3565 8.6562
20.0000 4.3532 10.3763
20.0000 4.3272 11.6828
20.0000 4.1713 12.0088
20.0000 3.4117 12.0661
20.0000 1.7202 12.0742
20.0000 0.0000 12.0750
&BPNODE TNODE=3, TNPC=0, TINTC=0, &END
&PATCH1 IREV=0, IDPAT=2, MAKE=0, KCOMP=1, KASS=1, IPATSYM=1, IPATCUP=0, &END
ROOT TRANSITION FORE STARBOARD
&SECT1 STX=0.0, STY=0.0, STZ=0.0, SCALE=1.0, ALF=0.0, THETA=0.0, INMODE=4,
TNODES=0, TNPS=0, TINTS=0, &END
20.0000 0.0000 0.0000
20.0000 1.7202 0.0007
20.0000 3.4256 0.0081
20.0000 4.1917 0.0673
20.0000 4.3314 0.4135
20.0000 4.3535 1.7754
20.0000 4.3564 3.4956
20.0000 4.3571 5.2158
20.0000 4.3571 6.9360
20.0000 4.3565 8.6562
20.0000 4.3532 10.3763
20.0000 4.3272 11.6828
20.0000 4.1713 12.0088
20.0000 3.4117 12.0661
20.0000 1.7202 12.0742
20.0000 0.0000 12.0750
&BPNODE TNODE=3, TNPC=0, TINTC=0, &END
&SECT1 STX=0.0, STY=0.0, STZ=0.0, SCALE=1.0, ALF=0.0, THETA=0.0, INMODE=4,
TNODES=0, TNPS=0, TINTS=0, &END
20.4440 0.0000 0.0000
20.4440 1.7171 0.0007
20.4440 3.4241 0.0078
20.4440 4.2151 0.0644
20.4440 4.3616 0.3949
20.4440 4.3850 1.7224
20.4440 4.3881 3.4395
20.4440 4.3888 5.1566
20.4440 4.3889 6.8736
20.4440 4.3885 8.5907
20.4440 4.3865 10.3078
20.4440 4.3707 11.8182
20.4440 4.2485 12.2579
20.4440 3.5302 12.3232
20.4440 1.7837 12.3310
20.4440 0.0000 12.3317
&BPNODE TNODE=3, TNPC=0, TINTC=0, &END
&SECT1 STX=0.0, STY=0.0, STZ=0.0, SCALE=1.0, ALF=0.0, THETA=0.0, INMODE=4,
TNODES=0, TNPS=0, TINTS=0, &END
21.6065 0.0000 0.0000
21.6065 1.7392 0.0007
21.6065 3.4719 0.0076
21.6065 4.2930 0.0637
21.6065 4.4441 0.3949

```

Jun 11 1997 05:30			froguav.in	Page 5
21.6065	4.4680	1.7396		
21.6065	4.4711	3.4788		
21.6065	4.4718	5.2180		
21.6065	4.4719	6.9572		
21.6065	4.4717	8.6964		
21.6065	4.4711	10.4355		
21.6065	4.4667	12.1724		
21.6065	4.3976	12.9316		
21.6065	3.6877	12.9989		
21.6065	1.8477	13.0035		
21.6065	0.0000	13.0039		
&BPNODE TNODE=3, TNPC=0, TINTC=0, &END				
&SECT1 STX=0.0, STY=0.0, STZ=0.0, SCALE=1.0, ALF=0.0, THETA=0.0, INMODE=4,				
TNODE=0, TNPS=0, TINTS=0, &END				
23.0435	0.0000	0.0000		
23.0435	1.7813	0.0007		
23.0435	3.5493	0.0083		
23.0435	4.3384	0.0714		
23.0435	4.4761	0.4540		
23.0435	4.4967	1.9224		
23.0435	4.4994	3.7037		
23.0435	4.4999	5.4850		
23.0435	4.5000	7.2664		
23.0435	4.5000	9.0477		
23.0435	4.4999	10.8290		
23.0435	4.4993	12.6104		
23.0435	4.4647	13.6074		
23.0435	3.4428	13.6337		
23.0435	1.7214	13.6342		
23.0435	0.0000	13.6343		
&BPNODE TNODE=3, TNPC=0, TINTC=0, &END				
&SECT1 STX=0.0, STY=0.0, STZ=0.0, SCALE=1.0, ALF=0.0, THETA=0.0, INMODE=4,				
TNODE=0, TNPS=0, TINTS=0, &END				
24.2060	0.0000	0.0000		
24.2060	1.8135	0.0008		
24.2060	3.6032	0.0090		
24.2060	4.3543	0.0795		
24.2060	4.4793	0.5138		
24.2060	4.4972	2.0834		
24.2060	4.4995	3.8970		
24.2060	4.5000	5.7105		
24.2060	4.5000	7.5240		
24.2060	4.5000	9.3376		
24.2060	4.5000	11.1511		
24.2060	4.5000	12.9647		
24.2060	4.2423	13.9775		
24.2060	2.8282	13.9775		
24.2060	1.4141	13.9775		
24.2060	0.0000	13.9775		
&BPNODE TNODE=3, TNPC=0, TINTC=0, &END				
&SECT1 STX=0.0, STY=0.0, STZ=0.0, SCALE=1.0, ALF=0.0, THETA=0.0, INMODE=4,				
TNODE=3, TNPS=0, TINTS=0, &END				
24.6500	0.0000	0.0000		
24.6500	1.8258	0.0008		
24.6500	3.6231	0.0094		
24.6500	4.3600	0.0829		
24.6500	4.4804	0.5384		
24.6500	4.4973	2.1449		
24.6500	4.4995	3.9708		
24.6500	4.5000	5.7966		
24.6500	4.5000	7.6225		
24.6500	4.5000	9.4483		
24.6500	4.5000	11.2742		
24.6500	4.5000	13.1000		
24.6500	4.2213	14.0848		
24.6500	2.8142	14.0848		
24.6500	1.4071	14.0848		
24.6500	0.0000	14.0848		
&BPNODE TNODE=3, TNPC=0, TINTC=0, &END				
&PATCH REV=0, IDPAT=2, MAKE=0, KCOMP=1, KASS=1, IPATSYM=1, IPATCOP=0, &END				
ROCK LOWER STARBOARD				
&SECT1 STX=0.0, STY=0.0, STZ=0.0, SCALE=1.0, ALF=0.0, THETA=0.0, INMODE=4,				
TNODE=0, TNPS=0, TINTS=0, &END				
24.6500	0.0000	0.0000		
24.6500	1.8258	0.0008		

Jun 11 1997 05:30			froguav.in	Page 6
24.6500	3.6231	0.0094		
24.6500	4.3600	0.0829		
24.6500	4.4804	0.5384		
24.6500	4.4973	2.1449		
24.6500	4.4995	3.9708		
24.6500	4.5000	5.7966		
24.6500	4.5000	7.6225		
24.6500	4.5000	9.4483		
24.6500	4.5000	11.2742		
24.6500	4.5000	13.1000		
&BPNODE TNODE=3, TNPC=0, TINTC=0, &END				
&SECT1 STX=0.0, STY=0.0, STZ=0.0, SCALE=1.0, ALF=0.0, THETA=0.0, INMODE=4,				
TNODE=0, TNPS=0, TINTS=0, &END				
24.8679	0.0000	0.0000		
24.8679	1.7867	0.0007		
24.8679	3.5584	0.0084		
24.8679	4.3412	0.0727		
24.8679	4.4766	0.4634		
24.8679	4.4968	1.9491		
24.8679	4.4994	3.7357		
24.8679	4.4999	5.5224		
24.8679	4.5000	7.3091		
24.8679	4.5000	9.0958		
24.8679	4.5000	10.8824		
24.8679	4.5000	12.6691		
&BPNODE TNODE=3, TNPC=0, TINTC=0, &END				
&SECT1 STX=0.0, STY=0.0, STZ=0.0, SCALE=1.0, ALF=0.0, THETA=0.0, INMODE=4,				
TNODE=0, TNPS=0, TINTS=0, &END				
25.5119	0.0000	0.0000		
25.5119	1.7519	0.0007		
25.5119	3.4973	0.0076		
25.5119	4.3223	0.0646		
25.5119	4.4728	0.4048		
25.5119	4.4962	1.7750		
25.5119	4.4992	3.5269		
25.5119	4.4999	5.2788		
25.5119	4.5000	7.0306		
25.5119	4.5000	8.7825		
25.5119	4.5000	10.5344		
25.5119	4.5000	12.2862		
&BPNODE TNODE=3, TNPC=0, TINTC=0, &END				
&SECT1 STX=0.0, STY=0.0, STZ=0.0, SCALE=1.0, ALF=0.0, THETA=0.0, INMODE=4,				
TNODE=0, TNPS=0, TINTS=0, &END				
26.5541	0.0000	0.0000		
26.5541	1.7230	0.0007		
26.5541	3.4441	0.0070		
26.5541	4.3050	0.0585		
26.5541	4.4691	0.3614		
26.5541	4.4956	1.6308		
26.5541	4.4991	3.3539		
26.5541	4.4999	5.0769		
26.5541	4.5000	6.7999		
26.5541	4.5000	8.5229		
26.5541	4.5000	10.2460		
26.5541	4.5000	11.9690		
&BPNODE TNODE=3, TNPC=0, TINTC=0, &END				
&SECT1 STX=0.0, STY=0.0, STZ=0.0, SCALE=1.0, ALF=0.0, THETA=0.0, INMODE=4,				
TNODE=0, TNPS=0, TINTS=0, &END				
27.9487	0.0000	0.0000		
27.9487	1.7011	0.0006		
27.9487	3.4020	0.0066		
27.9487	4.2909	0.0542		
27.9487	4.4660	0.3314		
27.9487	4.4951	1.5215		
27.9487	4.4990	3.2226		
27.9487	4.4998	4.9237		
27.9487	4.5000	6.6249		
27.9487	4.5000	8.3260		
27.9487	4.5000	10.0272		
27.9487	4.5000	11.7283		
&BPNODE TNODE=3, TNPC=0, TINTC=0, &END				
&SECT1 STX=0.0, STY=0.0, STZ=0.0, SCALE=1.0, ALF=0.0, THETA=0.0, INMODE=4,				
TNODE=0, TNPS=0, TINTS=0, &END				
29.6349	0.0000	0.0000		
29.6349	1.6863	0.0006		
29.6349	3.3725	0.0063		

Jun 11 1997 05:30

froguav.in

Page 7

```

29.6349 4.2808 0.0515
29.6349 4.4638 0.3122
29.6349 4.4947 1.4471
29.6349 4.4989 3.1333
29.6349 4.4998 4.8196
29.6349 4.5000 6.5059
29.6349 4.5000 8.1922
29.6349 4.5000 9.8784
29.6349 4.5000 11.5647
&BPNODE TNODE=3, TNPC=0, TINTC=0, &END
&SECT1 STX=0.0, STY=0.0, STZ=0.0, SCALE=1.0, ALF=0.0, THETA=0.0, INMODE=4,
TNODES=0, TNPS=0, TINTS=0, &END
31.5390 0.0000 0.0000
31.5390 1.6769 0.0006
31.5390 3.3538 0.0061
31.5390 4.2741 0.0499
31.5390 4.4623 0.3007
31.5390 4.4944 1.4001
31.5390 4.4989 3.0770
31.5390 4.4998 4.7539
31.5390 4.5000 6.4308
31.5390 4.5000 8.1077
31.5390 4.5000 9.7845
31.5390 4.5000 11.4614
&BPNODE TNODE=3, TNPC=0, TINTC=0, &END
&SECT1 STX=0.0, STY=0.0, STZ=0.0, SCALE=1.0, ALF=0.0, THETA=0.0, INMODE=4,
TNODES=0, TNPS=0, TINTS=0, &END
33.5777 0.0000 0.0000
33.5777 1.6712 0.0006
33.5777 3.3424 0.0060
33.5777 4.2700 0.0489
33.5777 4.4613 0.2939
33.5777 4.4943 1.3718
33.5777 4.4988 3.0430
33.5777 4.4998 4.7142
33.5777 4.5000 6.3855
33.5777 4.5000 8.0567
33.5777 4.5000 9.7279
33.5777 4.5000 11.3991
&BPNODE TNODE=3, TNPC=0, TINTC=0, &END
&SECT1 STX=0.0, STY=0.0, STZ=0.0, SCALE=1.0, ALF=0.0, THETA=0.0, INMODE=4,
TNODES=0, TNPS=0, TINTS=0, &END
35.6619 0.0000 0.0000
35.6619 1.6694 0.0006
35.6619 3.3388 0.0060
35.6619 4.2687 0.0486
35.6619 4.4610 0.2918
35.6619 4.4942 1.3627
35.6619 4.4988 3.0321
35.6619 4.4998 4.7015
35.6619 4.5000 6.3708
35.6619 4.5000 8.0402
35.6619 4.5000 9.7096
35.6619 4.5000 11.3790
&BPNODE TNODE=3, TNPC=0, TINTC=0, &END
&SECT1 STX=0.0, STY=0.0, STZ=0.0, SCALE=1.0, ALF=0.0, THETA=0.0, INMODE=4,
TNODES=0, TNPS=0, TINTS=0, &END
37.7006 0.0000 0.0000
37.7006 1.6701 0.0006
37.7006 3.3402 0.0060
37.7006 4.2692 0.0487
37.7006 4.4611 0.2926
37.7006 4.4942 1.3663
37.7006 4.4988 3.0365
37.7006 4.4998 4.7066
37.7006 4.5000 6.3767
37.7006 4.5000 8.0468
37.7006 4.5000 9.7170
37.7006 4.5000 11.3871
&BPNODE TNODE=3, TNPC=0, TINTC=0, &END
&SECT1 STX=0.0, STY=0.0, STZ=0.0, SCALE=1.0, ALF=0.0, THETA=0.0, INMODE=4,
TNODES=0, TNPS=0, TINTS=0, &END
39.6047 0.0000 0.0000
39.6047 1.6716 0.0006
39.6047 3.3432 0.0060
39.6047 4.2703 0.0490

```

Printed by pollard from hawkkeys

Jun 11 1997 05:30

froguav.in

Page 8

```

39.6047 4.4614 0.2944
39.6047 4.4943 1.3737
39.6047 4.4988 3.0452
39.6047 4.4998 4.7168
39.6047 4.5000 6.3884
39.6047 4.5000 8.0600
39.6047 4.5000 9.7316
39.6047 4.5000 11.4032
&BPNODE TNODE=3, TNPC=0, TINTC=0, &END
&SECT1 STX=0.0, STY=0.0, STZ=0.0, SCALE=1.0, ALF=0.0, THETA=0.0, INMODE=4,
TNODES=0, TNPS=0, TINTS=0, &END
41.2909 0.0000 0.0000
41.2909 1.6739 0.0006
41.2909 3.3479 0.0061
41.2909 4.2720 0.0494
41.2909 4.4618 0.2971
41.2909 4.4943 1.3894
41.2909 4.4988 3.0593
41.2909 4.4998 4.7332
41.2909 4.5000 6.4072
41.2909 4.5000 8.0811
41.2909 4.5000 9.7550
41.2909 4.5000 11.4290
&BPNODE TNODE=3, TNPC=0, TINTC=0, &END
&SECT1 STX=0.0, STY=0.0, STZ=0.0, SCALE=1.0, ALF=0.0, THETA=0.0, INMODE=4,
TNODES=0, TNPS=0, TINTS=0, &END
42.6855 0.0000 0.0000
42.6855 1.6764 0.0006
42.6855 3.3529 0.0061
42.6855 4.2738 0.0498
42.6855 4.4622 0.3001
42.6855 4.4944 1.3979
42.6855 4.4989 3.0743
42.6855 4.4998 4.7507
42.6855 4.5000 6.4272
42.6855 4.5000 8.1036
42.6855 4.5000 9.7800
42.6855 4.5000 11.4565
&BPNODE TNODE=3, TNPC=0, TINTC=0, &END
&SECT1 STX=0.0, STY=0.0, STZ=0.0, SCALE=1.0, ALF=0.0, THETA=0.0, INMODE=4,
TNODES=0, TNPS=0, TINTS=0, &END
43.7277 0.0000 0.0000
43.7277 1.6766 0.0007
43.7277 3.3528 0.0067
43.7277 4.2374 0.0530
43.7277 4.4194 0.3099
43.7277 4.4514 1.4174
43.7277 4.4558 3.0940
43.7277 4.4568 4.7706
43.7277 4.4570 6.4472
43.7277 4.4570 8.1238
43.7277 4.4570 9.8004
43.7277 4.4570 11.4770
&BPNODE TNODE=3, TNPC=0, TINTC=0, &END
&SECT1 STX=0.0, STY=0.0, STZ=0.0, SCALE=1.0, ALF=0.0, THETA=0.0, INMODE=4,
TNODES=0, TNPS=0, TINTS=0, &END
44.3717 0.0000 0.0000
44.3717 1.6650 0.0009
44.3717 3.3021 0.0097
44.3717 4.0431 0.0680
44.3717 4.2033 0.3596
44.3717 4.2341 1.5019
44.3717 4.2388 3.1680
44.3717 4.2398 4.8331
44.3717 4.2400 6.4981
44.3717 4.2400 8.1631
44.3717 4.2400 9.8282
44.3717 4.2400 11.4932
&BPNODE TNODE=3, TNPC=0, TINTC=0, &END
&SECT1 STX=0.0, STY=0.0, STZ=0.0, SCALE=1.0, ALF=0.0, THETA=0.0, INMODE=4,
TNODES=0, TNPS=0, TINTS=0, &END
44.5909 0.0000 0.0000
44.5909 1.6672 0.0010
44.5909 3.2859 0.0111
44.5909 3.9797 0.0752
44.5909 4.1306 0.3843

```

Jun 11 1997 05:30 froguav.in Page 9

```

44.5909 4.1604 1.5597
44.5909 4.1650 3.2268
44.5909 4.1660 4.8948
44.5909 4.1662 6.5612
44.5909 4.1662 8.2284
44.5909 4.1662 9.8955
44.5909 4.1662 11.5627
&BPNODE TNODE=3, TNPC=0, TINTC=0, &END

&PATCH1 IREV=0, IDPAT=2, MAKE=0, KCOMP=1, KASS=1, IPATSYM=1, IPATCOP=0, &END
ROOT UPPER STARBOARD
&SECT1 STX=0.0, STY=0.0, STZ=0.0, SCALE=1.0, ALF=0.0, THETA=0.0, INMODE=4,
TNODES=0, TNPS=0, TINTS=0, &END
24.6500 4.5000 13.1000
24.6500 4.2213 14.0848
24.6500 2.8142 14.0848
24.6500 1.4071 14.0848
24.6500 0.0000 14.0848
&BPNODE TNODE=3, TNPC=0, TINTC=0, &END
&SECT1 STX=0.0, STY=0.0, STZ=0.0, SCALE=1.0, ALF=0.0, THETA=0.0, INMODE=4,
TNODES=0, TNPS=0, TINTS=0, &END
24.8679 4.5000 13.5517
24.8679 4.2213 14.1334
24.8679 2.8142 14.1334
24.8679 1.4071 14.1334
24.8679 0.0000 14.1334
&BPNODE TNODE=3, TNPC=0, TINTC=0, &END
&SECT1 STX=0.0, STY=0.0, STZ=0.0, SCALE=1.0, ALF=0.0, THETA=0.0, INMODE=4,
TNODES=0, TNPS=0, TINTS=0, &END
25.5119 4.5000 13.9485
25.5119 4.2213 14.2622
25.5119 2.8142 14.2622
25.5119 1.4071 14.2622
25.5119 0.0000 14.2622
&BPNODE TNODE=3, TNPC=0, TINTC=0, &END
&SECT1 STX=0.0, STY=0.0, STZ=0.0, SCALE=1.0, ALF=0.0, THETA=0.0, INMODE=4,
TNODES=0, TNPS=0, TINTS=0, &END
26.5541 4.5000 14.2646
26.5541 4.2213 14.4272
26.5541 2.8142 14.4272
26.5541 1.4071 14.4272
26.5541 0.0000 14.4272
&BPNODE TNODE=3, TNPC=0, TINTC=0, &END
&SECT1 STX=0.0, STY=0.0, STZ=0.0, SCALE=1.0, ALF=0.0, THETA=0.0, INMODE=4,
TNODES=0, TNPS=0, TINTS=0, &END
27.9487 4.5000 14.4706
27.9487 4.2213 14.5653
27.9487 2.8142 14.5653
27.9487 1.4071 14.5653
27.9487 0.0000 14.5653
&BPNODE TNODE=3, TNPC=0, TINTC=0, &END
&SECT1 STX=0.0, STY=0.0, STZ=0.0, SCALE=1.0, ALF=0.0, THETA=0.0, INMODE=4,
TNODES=0, TNPS=0, TINTS=0, &END
29.6349 4.5000 14.5367
29.6349 4.2213 14.5971
29.6349 2.8142 14.5971
29.6349 1.4071 14.5971
29.6349 0.0000 14.5971
&BPNODE TNODE=3, TNPC=0, TINTC=0, &END
&SECT1 STX=0.0, STY=0.0, STZ=0.0, SCALE=1.0, ALF=0.0, THETA=0.0, INMODE=4,
TNODES=0, TNPS=0, TINTS=0, &END
31.5390 4.5000 14.4449
31.5390 4.2213 14.5447
31.5390 2.8142 14.5447
31.5390 1.4071 14.5447
31.5390 0.0000 14.5447
&BPNODE TNODE=3, TNPC=0, TINTC=0, &END
&SECT1 STX=0.0, STY=0.0, STZ=0.0, SCALE=1.0, ALF=0.0, THETA=0.0, INMODE=4,
TNODES=0, TNPS=0, TINTS=0, &END
33.5777 4.5000 14.2088
33.5777 4.2213 14.3864
33.5777 2.8142 14.3864
33.5777 1.4071 14.3864
33.5777 0.0000 14.3864
&BPNODE TNODE=3, TNPC=0, TINTC=0, &END
&SECT1 STX=0.0, STY=0.0, STZ=0.0, SCALE=1.0, ALF=0.0, THETA=0.0, INMODE=4,

```

Jun 11 1997 05:30 froguav.in Page 10

```

TNODES=0, TNPS=0, TINTS=0, &END
35.6619 4.5000 13.8627
35.6619 4.2213 14.0807
35.6619 2.8142 14.0807
35.6619 1.4071 14.0807
35.6619 0.0000 14.0807
&BPNODE TNODE=3, TNPC=0, TINTC=0, &END
&SECT1 STX=0.0, STY=0.0, STZ=0.0, SCALE=1.0, ALF=0.0, THETA=0.0, INMODE=4,
TNODES=0, TNPS=0, TINTS=0, &END
37.7006 4.5000 13.4473
37.7006 4.2213 13.6423
37.7006 2.8142 13.6423
37.7006 1.4071 13.6423
37.7006 0.0000 13.6423
&BPNODE TNODE=3, TNPC=0, TINTC=0, &END
&SECT1 STX=0.0, STY=0.0, STZ=0.0, SCALE=1.0, ALF=0.0, THETA=0.0, INMODE=4,
TNODES=0, TNPS=0, TINTS=0, &END
39.6047 4.5000 12.9980
39.6047 4.2213 13.1398
39.6047 2.8142 13.1398
39.6047 1.4071 13.1398
39.6047 0.0000 13.1398
&BPNODE TNODE=3, TNPC=0, TINTC=0, &END
&SECT1 STX=0.0, STY=0.0, STZ=0.0, SCALE=1.0, ALF=0.0, THETA=0.0, INMODE=4,
TNODES=0, TNPS=0, TINTS=0, &END
41.2909 4.5000 12.5573
41.2909 4.2213 12.6458
41.2909 2.8142 12.6458
41.2909 1.4071 12.6458
41.2909 0.0000 12.6458
&BPNODE TNODE=3, TNPC=0, TINTC=0, &END
&SECT1 STX=0.0, STY=0.0, STZ=0.0, SCALE=1.0, ALF=0.0, THETA=0.0, INMODE=4,
TNODES=0, TNPS=0, TINTS=0, &END
42.6855 4.5000 12.1606
42.6855 4.2213 12.2144
42.6855 2.8142 12.2144
42.6855 1.4071 12.2144
42.6855 0.0000 12.2144
&BPNODE TNODE=3, TNPC=0, TINTC=0, &END
&SECT1 STX=0.0, STY=0.0, STZ=0.0, SCALE=1.0, ALF=0.0, THETA=0.0, INMODE=4,
TNODES=0, TNPS=0, TINTS=0, &END
43.7277 4.4570 11.8400
43.7277 4.1900 11.8826
43.7277 2.8142 11.8826
43.7277 1.4071 11.8826
43.7277 0.0000 11.8826
&BPNODE TNODE=3, TNPC=0, TINTC=0, &END
&SECT1 STX=0.0, STY=0.0, STZ=0.0, SCALE=1.0, ALF=0.0, THETA=0.0, INMODE=4,
TNODES=0, TNPS=0, TINTS=0, &END
44.3717 4.2400 11.6336
44.3717 3.9900 11.6743
44.3717 2.8142 11.6743
44.3717 1.4071 11.6743
44.3717 0.0000 11.6743
&BPNODE TNODE=3, TNPC=0, TINTC=0, &END
&SECT1 STX=0.0, STY=0.0, STZ=0.0, SCALE=1.0, ALF=0.0, THETA=0.0, INMODE=4,
TNODES=3, TNPS=0, TINTS=0, &END
44.5909 4.1662 11.5627
44.5909 3.9300 11.6030
44.5909 2.8142 11.6030
44.5909 1.4071 11.6030
44.5909 0.0000 11.6030
&BPNODE TNODE=3, TNPC=0, TINTC=0, &END

&PATCH1 IREV=0, IDPAT=2, MAKE=0, KCOMP=1, KASS=1, IPATSYM=1, IPATCOP=0, &END
ROOT TRANSITION AFT STARBOARD
&SECT1 STX=0.0, STY=0.0, STZ=0.0, SCALE=1.0, ALF=0.0, THETA=0.0, INMODE=4,
TNODES=0, TNPS=0, TINTS=0, &END
44.5909 0.0000 0.0000
44.5909 1.6672 0.0010
44.5909 3.2859 0.0111
44.5909 3.9797 0.0222
44.5909 4.1306 0.3843
44.5909 4.1604 1.5597
44.5909 4.1650 3.2268
44.5909 4.1660 4.8948

```

Jun 11 1997 05:30      froguav.in      Page 11

```

44.5909 4.1662 6.5612
44.5909 4.1662 8.2284
44.5909 4.1662 9.8955
44.5909 4.1662 11.5627
44.5909 3.9300 11.6030
44.5909 2.8142 11.6030
44.5909 1.4071 11.6030
44.5909 0.0000 11.6030
&BPNODE TNODE=3, TNPC=0, TINTC=0, &END
&SECT1 STX=0.0, STY=0.0, STZ=0.0, SCALE=1.0, ALF=0.0, THETA=0.0, INMODE=4,
  TNODES=0, TNPS=0, TINTS=0, &END
44.9164 0.0000 0.0000
44.9164 1.6527 0.0012
44.9164 3.2292 0.0128
44.9164 3.8750 0.0819
44.9164 4.0206 0.4023
44.9164 4.0505 1.5694
44.9164 4.0553 3.2220
44.9164 4.0564 4.8747
44.9164 4.0566 6.5274
44.9164 4.0566 8.1800
44.9164 4.0566 9.8327
44.9164 4.0562 11.4773
44.9164 3.8438 11.5962
44.9164 2.8142 11.5962
44.9164 1.4071 11.5962
44.9164 0.0000 11.5962
&BPNODE TNODE=3, TNPC=0, TINTC=0, &END
&SECT1 STX=0.0, STY=0.0, STZ=0.0, SCALE=1.0, ALF=0.0, THETA=0.0, INMODE=4,
  TNODES=0, TNPS=0, TINTS=0, &END
45.7687 0.0000 0.0000
45.7687 1.6149 0.0016
45.7687 3.0609 0.0178
45.7687 3.6006 0.1009
45.7687 3.7321 0.4387
45.7687 3.7625 1.5799
45.7687 3.7679 3.1948
45.7687 3.7692 4.8097
45.7687 3.7695 6.4245
45.7687 3.7695 8.0394
45.7687 3.7693 9.6543
45.7687 3.7674 11.2536
45.7687 3.5600 11.5767
45.7687 2.8142 11.5857
45.7687 1.4071 11.5860
45.7687 0.0000 11.5861
&BPNODE TNODE=3, TNPC=0, TINTC=0, &END
&SECT1 STX=0.0, STY=0.0, STZ=0.0, SCALE=1.0, ALF=0.0, THETA=0.0, INMODE=4,
  TNODES=0, TNPS=0, TINTS=0, &END
46.8222 0.0000 0.0000
46.8222 1.5638 0.0025
46.8222 2.8199 0.0253
46.8222 3.2590 0.249
46.8222 3.3765 0.4866
46.8222 3.4068 1.5991
46.8222 3.4128 3.1628
46.8222 3.4143 4.7266
46.8222 3.4146 6.2903
46.8222 3.4146 7.8541
46.8222 3.4142 9.4178
46.8222 3.4111 10.9772
46.8222 3.3229 11.5231
46.8222 2.8650 11.5700
46.8222 1.4071 11.5733
46.8222 0.0000 11.5735
&BPNODE TNODE=3, TNPC=0, TINTC=0, &END
&SECT1 STX=0.0, STY=0.0, STZ=0.0, SCALE=1.0, ALF=0.0, THETA=0.0, INMODE=4,
  TNODES=0, TNPS=0, TINTS=0, &END
47.6745 0.0000 0.0000
47.6745 1.5223 0.0036
47.6745 2.6098 0.2323
47.6745 2.9827 0.1456
47.6745 3.0895 0.5253
47.6745 3.1192 1.6204
47.6745 3.1255 3.1427
47.6745 3.1271 4.6650

```

Jun 11 1997 05:30      froguav.in      Page 12

```

47.6745 3.1275 6.1873
47.6745 3.1275 7.7096
47.6745 3.1269 9.2319
47.6745 3.1232 10.7536
47.6745 3.0838 11.4579
47.6745 2.7717 11.5525
47.6745 1.4071 11.5627
47.6745 0.0000 11.5634
&BPNODE TNODE=3, TNPC=0, TINTC=0, &END
&SECT1 STX=0.0, STY=0.0, STZ=0.0, SCALE=1.0, ALF=0.0, THETA=0.0, INMODE=4,
  TNODES=0, TNPS=0, TINTS=0, &END
48.0000 0.0000 0.0000
48.0000 1.5058 0.0041
48.0000 2.5263 0.0352
48.0000 2.8769 0.1533
48.0000 2.9802 0.5421
48.0000 3.0094 1.6335
48.0000 3.0158 3.1393
48.0000 3.0175 4.6450
48.0000 3.0179 6.1508
48.0000 3.0178 7.6566
48.0000 3.0172 9.1624
48.0000 3.0134 10.6681
48.0000 2.9761 11.4292
48.0000 2.7054 11.5444
48.0000 1.4071 11.5586
48.0000 0.0000 11.5595
&BPNODE TNODE=3, TNPC=0, TINTC=0, &END
&PATCH IREV=0, IDPAT=2, MAKE=0, KCOMP=1, KASS=1, IPATSYM=1, IPATCOP=0,
&END
FUSELAGE_AFT
&SECT1 STX=0.0, STY=0.0, STZ=0.0, SCALE=1.0, ALF=0.0, THETA=0.0, INMODE=4,
  TNODES=0, TNPS=0, TINTS=0, &END
48.0000 0.0000 0.0000
48.0000 1.5058 0.0041
48.0000 2.5263 0.0352
48.0000 2.8769 0.1533
48.0000 2.9802 0.5421
48.0000 3.0094 1.6335
48.0000 3.0158 3.1393
48.0000 3.0175 4.6450
48.0000 3.0179 6.1508
48.0000 3.0178 7.6566
48.0000 3.0172 9.1624
48.0000 3.0134 10.6681
48.0000 2.9761 11.4292
48.0000 2.7054 11.5444
48.0000 1.5058 11.5586
48.0000 0.0000 11.5595
&BPNODE TNODE=3, TNPC=0, TINTC=0, &END
&SECT1 STX=0.0, STY=0.0, STZ=0.0, SCALE=1.0, ALF=0.0, THETA=0.0, INMODE=4,
  TNODES=0, TNPS=0, TINTS=0, &END
48.2093 0.0000 0.0000
48.2093 1.5001 0.0045
48.2093 2.4757 0.0375
48.2093 2.8105 0.1604
48.2093 2.9106 0.5614
48.2093 2.9390 1.6667
48.2093 2.9453 3.1668
48.2093 2.9469 4.6669
48.2093 2.9474 6.1670
48.2093 2.9473 7.6670
48.2093 2.9466 9.1671
48.2093 2.9424 10.6669
48.2093 2.9044 11.4175
48.2093 2.6462 11.5397
48.2093 1.4996 11.5559
48.2093 0.0000 11.5570
&BPNODE TNODE=3, TNPC=0, TINTC=0, &END
&SECT1 STX=0.0, STY=0.0, STZ=0.0, SCALE=1.0, ALF=0.0, THETA=0.0, INMODE=4,
  TNODES=0, TNPS=0, TINTS=0, &END
48.8055 0.0000 0.0000
48.8055 1.4733 0.0060
48.8055 2.3269 0.0446
48.8055 2.6221 0.1829

```

Jun 11 1997 05:30      froguav.in      Page 13

```

48.8055 2.7120 0.6123
48.8055 2.7385 1.7484
48.8055 2.7445 3.2309
48.8055 2.7462 4.7134
48.8055 2.7466 6.1959
48.8055 2.7465 7.6784
48.8055 2.7456 9.1609
48.8055 2.7404 10.6408
48.8055 2.7016 11.3810
48.8055 2.4736 11.5252
48.8055 1.4808 11.5480
48.8055 0.0000 11.5499
&BPNODE TNODE=3, TNPC=0, TINTC=0, &END
&SECT1 STX=0.0, STY=0.0, STZ=0.0, SCALE=1.0, ALF=0.0, THETA=0.0, INMODE=4,
TNODE=0, TNPS=0, TINTS=0, &END
49.6976 0.0000 0.0000
49.6976 1.3923 0.0085
49.6976 2.0943 0.0564
49.6976 2.3385 0.2185
49.6976 2.4154 0.6980
49.6976 2.4387 1.8818
49.6976 2.4441 3.3356
49.6976 2.4457 4.7894
49.6976 2.4461 6.2432
49.6976 2.4459 7.6970
49.6976 2.4448 9.1508
49.6976 2.4382 10.5961
49.6976 2.3950 11.3282
49.6976 2.2089 11.5012
49.6976 1.4448 11.5354
49.6976 0.0000 11.5393
&BPNODE TNODE=3, TNPC=0, TINTC=0, &END
&SECT1 STX=0.0, STY=0.0, STZ=0.0, SCALE=1.0, ALF=0.0, THETA=0.0, INMODE=4,
TNODE=0, TNPS=0, TINTS=0, &END
50.7500 0.0000 0.0000
50.7500 1.2503 0.0119
50.7500 1.8087 0.0723
50.7500 2.0016 0.2624
50.7500 2.0654 0.8001
50.7500 2.0851 2.0280
50.7500 2.0898 3.4449
50.7500 2.0912 4.8618
50.7500 2.0916 6.2787
50.7500 2.0914 7.6956
50.7500 2.0900 9.1125
50.7500 2.0826 10.5181
50.7500 2.0449 11.2629
50.7500 1.8881 11.4705
50.7500 1.3215 11.5194
50.7500 0.0000 11.5268
&BPNODE TNODE=3, TNPC=0, TINTC=0, &END
&SECT1 STX=0.0, STY=0.0, STZ=0.0, SCALE=1.0, ALF=0.0, THETA=0.0, INMODE=4,
TNODE=0, TNPS=0, TINTS=0, &END
51.8024 0.0000 0.0000
51.8024 1.0710 0.0155
51.8024 1.5126 0.0897
51.8024 1.6649 0.3144
51.8024 1.7158 0.9210
51.8024 1.7316 2.1843
51.8024 1.7355 3.5578
51.8024 1.7368 4.9313
51.8024 1.7371 6.3049
51.8024 1.7369 7.6784
51.8024 1.7353 9.0519
51.8024 1.7278 10.4187
51.8024 1.6936 11.1932
51.8024 1.5648 11.4376
51.8024 1.1343 11.5024
51.8024 0.0000 11.5143
&BPNODE TNODE=3, TNPC=0, TINTC=0, &END
&SECT1 STX=0.0, STY=0.0, STZ=0.0, SCALE=1.0, ALF=0.0, THETA=0.0, INMODE=4,
TNODE=0, TNPS=0, TINTS=0, &END
52.6945 0.0000 0.0000
52.6945 0.8991 0.0186
52.6945 1.2562 0.1053
52.6945 1.3782 0.3607

```

Jun 11 1997 05:30      froguav.in      Page 14

```

52.6945 1.4194 1.0318
52.6945 1.4320 2.3099
52.6945 1.4352 3.6427
52.6945 1.4363 4.9756
52.6945 1.4366 6.3084
52.6945 1.4363 7.6413
52.6945 1.4348 8.9741
52.6945 1.4280 10.3058
52.6945 1.3981 11.1267
52.6945 1.2909 11.4083
52.6945 0.9497 11.4877
52.6945 0.0000 11.5036
&BPNODE TNODE=3, TNPC=0, TINTC=0, &END
&SECT1 STX=0.0, STY=0.0, STZ=0.0, SCALE=1.0, ALF=0.0, THETA=0.0, INMODE=4,
TNODE=0, TNPS=0, TINTS=0, &END
53.2907 0.0000 0.0142
53.2907 0.7868 0.0350
53.2907 1.0933 0.1303
53.2907 1.1979 0.4106
53.2907 1.2330 1.1338
53.2907 1.2435 2.4132
53.2907 1.2463 3.7174
53.2907 1.2472 5.0216
53.2907 1.2475 6.3259
53.2907 1.2472 7.6301
53.2907 1.2458 8.9343
53.2907 1.2394 10.2385
53.2907 1.2120 11.0812
53.2907 1.1171 11.3809
53.2907 0.8219 11.4693
53.2907 0.0000 11.4876
&BPNODE TNODE=3, TNPC=0, TINTC=0, &END
&SECT1 STX=0.0, STY=0.0, STZ=0.0, SCALE=1.0, ALF=0.0, THETA=0.0, INMODE=4,
TNODE=0, TNPS=0, TINTS=0, &END
53.5000 0.0000 5.7500
53.5000 0.0000 5.7539
53.5000 0.0000 5.7578
53.5000 0.0000 5.7852
53.5000 0.0000 5.8447
53.5000 0.0000 5.9043
53.5000 0.0000 5.9639
53.5000 0.0000 6.0234
53.5000 0.0000 6.0830
53.5000 0.0000 6.1426
53.5000 0.0000 6.2021
53.5000 0.0000 6.2617
53.5000 0.0000 6.3213
53.5000 0.0000 6.3809
53.5000 0.0000 6.4404
53.5000 0.0000 6.5000
&BPNODE TNODE=3, TNPC=0, TINTC=0, &END
&PATCH1 IREV=0, IDPAT=1, MAKE=0, KCOMP=1, KASS=1, IPATSYM=1, IPATCOP=0, &END
MING_INBOARD
&SECT1 STX=0.0, STY=0.0, STZ=0.0, SCALE=1.0, ALF=0.0, THETA=0.0, INMODE=4,
TNODE=0, TNPS=0, TINTS=0, &END
44.5909 4.1662 11.5627
44.3717 4.2400 11.4932
43.7277 4.4570 11.4770
42.6855 4.5000 11.4565
41.2909 4.5000 11.4290
39.6047 4.5000 11.4032
37.7006 4.5000 11.3871
35.6619 4.5000 11.3790
33.5777 4.5000 11.3991
31.5390 4.5000 11.4614
29.6349 4.5000 11.5647
27.9487 4.5000 11.7283
26.5541 4.5000 11.9690
25.5119 4.5000 12.2862
24.8679 4.5000 12.6691
24.6500 4.5000 13.1000
24.8679 4.5000 13.5517
25.5119 4.5000 13.9485
26.5541 4.5000 14.2646
27.9487 4.5000 14.4706

```

Jun 11 1997 05:30			froguav.in	Page 15
29.6349	4.5000	14.5367		
31.5390	4.5000	14.4449		
33.5777	4.5000	14.2088		
35.6619	4.5000	13.8627		
37.7006	4.5000	13.4473		
39.6047	4.5000	12.9980		
41.2909	4.5000	12.5573		
42.6855	4.5000	12.1606		
43.7277	4.4570	11.8400		
44.3717	4.2400	11.6336		
44.5896	4.1662	11.5308		
&BPNODE TNODE=3, TNPC=0, TINTC=0, &END				
&SECT1 STX=0.0, STY=0.0, STZ=0.0, SCALE=1.0, ALF=0.0, THETA=0.0, INMODE=4,				
TNODES=0, TNPS=0, TINTS=0, &END				
44.5896	5.0188	11.5308		
44.3717	5.0188	11.4914		
43.7277	5.0188	11.4763		
42.6855	5.0188	11.4563		
41.2909	5.0188	11.4289		
39.6047	5.0188	11.4032		
37.7006	5.0188	11.3871		
35.6619	5.0188	11.3790		
33.5777	5.0188	11.3991		
31.5390	5.0188	11.4614		
29.6349	5.0188	11.5647		
27.9487	5.0188	11.7283		
26.5541	5.0188	11.9690		
25.5119	5.0188	12.2862		
24.8679	5.0188	12.6691		
24.6500	5.0188	13.1000		
24.8679	5.0188	13.5517		
25.5119	5.0188	13.9485		
26.5541	5.0188	14.2646		
27.9487	5.0188	14.4706		
29.6349	5.0188	14.5367		
31.5390	5.0188	14.4449		
33.5777	5.0188	14.2088		
35.6619	5.0188	13.8627		
37.7006	5.0188	13.4473		
39.6047	5.0188	12.9980		
41.2909	5.0188	12.5573		
42.6855	5.0188	12.1607		
43.7277	5.0188	11.8407		
44.3717	5.0188	11.6352		
44.5896	5.0188	11.5308		
&BPNODE TNODE=3, TNPC=0, TINTC=0, &END				
&SECT1 STX=0.0, STY=0.0, STZ=0.0, SCALE=1.0, ALF=0.0, THETA=0.0, INMODE=4,				
TNODES=0, TNPS=0, TINTS=0, &END				
44.5896	6.5553	11.5308		
44.3717	6.5553	11.4914		
43.7277	6.5553	11.4763		
42.6855	6.5553	11.4563		
41.2909	6.5553	11.4289		
39.6047	6.5553	11.4032		
37.7006	6.5553	11.3871		
35.6619	6.5553	11.3790		
33.5777	6.5553	11.3991		
31.5390	6.5553	11.4614		
29.6349	6.5553	11.5647		
27.9487	6.5553	11.7283		
26.5541	6.5553	11.9690		
25.5119	6.5553	12.2862		
24.8679	6.5553	12.6691		
24.6500	6.5553	13.1000		
24.8679	6.5553	13.5517		
25.5119	6.5553	13.9485		
26.5541	6.5553	14.2646		
27.9487	6.5553	14.4706		
29.6349	6.5553	14.5367		
31.5390	6.5553	14.4449		
33.5777	6.5553	14.2088		
35.6619	6.5553	13.8627		
37.7006	6.5553	13.4473		
39.6047	6.5553	12.9980		
41.2909	6.5553	12.5573		
42.6855	6.5553	12.1607		

124

Jun 11 1997 05:30			froguav.in	Page 16
43.7277	6.5553	11.8407		
44.3717	6.5553	11.6352		
44.5896	6.5553	11.5308		
&BPNODE TNODE=3, TNPC=0, TINTC=0, &END				
&SECT1 STX=0.0, STY=0.0, STZ=0.0, SCALE=1.0, ALF=0.0, THETA=0.0, INMODE=4,				
TNODES=0, TNPS=0, TINTS=0, &END				
44.5896	9.0503	11.5308		
44.3717	9.0503	11.4914		
43.7277	9.0503	11.4763		
42.6855	9.0503	11.4563		
41.2909	9.0503	11.4289		
39.6047	9.0503	11.4032		
37.7006	9.0503	11.3871		
35.6619	9.0503	11.3790		
33.5777	9.0503	11.3991		
31.5390	9.0503	11.4614		
29.6349	9.0503	11.5647		
27.9487	9.0503	11.7283		
26.5541	9.0503	11.9690		
25.5119	9.0503	12.2862		
24.8679	9.0503	12.6691		
24.6500	9.0503	13.1000		
24.8679	9.0503	13.5517		
25.5119	9.0503	13.9485		
26.5541	9.0503	14.2646		
27.9487	9.0503	14.4706		
29.6349	9.0503	14.5367		
31.5390	9.0503	14.4449		
33.5777	9.0503	14.2088		
35.6619	9.0503	13.8627		
37.7006	9.0503	13.4473		
39.6047	9.0503	12.9980		
41.2909	9.0503	12.5573		
42.6855	9.0503	12.1607		
43.7277	9.0503	11.8407		
44.3717	9.0503	11.6352		
44.5896	9.0503	11.5308		
&BPNODE TNODE=3, TNPC=0, TINTC=0, &END				
&SECT1 STX=0.0, STY=0.0, STZ=0.0, SCALE=1.0, ALF=0.0, THETA=0.0, INMODE=4,				
TNODES=0, TNPS=0, TINTS=0, &END				
44.5896	12.4081	11.5308		
44.3717	12.4081	11.4914		
43.7277	12.4081	11.4763		
42.6855	12.4081	11.4563		
41.2909	12.4081	11.4289		
39.6047	12.4081	11.4032		
37.7006	12.4081	11.3871		
35.6619	12.4081	11.3790		
33.5777	12.4081	11.3991		
31.5390	12.4081	11.4614		
29.6349	12.4081	11.5647		
27.9487	12.4081	11.7283		
26.5541	12.4081	11.9690		
25.5119	12.4081	12.2862		
24.8679	12.4081	12.6691		
24.6500	12.4081	13.1000		
24.8679	12.4081	13.5517		
25.5119	12.4081	13.9485		
26.5541	12.4081	14.2646		
27.9487	12.4081	14.4706		
29.6349	12.4081	14.5367		
31.5390	12.4081	14.4449		
33.5777	12.4081	14.2088		
35.6619	12.4081	13.8627		
37.7006	12.4081	13.4473		
39.6047	12.4081	12.9980		
41.2909	12.4081	12.5573		
42.6855	12.4081	12.1607		
43.7277	12.4081	11.8407		
44.3717	12.4081	11.6352		
44.5896	12.4081	11.5308		
&BPNODE TNODE=3, TNPC=0, TINTC=0, &END				
&SECT1 STX=0.0, STY=0.0, STZ=0.0, SCALE=1.0, ALF=0.0, THETA=0.0, INMODE=4,				
TNODES=0, TNPS=0, TINTS=0, &END				
44.5896	16.4996	11.5308		
44.3717	16.4996	11.4914		



Jun 11 1997 05:30      froguav.in      Page 17

```

43.7277 16.4996 11.4763
42.6855 16.4996 11.4563
41.2909 16.4996 11.4289
39.6047 16.4996 11.4032
37.7006 16.4996 11.3871
35.6619 16.4996 11.3790
33.5777 16.4996 11.3991
31.5390 16.4996 11.4614
29.6349 16.4996 11.5647
27.9487 16.4996 11.7283
26.5541 16.4996 11.9690
25.5119 16.4996 12.2862
24.8679 16.4996 12.6691
24.6500 16.4996 13.1000
24.8679 16.4996 13.5517
25.5119 16.4996 13.9485
26.5541 16.4996 14.2646
27.9487 16.4996 14.4706
29.6349 16.4996 14.5367
31.5390 16.4996 14.4449
33.5777 16.4996 14.2088
35.6619 16.4996 13.8627
37.7006 16.4996 13.4473
39.6047 16.4996 12.9980
41.2909 16.4996 12.5573
42.6855 16.4996 12.1607
43.7277 16.4996 11.8407
44.3717 16.4996 11.6352
44.5896 16.4996 11.5308
&BPNODE TNODE=3, TNPC=0, TINTC=0, &END
&SECT1 STX=0.0, STY=0.0, STZ=0.0, SCALE=1.0, ALF=0.0, THETA=0.0, INNODE=4,
  TNODES=0, TNPS=0, TINTS=0, &END
44.5896 21.1675 11.5308
44.3717 21.1675 11.4914
43.7277 21.1675 11.4763
42.6855 21.1675 11.4563
41.2909 21.1675 11.4289
39.6047 21.1675 11.4032
37.7006 21.1675 11.3871
35.6619 21.1675 11.3790
33.5777 21.1675 11.3991
31.5390 21.1675 11.4614
29.6349 21.1675 11.5647
27.9487 21.1675 11.7283
26.5541 21.1675 11.9690
25.5119 21.1675 12.2862
24.8679 21.1675 12.6691
24.6500 21.1675 13.1000
24.8679 21.1675 13.5517
25.5119 21.1675 13.9485
26.5541 21.1675 14.2646
27.9487 21.1675 14.4706
29.6349 21.1675 14.5367
31.5390 21.1675 14.4449
33.5777 21.1675 14.2088
35.6619 21.1675 13.8627
37.7006 21.1675 13.4473
39.6047 21.1675 12.9980
41.2909 21.1675 12.5573
42.6855 21.1675 12.1607
43.7277 21.1675 11.8407
44.3717 21.1675 11.6352
44.5896 21.1675 11.5308
&BPNODE TNODE=3, TNPC=0, TINTC=0, &END
&SECT1 STX=0.0, STY=0.0, STZ=0.0, SCALE=1.0, ALF=0.0, THETA=0.0, INNODE=4,
  TNODES=0, TNPS=0, TINTS=0, &END
44.5896 26.2326 11.5308
44.3717 26.2326 11.4914
43.7277 26.2326 11.4763
42.6855 26.2326 11.4563
41.2909 26.2326 11.4289
39.6047 26.2326 11.4032
37.7006 26.2326 11.3871
35.6619 26.2326 11.3790
33.5777 26.2326 11.3991
31.5390 26.2326 11.4614
29.6349 26.2326 11.5647
27.9487 26.2326 11.7283
26.5541 26.2326 11.9690
25.5119 26.2326 12.2862
24.8679 26.2326 12.6691
24.6500 26.2326 13.1000
24.8679 26.2326 13.5517
25.5119 26.2326 13.9485
26.5541 26.2326 14.2646
27.9487 26.2326 14.4706
29.6349 26.2326 14.5367
31.5390 26.2326 14.4449
33.5777 26.2326 14.2088
35.6619 26.2326 13.8627
37.7006 26.2326 13.4473
39.6047 26.2326 12.9980
41.2909 26.2326 12.5573
42.6855 26.2326 12.1607
43.7277 26.2326 11.8407
44.3717 26.2326 11.6352
44.5896 26.2326 11.5308

```

Jun 11 1997 05:30      froguav.in      Page 18

```

29.6349 26.2326 11.5647
27.9487 26.2326 11.7283
26.5541 26.2326 11.9690
25.5119 26.2326 12.2862
24.8679 26.2326 12.6691
24.6500 26.2326 13.1000
24.8679 26.2326 13.5517
25.5119 26.2326 13.9485
26.5541 26.2326 14.2646
27.9487 26.2326 14.4706
29.6349 26.2326 14.5367
31.5390 26.2326 14.4449
33.5777 26.2326 14.2088
35.6619 26.2326 13.8627
37.7006 26.2326 13.4473
39.6047 26.2326 12.9980
41.2909 26.2326 12.5573
42.6855 26.2326 12.1607
43.7277 26.2326 11.8407
44.3717 26.2326 11.6352
44.5896 26.2326 11.5308
&BPNODE TNODE=3, TNPC=0, TINTC=0, &END
&SECT1 STX=0.0, STY=0.0, STZ=0.0, SCALE=1.0, ALF=0.0, THETA=0.0, INNODE=4,
  TNODES=3, TNPS=0, TINTS=0, &END
44.5896 31.5000 11.5308
44.3717 31.5000 11.4914
43.7277 31.5000 11.4763
42.6855 31.5000 11.4563
41.2909 31.5000 11.4289
39.6047 31.5000 11.4032
37.7006 31.5000 11.3871
35.6619 31.5000 11.3790
33.5777 31.5000 11.3991
31.5390 31.5000 11.4614
29.6349 31.5000 11.5647
27.9487 31.5000 11.7283
26.5541 31.5000 11.9690
25.5119 31.5000 12.2862
24.8679 31.5000 12.6691
24.6500 31.5000 13.1000
24.8679 31.5000 13.5517
25.5119 31.5000 13.9485
26.5541 31.5000 14.2646
27.9487 31.5000 14.4706
29.6349 31.5000 14.5367
31.5390 31.5000 14.4449
33.5777 31.5000 14.2088
35.6619 31.5000 13.8627
37.7006 31.5000 13.4473
39.6047 31.5000 12.9980
41.2909 31.5000 12.5573
42.6855 31.5000 12.1607
43.7277 31.5000 11.8407
44.3717 31.5000 11.6352
44.5896 31.5000 11.5308
&BPNODE TNODE=3, TNPC=0, TINTC=0, &END
&PATCH1 IREV=0, IDPAT=1, MAKE=0, KCOMP=1, KASS=1, IPATSYM=1, IPATCOP=0, &END
WING_MID_AILERON
&SECT1 STX=0.0, STY=0.0, STZ=0.0, SCALE=1.0, ALF=0.0, THETA=0.0, INNODE=4,
  TNODES=0, TNPS=0, TINTS=0, &END
44.5896 31.5000 11.5308
44.3717 31.5000 11.4914
43.7277 31.5000 11.4763
42.6855 31.5000 11.4563
41.2909 31.5000 11.4289
39.6047 31.5000 11.4032
37.7006 31.5000 11.3871
35.6619 31.5000 11.3790
33.5777 31.5000 11.3991
31.5390 31.5000 11.4614
29.6349 31.5000 11.5647
27.9487 31.5000 11.7283
26.5541 31.5000 11.9690
25.5119 31.5000 12.2862
24.8679 31.5000 12.6691

```

Jun 11 1997 05:30			froguav.in	Page 19
24.6500	31.5000	13.1000		
24.8679	31.5000	13.5517		
25.5119	31.5000	13.9485		
26.5541	31.5000	14.2646		
27.9487	31.5000	14.4706		
29.6349	31.5000	14.5367		
31.5390	31.5000	14.4449		
33.5777	31.5000	14.2088		
35.6619	31.5000	13.8627		
37.7006	31.5000	13.4473		
39.6047	31.5000	12.9980		
41.2909	31.5000	12.5573		
42.6855	31.5000	12.1607		
43.7277	31.5000	11.8407		
44.3717	31.5000	11.6352		
44.5896	31.5000	11.5308		
&BPNODE TNODE=3, TNPC=0, TINTC=0, &END				
&SECT1 STX=0.0, STY=0.0, STZ=0.0, SCALE=1.0, ALF=0.0, THETA=0.0, INMODE=4,				
TNODES=0, TNPS=0, TINTS=0, &END				
44.5896	35.8000	11.5308		
44.3717	35.8000	11.4914		
43.7277	35.8000	11.4763		
42.6855	35.8000	11.4563		
41.2909	35.8000	11.4289		
39.6047	35.8000	11.4032		
37.7006	35.8000	11.3871		
35.6619	35.8000	11.3790		
33.5777	35.8000	11.3991		
31.5390	35.8000	11.4614		
29.6349	35.8000	11.5647		
27.9487	35.8000	11.7283		
26.5541	35.8000	11.9690		
25.5119	35.8000	12.2862		
24.8679	35.8000	12.6691		
24.6500	35.8000	13.1000		
24.8679	35.8000	13.5517		
25.5119	35.8000	13.9485		
26.5541	35.8000	14.2646		
27.9487	35.8000	14.4706		
29.6349	35.8000	14.5367		
31.5390	35.8000	14.4449		
33.5777	35.8000	14.2088		
35.6619	35.8000	13.8627		
37.7006	35.8000	13.4473		
39.6047	35.8000	12.9980		
41.2909	35.8000	12.5573		
42.6855	35.8000	12.1607		
43.7277	35.8000	11.8407		
44.3717	35.8000	11.6352		
44.5896	35.8000	11.5308		
&BPNODE TNODE=3, TNPC=0, TINTC=0, &END				
&SECT1 STX=0.0, STY=0.0, STZ=0.0, SCALE=1.0, ALF=0.0, THETA=0.0, INMODE=4,				
TNODES=0, TNPS=0, TINTS=0, &END				
44.5896	40.1000	11.5308		
44.3717	40.1000	11.4914		
43.7277	40.1000	11.4763		
42.6855	40.1000	11.4563		
41.2909	40.1000	11.4289		
39.6047	40.1000	11.4032		
37.7006	40.1000	11.3871		
35.6619	40.1000	11.3790		
33.5777	40.1000	11.3991		
31.5390	40.1000	11.4614		
29.6349	40.1000	11.5647		
27.9487	40.1000	11.7283		
26.5541	40.1000	11.9690		
25.5119	40.1000	12.2862		
24.8679	40.1000	12.6691		
24.6500	40.1000	13.1000		
24.8679	40.1000	13.5517		
25.5119	40.1000	13.9485		
26.5541	40.1000	14.2646		
27.9487	40.1000	14.4706		
29.6349	40.1000	14.5367		
31.5390	40.1000	14.4449		
33.5777	40.1000	14.2088		

Jun 11 1997 05:30			froguav.in	Page 20
35.6619	40.1000	13.8627		
37.7006	40.1000	13.4473		
39.6047	40.1000	12.9980		
41.2909	40.1000	12.5573		
42.6855	40.1000	12.1607		
43.7277	40.1000	11.8407		
44.3717	40.1000	11.6352		
44.5896	40.1000	11.5308		
&BPNODE TNODE=3, TNPC=0, TINTC=0, &END				
&SECT1 STX=0.0, STY=0.0, STZ=0.0, SCALE=1.0, ALF=0.0, THETA=0.0, INMODE=4,				
TNODES=0, TNPS=0, TINTS=0, &END				
44.5896	44.4000	11.5308		
44.3717	44.4000	11.4914		
43.7277	44.4000	11.4763		
42.6855	44.4000	11.4563		
41.2909	44.4000	11.4289		
39.6047	44.4000	11.4032		
37.7006	44.4000	11.3871		
35.6619	44.4000	11.3790		
33.5777	44.4000	11.3991		
31.5390	44.4000	11.4614		
29.6349	44.4000	11.5647		
27.9487	44.4000	11.7283		
26.5541	44.4000	11.9690		
25.5119	44.4000	12.2862		
24.8679	44.4000	12.6691		
24.6500	44.4000	13.1000		
24.8679	44.4000	13.5517		
25.5119	44.4000	13.9485		
26.5541	44.4000	14.2646		
27.9487	44.4000	14.4706		
29.6349	44.4000	14.5367		
31.5390	44.4000	14.4449		
33.5777	44.4000	14.2088		
35.6619	44.4000	13.8627		
37.7006	44.4000	13.4473		
39.6047	44.4000	12.9980		
41.2909	44.4000	12.5573		
42.6855	44.4000	12.1607		
43.7277	44.4000	11.8407		
44.3717	44.4000	11.6352		
44.5896	44.4000	11.5308		
&BPNODE TNODE=3, TNPC=0, TINTC=0, &END				
&SECT1 STX=0.0, STY=0.0, STZ=0.0, SCALE=1.0, ALF=0.0, THETA=0.0, INMODE=4,				
TNODES=0, TNPS=0, TINTS=0, &END				
44.5896	48.7000	11.5308		
44.3717	48.7000	11.4914		
43.7277	48.7000	11.4763		
42.6855	48.7000	11.4563		
41.2909	48.7000	11.4289		
39.6047	48.7000	11.4032		
37.7006	48.7000	11.3871		
35.6619	48.7000	11.3790		
33.5777	48.7000	11.3991		
31.5390	48.7000	11.4614		
29.6349	48.7000	11.5647		
27.9487	48.7000	11.7283		
26.5541	48.7000	11.9690		
25.5119	48.7000	12.2862		
24.8679	48.7000	12.6691		
24.6500	48.7000	13.1000		
24.8679	48.7000	13.5517		
25.5119	48.7000	13.9485		
26.5541	48.7000	14.2646		
27.9487	48.7000	14.4706		
29.6349	48.7000	14.5367		
31.5390	48.7000	14.4449		
33.5777	48.7000	14.2088		
35.6619	48.7000	13.8627		
37.7006	48.7000	13.4473		
39.6047	48.7000	12.9980		
41.2909	48.7000	12.5573		
42.6855	48.7000	12.1607		
43.7277	48.7000	11.8407		
44.3717	48.7000	11.6352		
44.5896	48.7000	11.5308		

Jun 11 1997 05:30      froguav.in      Page 21

```
&BPNODE TNODE=3, TNPC=0, TINTC=0, &END
&SECT1 STX=0.0, STY=0.0, STZ=0.0, SCALE=1.0, ALF=0.0, THETA=0.0, INMODE=4,
TNODE=3, TNPS=0, TINTS=0, &END
44.5896 53.0000 11.5308
44.3717 53.0000 11.4914
43.7277 53.0000 11.4763
42.6855 53.0000 11.4563
41.2909 53.0000 11.4289
39.6047 53.0000 11.4032
37.7006 53.0000 11.3871
35.6619 53.0000 11.3790
33.5777 53.0000 11.3991
31.5390 53.0000 11.4614
29.6349 53.0000 11.5647
27.9487 53.0000 11.7283
26.5541 53.0000 11.9690
25.5119 53.0000 12.2862
24.8679 53.0000 12.6691
24.6500 53.0000 13.1000
24.8679 53.0000 13.5517
25.5119 53.0000 13.9485
26.5541 53.0000 14.2646
27.9487 53.0000 14.4706
29.6349 53.0000 14.5367
31.5390 53.0000 14.4449
33.5777 53.0000 14.2088
35.6619 53.0000 13.8627
37.7006 53.0000 13.4473
39.6047 53.0000 12.9980
41.2909 53.0000 12.5573
42.6855 53.0000 12.1607
43.7277 53.0000 11.8407
44.3717 53.0000 11.6352
44.5896 53.0000 11.5308
&BPNODE TNODE=3, TNPC=0, TINTC=0, &END
```

```
&PATCH1 IREV=0, IDPAT=1, MAKE=0, KCOMP=1, KASS=1, IPATSYH=1, IPATCOP=0, &END
WING_OUTBOARD_TAPER
&SECT1 STX=0.0, STY=0.0, STZ=0.0, SCALE=1.0, ALF=0.0, THETA=0.0, INMODE=4,
TNODE=0, TNPS=0, TINTS=0, &END
44.5896 53.0000 11.5308
44.3717 53.0000 11.4914
43.7277 53.0000 11.4763
42.6855 53.0000 11.4563
41.2909 53.0000 11.4289
39.6047 53.0000 11.4032
37.7006 53.0000 11.3871
35.6619 53.0000 11.3790
33.5777 53.0000 11.3991
31.5390 53.0000 11.4614
29.6349 53.0000 11.5647
27.9487 53.0000 11.7283
26.5541 53.0000 11.9690
25.5119 53.0000 12.2862
24.8679 53.0000 12.6691
24.6500 53.0000 13.1000
24.8679 53.0000 13.5517
25.5119 53.0000 13.9485
26.5541 53.0000 14.2646
27.9487 53.0000 14.4706
29.6349 53.0000 14.5367
31.5390 53.0000 14.4449
33.5777 53.0000 14.2088
35.6619 53.0000 13.8627
37.7006 53.0000 13.4473
39.6047 53.0000 12.9980
41.2909 53.0000 12.5573
42.6855 53.0000 12.1607
43.7277 53.0000 11.8407
44.3717 53.0000 11.6352
44.5896 53.0000 11.5308
```

```
&BPNODE TNODE=3, TNPC=0, TINTC=0, &END
&SECT1 STX=0.0, STY=0.0, STZ=0.0, SCALE=1.0, ALF=0.0, THETA=0.0, INMODE=4,
TNODE=0, TNPS=0, TINTS=0, &END
43.8419 57.0000 11.5897
```

Jun 11 1997 05:30      froguav.in      Page 22

```
43.6322 57.0000 11.5517
43.0123 57.0000 11.5372
42.0092 57.0000 11.5180
40.6669 57.0000 11.4916
39.0439 57.0000 11.4668
37.2112 57.0000 11.4513
35.2490 57.0000 11.4436
33.2429 57.0000 11.4629
31.2806 57.0000 11.5229
29.4480 57.0000 11.6223
27.8250 57.0000 11.7798
26.4827 57.0000 12.0114
25.4796 57.0000 12.3168
24.8597 57.0000 12.6853
24.6500 57.0000 13.1000
24.8597 57.0000 13.5348
25.4796 57.0000 13.9167
26.4827 57.0000 14.2209
27.8250 57.0000 14.4192
29.4480 57.0000 14.4828
31.2806 57.0000 14.3944
33.2429 57.0000 14.1673
35.2490 57.0000 13.8341
37.2112 57.0000 13.4342
39.0439 57.0000 13.0018
40.6669 57.0000 12.5777
42.0092 57.0000 12.1959
43.0123 57.0000 11.8879
43.6322 57.0000 11.6901
43.8419 57.0000 11.5897
```

```
&BPNODE TNODE=3, TNPC=0, TINTC=0, &END
&SECT1 STX=0.0, STY=0.0, STZ=0.0, SCALE=1.0, ALF=0.0, THETA=0.0, INMODE=4,
TNODE=0, TNPS=0, TINTS=0, &END
```

```
43.2945 59.9282 11.6327
43.0908 59.9282 11.5959
42.4885 59.9282 11.5818
41.5141 59.9282 11.5631
40.2100 59.9282 11.5375
38.6334 59.9282 11.5134
36.8530 59.9282 11.4981
34.9467 59.9282 11.4908
32.9978 59.9282 11.5096
31.0915 59.9282 11.5679
29.3111 59.9282 11.6644
27.7344 59.9282 11.8174
26.4304 59.9282 12.0424
25.4560 59.9282 12.3391
24.8537 59.9282 12.6971
24.6500 59.9282 13.1000
24.8537 59.9282 13.5224
25.4560 59.9282 13.8934
26.4304 59.9282 14.1890
27.7344 59.9282 14.3815
29.3111 59.9282 14.4433
31.0915 59.9282 14.3575
32.9978 59.9282 14.1368
34.9467 59.9282 13.8132
36.8530 59.9282 13.4247
38.6334 59.9282 13.0046
40.2100 59.9282 12.5926
41.5141 59.9282 12.2217
42.4885 59.9282 11.9225
43.0908 59.9282 11.7303
43.2945 59.9282 11.6327
```

```
&BPNODE TNODE=3, TNPC=0, TINTC=0, &END
&SECT1 STX=0.0, STY=0.0, STZ=0.0, SCALE=1.0, ALF=0.0, THETA=0.0, INMODE=4,
TNODE=3, TNPS=0, TINTS=0, &END
```

```
43.0941 61.0000 11.6485
42.8926 61.0000 11.6120
42.2968 61.0000 11.5981
41.3325 61.0000 11.5796
40.0455 61.0000 11.5543
38.4831 61.0000 11.5304
36.7218 61.0000 11.5156
34.8760 61.0000 11.5081
32.9081 61.0000 11.5267
```

Jun 11 1997 05:30      froguav.in      Page 23

31.0223	61.0000	11.5843
29.2610	61.0000	11.6799
27.7013	61.0000	11.8312
26.4113	61.0000	12.0538
25.4473	61.0000	12.3473
24.8515	61.0000	12.7014
24.6500	61.0000	13.1000
24.8515	61.0000	13.5178
25.4473	61.0000	13.8848
26.4113	61.0000	14.1773
27.7013	61.0000	14.3678
29.2610	61.0000	14.4289
31.0223	61.0000	14.3440
32.9081	61.0000	14.1257
34.8360	61.0000	13.8055
36.7218	61.0000	13.4212
38.4831	61.0000	13.0057
40.0428	61.0000	12.5980
41.3329	61.0000	12.2311
42.2968	61.0000	11.9351
42.8926	61.0000	11.7451
43.0941	61.0000	11.6485

&BPNODE TNODE=3, TNPC=0, TINTC=0, &END

&PATCH1 IREV= 0, IDPAT= 1, MAKE= 17, KCOMP= 1, KASS= 1, IPATSYM=1, &END  
 IPATCOP=0,  
 WING\_TIP\_Half\_Round  
 &PATCH2 ITYP= 2, TNDS= 3, TNPS= 4, TINTS= 3, &END

&PATCH1 IREV=0, IDPAT=1, MAKE=0, KCOMP=1, KASS=1, IPATSYM=1, IPATCOP=0, &END  
 FOG\_HORIZONTAL\_TAIL  
 &SECT1 STX=0.0, STY=0.0, STZ=0.0, SCALE=1.0, ALF=0.0, THETA=0.0, INMODE=4,  
 TNODES=0, TNPS=0, TINTS=0, &END

96.0000	0.0000	8.0900
95.7266	0.0000	8.0641
94.9285	0.0000	8.0097
93.6703	0.0000	7.9337
92.0541	0.0000	7.8478
90.2106	0.0000	7.7664
88.2894	0.0000	7.7063
86.4459	0.0000	7.6850
84.8297	0.0000	7.7154
83.5715	0.0000	7.8000
82.7734	0.0000	7.9302
82.5000	0.0000	8.0900
82.7734	0.0000	8.2498
83.5715	0.0000	8.3800
84.8297	0.0000	8.4646
86.4459	0.0000	8.4950
88.2894	0.0000	8.4737
90.2106	0.0000	8.4136
92.0541	0.0000	8.3322
93.6703	0.0000	8.2463
94.9285	0.0000	8.1703
95.7266	0.0000	8.1159
96.0000	0.0000	8.0900

&BPNODE TNODE=3, TNPC=0, TINTC=0, &END

&SECT1 STX=0.0, STY=0.0, STZ=0.0, SCALE=1.0, ALF=0.0, THETA=0.0, INMODE=4,  
 TNODES=0, TNPS=0, TINTS=0, &END

96.0012	0.4864	8.0900
95.7298	0.4864	8.0643
94.9374	0.4864	8.0103
93.6882	0.4864	7.9348
92.0835	0.4864	7.8495
90.2533	0.4864	7.7687
88.3458	0.4864	7.7091
86.5156	0.4864	7.6879
84.9109	0.4864	7.7180
83.6618	0.4864	7.8021
82.8624	0.4864	7.9313
82.5070	0.4864	8.0900
82.8694	0.4864	8.2487
83.6618	0.4864	8.3779
84.9109	0.4864	8.4620
86.5156	0.4864	8.4921

Jun 11 1997 05:30      froguav.in      Page 24

88.3458	0.4864	8.4709
90.2533	0.4864	8.4113
92.0835	0.4864	8.3305
93.6882	0.4864	8.2452
94.9374	0.4864	8.1697
95.7298	0.4864	8.1157
96.0012	0.4864	8.0900

&BPNODE TNODE=3, TNPC=0, TINTC=0, &END

&SECT1 STX=0.0, STY=0.0, STZ=0.0, SCALE=1.0, ALF=0.0, THETA=0.0, INMODE=4,  
 TNODES=0, TNPS=0, TINTS=0, &END

96.0048	1.8979	8.0900
95.7390	1.8979	8.0648
94.9632	1.8979	8.0120
93.7402	1.8979	7.9381
92.1691	1.8979	7.8545
90.3772	1.8979	7.7755
88.5096	1.8979	7.7170
86.7177	1.8979	7.6963
85.1466	1.8979	7.7258
83.9236	1.8979	7.8081
83.1477	1.8979	7.9347
82.8820	1.8979	8.0900
83.1477	1.8979	8.2453
83.9236	1.8979	8.3719
85.1466	1.8979	8.4542
86.7177	1.8979	8.4837
88.5096	1.8979	8.4630
90.3772	1.8979	8.4045
92.1691	1.8979	8.3255
93.7402	1.8979	8.2419
94.9632	1.8979	8.1680
95.7390	1.8979	8.1152
96.0048	1.8979	8.0900

&BPNODE TNODE=3, TNPC=0, TINTC=0, &END

&SECT1 STX=0.0, STY=0.0, STZ=0.0, SCALE=1.0, ALF=0.0, THETA=0.0, INMODE=4,  
 TNODES=0, TNPS=0, TINTS=0, &END

96.0103	4.0964	8.0900
95.7534	4.0964	8.0657
95.0034	4.0964	8.0146
93.8211	4.0964	7.9432
92.3023	4.0964	7.8624
90.5701	4.0964	7.7859
88.7647	4.0964	7.7295
87.0324	4.0964	7.7094
85.5136	4.0964	7.7380
84.3313	4.0964	7.8175
83.5814	4.0964	7.9398
83.3244	4.0964	8.0900
83.5814	4.0964	8.2402
84.3313	4.0964	8.3625
85.5136	4.0964	8.4420
87.0324	4.0964	8.4706
88.7647	4.0964	8.4505
90.5701	4.0964	8.3941
92.3023	4.0964	8.3176
93.8211	4.0964	8.2368
95.0034	4.0964	8.1654
95.7534	4.0964	8.1143
96.0103	4.0964	8.0900

&BPNODE TNODE=3, TNPC=0, TINTC=0, &END

&SECT1 STX=0.0, STY=0.0, STZ=0.0, SCALE=1.0, ALF=0.0, THETA=0.0, INMODE=4,  
 TNODES=0, TNPS=0, TINTS=0, &END

95.0173	6.8666	8.0900
95.7715	6.8666	8.0667
95.0541	6.8666	8.0178
93.9231	6.8666	7.9495
92.4702	6.8666	7.8723
90.8131	6.8666	7.7991
89.0861	6.8666	7.7451
87.4290	6.8666	7.7259
85.9762	6.8666	7.7532
84.8452	6.8666	7.8293
84.1277	6.8666	7.9464
83.8820	6.8666	8.0900
84.1277	6.8666	8.2336
84.8452	6.8666	8.3507

Jun 11 1997 05:30 froguav.in Page 25

```

85.9762 6.8666 8.4268
87.4290 6.8666 8.4541
89.0861 6.8666 8.4349
90.8131 6.8666 8.3809
92.4702 6.8666 8.3077
93.9231 6.8666 8.2305
95.0541 6.8666 8.1622
95.7715 6.8666 8.1133
96.0173 6.8666 8.0900
&BPNODE TNODE=3, TNPC=0, TINTC=0, &END
&SECT1 STX=0.0, STY=0.0, STZ=0.0, SCALE=1.0, ALF=0.0, THETA=0.0, INMODE=4,
TNODS=0, TNPS=0, TINTS=0, &END
96.0250 9.9375 8.0900
95.7916 9.9375 8.0679
95.1102 9.9375 8.0215
94.0361 9.9375 7.9566
92.6563 9.9375 7.8832
91.0826 9.9375 7.8138
89.4424 9.9375 7.7625
87.8687 9.9375 7.7442
86.4889 9.9375 7.7702
85.4148 9.9375 7.8424
84.7334 9.9375 7.9536
84.5000 9.9375 8.0900
84.7334 9.9375 8.2264
85.4148 9.9375 8.3376
86.4889 9.9375 8.4098
87.8687 9.9375 8.4358
89.4424 9.9375 8.4175
91.0826 9.9375 8.3662
92.6563 9.9375 8.2968
94.0361 9.9375 8.2234
95.1102 9.9375 8.1595
95.7916 9.9375 8.1121
96.0250 9.9375 8.0900
&BPNODE TNODE=3, TNPC=0, TINTC=0, &END
&SECT1 STX=0.0, STY=0.0, STZ=0.0, SCALE=1.0, ALF=0.0, THETA=0.0, INMODE=4,
TNODS=0, TNPS=0, TINTS=0, &END
96.0327 13.0084 8.0900
95.8117 13.0084 8.0691
95.1664 13.0084 8.0251
94.1492 13.0084 7.9637
92.8424 13.0084 7.8942
91.3520 13.0084 7.8284
89.7987 13.0084 7.7798
88.3083 13.0084 7.7625
87.0016 13.0084 7.7871
85.9844 13.0084 7.8555
85.3391 13.0084 7.9608
85.1180 13.0084 8.0900
85.3391 13.0084 8.2192
85.9844 13.0084 8.3245
87.0016 13.0084 8.3929
88.3083 13.0084 8.4175
89.7987 13.0084 8.4002
91.3520 13.0084 8.3516
92.8424 13.0084 8.2858
94.1492 13.0084 8.2163
95.1664 13.0084 8.1549
95.8117 13.0084 8.1109
96.0327 13.0084 8.0900
&BPNODE TNODE=3, TNPC=0, TINTC=0, &END
&SECT1 STX=0.0, STY=0.0, STZ=0.0, SCALE=1.0, ALF=0.0, THETA=0.0, INMODE=4,
TNODS=0, TNPS=0, TINTS=0, &END
96.0397 15.7786 8.0900
95.8298 15.7786 8.0701
95.2171 15.7786 8.0284
94.2512 15.7786 7.9700
93.0103 15.7786 7.9040
91.5951 15.7786 7.8416
90.1201 15.7786 7.7955
88.7049 15.7786 7.7790
87.4641 15.7786 7.8024
86.4982 15.7786 7.8674
85.8855 15.7786 7.9673
85.6756 15.7786 8.0900

```

Jun 11 1997 05:30 froguav.in Page 26

```

85.8855 15.7786 8.2127
86.4982 15.7786 8.3126
87.4641 15.7786 8.3776
88.7049 15.7786 8.4010
90.1201 15.7786 8.3845
91.5951 15.7786 8.3384
93.0103 15.7786 8.2760
94.2512 15.7786 8.2100
95.2171 15.7786 8.1516
95.8298 15.7786 8.1099
96.0397 15.7786 8.0900
&BPNODE TNODE=3, TNPC=0, TINTC=0, &END
&SECT1 STX=0.0, STY=0.0, STZ=0.0, SCALE=1.0, ALF=0.0, THETA=0.0, INMODE=4,
TNODS=0, TNPS=0, TINTS=0, &END
96.0452 17.9771 8.0900
95.8442 17.9771 8.0710
95.2573 17.9771 8.0310
94.3321 17.9771 7.9751
93.1436 17.9771 7.9119
91.7880 17.9771 7.8521
90.3752 17.9771 7.8079
89.0197 17.9771 7.7921
87.8312 17.9771 7.8145
86.9060 17.9771 7.8767
86.3191 17.9771 7.9725
86.1180 17.9771 8.0900
86.3191 17.9771 8.2075
86.9060 17.9771 8.3033
87.8312 17.9771 8.3655
89.0197 17.9771 8.3879
90.3752 17.9771 8.3721
91.7880 17.9771 8.3279
93.1436 17.9771 8.2681
94.3321 17.9771 8.2049
95.2573 17.9771 8.1490
95.8442 17.9771 8.1090
96.0452 17.9771 8.0900
&BPNODE TNODE=3, TNPC=0, TINTC=0, &END
&SECT1 STX=0.0, STY=0.0, STZ=0.0, SCALE=1.0, ALF=0.0, THETA=0.0, INMODE=4,
TNODS=0, TNPS=0, TINTS=0, &END
96.0488 19.3886 8.0900
95.8534 19.3886 8.0715
95.2831 19.3886 8.0326
94.3841 19.3886 7.9783
93.2291 19.3886 7.9169
91.9119 19.3886 7.8588
90.5390 19.3886 7.8158
89.2218 19.3886 7.8006
88.0668 19.3886 7.8223
87.1678 19.3886 7.8828
86.5975 19.3886 7.9758
86.4021 19.3886 8.0900
86.5975 19.3886 8.2042
87.1678 19.3886 8.2972
88.0668 19.3886 8.3577
89.2218 19.3886 8.3794
90.5390 19.3886 8.3642
91.9119 19.3886 8.3212
93.2291 19.3886 8.2631
94.3841 19.3886 8.2017
95.2831 19.3886 8.1474
95.8534 19.3886 8.1085
96.0488 19.3886 8.0900
&BPNODE TNODE=3, TNPC=0, TINTC=0, &END
&SECT1 STX=0.0, STY=0.0, STZ=0.0, SCALE=1.0, ALF=0.0, THETA=0.0, INMODE=4,
TNODS=0, TNPS=0, TINTS=0, &END
96.0500 19.8750 8.0900
95.8566 19.8750 8.0717
95.2920 19.8750 8.0332
94.4020 19.8750 7.9795
93.2586 19.8750 7.9186
91.9546 19.8750 7.8611
90.5954 19.8750 7.8186
89.2914 19.8750 7.8035
88.1480 19.8750 7.8250
87.2580 19.8750 7.8848

```

Jun 11 1997 05:30      froguav.in      Page 27

```

86.6934 19.8750 7.9770
86.5000 19.8750 8.0900
86.6934 19.8750 8.2030
87.2580 19.8750 8.2952
88.1480 19.8750 8.3550
89.2914 19.8750 8.3765
90.5954 19.8750 8.3614
91.9546 19.8750 8.3189
93.2586 19.8750 8.2614
94.4020 19.8750 8.2005
95.2920 19.8750 8.1468
95.8566 19.8750 8.1083
96.0500 19.8750 8.0900
&BPNODE TNODE=3, TNPC=0, TINTC=0, &END

&PATCH1 IREV=0, IDPAT=1, MAKE=0, KCOMP=1, KASS=1, IPATSYM=0, IPATCOP=0, &END
FOG_VERTICAL_TAIL
&SECT1 STX=0.0, STY=0.0, STZ=0.0, SCALE=1.0, ALF=0.0, THETA=0.0, INMODE=4,
TNODES=0, TNPS=0, TINTS=0, &END
97.5000 0.0000 10.4000
96.8969 0.0548 10.4000
95.1604 0.1657 10.4000
92.5000 0.3161 10.4000
89.2365 0.4671 10.4000
85.7635 0.5752 10.4000
82.5000 0.5942 10.4000
79.8396 0.4945 10.4000
78.1031 0.2842 10.4000
77.5000 0.0000 10.4000
78.1031 -0.2842 10.4000
79.8396 -0.4945 10.4000
82.5000 -0.5942 10.4000
85.7635 -0.5752 10.4000
89.2365 -0.4671 10.4000
92.5000 -0.3161 10.4000
95.1604 -0.1657 10.4000
96.8969 -0.0548 10.4000
97.5000 0.0000 10.4000
&BPNODE TNODE=3, TNPC=0, TINTC=0, &END
&SECT1 STX=0.0, STY=0.0, STZ=0.0, SCALE=1.0, ALF=0.0, THETA=0.0, INMODE=4,
TNODES=0, TNPS=0, TINTS=0, &END
97.6846 0.0000 10.9614
97.0930 0.0537 10.9614
95.3896 0.1625 10.9614
92.7797 0.3101 10.9614
89.5783 0.4582 10.9614
86.1715 0.5643 10.9614
82.9700 0.5829 10.9614
80.3602 0.4851 10.9614
78.6568 0.2788 10.9614
78.0652 0.0000 10.9614
78.6568 -0.2788 10.9614
80.3602 -0.4851 10.9614
82.9700 -0.5829 10.9614
86.1715 -0.5643 10.9614
89.5783 -0.4582 10.9614
92.7797 -0.3101 10.9614
95.3896 -0.1625 10.9614
97.0930 -0.0537 10.9614
97.6846 0.0000 10.9614
&BPNODE TNODE=3, TNPC=0, TINTC=0, &END
&SECT1 STX=0.0, STY=0.0, STZ=0.0, SCALE=1.0, ALF=0.0, THETA=0.0, INMODE=4,
TNODES=0, TNPS=0, TINTS=0, &END
98.2103 0.0000 12.5601
97.6514 0.0508 12.5601
96.0420 0.1536 12.5601
93.5764 0.2929 12.5601
90.5518 0.4329 12.5601
87.3332 0.5331 12.5601
84.3086 0.5507 12.5601
81.8430 0.4583 12.5601
80.2336 0.2634 12.5601
79.6747 0.0000 12.5601
80.2336 -0.2634 12.5601

```

Jun 11 1997 05:30      froguav.in      Page 28

```

81.8430 -0.4583 12.5601
84.3086 -0.5507 12.5601
87.3332 -0.5331 12.5601
90.5518 -0.4329 12.5601
93.5764 -0.2929 12.5601
96.0420 -0.1536 12.5601
97.6514 -0.0508 12.5601
98.2103 0.0000 12.5601
&BPNODE TNODE=3, TNPC=0, TINTC=0, &END
&SECT1 STX=0.0, STY=0.0, STZ=0.0, SCALE=1.0, ALF=0.0, THETA=0.0, INMODE=4,
TNODES=0, TNPS=0, TINTS=0, &END
98.9970 0.0000 14.9527
98.4870 0.0463 14.9527
97.0185 0.1401 14.9527
94.7686 0.2673 14.9527
92.0088 0.3950 14.9527
89.0718 0.4864 14.9527
86.3119 0.5025 14.9527
84.0621 0.4182 14.9527
82.5936 0.2404 14.9527
82.0836 0.0000 14.9527
82.5936 -0.2404 14.9527
84.0621 -0.4182 14.9527
86.3119 -0.5025 14.9527
89.0718 -0.4864 14.9527
92.0088 -0.3950 14.9527
94.7686 -0.2673 14.9527
97.0185 -0.1401 14.9527
98.4870 -0.0463 14.9527
98.9970 0.0000 14.9527
&BPNODE TNODE=3, TNPC=0, TINTC=0, &END
&SECT1 STX=0.0, STY=0.0, STZ=0.0, SCALE=1.0, ALF=0.0, THETA=0.0, INMODE=4,
TNODES=0, TNPS=0, TINTS=0, &END
99.9250 0.0000 17.7750
99.4727 0.0411 17.7750
98.1703 0.1243 17.7750
96.1750 0.2371 17.7750
93.7274 0.3503 17.7750
91.1226 0.4314 17.7750
88.6750 0.4456 17.7750
86.6797 0.3709 17.7750
85.3773 0.2132 17.7750
84.9250 0.0000 17.7750
85.3773 -0.2132 17.7750
86.6797 -0.3709 17.7750
88.6750 -0.4456 17.7750
91.1226 -0.4314 17.7750
93.7274 -0.3503 17.7750
96.1750 -0.2371 17.7750
98.1703 -0.1243 17.7750
99.4727 -0.0411 17.7750
99.9250 0.0000 17.7750
&BPNODE TNODE=3, TNPC=0, TINTC=0, &END
&SECT1 STX=0.0, STY=0.0, STZ=0.0, SCALE=1.0, ALF=0.0, THETA=0.0, INMODE=4,
TNODES=0, TNPS=0, TINTS=0, &END
100.8530 0.0000 20.5973
100.4584 0.0358 20.5973
99.3222 0.1084 20.5973
97.5814 0.2068 20.5973
95.4459 0.3056 20.5973
93.1735 0.3764 20.5973
91.0381 0.3888 20.5973
89.2973 0.3236 20.5973
88.1610 0.1860 20.5973
87.7664 0.0000 20.5973
88.1610 -0.1860 20.5973
89.2973 -0.3236 20.5973
91.0381 -0.3888 20.5973
93.1735 -0.3764 20.5973
95.4459 -0.3056 20.5973
97.5814 -0.2068 20.5973
99.3222 -0.1084 20.5973
100.4584 -0.0358 20.5973
100.8530 0.0000 20.5973
&BPNODE TNODE=3, TNPC=0, TINTC=0, &END
&SECT1 STX=0.0, STY=0.0, STZ=0.0, SCALE=1.0, ALF=0.0, THETA=0.0, INMODE=4,

```

Jun 11 1997 05:30      froguav.in      Page 29

```

TNODES=0, TNPS=0, TINTS=0, &END
101.6397 0.0000 22.9899
101.2940 0.0314 22.9899
100.2986 0.0950 22.9899
98.7736 0.1812 22.9899
96.9029 0.2677 22.9899
94.9121 0.3297 22.9899
93.0414 0.3406 22.9899
91.5164 0.2835 22.9899
90.5210 0.1629 22.9899
90.1753 0.0000 22.9899
90.5210 -0.1629 22.9899
91.5164 -0.2835 22.9899
93.0414 -0.3406 22.9899
94.9121 -0.3297 22.9899
96.9029 -0.2677 22.9899
98.7736 -0.1812 22.9899
100.2986 -0.0950 22.9899
101.2940 -0.0314 22.9899
101.6397 0.0000 22.9899
&BPNODE TNODE=3, TNPC=0, TINTC=0, &END
&SECT1 STX=0.0, STY=0.0, STZ=0.0, SCALE=1.0, ALF=0.0, THETA=0.0, INMODE=4,
TNODES=0, TNPS=0, TINTS=0, &END
102.1654 0.0000 24.5886
101.8524 0.0284 24.5886
100.9511 0.0860 24.5886
99.5703 0.1641 24.5886
97.8764 0.2424 24.5886
96.0738 0.2986 24.5886
94.3800 0.3084 24.5886
92.9991 0.2567 24.5886
92.0978 0.1475 24.5886
91.7848 0.0000 24.5886
92.0978 -0.1475 24.5886
92.9991 -0.2567 24.5886
94.3800 -0.3084 24.5886
96.0738 -0.2986 24.5886
97.8764 -0.2424 24.5886
99.5703 -0.1641 24.5886
100.9511 -0.0860 24.5886
101.8524 -0.0284 24.5886
102.1654 0.0000 24.5886
&BPNODE TNODE=3, TNPC=0, TINTC=0, &END
&SECT1 STX=0.0, STY=0.0, STZ=0.0, SCALE=1.0, ALF=0.0, THETA=0.0, INMODE=4,
TNODES=3, TNPS=0, TINTS=0, &END
102.3500 0.0000 25.1500
102.0485 0.0274 25.1500
101.1802 0.0828 25.1500
99.8500 0.1580 25.1500
98.2182 0.2335 25.1500
96.4818 0.2876 25.1500
94.8500 0.2971 25.1500
93.5198 0.2473 25.1500
92.6515 0.1421 25.1500
92.3500 0.0000 25.1500
92.6515 -0.1421 25.1500
93.5198 -0.2473 25.1500
94.8500 -0.2971 25.1500
96.4818 -0.2876 25.1500
98.2182 -0.2335 25.1500
99.8500 -0.1580 25.1500
101.1802 -0.0828 25.1500
102.0485 -0.0274 25.1500
102.3500 0.0000 25.1500
&BPNODE TNODE=3, TNPC=0, TINTC=0, &END

&PATCH1 IREV=0, IDPAT=2, MAKE=0, KCOMP=1, KASS=1, IPATSYM=1, IPATCOP=0, &END
FOG_PYLON
&SECT1 STX=0.0, STY=0.0, STZ=0.0, SCALE=1.0, ALF=0.0, THETA=0.0, INMODE=4,
TNODES=0, TNPS=0, TINTS=0, &END
25.8000 0.0000 14.3100
25.8000 0.0000 14.3516
25.8000 0.0000 14.5358
25.8000 0.0000 14.7201
25.8000 0.0000 14.9044

```

Jun 11 1997 05:30      froguav.in      Page 30

```

25.8000 0.0000 15.0886
25.8000 0.0000 15.2729
25.8000 0.0000 15.4572
25.8000 0.0000 15.6415
25.8000 0.0000 15.8257
25.8000 0.0000 16.0100
&BPNODE TNODE=3, TNPC=0, TINTC=0, &END
&SECT1 STX=0.0, STY=0.0, STZ=0.0, SCALE=1.0, ALF=0.0, THETA=0.0, INMODE=4,
TNODES=0, TNPS=0, TINTS=0, &END
25.9300 0.5302 14.3377
25.9300 0.5302 14.3753
25.9300 0.5302 14.5558
25.9300 0.5302 14.7362
25.9300 0.5302 14.9167
25.9300 0.5302 15.0971
25.9300 0.5302 15.2776
25.9300 0.5302 15.4581
25.9300 0.5302 15.6385
25.9300 0.5302 15.8190
25.9300 0.5302 15.9995
&BPNODE TNODE=3, TNPC=0, TINTC=0, &END
&SECT1 STX=0.0, STY=0.0, STZ=0.0, SCALE=1.0, ALF=0.0, THETA=0.0, INMODE=4,
TNODES=0, TNPS=0, TINTS=0, &END
26.3144 0.9601 14.4108
26.3144 0.9601 14.4384
26.3144 0.9601 14.6089
26.3144 0.9601 14.7793
26.3144 0.9601 14.9497
26.3144 0.9601 15.1201
26.3144 0.9601 15.2905
26.3144 0.9601 15.4609
26.3144 0.9601 15.6313
26.3144 0.9601 15.8017
26.3144 0.9601 15.9721
&BPNODE TNODE=3, TNPC=0, TINTC=0, &END
&SECT1 STX=0.0, STY=0.0, STZ=0.0, SCALE=1.0, ALF=0.0, THETA=0.0, INMODE=4,
TNODES=0, TNPS=0, TINTS=0, &END
26.9363 1.2810 14.5052
26.9363 1.2810 14.5199
26.9363 1.2810 14.6773
26.9363 1.2810 14.8348
26.9363 1.2810 14.9922
26.9363 1.2810 15.1496
26.9363 1.2810 15.3070
26.9363 1.2810 15.4644
26.9363 1.2810 15.6219
26.9363 1.2810 15.7793
26.9363 1.2810 15.9367
&BPNODE TNODE=3, TNPC=0, TINTC=0, &END
&SECT1 STX=0.0, STY=0.0, STZ=0.0, SCALE=1.0, ALF=0.0, THETA=0.0, INMODE=4,
TNODES=0, TNPS=0, TINTS=0, &END
27.7687 1.4893 14.5940
27.7687 1.4893 14.6334
27.7687 1.4893 14.7408
27.7687 1.4893 14.8859
27.7687 1.4893 15.0309
27.7687 1.4893 15.1759
27.7687 1.4893 15.3210
27.7687 1.4893 15.4660
27.7687 1.4893 15.6110
27.7687 1.4893 15.7561
27.7687 1.4893 15.9011
&BPNODE TNODE=3, TNPC=0, TINTC=0, &END
&SECT1 STX=0.0, STY=0.0, STZ=0.0, SCALE=1.0, ALF=0.0, THETA=0.0, INMODE=4,
TNODES=0, TNPS=0, TINTS=0, &END
28.7750 1.5866 14.6549
28.7750 1.5866 14.6638
28.7750 1.5866 14.7837
28.7750 1.5866 14.9196
28.7750 1.5866 15.0555
28.7750 1.5866 15.1914
28.7750 1.5866 15.3273
28.7750 1.5866 15.4632
28.7750 1.5866 15.5991
28.7750 1.5866 15.7351
28.7750 1.5866 15.8710

```

Jun 11 1997 05:30

froguav.in

Page 31

```

&BPNODE TNODE=3, TNPC=0, TINTC=0, &END
&SECT1 STX=0.0, STY=0.0, STZ=0.0, SCALE=1.0, ALF=0.0, THETA=0.0, INMODE=4,
TNODES=0, TNPS=0, TINTS=0, &END
29.9113 1.5803 14.6732
29.9113 1.5803 14.6818
29.9113 1.5803 14.7940
29.9113 1.5803 14.9260
29.9113 1.5803 15.0580
29.9113 1.5803 15.1900
29.9113 1.5803 15.3220
29.9113 1.5803 15.4540
29.9113 1.5803 15.5860
29.9113 1.5803 15.7180
29.9113 1.5803 15.8500
&BPNODE TNODE=3, TNPC=0, TINTC=0, &END
&SECT1 STX=0.0, STY=0.0, STZ=0.0, SCALE=1.0, ALF=0.0, THETA=0.0, INMODE=4,
TNODES=0, TNPS=0, TINTS=0, &END
31.1281 1.4826 14.6416
31.1281 1.4826 14.6504
31.1281 1.4826 14.7667
31.1281 1.4826 14.9009
31.1281 1.4826 15.0351
31.1281 1.4826 15.1694
31.1281 1.4826 15.3036
31.1281 1.4826 15.4379
31.1281 1.4826 15.5721
31.1281 1.4826 15.7063
31.1281 1.4826 15.8406
&BPNODE TNODE=3, TNPC=0, TINTC=0, &END
&SECT1 STX=0.0, STY=0.0, STZ=0.0, SCALE=1.0, ALF=0.0, THETA=0.0, INMODE=4,
TNODES=0, TNPS=0, TINTS=0, &END
32.3719 1.3110 14.5598
32.3719 1.3110 14.5691
32.3719 1.3110 14.7023
32.3719 1.3110 14.8450
32.3719 1.3110 14.9877
32.3719 1.3110 15.1304
32.3719 1.3110 15.2731
32.3719 1.3110 15.4158
32.3719 1.3110 15.5585
32.3719 1.3110 15.7012
32.3719 1.3110 15.8439
&BPNODE TNODE=3, TNPC=0, TINTC=0, &END
&SECT1 STX=0.0, STY=0.0, STZ=0.0, SCALE=1.0, ALF=0.0, THETA=0.0, INMODE=4,
TNODES=0, TNPS=0, TINTS=0, &END
33.5886 1.0866 14.4337
33.5886 1.0866 14.4475
33.5886 1.0866 14.6044
33.5886 1.0866 14.7614
33.5886 1.0866 14.9184
33.5886 1.0866 15.0754
33.5886 1.0866 15.2324
33.5886 1.0866 15.3894
33.5886 1.0866 15.5464
33.5886 1.0866 15.7034
33.5886 1.0866 15.8604
&BPNODE TNODE=3, TNPC=0, TINTC=0, &END
&SECT1 STX=0.0, STY=0.0, STZ=0.0, SCALE=1.0, ALF=0.0, THETA=0.0, INMODE=4,
TNODES=0, TNPS=0, TINTS=0, &END
34.7250 0.8337 14.2747
34.7250 0.8337 14.3074
34.7250 0.8337 14.4831
34.7250 0.8337 14.6589
34.7250 0.8337 14.8347
34.7250 0.8337 15.0105
34.7250 0.8337 15.1863
34.7250 0.8337 15.3621
34.7250 0.8337 15.5379
34.7250 0.8337 15.7137
34.7250 0.8337 15.8895
&BPNODE TNODE=3, TNPC=0, TINTC=0, &END
&SECT1 STX=0.0, STY=0.0, STZ=0.0, SCALE=1.0, ALF=0.0, THETA=0.0, INMODE=4,
TNODES=0, TNPS=0, TINTS=0, &END
35.7313 0.5784 14.0992
35.7313 0.5784 14.1537
35.7313 0.5784 14.3510

```

Jun 11 1997 05:30

froguav.in

Page 32

```

35.7313 0.5784 14.5484
35.7313 0.5784 14.7457
35.7313 0.5784 14.9430
35.7313 0.5784 15.1403
35.7313 0.5784 15.3377
35.7313 0.5784 15.5350
35.7313 0.5784 15.7323
35.7313 0.5784 15.9296
&BPNODE TNODE=3, TNPC=0, TINTC=0, &END
&SECT1 STX=0.0, STY=0.0, STZ=0.0, SCALE=1.0, ALF=0.0, THETA=0.0, INMODE=4,
TNODES=0, TNPS=0, TINTS=0, &END
36.5637 0.3462 13.9276
36.5637 0.3462 14.0041
36.5637 0.3462 14.2235
36.5637 0.3462 14.4428
36.5637 0.3462 14.6622
36.5637 0.3462 14.8815
36.5637 0.3462 15.1009
36.5637 0.3462 15.3203
36.5637 0.3462 15.5396
36.5637 0.3462 15.7590
36.5637 0.3462 15.9783
&BPNODE TNODE=3, TNPC=0, TINTC=0, &END
&SECT1 STX=0.0, STY=0.0, STZ=0.0, SCALE=1.0, ALF=0.0, THETA=0.0, INMODE=4,
TNODES=0, TNPS=0, TINTS=0, &END
37.1856 0.1609 13.7823
37.1856 0.1609 13.8781
37.1856 0.1609 14.1173
37.1856 0.1609 14.3565
37.1856 0.1609 14.5957
37.1856 0.1609 14.8349
37.1856 0.1609 15.0741
37.1856 0.1609 15.3134
37.1856 0.1609 15.5526
37.1856 0.1609 15.7918
37.1856 0.1609 16.0310
&BPNODE TNODE=3, TNPC=0, TINTC=0, &END
&SECT1 STX=0.0, STY=0.0, STZ=0.0, SCALE=1.0, ALF=0.0, THETA=0.0, INMODE=4,
TNODES=0, TNPS=0, TINTS=0, &END
37.5700 0.0413 13.6845
37.5700 0.0413 13.7951
37.5700 0.0413 14.0489
37.5700 0.0413 14.3025
37.5700 0.0413 14.5562
37.5700 0.0413 14.8099
37.5700 0.0413 15.0636
37.5700 0.0413 15.3173
37.5700 0.0413 15.5710
37.5700 0.0413 15.8247
37.5700 0.0413 16.0784
&BPNODE TNODE=3, TNPC=0, TINTC=0, &END
&SECT1 STX=0.0, STY=0.0, STZ=0.0, SCALE=1.0, ALF=0.0, THETA=0.0, INMODE=4,
TNODES=3, TNPS=0, TINTS=0, &END
37.7000 0.0000 13.6500
37.7000 0.0000 13.7663
37.7000 0.0000 14.0256
37.7000 0.0000 14.2849
37.7000 0.0000 14.5442
37.7000 0.0000 14.8035
37.7000 0.0000 15.0628
37.7000 0.0000 15.3221
37.7000 0.0000 15.5814
37.7000 0.0000 15.8407
37.7000 0.0000 16.1000
&BPNODE TNODE=3, TNPC=0, TINTC=0, &END
&PATCH1 IREV=0, IDPAT=2, MAKE=0, KCOMP=1, KASS=1, IPATSYM=1, IPATCOP=0, &END
FOG_ENGINE_POD
&SECT1 STX=0.0, STY=0.0, STZ=0.0, SCALE=1.0, ALF=0.0, THETA=0.0, INMODE=4,
TNODES=0, TNPS=0, TINTS=0, &END
16.5000 0.0000 20.4000
16.5000 0.0000 20.4000
16.5000 0.0000 20.4000
16.5000 0.0000 20.4000

```



Jun 11 1997 05:30      froguav.in      Page 33

```

16.5000 0.0000 20.4000
16.5000 0.0000 20.4000
16.5000 0.0000 20.4000
16.5000 0.0000 20.4000
16.5000 0.0000 20.4000
16.5000 0.0000 20.4000
16.5000 0.0000 20.4000
&BPNODE TNODE=3, TNPC=0, TINTC=0, &END
&SECT1 STX=0.0, STY=0.0, STZ=0.0, SCALE=1.0, ALF=0.0, THETA=0.0, INMODE=4,
TNODES=0, TNPS=0, TINTS=0, &END
16.7895 0.0000 19.7036
16.7895 0.1802 19.7381
16.7895 0.3338 19.8311
16.7895 0.4530 19.9692
16.7895 0.5342 20.1491
16.7895 0.5642 20.3542
16.7895 0.5363 20.5590
16.7895 0.4556 20.7374
16.7895 0.3349 20.8747
16.7895 0.1800 20.9661
16.7895 0.0000 20.9995
&BPNODE TNODE=3, TNPC=0, TINTC=0, &END
&SECT1 STX=0.0, STY=0.0, STZ=0.0, SCALE=1.0, ALF=0.0, THETA=0.0, INMODE=4,
TNODES=0, TNPS=0, TINTS=0, &END
17.6455 0.0000 18.9621
17.6455 0.4134 19.0316
17.6455 0.7696 19.2229
17.6455 1.0398 19.5042
17.6455 1.2183 19.8707
17.6455 1.2728 20.2955
17.6455 1.1966 20.7383
17.6455 1.0093 21.1240
17.6455 0.7418 21.4169
17.6455 0.3972 21.6150
17.6455 0.0000 21.6870
&BPNODE TNODE=3, TNPC=0, TINTC=0, &END
&SECT1 STX=0.0, STY=0.0, STZ=0.0, SCALE=1.0, ALF=0.0, THETA=0.0, INMODE=4,
TNODES=0, TNPS=0, TINTS=0, &END
19.0305 0.0000 17.6702
19.0305 0.7979 17.7380
19.0305 1.3113 17.9554
19.0305 1.6163 18.3439
19.0305 1.7872 18.9932
19.0305 1.8434 19.9738
19.0305 1.7865 20.8477
19.0305 1.5906 21.4633
19.0305 1.2554 21.8603
19.0305 0.7367 22.0950
19.0305 0.0000 22.1718
&BPNODE TNODE=3, TNPC=0, TINTC=0, &END
&SECT1 STX=0.0, STY=0.0, STZ=0.0, SCALE=1.0, ALF=0.0, THETA=0.0, INMODE=4,
TNODES=0, TNPS=0, TINTS=0, &END
20.8840 0.0000 16.8347
20.8840 1.3042 16.8570
20.8840 1.8746 16.9602
20.8840 2.0812 17.2524
20.8840 2.1525 18.0117
20.8840 2.1689 19.5462
20.8840 2.1572 21.0957
20.8840 2.0882 21.8715
20.8840 1.8780 22.1653
20.8840 1.3111 22.2650
20.8840 0.0000 22.2869
&BPNODE TNODE=3, TNPC=0, TINTC=0, &END
&SECT1 STX=0.0, STY=0.0, STZ=0.0, SCALE=1.0, ALF=0.0, THETA=0.0, INMODE=4,
TNODES=0, TNPS=0, TINTS=0, &END
23.1250 0.0000 16.3511
23.1250 1.4033 16.3708
23.1250 2.0127 16.4691
23.1250 2.2204 16.7715
23.1250 2.2622 17.5999
23.1250 2.2994 19.2276
23.1250 2.2915 20.8939
23.1250 2.2329 21.7791
23.1250 2.0307 22.0844
23.1250 1.4246 22.1766

```

Jun 11 1997 05:30      froguav.in      Page 34

```

23.1250 0.0000 22.1945
&BPNODE TNODE=3, TNPC=0, TINTC=0, &END
&SECT1 STX=0.0, STY=0.0, STZ=0.0, SCALE=1.0, ALF=0.0, THETA=0.0, INMODE=4,
TNODES=0, TNPS=0, TINTS=0, &END
25.6555 0.0000 16.0481
25.6555 1.4141 16.0679
25.6555 2.0188 16.1668
25.6555 2.2226 16.4703
25.6555 2.2870 17.3089
25.6555 2.2999 18.9446
25.6555 2.2912 20.6132
25.6555 2.2327 21.5039
25.6555 2.0316 21.8124
25.6555 1.4305 21.9057
25.6555 0.0000 21.9240
&BPNODE TNODE=3, TNPC=0, TINTC=0, &END
&SECT1 STX=0.0, STY=0.0, STZ=0.0, SCALE=1.0, ALF=0.0, THETA=0.0, INMODE=4,
TNODES=0, TNPS=0, TINTS=0, &END
28.3650 0.0000 15.8494
28.3650 1.4144 15.8682
28.3650 2.0199 15.9622
28.3650 2.2237 16.2532
28.3650 2.2875 17.0611
28.3650 2.3000 18.6632
28.3650 2.2900 20.2862
28.3650 2.2287 21.1215
28.3650 2.0240 21.4109
28.3650 1.4190 21.4999
28.3650 0.0000 21.5175
&BPNODE TNODE=3, TNPC=0, TINTC=0, &END
&SECT1 STX=0.0, STY=0.0, STZ=0.0, SCALE=1.0, ALF=0.0, THETA=0.0, INMODE=4,
TNODES=0, TNPS=0, TINTS=0, &END
31.1350 0.0000 15.7474
31.1350 1.3961 15.7637
31.1350 2.0103 15.8456
31.1350 2.2203 16.1006
31.1350 2.2865 16.8111
31.1350 2.3000 18.3044
31.1350 2.2868 19.8200
31.1350 2.2242 20.5497
31.1350 2.0130 20.8000
31.1350 1.3979 20.8773
31.1350 0.0000 20.8925
&BPNODE TNODE=3, TNPC=0, TINTC=0, &END
&SECT1 STX=0.0, STY=0.0, STZ=0.0, SCALE=1.0, ALF=0.0, THETA=0.0, INMODE=4,
TNODES=0, TNPS=0, TINTS=0, &END
33.8445 0.0000 15.8093
33.8445 1.3627 15.8218
33.8445 1.9940 15.8864
33.8445 2.2152 16.0907
33.8445 2.2852 16.6649
33.8445 2.3000 17.9747
33.8445 2.2868 19.3038
33.8445 2.2166 19.8875
33.8445 1.9942 20.0845
33.8445 1.3615 20.1457
33.8445 0.0000 20.1575
&BPNODE TNODE=3, TNPC=0, TINTC=0, &END
&SECT1 STX=0.0, STY=0.0, STZ=0.0, SCALE=1.0, ALF=0.0, THETA=0.0, INMODE=4,
TNODES=0, TNPS=0, TINTS=0, &END
36.3750 0.0000 15.9892
36.3750 1.3053 15.9975
36.3750 1.9691 16.0428
36.3750 2.2080 16.1903
36.3750 2.2835 16.6129
36.3750 2.3000 17.6647
36.3750 2.2844 18.7297
36.3750 2.2062 19.1542
36.3750 1.9627 19.2941
36.3750 1.2912 19.3366
36.3750 0.0000 19.3443
&BPNODE TNODE=3, TNPC=0, TINTC=0, &END
&SECT1 STX=0.0, STY=0.0, STZ=0.0, SCALE=1.0, ALF=0.0, THETA=0.0, INMODE=4,
TNODES=0, TNPS=0, TINTS=0, &END
38.6160 0.0000 16.2138
38.6160 1.1972 16.2181

```

Jun 11 1997 05:30      froguav.in      Page 35

```

38.6160 1.9280 16.2456
38.6160 2.1972 16.3400
38.6160 2.2813 16.6192
38.6160 2.3000 17.3609
38.6160 2.2827 18.1311
38.6160 2.1968 18.4163
38.6160 1.9293 18.5068
38.6160 1.2029 18.5335
38.6160 0.0000 18.5378
&BPNODE TNODE=3, TNPC=0, TINTC=0, &END
&SECT1 STX=0.0, STY=0.0, STZ=0.0, SCALE=1.0, ALF=0.0, THETA=0.0, INMODE=4,
TNODES=0, TNPS=0, TINTS=0, &END
40.4695 0.0000 16.4386
40.4695 1.0541 16.4404
40.4695 1.8638 16.4540
40.4695 2.1814 16.5048
40.4695 2.2786 16.6646
40.4695 2.3000 17.1216
40.4695 2.2796 17.6011
40.4695 2.1790 17.7620
40.4695 1.8677 17.8097
40.4695 1.0610 17.8229
40.4695 0.0000 17.8247
&BPNODE TNODE=3, TNPC=0, TINTC=0, &END
&SECT1 STX=0.0, STY=0.0, STZ=0.0, SCALE=1.0, ALF=0.0, THETA=0.0, INMODE=4,
TNODES=0, TNPS=0, TINTS=0, &END
41.8545 0.0000 16.6286
41.8545 0.8776 16.6291
41.8545 1.7102 16.6332
41.8545 2.1282 16.6520
41.8545 2.2589 16.7231
41.8545 2.2846 16.9507
41.8545 2.2559 17.1850
41.8545 2.1229 17.2486
41.8545 1.7061 17.2659
41.8545 0.8776 17.2699
41.8545 0.0000 17.2703
&BPNODE TNODE=3, TNPC=0, TINTC=0, &END
&SECT1 STX=0.0, STY=0.0, STZ=0.0, SCALE=1.0, ALF=0.0, THETA=0.0, INMODE=4,
TNODES=0, TNPS=0, TINTS=0, &END
42.7105 0.0000 16.7554
42.7105 0.6609 16.7566
42.7105 1.2924 16.7619
42.7105 1.7606 16.7743
42.7105 2.0332 16.7974
42.7105 2.1274 16.8434
42.7105 2.0340 16.8795
42.7105 1.7674 16.9014
42.7105 1.3047 16.9135
42.7105 0.6710 16.9187
42.7105 0.0000 16.9198
&BPNODE TNODE=3, TNPC=0, TINTC=0, &END
&SECT1 STX=0.0, STY=0.0, STZ=0.0, SCALE=1.0, ALF=0.0, THETA=0.0, INMODE=4,
TNODES=3, TNPS=0, TINTS=0, &END
43.0000 0.0000 16.8000
43.0000 0.0000 16.8000
43.0000 0.0000 16.8000
43.0000 0.0000 16.8000
43.0000 0.0000 16.8000
43.0000 0.0000 16.8000
43.0000 0.0000 16.8000
43.0000 0.0000 16.8000
43.0000 0.0000 16.8000
43.0000 0.0000 16.8000
&BPNODE TNODE=3, TNPC=0, TINTC=0, &END

&PATCH1 IREV=0, IDPAT=2, MAKE=0, KASS=1, IPATSYM=1, IPATCOP=0, &END
FOG_UAV_BOOM (10X12) CLOSED ENDS
&SECT1 STX=0.0, STY=0.0, STZ=0.0, SCALE=1.0, ALF=0.0, THETA=0.0, INMODE=4,
TNODES=0, TNPS=0, TINTS=0, &END
53.5000 0.0000 9.3750
53.5000 0.0000 9.3750
53.5000 0.0000 9.3750
53.5000 0.0000 9.3750

```

Jun 11 1997 05:30      froguav.in      Page 36

```

53.5000 0.0000 9.3750
53.5000 0.0000 9.3750
53.5000 0.0000 9.3750
53.5000 0.0000 9.3750
53.5000 0.0000 9.3750
53.5000 0.0000 9.3750
53.5000 0.0000 9.3750
&BPNODE TNODE=3, TNPC=0, TINTC=0, &END
&SECT1 STX=0.0, STY=0.0, STZ=0.0, SCALE=1.0, ALF=0.0, THETA=0.0, INMODE=4,
TNODES=0, TNPS=0, TINTS=0, &END
53.5000 0.0000 8.5178
53.5000 0.2731 8.5625
53.5000 0.5094 8.6857
53.5000 0.6900 8.8665
53.5000 0.8127 9.1024
53.5000 0.8572 9.3738
53.5000 0.8121 9.6495
53.5000 0.6885 9.8855
53.5000 0.5074 10.0658
53.5000 0.2712 10.1882
53.5000 0.0000 10.2322
&BPNODE TNODE=3, TNPC=0, TINTC=0, &END
&SECT1 STX=0.0, STY=0.0, STZ=0.0, SCALE=1.0, ALF=0.0, THETA=0.0, INMODE=4,
TNODES=0, TNPS=0, TINTS=0, &END
55.1002 0.0000 8.5000
55.1002 0.2785 8.5455
55.1002 0.5195 8.6711
55.1002 0.7046 8.8564
55.1002 0.8296 9.0971
55.1002 0.8750 9.3739
55.1002 0.8290 9.6548
55.1002 0.7031 9.8956
55.1002 0.5175 10.0804
55.1002 0.2766 10.2051
55.1002 0.0000 10.2500
&BPNODE TNODE=3, TNPC=0, TINTC=0, &END
&SECT1 STX=0.0, STY=0.0, STZ=0.0, SCALE=1.0, ALF=0.0, THETA=0.0, INMODE=4,
TNODES=0, TNPS=0, TINTS=0, &END
57.1102 0.0000 8.5000
57.1102 0.2785 8.5455
57.1102 0.5195 8.6711
57.1102 0.7046 8.8564
57.1102 0.8296 9.0971
57.1102 0.8750 9.3739
57.1102 0.8290 9.6548
57.1102 0.7031 9.8956
57.1102 0.5175 10.0804
57.1102 0.2766 10.2051
57.1102 0.0000 10.2500
&BPNODE TNODE=3, TNPC=0, TINTC=0, &END
&SECT1 STX=0.0, STY=0.0, STZ=0.0, SCALE=1.0, ALF=0.0, THETA=0.0, INMODE=4,
TNODES=0, TNPS=0, TINTS=0, &END
59.9757 0.0000 8.5000
59.9757 0.2785 8.5455
59.9757 0.5195 8.6711
59.9757 0.7046 8.8564
59.9757 0.8296 9.0971
59.9757 0.8750 9.3739
59.9757 0.8290 9.6548
59.9757 0.7031 9.8956
59.9757 0.5175 10.0804
59.9757 0.2766 10.2051
59.9757 0.0000 10.2500
&BPNODE TNODE=3, TNPC=0, TINTC=0, &END
&SECT1 STX=0.0, STY=0.0, STZ=0.0, SCALE=1.0, ALF=0.0, THETA=0.0, INMODE=4,
TNODES=0, TNPS=0, TINTS=0, &END
63.8927 0.0000 8.5000
63.8927 0.2785 8.5455
63.8927 0.5195 8.6711
63.8927 0.7046 8.8564
63.8927 0.8296 9.0971
63.8927 0.8750 9.3739
63.8927 0.8290 9.6548
63.8927 0.7031 9.8956
63.8927 0.5175 10.0804
63.8927 0.2766 10.2051

```

Jun 11 1997 05:30      froguav.in      Page 37

```

63.8927 0.0000 10.2500
&BPNODE TNODE=3, TNPC=0, TINTC=0, &END
&SECT1 STX=0.0, STY=0.0, STZ=0.0, SCALE=1.0, ALF=0.0, THETA=0.0, INMODE=4,
TNODS=0, TNPS=0, TINTS=0, &END
71.0000 0.0000 8.5000
71.0000 0.2785 8.5455
71.0000 0.5195 8.6711
71.0000 0.7046 8.8564
71.0000 0.8296 9.0971
71.0000 0.8750 9.3739
71.0000 0.8290 9.6548
71.0000 0.7031 9.8956
71.0000 0.5175 10.0804
71.0000 0.2766 10.2051
71.0000 0.0000 10.2500
&BPNODE TNODE=3, TNPC=0, TINTC=0, &END
&SECT1 STX=0.0, STY=0.0, STZ=0.0, SCALE=1.0, ALF=0.0, THETA=0.0, INMODE=4,
TNODS=0, TNPS=0, TINTS=0, &END
78.1073 0.0000 8.5000
78.1073 0.2785 8.5455
78.1073 0.5195 8.6711
78.1073 0.7046 8.8564
78.1073 0.8296 9.0971
78.1073 0.8750 9.3739
78.1073 0.8290 9.6548
78.1073 0.7031 9.8956
78.1073 0.5175 10.0804
78.1073 0.2766 10.2051
78.1073 0.0000 10.2500
&BPNODE TNODE=3, TNPC=0, TINTC=0, &END
&SECT1 STX=0.0, STY=0.0, STZ=0.0, SCALE=1.0, ALF=0.0, THETA=0.0, INMODE=4,
TNODS=0, TNPS=0, TINTS=0, &END
82.0243 0.0000 8.5000
82.0243 0.2785 8.5455
82.0243 0.5195 8.6711
82.0243 0.7046 8.8564
82.0243 0.8296 9.0971
82.0243 0.8750 9.3739
82.0243 0.8290 9.6548
82.0243 0.7031 9.8956
82.0243 0.5175 10.0804
82.0243 0.2766 10.2051
82.0243 0.0000 10.2500
&BPNODE TNODE=3, TNPC=0, TINTC=0, &END
&SECT1 STX=0.0, STY=0.0, STZ=0.0, SCALE=1.0, ALF=0.0, THETA=0.0, INMODE=4,
TNODS=0, TNPS=0, TINTS=0, &END
84.8898 0.0000 8.5000
84.8898 0.2785 8.5455
84.8898 0.5195 8.6711
84.8898 0.7046 8.8564
84.8898 0.8296 9.0971
84.8898 0.8750 9.3739
84.8898 0.8290 9.6548
84.8898 0.7031 9.8956
84.8898 0.5175 10.0804
84.8898 0.2766 10.2051
84.8898 0.0000 10.2500
&BPNODE TNODE=3, TNPC=0, TINTC=0, &END
&SECT1 STX=0.0, STY=0.0, STZ=0.0, SCALE=1.0, ALF=0.0, THETA=0.0, INMODE=4,
TNODS=0, TNPS=0, TINTS=0, &END
86.8998 0.0000 8.5000
86.8998 0.2785 8.5455
86.8998 0.5195 8.6711
86.8998 0.7046 8.8564
86.8998 0.8296 9.0971
86.8998 0.8750 9.3739
86.8998 0.8290 9.6548
86.8998 0.7031 9.8956
86.8998 0.5175 10.0804
86.8998 0.2766 10.2051
86.8998 0.0000 10.2500
&BPNODE TNODE=3, TNPC=0, TINTC=0, &END
&SECT1 STX=0.0, STY=0.0, STZ=0.0, SCALE=1.0, ALF=0.0, THETA=0.0, INMODE=4,
TNODS=0, TNPS=0, TINTS=0, &END
88.5002 0.0000 8.5178
88.5002 0.2731 8.5625

```

Jun 11 1997 05:30      froguav.in      Page 38

```

88.5002 0.5094 8.6857
88.5002 0.6900 8.8665
88.5002 0.8127 9.1024
88.5002 0.8572 9.3738
88.5002 0.8121 9.6495
88.5002 0.6885 9.8855
88.5002 0.5074 10.0658
88.5002 0.2712 10.1882
88.5002 0.0000 10.2322
&BPNODE TNODE=3, TNPC=0, TINTC=0, &END
&SECT1 STX=0.0, STY=0.0, STZ=0.0, SCALE=1.0, ALF=0.0, THETA=0.0, INMODE=4,
TNODS=5, TNPS=0, TINTS=0, &END
88.5000 0.0000 9.3750
88.5000 0.0000 9.3750
88.5000 0.0000 9.3750
88.5000 0.0000 9.3750
88.5000 0.0000 9.3750
88.5000 0.0000 9.3750
88.5000 0.0000 9.3750
88.5000 0.0000 9.3750
88.5000 0.0000 9.3750
88.5000 0.0000 9.3750
&BPNODE TNODE=3, TNPC=0, TINTC=0, &END

&WAKE1 IDWAK=1, IFLXW=1, ITRFTZ= 1, INTRW= 0, &END
&WAKE2 RIGHT_WING_WAKE KWPACH=17, KWSIDE=4, KWLIN=1, KWPAN1=0, &END
&WAKE2 KWPACH=15, KWSIDE=4, KWLIN=1, KWPAN1=0, &END
&WAKE2 KWPACH=13, KWSIDE=4, KWLIN=1, KWPAN1=0, &END
&WAKE2 KWPACH=11, NODEW=3, INITIAL=0, &END

&WAKE1 IDWAK=1, IFLXW=1, ITRFTZ= 1, INTRW= 0, &END
&WAKE2 LEFT_WING_WAKE KWPACH=18, KWSIDE=4, KWLIN=1, KWPAN1=0, &END
&WAKE2 KWPACH=16, NODEW=0, INITIAL=0, KWPAN1=0, &END
&WAKE2 KWPACH=14, KWSIDE=4, KWLIN=1, KWPAN1=0, &END
&WAKE2 KWPACH=12, NODEW=3, INITIAL=0, &END

&WAKE1 IDWAK=1, IFLXW=1, ITRFTZ= 1, INTRW= 0, &END
&WAKE2 RIGHT_HORIZ_TAIL_WAKE KWPACH=21, KWSIDE=4, KWLIN=1, KWPAN1=0, &END
&WAKE2 KWPACH=20, NODEW=3, INITIAL=0, &END

&WAKE1 IDWAK=1, IFLXW=1, ITRFTZ= 1, INTRW= 0, &END
&WAKE2 LEFT_HORIZ_TAIL_WAKE KWPACH=22, KWSIDE=4, KWLIN=1, KWPAN1=0, &END
&WAKE2 KWPACH=20, NODEW=3, INITIAL=0, &END

&WAKE1 IDWAK=1, IFLXW=1, ITRFTZ= 1, INTRW= 1, &END
&WAKE2 VERT_TAIL_WAKE KWPACH=23, KWSIDE=4, KWLIN=1, KWPAN1=0, &END
&WAKE2 KWPACH=20, NODEW=5, INITIAL=0, &END

&WAKE1 IDWAK=1, IFLXW=1, ITRFTZ= 1, INTRW= 1, &END
&WAKE2 ENGINE_PYLON_WAKE KWPACH=24, KWSIDE=3, KWLIN=0, KWPAN1=0, &END
&WAKE2 KWPACH=20, NODEW=3, INITIAL=0, &END

&WAKE1 IDWAK=1, IFLXW=0, ITRFTZ= 1, INTRW= 1, &END
&WAKE2 LEFT_ENGINE_POD_WAKE KWPACH=27, KWSIDE=1, KWLIN=15, KWPAN1=6, &END
&WAKE2 KWPACH=20, NODEW=5, INITIAL=0, &END

&WAKE1 IDWAK=1, IFLXW=0, ITRFTZ= 1, INTRW= 1, &END
&WAKE2 RIGHT_ENGINE_POD_WAKE KWPACH=26, KWSIDE=1, KWLIN=15, KWPAN1=6, &END
&WAKE2 KWPACH=20, NODEW=3, INITIAL=0, &END

```

Jun 11 1997 05:30

froguav.in

Page 39

```

&ONSTRM NONSL =0, KPSL =
1,2,3,4,5,6,7,8,9,10,11,117,115,113,111,109,107,105,103,102,197,195,193,191,
189,187,185,183,1937,1938,1939,1940,1941,2890,2908,2926,2944,2962,2980,
2998,1073,1045,1017,989,961,933,905,2638,2616,2594,2572,2550,2528,2506,2584,      &EN
D

&BLPARAM RN =929000, VISC = 0.022641, NSLBL = 1,2,3,4,5,6,7,8,9,10,11,
12,13,14,15,16,17,18,19,20,21,22,23,24,25,26,27,28,29,30,31,32,33,34,35,36,37,38,
39,40,41,42,43,44,45,46,47,48,49,50,51,52,53,54,55,      &END

&VS1 NVOLR= 0, NVOLC= 0,      &END
&VS2 X0= -0.1000, Y0= 1.5000, Z0= -0.1000, INTVSR= 1,      &END
&VS3 X1= -0.1000, Y1= 1.5000, Z1= 0.1000, NPT1= 0,      &END
&VS4 X2= -0.1000, Y2= 1.5000, Z2= 0.1000, NPT2= 20,      &END
&VS5 X3= 1.1000, Y3= 1.5000, Z3= -0.1000, NPT3= 25,      &END

&VS6 XR0= 2.0000, YR0= 2.0000, ZR0= 0.0000, INTVSC= 1,      &END
&VS7 XR1= 4.0000, YR1= 2.0000, ZR1= 0.0000,      &END
&VS8 XR2= 2.0000, YR2= 2.0000, ZR2= 1.0000,      &END
&VS9 R1= 0.1000, R2= 1.0000, PHI1= 0.0, PHI2=360.0,      &END
NRAD= 5, NPFI= 12, NLEN= 3,      &END

&SLIN1 NSTLIN=4,      &END
&SLIN2 SX0= -6.5000, SY0= 2.50000, SZ0= 7.5000,      &END
SU= 2.0000, SD= 2.0000, DS= 0.100, INTSL= 1,      &END
&SLIN2 SX0= -8.25000, SY0= 0.00000, SZ0= 7.5000,      &END
SU= 2.0000, SD= 2.0000, DS= 0.100, INTSL= 1,      &END
&SLIN2 SX0= -6.5000, SY0= 2.50000, SZ0= 7.5000,      &END
SU= 15.0000, SD= 100.0000, DS= 0.500, INTSL= 1,      &END
&SLIN2 SX0= -8.25000, SY0= 0.00000, SZ0= 7.5000,      &END
SU= 15.0000, SD= 100.0000, DS= 0.500, INTSL= 1,      &END

```

## LIST OF REFERENCES

1. Papageorgiou, E., "Development of a Dynamic Model for a UAV," Master's Thesis, Naval Postgraduate School, Monterey, CA, March 1997.
2. Garrison, P., and Pinella, D., *CMARC User's Guide*, AeroLogic, Inc., <http://www.iac.net/~aerol>, 1996.
3. Bertin, J. J., and Smith, M. L., *Aerodynamics for Engineers*, Prentice Hall, 1989.
4. Ashby, D. L., Dudley, M. R., Iguchi, S. K., Browne, L., and Katz, J., *Potential Flow Theory and Operation Guide for the Panel Code PMARC\_12*, NASA TM-102851, Ames Research Center, Moffet Field, CA., December 1992.
5. Anderson, J. D., *Fundamentals of Aerodynamics*, McGraw-Hill, Inc., 1991.
6. Lambert, M. A., *Evaluation of the NASA-AMES Panel Method (PMARC) for Aerodynamic Missile Design*, Master's Thesis, Naval Postgraduate School, CA, September, 1995.
7. Tuncer, I. H., and Platzer, M. F., *PMARC Potential Flow Solutions with Wakes Over an Ogive Cylinder at High Incidence*, AIAA Paper No. 97-1968, American Institute of Aeronautics and Astronautics, June 1997.
8. Cebeci, T., "Computation of Three-Dimensional Boundary Layers Including Separation," VKI Lecture Series, Douglas Aircraft Company, April 1986.
9. Young, A. D., *Boundary Layers*, American Institute of Aeronautics, 1989.
10. Jones, K. D., and Center, K. B., "Numerical Wake Visualization for Airfoils Undergoing Forced and Aeroelastic Motions," AIAA Paper No. 96-0055, January 1996.
11. Nowak, L. M., *Computational Investigations of a NACA 0012 Airfoil in Low Reynolds Number Flows*, Master's Thesis, Naval Postgraduate School, Monterey, CA, September 1992.
12. Kreplin, H. P., "Three-Dimensional Boundary Layer and Flow Field Data of an Inclined Prolate Spheroid," *AGARD Advisory Report No. 303: A Selection of Experimental Test Cases for the Validation of CFD Codes*, Volumes I and II, North Atlantic Treaty Organization, August 1994.

13. *Performance Phase Textbook-Volume I*, USAF Test Pilot School, Edwards AFB, CA., June 1988.
14. Nicolai, L. M., *Fundamentals of AIRCRAFT DESIGN*, METs, Inc., 1984.
15. Walden, A. B., van Dam, C. P., and Brandon, J. M., *Modeling of the Interaction Between a Lifting Wing and a Following Aircraft and Comparison with Experimental Results*, AIAA 96-0771, 34<sup>th</sup> Aerospace Sciences Meeting and Exhibit, Reno, NV, January 1996.

## INITIAL DISTRIBUTION LIST

1. Defense Technical Information Center..... 2  
8725 John J. Kingman Road, Ste 0944  
Ft. Belvoir, VA 22060-6218
  
2. Dudley Knox Library..... 2  
Naval Postgraduate School  
411 Dyer Rd.  
Monterey, CA 93943-5101
  
3. Chairman..... 1  
Department of Aeronautics and Astronautics, Code AA  
Naval Postgraduate School  
699 Dyer Road, Room 137  
Monterey, CA 93943-5106
  
4. Dr. Max F. Platzer..... 5  
Department of Aeronautics and Astronautics, Code AA/PL  
Naval Postgraduate School  
699 Dyer Road, Room 137  
Monterey, CA 93943-5106
  
5. Dr. Ismail H. Tuncer..... 1  
Department of Aeronautics and Astronautics, Code AA  
Naval Postgraduate School  
699 Dyer Road, Room 137  
Monterey, CA 93943-5106
  
6. Dr. Kevin Jones..... 1  
Department of Aeronautics and Astronautics, Code AA  
Naval Postgraduate School  
699 Dyer Road, Room 137  
Monterey, CA 93943-5106
  
7. LCDR Stephen J. Pollard..... 2  
Department of Aviation Safety  
Naval Postgraduate School  
1 University Circle  
Monterey, CA 93943-5106

8. Peter Garrison..... 1  
AeroLogic, Inc.  
1613 Altivo Way  
Los Angeles, CA 90026